DOTTORATO DI RICERCA IN

CHIMICA

Ciclo XXVIII

Settore Concorsuale di afferenza: **03/C2**

Settore Scientifico disciplinare: CHIM/04

SUSTAINABLE CATALYTIC PROCESSES
FOR THE SYNTHESIS AND USE OF ORGANIC CARBONATES

Presentata da: **Tommaso Tabanelli**

Coordinatore Dottorato   *Relatore*

Prof. Aldo Roda   **Prof. Fabrizio Cavani**

Esame finale anno 2016

I would like to dedicate this Thesis to my grandpa Ermanno, who is always in my thoughts

Key words

Carbon Dioxide (CO$_2$)

Organic Carbonates

Reactive Distillation

Dimethyl Carbonate (DMC)

Pyrocatechol Carbonate (PCC)

Carbonate Interchange Reaction

Glycerol Carbonate (GlyC)

Heterogeneous Catalyst

Phenol Alkylation

Gas-phase

Abstract

The present study is focused on the development and improvement of sustainable catalytic processes for the synthesis of organic carbonates.

In particular, the condensation reaction between carbon dioxide and several alcohols and diols has been investigated using a new generation of mesoporous nanosilicas functionalized by the insertion of amino groups on the catalyst surface. This reaction were performed in a high-pressure batch vessel (autoclave).

Moreover, the carbonate interchange reaction (CIR) of the simplest linear organic carbonate, dimethyl carbonate (DMC) with several alcohols has been implemented by means of a new lab-scale reactive distillation system.

In this new system, the distilled mixture is continuously passed over molecular sieves able to promote a selective adsorption of methanol (co-product of the reactions) while DMC is continuously refluxed back into the reaction batch.

In this way, we were able to promote an efficient shift of the reaction equilibria toward the formation of the desired products.

This system allowed us to achieve up to 90% isolated yield of pyrocatechol carbonate (PCC), a new and previously scarcely investigated carbonate.

The PCC has been used as a new and more efficient carbonate source for the selective synthesis of symmetric carbonates and for the synthesis of glycerol carbonate (GlyC).

GlyC has been also used as glycidol intermediate, for the condensation reaction with catechol in order to obtain the efficient synthesis of 2-hydroxymethy-1,4-benzodioxane (HMB) an important intermediate for the pharma industry.

Finally, some of the synthesized carbonates were tested for the gas-phase phenol alkylation showing an interesting reactivity that could be properly modulated by changing the reaction conditions and the catalyst acid-base properties.

Summary

NOMENCLATURE

BC: Butylene Carbonate;

BET: Brunauer–Emmett–Teller surface area analysis;

CCS: Carbon dioxide Capture and Storage;

CIR: Carbonate Interchange Reaction;

CLC: Chemical-Looping Combustion;

DAC: DiAllyl Carbonate;

DBC: DiButyl Carbonate;

DCC: DiCyclohexyl Carbonate;

DCM: DiChloroMethane;

DEC: DiEthyl Carbonate;

DEE: DiEthyl Ether;

DMC: DiMethyl Carbonate;

DMeC: DiMenthyl Carbonate;

DIPC: DiIsoPropyl Carbonate;

DPC: DiPhenyl Carbonate;

EC: Ethylene Carbonate;

EG: Ethylene Glycol;

EO: Ethylene Oxide;

FT-IR: Fourier Transform InfraRed spectroscopy analysis;

GlyC: Glycerol Carbonate;

IPCC: Intergovernmental Panel on Climate Change

MBC: Methyl Butyl Carbonate;

MDR: Methane Dry Reforming;

MgO: Magnesium Oxide;

Mg/Al/O: Magnesium and Aluminum mixed oxide;

MMeC: Methyl Menthyl Carbonate;

MOFs: Metal-Organic Frameworks;

MPC: MethylPhenyl Carbonate;

PC: Propylene Carbonate;

PCC: PyroCatechol Carbonate;

RDS: Reactive Distillation Systems;

RWGS: Reverse Water Gas Shift reaction;

SBA-15/APTS: 3-aminopropyltrimethoxysilane functionalized mesoporous nanosilicas;

SBA-15/EAPTS: 3-(2-aminoethyl) aminopropyltrimethoxysilane functionalized mesoporous nanosilicas;

SBA-15/PAPTS: 3-[2-(2-aminoethyl)aminoethyl] aminopropyltrimethoxysilane functionalized mesoporous nanosilicas;

sc-CO$_2$: super critical carbon dioxide;

τ: residence time;

TGA: ThermoGravimetric Analysis;

TOF: Turnover Frequency;

TON: Turnover Number;

VOCs: Volatile Oorganic Compounds;

X: Conversion;

XRD: X-ray Diffraction analysis;

Y: Yield;

WGS: Water Gas Shift reaction.

ACKNOWLEDGEMENTS

1 INTRODUCTION

1.1 General introduction

Over the course of the past decades, the world has seen the rapid increase of its population and the explosion of the energy demand and consumption.

The increasing public awareness about the environmental problems linked to the anthropogenic activities is moving governments to issue more restrictive and binding laws in terms of emissions of pollutants and about environmental and human safety in general.

In this way, the research of both chemical industries and academia plays a key role in the development of new cleaner technologies, planning and designing chemical products and processes able to reduce or eliminate the use and generation of hazardous substances; all this without forgetting economics.

This concept, expressed in the term "Green Chemistry", was initially developed as a response to the Pollution Prevention Act in 1990 which declared that U.S. National policy should eliminate pollution by improved design, including cost-effective changes in processes, products, use of raw materials, and recycling; instead of treatment and disposal of harmful wastes.

During the latest years, green chemistry has demonstrated how essential scientific methodologies can be in the aim of protecting both human health and environment in an economically beneficial manner.

Noteworthy, improvements are being made in several key research areas, for instance the development of new and more efficient catalysts, the progressive abandonment of the more toxic and harmful reagents by replacing them with safer chemicals or the use of environmentally benign solvents. This trend also corresponds to an exponential increase of the studies on new platform molecules, no longer derived from fossil fuels but based on renewable feedstocks (biomass).

In this way, current and future chemists are striving to work at molecular level to achieve the sustainability of the future processes and products, with an increased awareness for problems related to environmental impact.[1]

It is therefore evident that the chemical industry has a key role in creating a sustainable and resource-efficient economy and society.[2]

The guiding framework of Green Chemistry is summarized in the Twelve Principles, which were introduced for the first time in 1998 by Paul Anastas and John Warner.

They can be applied to all the aspects of chemical processes; moreover, the complete life-cycle of every product should be taken into account, from the raw materials used and their transformation efficiency until the toxicity and biodegradability of products and reagents used.

The twelve principles of Green Chemistry are reported below (from the American Chemical Society website).

1) Waste Prevention: it is better to prevent waste than to treat or clean up waste after it has been created.

2) Atom Economy: synthetic methods should be designed to maximize the incorporation of all materials used in the process into the final product.

3) Less Hazardous Chemical Syntheses: wherever practicable, synthetic methods should be designed to use and generate substances that possess little or no toxicity to human health and the environment.

4) Designing Safer Chemicals: chemical products should be designed to affect their desired function while minimizing their toxicity.

5) Safer Solvents and Auxiliaries: the use of auxiliary substances (e.g., solvents, separation agents, etc.) should be made unnecessary wherever possible and innocuous when used.

6) Design for Energy Efficiency: energy requirements of chemical processes should be recognized for their environmental and economic impacts and should be minimized. If possible, synthetic methods should be conducted at ambient temperature and pressure.

7) Use of Renewable Feedstocks: a raw material or feedstock should be renewable rather than depleting whenever technically and economically practicable.

8) Reduce Derivatives: unnecessary derivatization (use of blocking groups, protection/ deprotection, temporary modification of physical/chemical processes) should be minimized or avoided if possible, because such steps require additional reagents and can generate waste.

9) Catalysts (vs Stoichiometric): catalytic reagents (as selective as possible) are superior to stoichiometric reagents.

10) Design for Degradation: chemical products should be designed so that at the end of their function they break down into innocuous degradation products and do not persist in the environment.

11) Real-time analysis for Pollution Prevention: analytical methodologies need to be further developed to allow for real-time, in-process monitoring and control prior to the formation of hazardous substances.

12) Inherently Safer Chemistry for Accident Prevention: substances and the form of a substance used in a chemical process should be chosen to minimize the potential for chemical accidents, including releases, explosions, and fires.[3]

After the publication of these cornerstones, there was a general international awareness that resulted in the creation of hundreds of programs and governmental

initiatives on Green Chemistry around the world, with leading programs located in the U.S., United Kingdom, and also in Italy.[4]

1.2 Carbon dioxide (CO₂)

1.2.1 Historical background and physicochemical properties

Carbon dioxide (CO_2, CAS number 124-38-9, molecular weight 44.010 g/mol) is a colorless, odorless, nonflammable gas.

Detailed information about the physical, thermodynamic and physicochemical properties of carbon dioxide are available;[5,6,7] some of them are summarized in the following table for convenience (Table 1.1); the pressure-temperature phase diagram of pure CO_2 is also reported (Fig. 1.1).

Gas density (0°C, 0,1 MPa)	1,977 kg/m³	Critical data: T (°C)	31,04
Molar heat Cp at 25°C	37,13 J/mol*K	Critical data: P (MPa)	7,383
Entropy (S₀)	213 J/mol*K	Critical data: density (kg/m³)	468
Heat of formation (ΔH)	-393,51 kJ/mol	Triple point: T (°C)	-56,57
Free energy of formation (ΔG₀)	-394,2 kJ/mol	Triple point: P (kPa)	518
Heat of vaporisation	347,86 J/g	Sublimation point: T (°C)	-78,92
Heat of fusion	195,82 J/g	Sublimation point: P (kPa)	98,07
Heat of sublimation	573,02 J/g	Dielectric constant ε (liquid 0°C)	1,58

Table 1.1 Physicochemical properties of carbon dioxide.
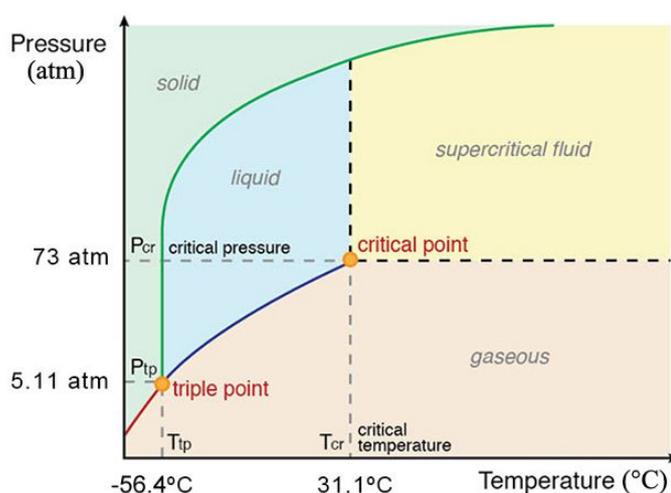
Fig. 1.1 The pressure-temperature phase diagram for carbon dioxide. The filled circles represent the triple point and critical point respectively. The solid lines illustrate an equilibrium between two phases.

The carbon dioxide existence has been known since primitive times; however, it was first recognized as a distinct gas by Van Helmont (1577–1644).[8]

About a century later, the French chemist Antoine-Laurent de Lavoisier was the first to study and prove that the combustion is a process that involves the combination of a substance and oxygen. In particular, heating carbon in oxygen results in a gas, which he named "carbonic acid", that was found to contain 23.5–28.9 parts by mass of carbon and 71.1–76.5 parts by mass of oxygen.[9]

In 1804 Nicolas-Théodore de Saussure was the first to hypothesize that CO_2 is essential for the plant growth.[10]

In the same period Joseph Priestly recognized that green plants are able to remove CO_2 from the air, producing oxygen and increasing in weight.[11]

Nowadays this process has been deeply studied and investigated and is known as photosynthesis (Scheme 1.1).

$$6 \; CO_2 \; + \; 6 \; H_2O \; \xrightarrow{\text{Light}} \; C_6H_{12}O_6 \; + \; 6 \; O_2$$
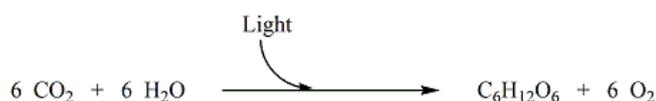
Scheme 1.1 Photosynthesis, general formula.

Later in the 19th century, Michael Faraday firstly succeeded in liquefying carbon dioxide in a bent glass tube in 1823 and finally, in 1845, he made larger quantities of liquid and solid carbon dioxide using a hydraulic pump. [12,13]

Afterward, J. Natterer invented a mechanical compressor (a prototype of the modern multistage type), which was used to make liquid carbon dioxide.[14]

This new liquid became important for its uses in refrigeration and ice-making and as fire extinguisher.

For these reasons, the industrial production of liquid CO_2 started in Germany in 1884, but the development of the industry continued as more uses of this compound were discovered.[15]

But it was in the beginning of the twentieth century that many uses for carbon dioxide were identified, and several other methods of manufacture assumed commercial relevance; some of these will be discussed in detail in the following chapters.

1.2.2 *CO_2 in the atmosphere: the greenhouse effect*

CO_2 is a linear molecule and represents the most oxidized form of carbon (+4).

It is the natural product of the complete combustion of any carbon-based fuel in the presence of enough oxygen.

After the industrial revolution, the increase of the world population and the corresponding explosion in the energy demand led to the significant increase of the fossil fuels (coal, oil, natural gas) consumption; so, it is not surprising that the atmospheric concentration of carbon dioxide has risen from a preindustrial level of 278 ppm to 397 ppm in 2013 and nowadays (November 2015) it stand at 400 ppm with a steadily increase of 1,9 ppm/year.[16]

In 2008 fossil fuels provided over 85% of our energy supply and emitted over 30 Gt of carbon dioxide (CO_2) into the atmosphere.

Moreover, CO_2 is known to be transparent to the sun's high-energy UV-visible radiation, but it's an IR active molecule able to absorb the longwave radiation emanating from the earth's surface and emits it again in all the possible directions.

This mechanism is the basis of the "greenhouse effect" that is raising the planet temperature.

The first scientists who hypothesized and understood these mechanisms were Arrhenius, Fourier and Tyndall in the 19th century, on the basis of simple calculations.

In particular, Tyndall in 1859 identified the molecules able to create the heat-trapping effect (such as carbon dioxide and water vapour)[17,18] and Arrhenius made a step further showing that doubling the concentration of CO_2 in the atmosphere would lead to significant changes in the surface temperatures.[19]

A lot of molecules in the atmosphere are able to absorb the infrared radiation from the surface but, among these greenhouse gases, CO_2 contributes to 60% of global warming effects, although methane and chlorofluorocarbons have much higher green-house effect as per mass of gases.[20]

However, stabilizing greenhouse gas concentrations in the atmosphere is critical to avoid dangerous interference with the climate system and it will require to reduce the overall emissions by an estimated 50–80% by 2050.[21]

There are four main ways to fight the increase of this greenhouse gases concentration in the atmosphere, in order to mitigate the effect of the global warming:

> To reduce energy intensity promoting an efficient use of energy;
>
> To reduce the carbon intensity, avoiding the utilization of fossil fuels and shifting toward renewable and environmental friendly energy sources (e.g. hydrogen and renewable electricity);
>
> To enhance the sequestration of CO_2 by the carbon capture and storage systems;
>
> To improve the CO_2 recyclability and valorization by its chemical transformation to other high value products or the reduction of CO_2 to fuels.

In particular, the last two points of this index and the main industrial processes that lead to the formation of a huge amount of CO_2 will be discussed in the following chapters.

1.2.3 *Industrial production of CO$_2$*

The IPCC of 2005 underlined that the energy and industry sectors dominate current global CO$_2$ emissions, accounting for about 60% of the total.[30]
Alongside the power plants in which fossil fuels are used to produce steam in order to generate electricity, the most of the carbon dioxide generated by industrial processes is a by-product of the ammonia (NH$_3$) and H$_2$ productions. Other important processes that lead to the formation of CO$_2$ are:

➢ the utilisation of fuels as feedstocks in petrochemical processes;
➢ the use of carbon as reducing agent in the metal manufactures from ores;
➢ the calcinations of limestone (CaCO$_3$) and dolomite (CaMg(CO$_3$)$_2$) in cement and lime productions;
➢ the fermentation of biomass, from sugars to alcohols.

In the following table, the profile of some of the worldwide larger CO$_2$ stationary sources are summarized (Table 1.2).[22]

Process	CO$_2$ conc. in the gas stream % by vol.	Number of sources	Emissions (MtCO3)	% of total CO$_2$ emissions
Coal power plant	12 to 15	2025	7984	59,7
Natural gas power plant	7 to 10	743	752	5,7
Fuel oil power plant	8	515	654	4,9
Cement production	20	1175	932	7,0
Ethylene process	12	240	258	1,9
Ethylene oxide process	100	17	3	0,020
Ammonia process	100	194	113	0,84
Fermentation processes	100	90	17,6	/

Table 1.2 Main industrial processes that lead to large carbon dioxide emissions.

1.2.4 Carbon Capture and Storage (CCS)

In a global context, almost all the industries use fossil-fuels to power their production, but, among them, the fossil-fueled power plants represent the more concentrated and localized sources of CO_2. Indeed, these plants (the coal-fired plant in particular) are responsible for roughly 40% of the total emissions.[23,24]

It is on these sites that the CO_2 capture and storage technology could be useful and make the difference, enhancing the direct artificial CO_2 sequestration, for example pumping and injecting the carbon dioxide into geological formations and oceans.

The principal benefit of this strategy, namely the Carbon dioxide Capture and Storage (CCS), is that it provides a mid-term solution to mitigate environmental impacts of climate changes, slowing the growth of the emissions and prolonging the possibility to use fossil fuels until the energy revolution to renewable technologies will be developed and mature enough to be scaled-up and meet current and growing energy demands.[25]

Moreover, over the longer term, CCS could be used to reduce emissions from sources that are difficult to eliminate in other ways, for example energy intensive industrial processes, natural gas cleanup, hydrogen production, fossil fuel refining, petrochemical industries, and steel and cement manufacturing.

Furthermore, CCS becomes more and more important for heavily coal-dependent and coal-rich counties such as Australia, Canada, China, India, the United States, and Russia, since it will be difficult to provide adequate energy supplies and simultaneously reduce emissions if CCS is not widely applied. In fact, a large new coal plant is able to emit over 100 $MtCO_2$ over its lifetime (30-40 years).

Finally, considering the full life-cycle emissions, this technology could reduce up to 65‑85% of CO_2 emissions from fossil fuel combustion in stationary sources.[26]

CCS involves the integration of the following four elements:

 ➢ CO_2 separation and purification (if necessary);
 ➢ CO_2 compression from gas to liquid or a denser gas;
 ➢ Transportation of this pressurized product to the storage location;
 ➢ Isolation from the atmosphere by pumping and storage in deep underground rock formation.

Unfortunately, with today's capture technology, CCS remains a relatively expensive mitigation option, so it can be considered as an insurance policy on the health of the planet.[27]

In particular, from 10 to 30% of the output of the power plant would be consumed by the CO_2 capture unit, depending on the capture technology, the type of power plant and the degree of systems integration.[26]

Advances not only in capture technology, but also ongoing improvements in the efficiency of power generation will be needed. An enormous effort is now devoted to advancing this technology and offset the energy penalty for the CO_2 capture with hundreds of active or planned projects.[28]

In particular, the first and most energy intensive step of CCS is the CO_2 separation and capture step. It contributes to roughly 75% of the overall CCS cost and, if applied to the fossil-fueled power plant, CCS should increase the electricity production cost by roughly the 50%.[29]

Cutting this capture cost is the most important issue to make CCS acceptable to the energy industries, so current researches are focused on improving the technologies or developing new approaches for the CO_2 separation and capture.

Moreover, to study the effects of the impurities in the CO_2 stream (e.g water) in the subsequent steps of pressurizing and transport is also important.

In particular, CCS can be divided into several scenarios, depending on the technology used:

> ➢ pre-combustion processes for gasification or reforming;
> ➢ post-combustion processes (e.g. for a traditional coal-fired plant);
> ➢ oxy-combustion (pure oxygen is sent to the combustion chamber and the flue gas is recycled several times in order to increase the CO_2 concentration up to 90% by volume on a dry basis);[29]
> ➢ chemical-looping combustion (CLC), a particular integrated process that will be discussed in detail in the following chapters.

In 2005, the IPCC SRCCS classified a wide range of emerging CO_2 capture technologies and recognized the large potential for developing and scaling up this procedure up to industrial scale.[30]

The main promising technologies for the CO_2 capture and purification are described below.

1.2.4.1 Chemical absorption (gas–liquid)

Especially for the post-combustion CCS processes, the CO_2 capture can be performed via chemical absorption, for example using monoethanolamine (MEA) to form the corresponding carbamate.

The MEA carbamate-rich solution is then sent to a stripper and heated again to release CO_2, after that the MEA solution is recycled back to the absorber.[24]

The advantages of this technique are related to the high purity of the final CO_2 (after desorption) and to the knowledge gained with these kind of processes (widely used in the natural gas industries for over 60 years).

On the other hand, the utilization of toxic and corrosive reagents, the low carbon dioxide loading capability and the fast degradation of the amine (with consequent high absorbent make-up rate), the size and cost of the equipment and the energy consumption (the absorber will consume around 25-30% of the total steam), contribute to both the poor economics of the process and the increase of the footprint of the host plant by the 60%.[31,32]

Many papers report about the possibility to use other liquid absorbents, especially aqueous ammonia.[33,34]

The main products are ammonium carbonate and bicarbonate, that have to be thermally decomposed to regenerate the absorbent and release CO_2. However, this process will save up to 60% of the energy if compared to the monoethanolamine process.

1.2.4.2 Solid sorbents (low temperature, gas–solid)

Solid sorbents can be easily recovered and managed in order to promote a versatile and cost-effective technology for a variety of carbon sequestration processes.[24]

In particular, well-designed molecular sieves are able to effectively separate molecules within certain size or weight.

In order to improve the CO_2 adsorption, the chemical treatment of the surface of high-surface-area inorganic supports and molecular sieves was investigated.

In this manner, the incorporation of basic organic groups (usually amines) over a porous support is able to enhance the performance in CO_2 sequestration.

In this category of materials, functionalized mesoporous nanosilicas (SBA-1, SBA-15, MCM-41 and MCM-48 to name a few), are of particular interest because they are characterized by the presence of pores large enough to be functionalized by molecules containing the amino groups. Both the porosity and the basic groups density on the surface are critical for the effectiveness in CO_2 sequestration.[35,36,37,38,39]

The interaction between CO_2 and the amino groups on the surface depend on the presence of water.

As a matter of fact, the presence of water leads to the formation of ammonium bicarbonate and carbonate species (1.0 mol CO_2/mol surface-bound amine of adsorption capacity), which halves in anhydrous conditions with the formation of ammonium carbonate (Scheme 1.2).[40]
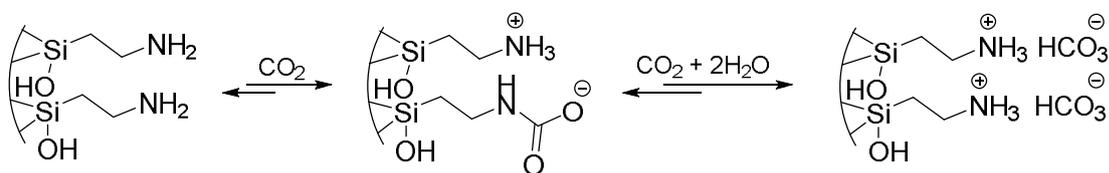
Scheme 1.2 Surface reaction of CO_2 with the amino groups.

Similar systems obtained by the impregnation of MCM-41 with polyethylenimine (PEI), described by Xu et al in 2002 and named as "molecular baskets", have proven to be effective and selective for CO_2 separation from a simulated power-plant flue gas.[37,41]

Finally, also adsorbent systems based on activated carbon (e.g., steam-activated anthracite) were found to be active for CO_2 sequestration.[42]

Noteworthy, also metal-organic frameworks (MOFs) have been studied for their CO_2 adsorption capacity and their tunable characteristics.

Indeed, MOFs are characterized by a three-dimensional, microporous crystalline structure, where the central metallic cations are joined through multiple metal-ligand bonds, by organic linkers.[43,44]

Unfortunately these materials are quite expensive, but their properties (such as surface area and pore size) can be tuned by a carefully design of the organic linker or the metal clusters.[45]

Moreover some MOFs have flexible structures enabling pressure-dependent structural changes that make this systems particularly useful for pre-combustion capture or CO_2 storage under pressure.

However, for post-combustion scenarios, the flue gas has to be dried, cooled at room temperature and made free from impurities that can compete with CO_2 for the adsorption sites in order to achieve good CO_2 adsorption capacity.

Conversely, amine-functionalized MOFs to enhance chemisorption or zeolite-like MOFs have been studied to mitigate these shortcomings.[45]

1.2.4.3 Membranes

A membrane is a thin layer that allows the selective passage of certain molecules and blocks the others. Their use and applications have been extensively studied since the early 80's. There are divided into two main categories: polymeric (the most used in industry) and inorganic.

A gas stream is divided by a membrane in a permeate (the part of the stream able to diffuse through the membrane), and a retentate (the gas unable to diffuse through the membrane).

Membranes are able to separate different kind of molecules depending on the diffusional characteristics of a particular gas through the given membrane. This is related to the membrane physical and chemical properties, and to the nature of the permeant species that lead to a particular interaction with the membrane and allow a specific sorptivity or solubility of the gas in the membrane itself.[46]

Additionally, the creation of a pressure difference across the membrane is necessary to enhance the separation, but requires a significant amount of power.

The advantages of using membranes are several:[47],[48]

- ➢ relatively small footprint;
- ➢ no phase change and steady-state operating conditions;
- ➢ simple mechanical system;
- ➢ easy scale-up and great flexibility.

Moreover, the CCS processes using inorganic or polymeric membranes are expected to be more convenient that conventional CO_2 separation processes when high purity is not a vital requisite.[49]

However, there are a number of issues associated to the capture of CO_2 which limit the use of membranes. Firstly, the flue gas is composed of a majority of nitrogen and oxygen, while the concentration of carbon dioxide is generally low, which means that huge quantities of gases will have to be processed.

Moreover, the membranes need to be chemically resistant to the harsh chemicals contained within flue gases or these chemicals need to be removed prior the CO_2 capture apparatus. Furthermore, the flue gas needs to be cooled down until below 100°C in order to prevent membrane decomposition (if polymeric).[50]

The performances of some polymeric membranes for CO_2 capture from a CO_2/N_2 mixture, summarized by Powell and Qiao in 2006, are reported in the following table (Table 1.3).

Material	Permeance (m³/m²*Pa*s)	Selectivity CO₂/N₂
Polyimide	735	43
Polydimethylphenylene oxide	2750	19
Polysulfone	450	31
Polyethersulfone	665	24.7
Polyacrylonitrile with PEG	91	27.9
Poly(amide-6-b-ethylene oxide)	608	61

Table 1.3 Polymeric membranes performance in the CO_2 capture from a mixture with nitrogen

The other main type of membranes is based on inorganic materials. These membranes can be classified into two categories depending on their structure: dense and porous. The dense membranes consist of a thin layer of metal (Pd or its alloys) or solid electrolytes (e.g zirconia).

However, these membranes are highly selective for hydrogen and oxygen separation but not useful for CO_2 sequestration.

Porous membranes are characterized by the presence of a thin selective porous layer, casted on a porous metal or ceramic support, able to provide mechanical strength with the minimum mass-transfer resistance.

The main porous inorganic membranes are based on the following materials:

- alumina;
- carbon;
- silica;
- titania;
- zirconia;
- zeolites;
- mixed matrix and hybrid membranes.

Many reviews make a complete analysis of these membranes.[50,51]

However, although they are characterized by better thermal stability with operating temperatures up to 1000°C that allow to combine reaction and separation in the same device, they suffer from almost the same drawbacks as polymeric membranes.

There are four main transport mechanisms describing the gas separation process using porous inorganic membranes namely:

Knudsen diffusion, surface diffusion, capillary condensation, and molecular sieving.[52]

Please refer to the references for a detailed explanation.

1.2.4.4 Chemical-looping combustion (CLC) and high temperatures solid looping systems

Chemical-looping combustion (CLC) is a newly emerged technology able to significantly reduce the complexity of CO_2 separation from the exhaust gas stream.

It's a two-step combustion process in which the direct contact between the fuel and air is avoided.

This "unmixed" combustion is performed using two different reactors:

the combustion reaction in which the oxidation of the fuel is carried out on small particles of a suitable inorganic oxygen carrier (especially metal oxides) and the regeneration reactor in which air is flown in order to oxidize again the inorganic carrier (Scheme 1.3)[53]

Small particles of Fe_2O_3, NiO, CuO or Mn_2O_3 are good candidates as suitable oxygen carriers. However, in 2011 Lyngfelt et al. reviewed more than 900 oxygen-carrier materials.[54]

This system allows to obtain highly concentrated CO_2 in the output stream.
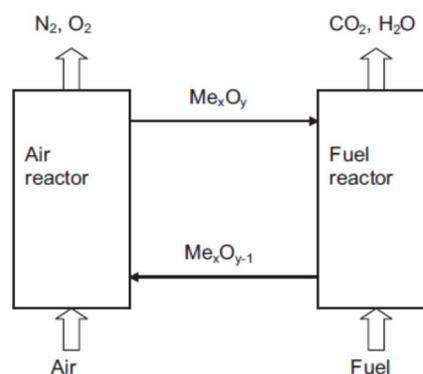
Scheme 1.3 Scheme of a chemical-looping combustion system with recirculating oxygen carriers.

An in-situ CO_2 capture at high temperature with different solid adsorbent is possible.

For example, many papers report the possibility to achieve an in-situ capture of CO_2 using a high temperature (ca. 700°C) carbonation reaction of CaO to produce $CaCO_3$.

This process, namely calcium-looping system, is similar to CLC, again consists of two reactors: a primary fuel reactor in which both the combustion and the carbonation reactions take place and a calciner in which calcium carbonate is decomposed to obtain again calcium oxide and CO_2.

It's clear that the second step requires a lot of energy; however, the overall thermal efficiency has been shown to be comparable to that of a current combustion system without any CO_2 capture apparatus.[55,56,57]
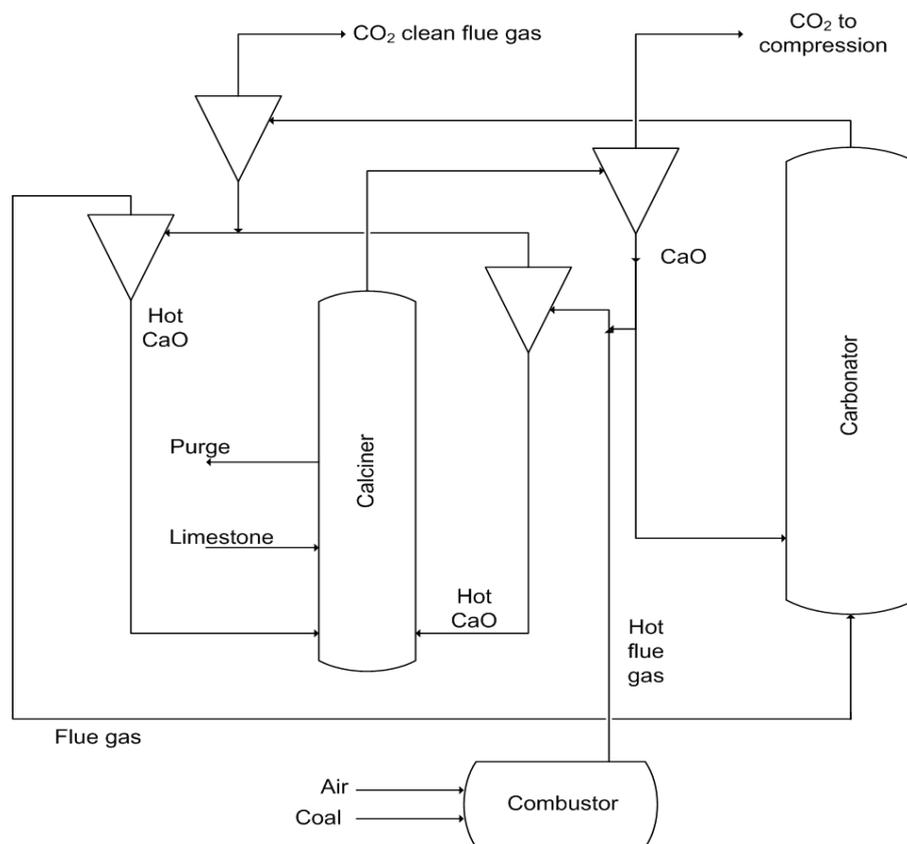
Scheme 1.4 Schemes of different calcium looping processes.
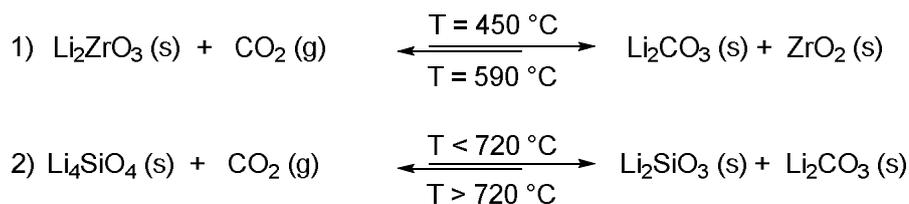Post-combustion CO_2 capture (left side); Integrated process that avoids the need for an air separation unit by supplying heat for calcination from the combustion chamber (middle); direct heat transfer using suspension preheaters (right side).[51]

Other high-temperature solid absorbents with favorable CO_2 sorption characteristics such as hydrotalcites[58], lithium zirconate (Li_2ZrO_3)[59] and lithium silicate (Li_4SiO_4), have been investigated.

In particular, Nakagawa et al. found that the capacity of lithium silicate is much larger compared to lithium zirconate; moreover, the rapid absorption of CO_2 in a wide range of temperature and concentrations and a good stability make this compound a good candidate for developing commercially competitive CO_2 adsorbents.[60,61]

The reaction mechanism of both compounds and the corresponding reaction temperature range are reported in the following scheme (Scheme 1.5).

$$1)\ Li_2ZrO_3\ (s)\ +\ CO_2\ (g) \quad \underset{T = 590\ °C}{\overset{T = 450\ °C}{\rightleftarrows}} \quad Li_2CO_3\ (s)\ +\ ZrO_2\ (s)$$

$$2)\ Li_4SiO_4\ (s)\ +\ CO_2\ (g) \quad \underset{T > 720\ °C}{\overset{T < 720\ °C}{\rightleftarrows}} \quad Li_2SiO_3\ (s)\ +\ Li_2CO_3\ (s)$$

Scheme 1.5 High-temperature reactions of lithium zirconate and lithium silicate with carbon dioxide.

1.2.5 CO$_2$ applications and valorisation as "carbon pool"

Carbon dioxide (CO$_2$) has been considered for long time by industries as a waste and, in recent years, due to the new carbon taxes applied by many countries, also as a cost.

However, in the last decades the interest toward the chemical utilisation of this abundant, non-toxic, economical and renewable carbon (C1) feedstock is rising.[62,63,64,65,66]

Hence, any efficient reaction leading to valuable products that uses CO$_2$ as the reagent may potentially have positive effects on the global effort toward the promotion of a "carbon circular economy" which is essential for the low-carbon chemical and energy industry of the future.

Noteworthy, the application of CO$_2$ as reagent and building block for the chemical industry is not enough by itself to solve the problems associated to the emission of this greenhouse gas in the atmosphere.

To put it in a perspective, the 2005 Intergovernmental Panel on Climate Change (IPCC) reported that the total industrial use of CO$_2$ is approximately 115 MtCO$_2$/yr. However, although this value is constantly increasing, it corresponds to only 0.5% of total anthropogenic CO$_2$ emissions: about 24 Gt CO$_2$/yr.[67]

The main drawback and obstacle in the aim of developing industrial processes based on CO$_2$ as a raw material is its low energy value. Indeed, CO$_2$ is the most oxidized state of carbon and is the end product of chemical and energy manufacture.

In other words, a large energy input and the development of efficient catalytic systems are usually required to transform carbon dioxide into useful chemicals. This is the main reason why currently the toxic carbon monoxide (CO), is preferred as a C1 building unit for many industrial processes.

Although CO$_2$ is a thermodynamically and kinetically stable compound, it is also characterized by an electron deficiency on the carbon atom.

This property gives CO$_2$ a good affinity toward electron-donating reagents or nucleophiles in general.

Moreover, due to its acidity (CO$_2$ can be considered also as an "anhydrous carbonic acid") can readily react with basic compounds.

Four main strategies have been developed in order to overcome the problem associated to its thermodynamic stability and which may lead to a negative Gibbs energy for a particular reaction with CO$_2$:

> ➤ React CO_2 with high-energy starting materials such as hydrogen, epoxides or other small-membered ring compounds, unsaturated molecules and organometallic compounds (e.g, Grignard's reagents);
> ➤ Choose highly oxidized low-energy molecules as synthetic target, for example organic carbonates or carbamates;
> ➤ Use the Le Châtelier equilibrium principle,[68] removing a particular compound in order to shift the equilibrium toward the products side;
> ➤ Perform CO_2 reduction under photoirradiation (UV light) or under electrolytic conditions.

Hereafter, an overview on the organic synthesis starting from CO_2 is schematically reported (Scheme 1.6). Many of them are discussed in detail in the following chapters.
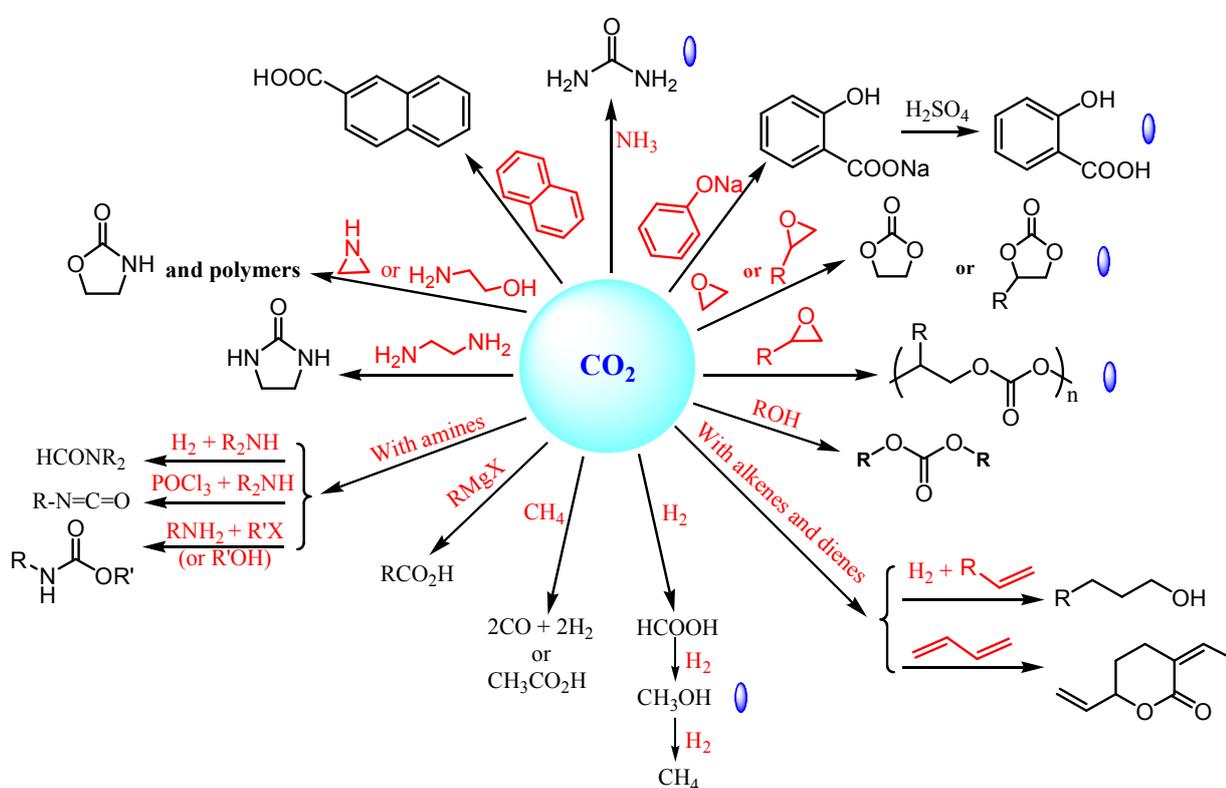
Scheme 1.6 Schematically overview on the organic synthesis with carbon dioxide. ⬭ represent the industrialized processes.

Noteworthy, we can consider these products as a temporary form of stored carbon with a certain lifetime before they will degraded again to CO_2 which will be finally emitted in the atmosphere.

Finally CO_2, apart from the possible uses to produce chemicals, is a valuable gas with a large number of applications: as an inert agent for food packaging, refrigeration systems, beverages, fire extinguishers, welding systems, water treatment processes

and as precipitating agent to yield calcium carbonate for the paper industry, to name a few.

1.2.5.1 *Urea (CO(NH₂)₂) production*

In 2011 the urea production, with a roughly yearly market of 154 Mt/yr was (and still it is) the largest consumer of CO_2, with around 113 Mt/yr, equivalent to over 60% of the total CO_2 used for chemicals productions.[69]
The two step synthesis is known as the Bosch-Meiser process and is shown in the following reaction scheme (Scheme 1.7).

$$2\,NH_3 + CO_2 \rightleftharpoons H_2NCOO^{\ominus}\,{}^{\oplus}NH_4 \rightleftharpoons H_2N-\overset{\overset{\displaystyle O}{\|}}{C}-NH_2$$

Scheme 1.7 Two-step synthesis of urea from carbon dioxide and ammonia.

This process requires high temperatures (T from 150 to 200 °C) and pressures (P from 150 to 250 bar).
Usually the urea manufacturing is integrated and coupled with the ammonia synthesis plant and the CO_2 source is the stream reforming process to produce H_2 for NH_3 synthesis.
Urea is widely used as a fertilizer in agriculture, as an additive for animal feed and for the synthesis of resins.

1.2.5.2 *CO₂ hydrogenation: methanol and fuels productions*

Methanol is a large commodity compound with 58 Mt/yr of production.
However, it is usually produced by the reaction of syngas (CO and H_2), obtained via steam reforming of natural gas or partial oxidation of coal.
In this reaction, usually catalyzed by supported copper and zinc oxides, only a minor part of carbon dioxide is involved with an overall consumption around 2 or 3 Mt/yr (Scheme 1.8).[70]

$$3\,CO + 9\,H_2 + CO_2 \longrightarrow 4\,CH_3OH + H_2O$$

Scheme 1.8 Methanol synthesis from syngas containing CO_2 as additive.

Another possible way to use CO_2 is the methane dry reforming (MDR) process.
This pathway produces syngas by methane reforming replacing water (steam) with carbon dioxide as shown below (Scheme 1.9).

$$CH_4 + CO_2 \longrightarrow 2\,CO + 2\,H_2 \qquad \triangle H_{298K} = 247 \text{ kJ/mol}$$
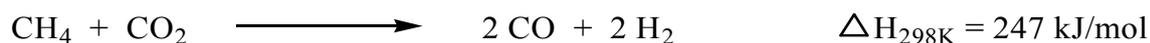
Scheme 1.9 Syngas synthesis from methane by means of dry reforming with CO_2.

This is a reaction of both scientific and industrial relevance; it was first studied in 1928 by Fischer and Tropsch (most known for the utilization of syngas to produce higher alkanes and oxygenates).[71]

Unfortunately, this reaction suffers from several drawbacks.

Firstly, MDR is a strongly endothermic reaction that requires operating temperatures of 800–1000 °C to obtain high equilibrium conversion of CH_4 and CO_2, and to minimize the thermodynamic driving force for carbon deposition. In particular, the carbon deposition over the catalyst surface is the main responsible of the severe deactivation problems met with catalysts.
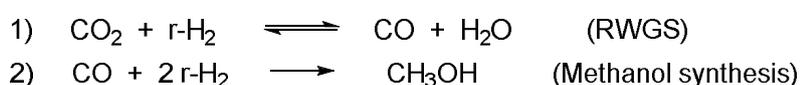
These are usually based on Nickel compounds, but noble metals (Pt, Rh and Ru) have also been studied and are typically found to be more resistant toward carbon deposition but more expensive.[72]

Hydrogen (r-H_2) production from electrolytic water cleavage using renewable energies (RE such as wind, photovoltaic etc.), opens up an important route to the conversion of CO_2 to higher energy density products.

One of the best ways to insert RE in the chemical production chain is the production of "renewable methanol" from CO_2 and r-H_2. This represents an interest future renewable transport fuel as established by the Renewable Energy Directives of the European Union.[73]

Moreover, the same catalyst used for methanol production from syngas may be applied for this new synthetic route.[74]

The general approach consists in a two-step synthesis in which a reverse water gas shift reaction (RWGS) first reduces CO_2 to CO followed by CO reduction to methanol (Scheme 1.10).

$$1) \quad CO_2 + \text{r-}H_2 \rightleftharpoons CO + H_2O \qquad (RWGS)$$
$$2) \quad CO + 2\,\text{r-}H_2 \longrightarrow CH_3OH \qquad (\text{Methanol synthesis})$$

Scheme 1.10 Synthesis of renewable methanol from CO_2 and r-H_2.

A typical catalytic system is based on copper supported over different metal oxides (Cu/ZnO/Al_2O_3 including ZrO_2, Ga_2O_3 and SiO_2 as additives) working at 250°C.[75]

However, the complex equilibria involving all the species that take part in the reactions make the performance critically dependent on feed composition.

Another problem regards water. Water is the co-product of the RWGS reaction and can act as an inhibitor (see also Scheme 1.8). A partial solution is continuous water

removal through condensation or membranes; in this way the two-step process, with intermediate water removal, allows a three times higher productivity in comparison with the single step process ("Camere" process, Fig. 1.2).[76]
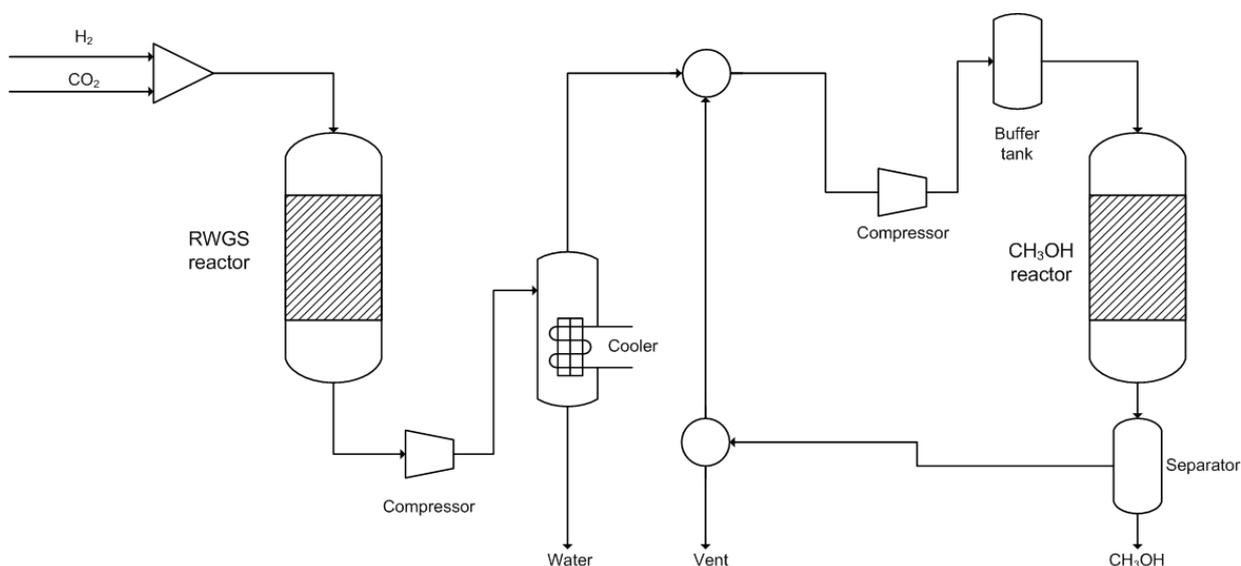

Fig. 1.2 The two-stage CAMERE process for the synthesis of methanol

This route is already applied for example in Iceland where in 2011 CRI opened a plant for the production of 5 Mton/yr of methanol from CO_2 using electrolytically produced H_2 from geothermal renewable energy sources.[77]

Other two possible strategies to insert r-H_2 in the chemical chain for CO_2 valorisation are formic acid production and methanation process.
The first one is mainly considered as a way to store and easily transport H_2 in liquid form.
The hydrogenation reaction (Scheme 1.11) is thermodynamically unfavored and requires the removal of the produced formic acid to enhance the conversion.

$$CO_2 \; + \; H_2 \; \rightleftharpoons \; HCOOH$$

Scheme 1.11 CO_2 hydrogenation to formic acid.

Nowadays the formic acid market is below 1 Mtons/yr.[78]
Recent developments in this reaction includes the utilization of new organo-Iridium complexes as efficient catalysts for the interconversion between hydrogen (and carbon dioxide) and formic acid at room temperature and ambient pressure.[79,80]
DVN GL has developed a pilot unit for the CO_2 electrochemical reduction to formate salts and formic acid.[81]

Finally, the CO_2 methanation reaction is known since 1913 when it was discovered by Paul Sabatier (Scheme 1.12).

$$CO_2 + 4H_2 \longrightarrow CH_4 + 2H_2O \qquad \triangle H = \text{-165.0 kJ/mol}$$
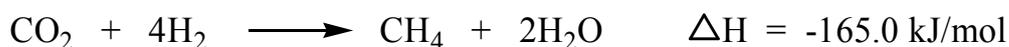
Scheme 1.12 Carbon dioxide methanation.

It is an exothermic reaction which involves eight electrons in order to reduce the fully oxidized carbon of CO_2 to CH_4 in the presence of an appropriate catalyst. In particular, Ni-based catalysts have been extensively investigated because of their low price and high activity using activated carbon or metal oxides (Al_2O_3, SiO_2, ZrO_2, $Ce_xZr_{1-x}O_2$, CeO_2) as support.[82]

Normally operating temperature are between 300 and 400°C.

In particular, a 10 wt% Ni/CeO_2 catalyst shows both high CO_2 conversion and CH_4 selectivity at lower temperatures.[83]

However, the Sabatier reaction requires high H_2/CO_2 ratio and a lot of energy input to start the reaction compared to the conversion of CO_2 to methanol, formic acid or other Fischer-Tropsch products.

Recently, a catalyst base on ruthenium nanoparticles (mean diameter 2,5 nm) supported on TiO_2 that allows to realize 100% CH_4 yield at very low temperature (ca. 160 °C), has been developed.[84]

Recently, in Norway, RCO2 AS has developed a pilot scale process in which CO_2 is recovered from flue stream gas and converted to CH_4 using the excess of electrical energy produced using renewable sources (power-to-gas approach).[85]

1.2.5.3 *Salicylic acid production: the Kolbe-Schmitt reaction*

Salicylic acid is an important intermediate in the synthesis of the acetylsalicylic acid (ASA or aspirin) a wide used drug for its antipyretic, anti-inflammatory, analgesic properties.

The synthesis of salicylic acid from sodium phenolate and carbon dioxide was firstly discovered in 1860 by Hermann Kolbe and then has been industrialized since 1890.[86,87]

This reaction, show in the following scheme (Scheme 1.13), is still used and the yield into the desired product has been improved from 50 to roughly 90% by using CO_2 at high pressure (>100 bar) and 125°C and currently consumes around 25 thousands tons per year of this molecule.[78]
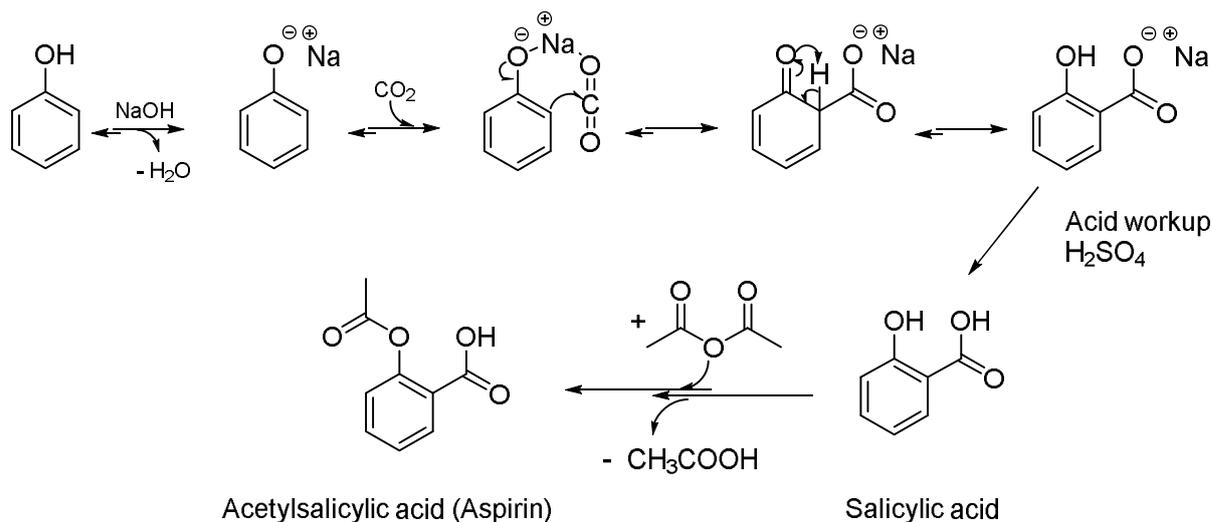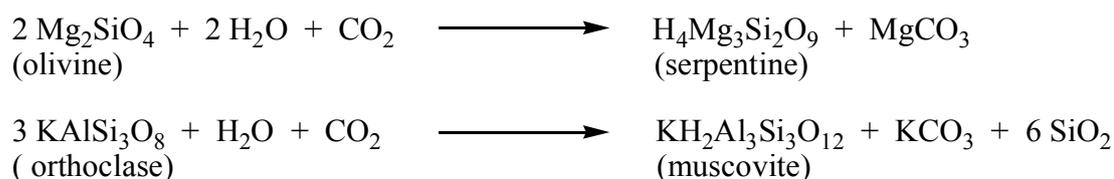
Scheme 1.13 Kolbe-Schmitt reaction for the synthesis of salicylic acid, an important intermediate for the production of acetylsalicylic acid (Aspirin).

1.2.5.4 *The mineral carbonation: inorganic carbonates synthesis*

Large quantities of CO_2 are fixed every day in the oceans by the reaction of $CaCO_3$, CO_2 and water to form $Ca(HCO_3)_2$, although it is kinetically slow.
The total CO_2 content in the seas and oceans is estimated around $1,4*10^{14}$ tons.[78]
However, the CO_2 reactions with suitable inorganic minerals such as silicates to form the corresponding carbonates are thermodynamically favored but kinetically limited (Scheme 1.14).[88]

$$2\,Mg_2SiO_4 + 2\,H_2O + CO_2 \longrightarrow H_4Mg_3Si_2O_9 + MgCO_3$$
(olivine) (serpentine)

$$3\,KAlSi_3O_8 + H_2O + CO_2 \longrightarrow KH_2Al_3Si_3O_{12} + KCO_3 + 6\,SiO_2$$
(orthoclase) (muscovite)

Scheme 1.14 Mineralization of CO_2 with olivine and orthoclase to yield the corresponding carbonates.

1.2.5.5 *Organic carbonates and carbamates synthesis*

Recently, new synthetic strategies to organic carbonates involving the direct CO_2 conversion in the so-called "carbonyl green route", avoiding the use of toxic phosgene, have been reported and they will be explained in details in Chapter 1.3.4.
Moreover, the synthesis of carbamates from amine and CO_2 in the presence of organic halides or alcohols is reported on lab scale with very good yields, in some case up to 90% depending on the specific starting material and synthetic route adopted.[89]

The general reaction of CO_2 and an amine in the presence of organic halides is reported for convenience (Scheme 1.15).

$$+ R'X$$

$$2\ RNH_2\ +\ CO_2\ \rightleftharpoons\ [RNHCOO]\ \text{-}\ [RNH_3]^+\ \longrightarrow\ RNHCOOR'\ +\ RNH_2\ +\ HX$$
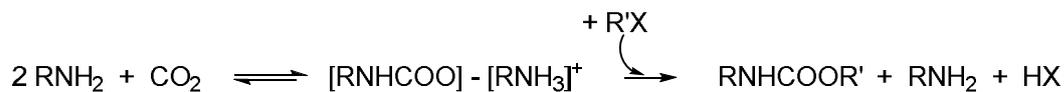
Scheme 1.15 Synthetic route to carbamates starting from CO_2 and amines.

1.2.5.6 *Aldehydes and alcohols synthesis*

Alkenes can be hydroformylated using high-pressure CO_2 and hydrogen to yield alcohols and aldehydes in the presence of ruthenium complexes.[90]
The reaction probably proceeds via CO formation with a reverse water gas shift reaction (RWGS) and then CO is the real reactant.
Similar reactivity is shown for methanol homologation with CO_2 to yield ethanol.[91,92]
Of particular interest is the synthesis of valeraldehyde from CO_2 and *n*-butane via alkane dehydrogenation to 1-butene, reported in a patent.[93]

1.2.5.7 *Electrochemical reduction routes*

CO_2 reduction at a number of metal electrodes has been investigated.[94,95]
The electrochemical reduction of CO_2 alone results in the non-selective formation of oxalic acid and its derivates (glycolic acid and glyoxylic acid).[96]
With similar electrochemical processes between CO_2 and alkenes, ketones or organic halides, carboxylic group can be introduced into organic moieties.[97]
Noteworthy, the electrochemical carboxylation with $scCO_2$ of a benzylic chloride was applied to Ibuprofen synthesis.[98]

1.3 Organic carbonates

1.3.1 General introduction

Organic carbonates represent an important class of molecules characterized by the functional group: R-O-C(O)O-R.

The industrial and scientific interest toward these molecules has increased exponentially in the last three decades because of their promising properties and because new synthesis starting from carbon dioxide have been discovered, which can replace the traditional phosgene route.

Organic carbonates are generally characterized by a very low toxicity, good biodegradability and because of their high boiling point, that lowers the emission of volatile organic compounds in the atmosphere (VOCs), and high solvency, they find wide utilisation as aprotic polar solvents for cellulose ethers and esters, polymers and in pharmaceutical and cosmetics preparations.[99,100,113]

Among these molecules, allyl and vinyl carbonates are reported to have outstanding properties for the preparation of optical plastics.[113]

Moreover, organic carbonates are very interesting chemical intermediates, with a versatile reactivity that strictly depends on the reaction conditions and catalytic system applied.

These peculiar properties make organic carbonates the best and safest candidates to replace other old and toxic reagents such as phosgene (for carbonylation reactions) and dimethyl sulphate or alkyl halides as alkylating agents[101], for the production of pharmaceuticals and fine chemicals.[102,103]

They find other applications in the bio-medical sector in the drug-delivery systems and as materials for prothesis;[104,105,106] in lubricants productions,[107,108] as fuels additives,[109] in the electronic industries for the production of capacitators and photoresistors,[110] and batteries (as electrolyte and solvents in lithium batteries).[111]

Moreover, they are useful monomers for the synthesis of high-performance polymers such as polycarbonates and polyurethanes.[112]

Organic carbonates can be divided into different categories: linear and cyclic; saturated and unsaturated; aliphatic and aromatic; symmetrical and unsymmetrical.

To clarify these categories a schematic classification of organic carbonates is reported in the following page (Fig 1.3).
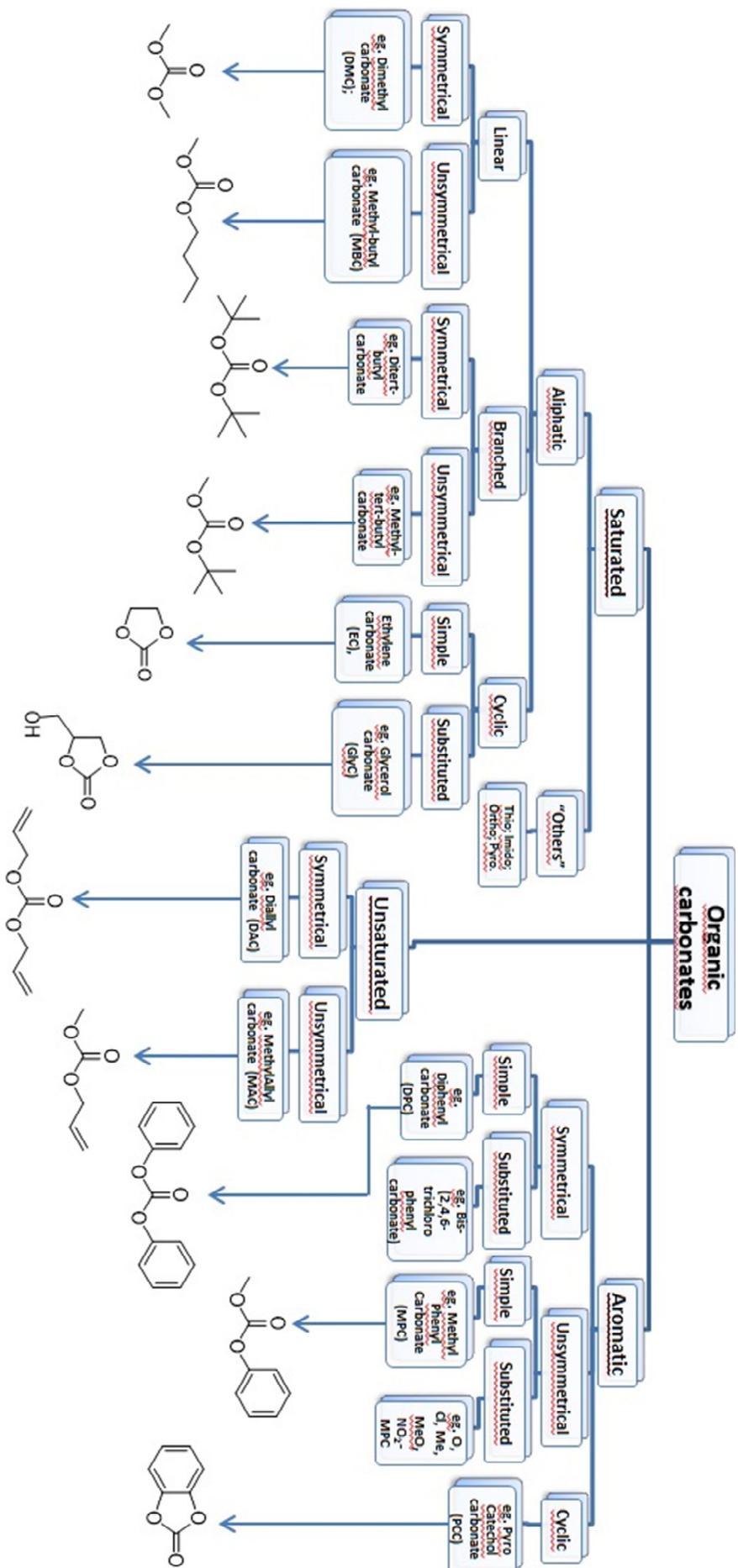
Fig. 1.3
Classification of organic carbonates.

Generally, all dialkyl carbonates are colourless liquids (some with pleasant odours), and diaryl or cyclic carbonates are crystalline compounds with relatively low melting point.

Moreover, most of these compounds are insoluble in water except for the simpler cyclic aliphatic carbonates (such as ethylene carbonate (EC) and propylene carbonate (PC)) and for the shorter-chain dialkyl carbonates (namely dimethyl carbonate (DMC) and diethyl carbonate (DEC)) that are only sparingly soluble in water. On the other hand, all the carbonates readily dissolve in polar organic solvents like alcohols, esters, ketones, ethers and some substituted aromatic hydrocarbons.[113]

Finally, it is known that the lower aliphatic carbonates form azeotropic mixtures with a number of organic solvents;[114] in particular DMC and EC form azeotropes with the alcohols from which they are derived, methanol and ethylene glycol respectively, as reported in the following table (Table 1.4).[115,116]

Component 1	*Component 2*	y^1_{az}	T_{az} *(K)*	P_{az} *(KPa)*
Methanol	DMC	0.85	337.25	102.52
Ethylene glycol	EC	0.19	361.25	1.33

Table 1.4 Azeotropic mixtures between carbonates and their alcohols

Moreover, some physical properties of the most common organic carbonates are presented in Table 1.5.

| Organic carbonate	mp (°C)	bp/P (°C/kPa)	d^{20}_4	n^{20}_D	Flash point (°C)
Dimethyl carbonate (DMC)	4	90.2/101.3	1.073	1.3687	14 (closed cup)
Diethyl carbonate (DEC)	-43	125.8/101.3	0.9764	1.3843	33 (closed cup)
Diallyl carbonate (DAC)	/	97/8.13	/	1.4280	59 (closed cup)
Diphenyl carbonate (DPC)	78.8	302/101.3	1.1215^{87}_4	/	168 (closed cup)
Ethylene carbonate (EC)	39	248/101.3	1.3218^{39}_4	1.4158^{50}	143 (closed cup)
Propylene carbonate (PC)	-48.8	242/101.3	1.2069^{20}_{20}	1.4189	/

Table 1.5 Physical properties of industrially important organic carbonates.

1.3.2 *Organic carbonates: general reactivity behaviours*

Organic carbonates exhibit a versatile and tuneable chemical reactivity that depends on the reaction conditions and the characteristic of the other reagents.

In particular, they can readily react with a wide series of nucleophiles (Nu⁻) in the presence of a catalytic amount of base.

The next considerations mainly regard dimethyl carbonate (DMC), but can be extended to the whole category of organic carbonates.

Indeed, carbonates are characterized by the presence of two different electrophilic sites (Scheme 1.16).
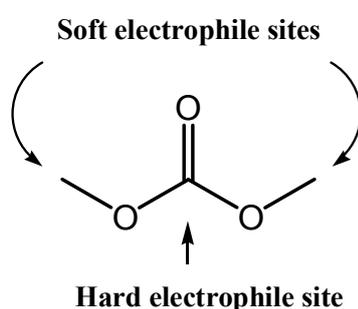
Scheme 1.16 Different electrophile sites on the DMC molecule.

For example, in the DMC moiety, two different active centers are present: a sp^2-hybridized carbonyl carbon (C=O) and sp^3-hybridized methyl carbons (-CH_3).

The former may be regarded as a hard electrophile site (or acid center) because of the partial positive charge due to the polarization of the C=O bond, correspondingly the latter are considered as soft electrophile sites.

The general rule is that hard nucleophiles prefer to react with hard electrophile and soft nucleophile with soft electrophile.

A broad classification of nucleophiles is reported in the table below (Table 1.6).[117]

Hard nucleophiles			Borderline			Soft nucleophiles		
F⁻; Cl⁻	OH⁻ ;H_2O	RO⁻ ;ROH	N^{3-}	CN⁻	Br⁻	I⁻	RSe⁻	S^{2-}
SO_4^{2-}	ROR	RCOR′		RNH_2		RS⁻	RSH	RSR′
NH_3	RMgBr	RLi		RR′NH		R_3P	alkenes	aromatics

Table 1.6 Classification of nucleophiles.

If we consider generic alcohols ROH they can act as nucleophile (in the presence of a catalyst) reacting with the organic carbonates.

Alcohols and alkoxides (in red in the table) are considered as hard nucleophiles because of the small, electronegative oxygen atom, promoting the reaction on the hard electrophile carbonyl site of the carbonate.

However, in the case of aromatic alcohols (phenols), the conjugation of lone-pair electrons in the oxygen atom with the benzene ring decreases the nucleophilic nature of phenol, making the phenolate a softer base (and nucleophile), thus facilitating the reaction on the methyl groups (softer electrophile).[118]

For these reasons, aliphatic and aromatic nucleophiles show different behavior in reaction with organic carbonates as it will be discussed in the following Chapters.

For the same reason, water (in blue in the table) could readily react on the carbonyl group of the carbonate moiety, destroying the molecule by hydrolysis, through the formation of an unstable monoester of the carbonic acid.

Another key parameter of the reactivity behavior of organic carbonates is the temperature.

Indeed, Tundo et al. in 2002 underlined that DMC can react either as a methoxycarbonylating agent (replacing phosgene) or as a methylating agent (replacing the poisonous and mutagenic methyl halides and dimethyl sulfate) depending on the experimental conditions.[65]

As a matter of fact, it is generally observed that at reflux temperature ($\approx$90°C or other relatively low temperatures) DMC acts primarily as a methoxycarbonylating agent by a (bimolecular, base-catalyzed, acyl cleavage, nucleophilic substitution) $B_{AC}2$ mechanism where the nucleophile attacks the carbonyl carbon of DMC, giving the transesterification product.

Interestingly, if the nucleophile is an alcohol or an alkoxide, this reaction is named carbonate interchange reaction (CIR) and lead to the formation of different organic carbonates (see Chapter 1.3.5).

On the other hand, at higher temperatures (usually T > 160 °C), DMC acts primarily as a methylating agent. A $B_{AL}2$ (bimolecular, base-catalyzed, alkyl cleavage, nucleophilic substitution) mechanism predominates and the nucleophile attacks the methyl group of DMC.

While the methoxycarbonylation is an equilibrium reaction, the methylation is irreversible, because the CH_3OCO_2H that is formed decomposes to methanol and CO_2. In principle, the methanol produced by these reactions can be recycled for the production of new DMC.[119]

On the contrary, methylation with methyl halides or DMS, and carbonylation with phosgene generate stoichiometric amounts of inorganic salts.

Finally, another possible pathway that lead to the formation of the alkylation products at high temperatures, is the reaction between hard nucleophiles on the carbonyl site of the carbonate, followed by the thermal decomposition through decarboxylation.

All these reaction pathways are reported in the following scheme (Scheme 1.17).
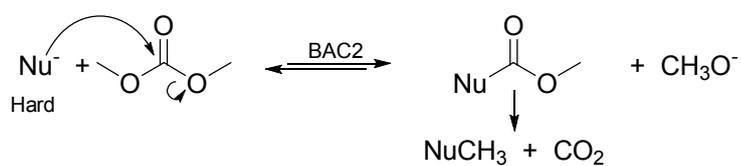
Methoxycarbonylation (low temperatures e.g. 90°C):
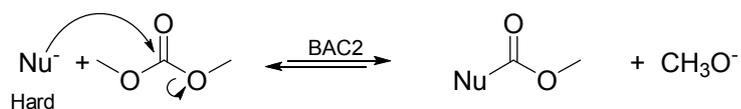
Methylation (higher temperatures T > 120°C):

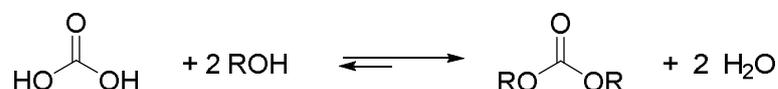Methylation: alternative mechanism (higher temperatures T > 120°C):

Scheme 1.17 Different nucleophilic substitution mechanisms on the DMC molecule.

1.3.3 Synthetic pathways toward organic carbonates

Formally, organic carbonates can be considered as the products of the esterification reactions of carbonic acid and alcohols (Scheme 1.18).

Scheme 1.18 Carbonic acid esterification with alcohols.

However, there are many ways to synthesize organic carbonates and they will be discussed in the following pages.

1.3.3.1 The Phosgenation method

With this method, alcohols and diols (aliphatic and aromatic) can be converted into the corresponding organic carbonates.
The hydroxyl compound is firstly dissolved in an anhydrous and inert solvent (benzene, toluene, dichloromethane or chloroform preferentially) or a mixture of them. Then it is phosgenated below room temperature.
An excess of pyridine is generally used in this reaction because it acts as acid acceptor, reacting with phosgene and forming an adduct more reactive than the corresponding chlorocarbonic acid esters (Scheme 1.19).[120]
This reaction can be carried out continuously and very good yield of the desired products are generally obtained.
However, this process involves the use of hazardous and toxic reagents like phosgene and pyridine. Moreover the reaction mixture has to be washed with dilute HCl to neutralize the excess pyridine and then with water to remove the salts formed with the consequent formation of a big amount of an aqueous effluent that has to be separated and disposed.
Nearly all the carbonates can be obtained by this method; however, aromatic hydroxyl compounds show slower reactivity compared to aliphatic alcohols.[121]
Nemirowsky was one of the first to use this technique, reacting phosgene and ethylene glycol to produce ethylene carbonate.[122]
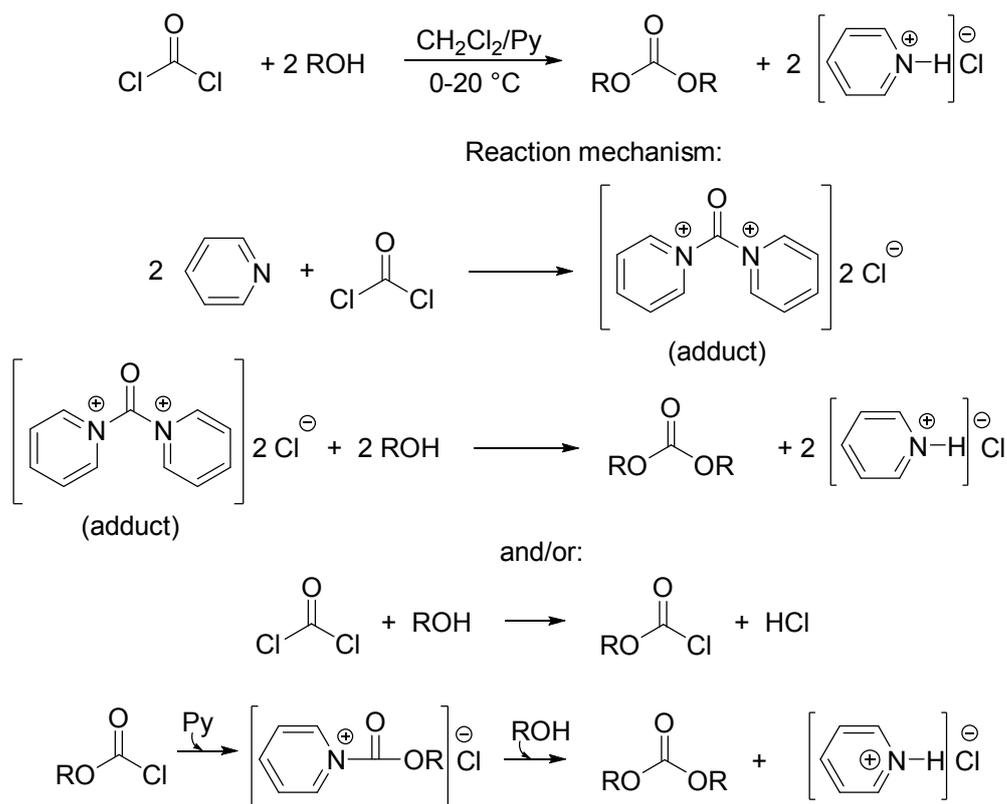
Scheme 1.19 Synthesis of organic carbonates: phosgenation of alcohols and diols.

1.3.3.2 The oxidative carbonylation of alcohols and phenols

The synthesis of dialkyl carbonates from alcohols and CO seems to be both economically and ecologically desirable.

This reaction was studied and patented since the 1960s using different CO-binding metal salts with an oxidative catalytic effect.[123]

Copper-based compounds seem to be the most effective catalysts for this reaction, while other systems based on N-bases, onium salts and complexing agents are claimed to accelerate the reaction but are unstable and generally difficult to separate from the reaction mixture.[113]

In 1983 in Ravenna, ENI (now Versalis) developed a process to produce DMC by reacting methanol with CO and O_2, using a slurry reactor with copper chloride as catalyst. This process is characterized by almost total selectivity into the desired product based on methanol and 80% selectivity based on CO.[124,125]

The plant was expanded in 1993 to an annual capacity of 12000 tons.[126] It was then stopped some years later.

The reaction takes place in two steps: firstly cuprous chloride is oxidized by the reaction with oxygen and methanol to cupric methoxy chloride and then this

intermediate is reduced by CO to form the desired product and regenerates the catalyst (Scheme 1.20).
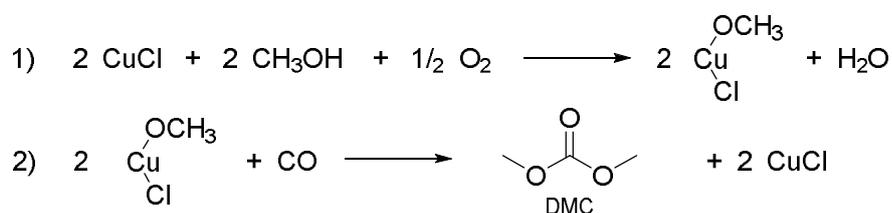
Scheme 1.20 Redox cycle mechanism of the oxidative carbonylation of methanol for the production of dimethyl carbonate (DMC).

The main by-products of this reaction are carbon dioxide and small amounts of methyl chloride and dimethyl ether.

The main drawback of this reaction concerns the toxicity of CO and the negative effect of the co-product water.

Indeed, water in high concentration displaces methanol from the Cu complex and is detrimental for the reaction, while small quantities seem to accelerate the formation of DMC.[127]

This reaction was also studied for a gas-phase application with copper chloride supported either on activated carbon or metal oxides, and promoted with salts of alkali and alkaline earth metals, bases and borates in order to improve the stability of the catalyst and selectivity to DMC.[128,129]

Also cobalt complexes were found to be active and less sensitive to water in this reaction, but when supported and used in the gas phase the ligands were not stable enough.[130,131]

Similarly to the oxidative carbonylation of alcohols, also phenols can react with CO to form the corresponding carbonates, however these reactions are less effective and the products are obtained with moderate yield.

In particular, diphenyl carbonate (DPC) can be synthesized reacting phenol with CO in the presence of Pd compounds.[132]

In this case, water shows a far more disruptive effect compared to the case of DMC synthesis, therefore it has to be readily removed by the use of molecular sieves adsorption,[133] or flushed out with an excess CO, or by means of dewatering at reduced pressure by distillation.[134,135]

In this way, diphenyl carbonate (DPC) is produced by a continuous process in a multistage distillation column (water removed as steam), with a yield of 39,5% and 99% of selectivity (Scheme 1.21).
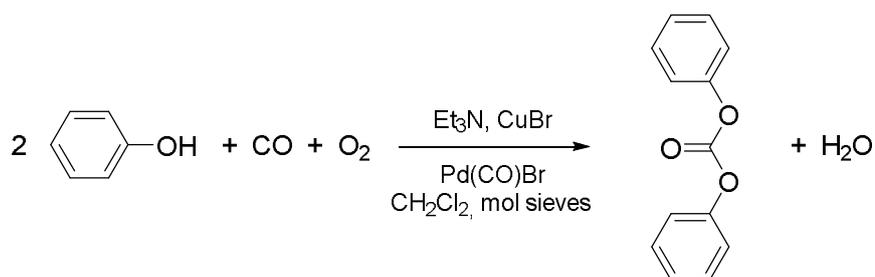
Scheme 1.21 Oxidative carbonylation of phenol for the production of diphenyl carbonate (DPC).

However, the low yield achieved, due to the lower reactivity of phenol (softer nucleophile that can delocalize the negative charge on the aromatic ring), combined with an expensive catalytic system have precluded a commercial process based on the oxidative carbonylation of phenols.

1.3.3.3 Urea alcoholysis

In 1946, Paquin discovered that reacting urea and alcohols in the presence of a metal salt (such as zinc and lead acetate) leads to the formation of carbamates and, prolonging the reaction, to carbonates; while isocyanuric is the major by-product (Scheme 1.22).[136]
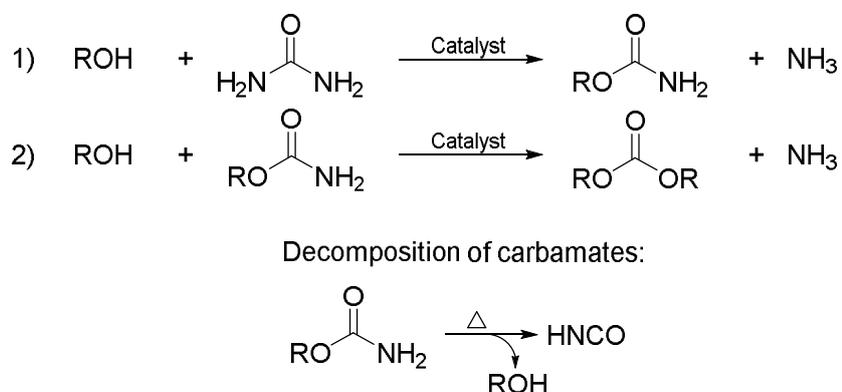
Scheme 1.22 Urea alcoholysis toward the formation of carbamates (first step) and organic carbonates (second step).

This reaction is generally performed at elevated temperatures (between 150 and 220°C) but the two steps, both catalytic, can be conducted separately and either carbamates or carbonates are obtained in high yields (ca 98%).[137,138,139]

The catalytic system has been improved and the formation of isocyanuric acid, which is observed with zinc acetate and triphenylphosphine, can be effectively limited by the use of titanium, aluminium and zirconium alcoxides in combination with suitable co-catalysts.[140]

Moreover, catalysts like dibutyloxide or dimethoxide and triphenyltin chloride have been found to give high yields of carbonates.

Qibiao Li et al. studied the reaction of aliphatic diols and urea using a wide series of heterogeneous catalysts based on different metal oxides, working at 150°C in vacuum, in order to improve the continuous removal of the NH_3 formed so shifting the equilibrium toward the desired products. In this way, they found a correlation between the acid and basic sites on the catalyst surface and the formation of by-products; zinc oxide (ZnO), with similar basic and acid properties was found to be the best catalyst for this reaction.[141]

This synthetic pathway leads to the formation of big quantities of ammonia as a co-product, which can be recycled for the synthesis of urea. So, for an industrial application the plant should be located near a urea manufacturing facility.

The reaction of urea with aromatic hydroxyl compounds was also investigated using various combinations of catalysts. However, the resulting aryl carbamates are thermally unstable in the reaction conditions and decompose to isocyanuric acid and phenols. In this way, the reaction cannot continue toward the desired organic carbonates products. Indeed the reaction of phenol and urea generates ammonia but only little amount of DPC.[142]

1.3.3.4 *Reaction of metal carbonates and alkyl halides*

Another possible pathway toward the synthesis of organic carbonates is the reaction between inorganic (metal) carbonates and alkyl halides by the following general scheme (Scheme 1.23).
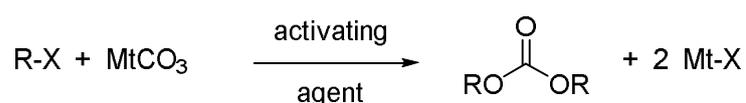
Scheme 1.23 Reaction of metal carbonates and alkyl halides toward organic carbonates.

The main difficulty derives from the low solubility of inorganic carbonates in a wide range of organic solvents.

A number of solvents, catalyst and reaction systems (like biphasic system in the presence of both activating agents and an appropriate phase-transfer catalyst) have been investigated.[143,144,145,146,147]

Recently, enhanced systems using ionic liquids for the synthesis of symmetric organic carbonates have been developed.[148]

However, this method leads to the formation of large quantities of inorganic salt waste that have to be separated and disposed; moreover the solubility

problems, the generally high temperature and long reaction time required make this reaction even less desirable.

Finally, this method is not applicable for the preparation of diaryl or activated dialkyl carbonates.[149]

Other synthetic strategies toward organic carbonates, namely the reaction of CO_2 with epoxides and the carbonate interchange reaction (CIR) between carbonates and alcohols, are so important to deserve separate chapters.

1.3.4 The "carbonyl green route": reactions with CO_2

Carbon dioxide represents an abundant, non-toxic and renewable C1 feedstock for the chemical industry.

The main limitation to its utilisation derives from its stability that often requires harsh reaction conditions compared to other synthetic strategies.

However, choosing the right synthetic targets and developing efficient catalytic systems is often the key to the success in recycling CO_2 inside the production chain.

In this way, the highly oxidized and low-energy organic carbonates represent the perfect target for CO_2 conversion.

Indeed, CO_2 can be used for the synthesis of organic carbonates using two main synthetic pathways:

> ➢ CO_2 cycloaddition reaction on epoxides: synthesis of cyclic carbonates;
> ➢ CO_2 direct condensation reaction with alcohols and diols.

These methods will be discussed in detail in the following pages.

Noteworthy, other alternative processes for the production of organic carbonates have also been investigated:

- Electrochemical reaction of CO_2 with diols in ionic liquids;[150]
- Oxidative addiction of CO_2 to olefins (Nb-catalyzed);[151,152]
- Cyclic ketals reaction with scCO$_2$ toward cyclic carbonates (Fe or Cu-catalyzed).[153]

1.3.4.1 *CO$_2$ cycloaddition reaction over oxiranes (and oxetanes)*

Epoxides and oxetanes represent the perfect high-energy substrates able to undergo cycloaddition reaction with the stable CO_2 in order to obtain five and six membered ring cyclic carbonates, respectively, according to the general scheme reported below (Scheme 1.24).
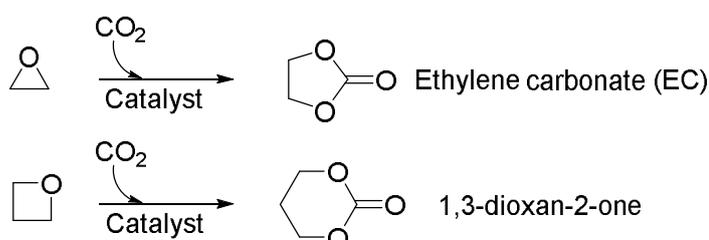
Scheme 1.24 General cycloaddition reaction of CO_2 with oxiranes and oxetanes.

In this way, ethylene and propylene oxides are successfully employed for the industrial production of five-membered cyclic carbonates (ethylene carbonate EC and propylene carbonate PC, respectively) with CO_2 since the 1950s, with a production volume around 100.000 tons per year.[154].

These reactions are highly exothermic (ΔH_R=-140 kJ/mol for EC synthesis) and usually both Lewis acid and base catalysts are used.

CO_2 cycloaddition on epoxides requires catalytic systems able to initiate the reaction by activating either CO_2 or the epoxide, or both at the same time.

CO_2 is typically activated by a Lewis base acting as a nucleophile while the epoxide is activated by the interaction of the oxygen atom of the ring with a Lewis acid.

A wide number of catalytic systems have been investigated and have been reported to be active for this reaction, both homogeneous:

- Metal complexes of different metals (Al,[155,156] Cr,[157,158] Co,[159,160] Zn,[159] and Sn[161]) and ligands (especially salen complexes);
- Metal halides (KI, NaI, ZnBr$_2$, LiBr);[182]
- Onium salts.[182]
- Ionic liquids.[162,163,164]

and heterogeneous:

- Supported halides salts on oxides (ZnO and SiO_2), carbon or zeolites;[165,166,167]
- Metal oxides like MgO,[168] Al-Mg mixed oxides[169] and $ZnO-SiO_2$[170];
- SmOCl;[171]
- Cs modified zeolites[172] and $Cs-P-SiO_2$[173];
- Smectites,[174] hydroxyapatites[175] and zinc-substituted heteropolyacids[176];
- Amine-functionalized silica catalysts;[177]
- Supported ionic liquids.[178]

However, the typical process uses an onium salt like tetraethyl ammonium bromide (TEAB), tert-butyl ammonium bromide (TBAB) and tetrabutylammonium iodide (TBAI), or metal halides and complexes (or a combination of the two) as catalysts.[154,179,180,181]

In particular, KI, being more durable, economical and more soluble in the cyclic carbonates formed compared to other catalytic systems, seems to be one of the best catalysts to apply in industrial processes.[182]

The possible mechanisms in the presence of generic metal halides is reported below (Scheme 1.25).[183]
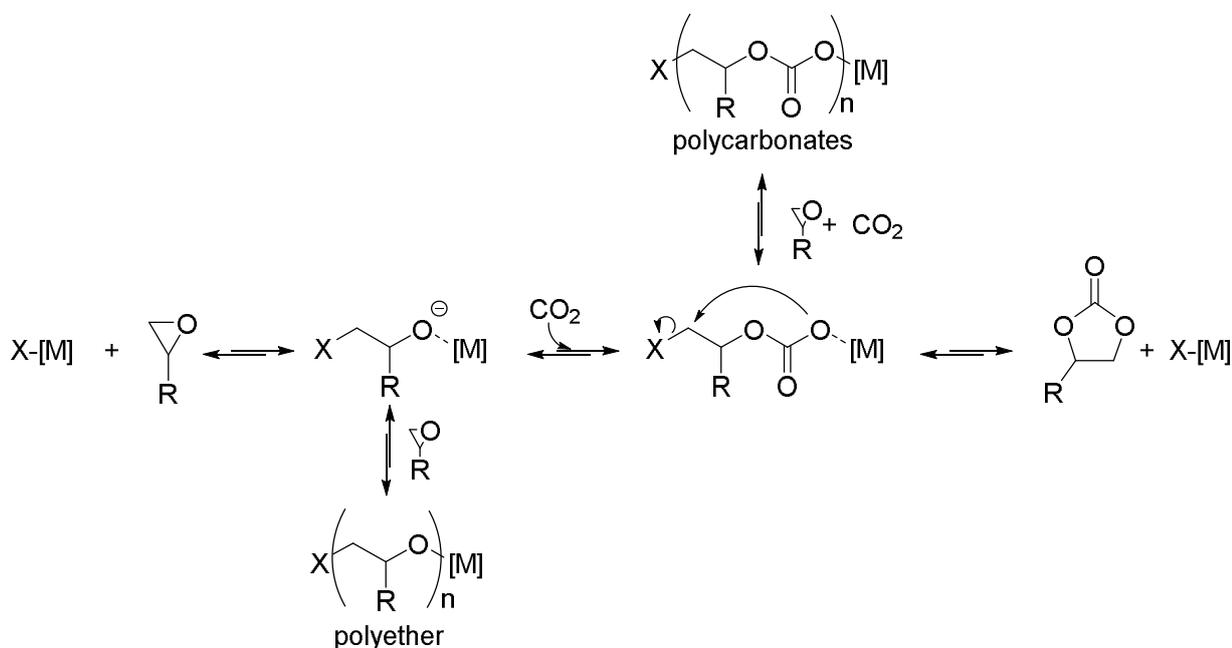
Scheme 1.25 Mechanism of the cycloaddition reaction of CO_2 with oxiranes with metal halides as catalytic systems.

Although this reaction is rather selective, the reaction conditions and the catalyst have to be carefully selected in order to prevent the two possible polymerization mechanisms (of course if the synthetic target is the cyclic carbonate and not one of the possible polymers):

- the alternating copolymerization of oxiranes and CO_2 that yields to polycarbonates;
- the homopolymerization of oxiranes to polyethers;
- a mixture of the two pathways that lead to polycarbonate containing ether linkages.

Although aliphatic polycarbonates produced by this reaction are characterized by less suitable properties compared to the diphenyl carbonate (DPC), bisphenol-based polycarbonates (holding excellent mechanical, physical and optical properties), they show very good biodegradability, low oxygen permeability and complete thermal depolymerisation to give cyclic carbonates. The relatively low glass transition temperature (35-40°C of polypropylene carbonate) can be improved by changing the starting material (epoxide). For example polycyclohexene carbonate (Tg=115°C) is expected to be a suitable substitute for polystyrene.[182]

The production of aliphatic polycarbonates by the reaction between CO_2 and epoxides has been recently industrialized in China.[184]

In particular, it is known that a stronger metal-oxygen bond leads to a better activation of the epoxides but can facilitate the propagation reactions; on the other hand, a weaker interaction leads to a weaker activation but increases the selectivity toward the intra-molecular cyclization to the cyclic carbonate.

It is also known that the cyclization reaction is thermodynamically more favorable that the polycarbonates formation, but it generally requires higher activation energy (polymers represents the kinetically preferred products while cyclic carbonates are the thermodynamic ones).[185] For this reason high operating temperature and pressure are generally required.[186]

However, this means that it is possible to selectively produce either cyclic carbonate or polycarbonate by tuning the reaction conditions and selecting a suitable catalyst.

For a complete dissertation on the reaction conditions, the catalytic systems and the mechanisms able to promote the polymerization or the cyclization toward carbonates see the work by P. Pescarmona et al., 2012.[187]

Finally, also the utilization of supercritical CO_2 (scCO_2) has attracted much interest since it is able to facilitate these chemical processes.

In effect, both propylene and ethylene oxide are soluble in scCO_2 while their products (PC and EC respectively) are not. In this way, carbonates are easily

separated from the supercritical phase, shifting the reaction balances toward the desired products. LiBr and perfluorophosphonium salts are suitable catalysts for scCO$_2$ processes (Fig. 1.4).[188,189]
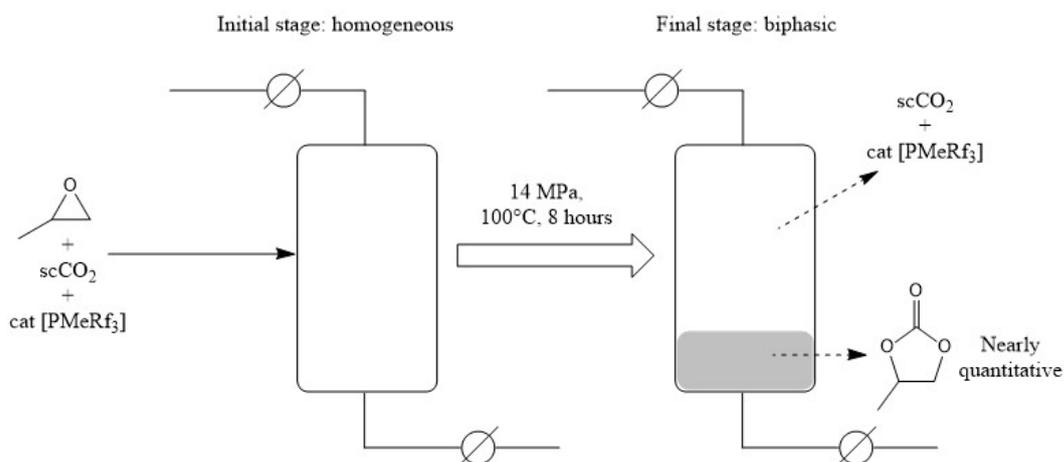

Fig. 1.4 Propylene carbonate (PC) synthesis from propylene oxide (PO) and scCO$_2$ with an highly soluble perfluorophosphonium salts as catalyst.

1.3.4.2 *CO₂ reactions with alcohols and diols*

The fundamental aspect on which the success of the previous synthetic pathway is based, is the excellent reactivity of the epoxides due to the ring strain.

On the other hand, oxiranes and oxetanes are often toxic and explosive compounds.

Replacing these compounds with the safer alcohols and diols would lead to a direct synthesis of both linear and cyclic carbonates, directly from CO_2 with water as the only co-product of the reaction, so enhancing the green aspects of this approach (Scheme 1.26).
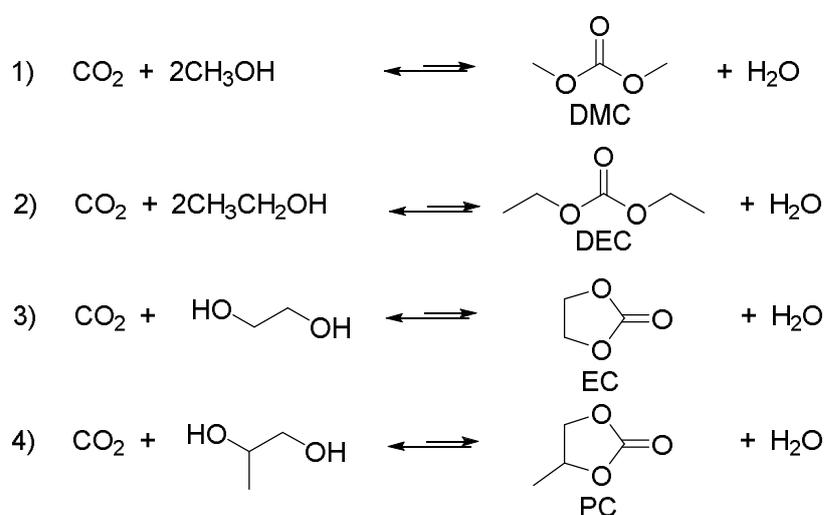
Scheme 1.26 Condensation reactions of CO_2 with alcohols and diols for the production of: 1) dimethyl carbonate (DMC); 2) diethyl carbonate (DEC); 3) ethylene carbonate (EC); 4) propylene carbonate (PC).

Unfortunately, several bottlenecks are known to be associated with this reaction:

- the yields of organic carbonates achieved so far are very low due to the strictly thermodynamic equilibrium limitations;
- difficult activation of CO_2;
- the formation of water as a co-product promotes the hydrolysis of the products, shifting the equilibrium back to the reactant side;
- difficulties in water in-situ separation under reaction conditions (large amount of alcohols, high temperature and high CO_2 pressure).

A complete study on the thermodynamic data on the synthesis of DMC (Scheme 1.26, reaction 1) was reported. In particular, the reaction is exothermic ($\Delta_r H^0_{298K}$ =-27,90kJ/mol), but it does not occur spontaneously at room temperature because of the Gibb's free energy value of $\Delta_r G^0_{298K} = 26,21$kJ/mol.[190]

In order to outflank the thermodynamic limitations it is crucial to develop highly efficient catalytic systems, remove water from the right-side of the equilibrium, using an adequate drying agent or to increase the CO_2 concentration by applying high pressure.

Many catalytic systems have been investigated for this reaction, in particular based on homogeneous metal complexes (titanium alkoxide with polyether ligands, cobalt, nickel and niobium complexes);[191,192,193,194,195] and organic bases such as triazabicyclodecene (TBD), diazabicycloundecene (DBU) and triethylamine.[196]

However, the most intensively studied complexes are based on tin alkoxides and in particular [$Bu_2Sn(OCH_3)_2$].[197,198]

Indeed, the reaction of this compound with CO_2, that lead to the formation of a methyl carbonate tin complex (intermediate of the reaction), is known since 1967.[199]

This intermediate can lead to the formation of DMC by thermolysis.[200]

Nevertheless, without any efficient dehydrating system, DMC yield in the reaction between methanol and CO_2 is normally less than 2% (based on the alcohol), with a turnover number less than one (TON<1), indicating that the reaction is stoichiometric rather than catalytic.[182]

Moreover, the organotin alkoxides could be hydrolyzed by the side-product water in the reaction conditions.[201]

Also heterogeneous catalytic systems have been studied for this reaction; in particular solid acid-base catalysts such as zirconia (ZrO_2)[202,203], $Ce_xZr_{1-x}O_2$[204], CeO_2[205,206] or heteropoly acid-modified zirconia[207] and Vanadium oxide based catalysts such as H_3PO_4/V_2O_5[208] and $Cu-Ni/V_2O_5-SiO_2$[209], have been applied for use in gas-phase reactions.

With heterogeneous catalytic systems (eg ZrO_2), the mechanism was investigated by means of infrared spectroscopy and was found to be composed of the following steps:

- dissociative adsorption of methanol over the surface (metal coordination), to form the methoxide species;
- CO_2 insertion and formation of the monomethyl carbonate (reaction intermediate);
- transfer of a neighboring adsorbed methyl group to the monomethyl carbonate and desorption of DMC.

The key point for success in this reaction is the set-up of an effective dehydrating system, which may promote the continuous removal of water and shift the unfavorable equilibrium toward the products.

Using the typical inorganic drying agents such as molecular sieves (zeolites), sodium or magnesium sulfate, dicyclohexyl carbodiimide and trimethyl phosphate, have the following merits compared to the organic ones:

easy separation from the reaction mixture by filtration and facile regeneration by drying at high temperature.

However, the addition of these dehydrating agents does not improve the DMC yield in the reaction between methanol and CO_2.[210]

This is probably due to the low capability of these systems as drying agents under the reaction conditions used, especially at high temperatures.

A possible way to overcome this problem is to design a process with separation of the high-temperature reactor from the room-temperature dehydrating section (eg, with selective adsorption over 3Å molecular sieves), and circulating the mixture between these two sections.[182]

The apparatus and the yield obtained are shown in the following figures (Fig. 1.5).
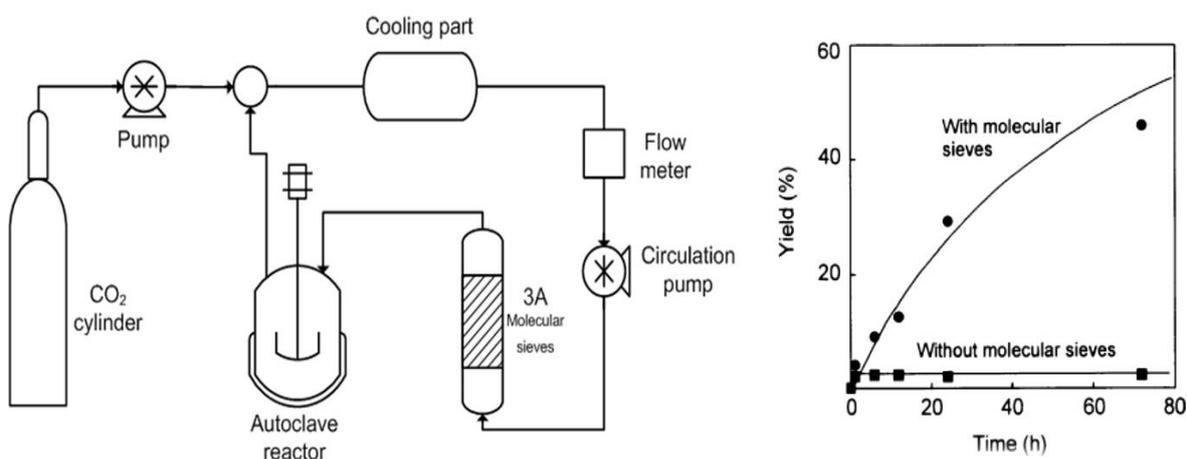

Fig. 1.5 Schematically representation of the apparatus used for the synthesis of DMC from methanol and CO_2 (left) and yield trends with and without the utilization of molecular sieves; adapted from reference.[182] Reaction condition: autoclave with internal recycle, catalyst dibutyltin dimethoxide (2.0 mmol), methanol (100 mmol), 15 grams of molecular sieves (3Å), carbon dioxide (300 atm), 180°C. Yields based on methanol.

Although this method can lead to an outstanding 50% DMC yield (based on methanol), it requires long reaction time (80 hours) and a lot of energy input in order to compress and pump the mixture.

On the other hand, many organic dehydrating agents have been investigated to promote the synthesis of organic carbonates from alcohols and diols with CO_2. In this case there are two possible strategies to follow:

- to substitute the alcohols with their corresponding dehydrated derivatives, such as epoxides and ketals (products of the dehydrative condensation of alcohols and ketones) and ortho-esters (however the synthesis from alcohols and esters is difficult);

in this way the removal of water is done before the reaction and further dehydrating is unnecessary;[182]

- to couple a parallel hydration reaction, using molecules able to readily react with water in the reaction conditions, like, for instance, nitriles.

The schematic representation of these different synthetic strategies is reported below (Scheme 1.27).
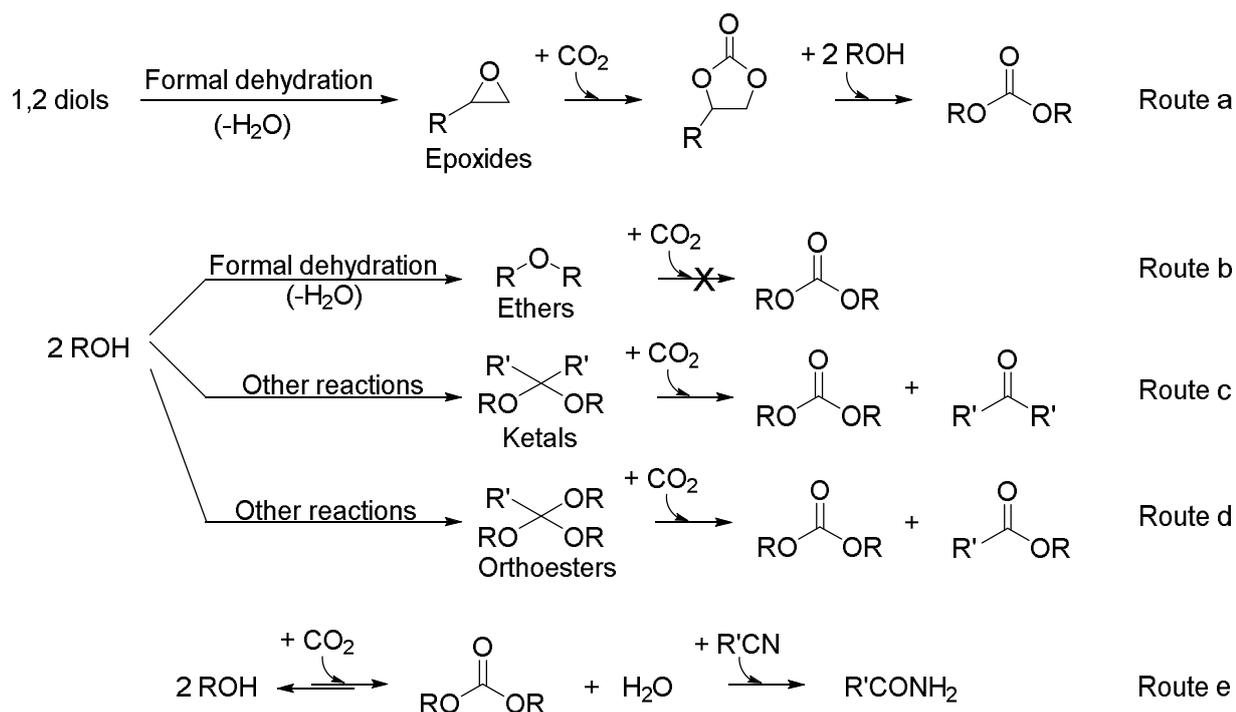
Scheme 1.27 Synthetic strategies for the synthesis of linear carbonates from alcohols and diols.

"Route a" represents the dehydration of 1,2 diols to yield epoxides which can readily react with CO_2 (as described in the previous chapter), to give cyclic carbonates. Cyclic carbonates can undergo further reaction with alcohols in order to obtain linear carbonates in the so called carbonates interchange reaction (CIR). This reaction is described in detail in the following chapter.

As epoxides are the dehydration products of 1,2-diols, linear ethers are the products of the condensation reaction of two alcohols moieties. However, without the ring strain, linear ethers are much less reactive compared to the cyclic epoxides (route b).[211] "Route c" and "Route d" use ketals and ortho-esters, respectively, as formal derivatives of alcohols. However, important differences between the two routes, that underline the presence of different mechanisms, are listed in the next page:

- ortho-esters react with CO_2 also in the absence of alcohols, while ketals need the alcohol in the reaction mixture (different reaction mechanisms);[212]
- ortho-esters have an optimal pressure to optimize the carbonate yield, while an higher pressure gives higher yield using ketals;
- the main by-product using ortho-esters are dialkyl ethers, while with ketals are enol ethers;
- easy regeneration of ketals from the ketones (the product of hydrolysis) through a dehydrative condensation with alcohols, while the regeneration of ortho-esters from esters is difficult;[213]
- ortho-esters are a much more expensive starting material compared to ketals.

For these reasons, ketals are usually preferred to ortho-esters.

In particular, 2,2-dimethoxypropane appears to be the most convenient ketal because of both its cost and availability, and because it is synthesized from acetone.

One typical synthesis with ketal using tin alkoxides and a small amount of an acidic co-catalyst ($RNH_3(OTf)$) is reported below (Scheme 1.28).
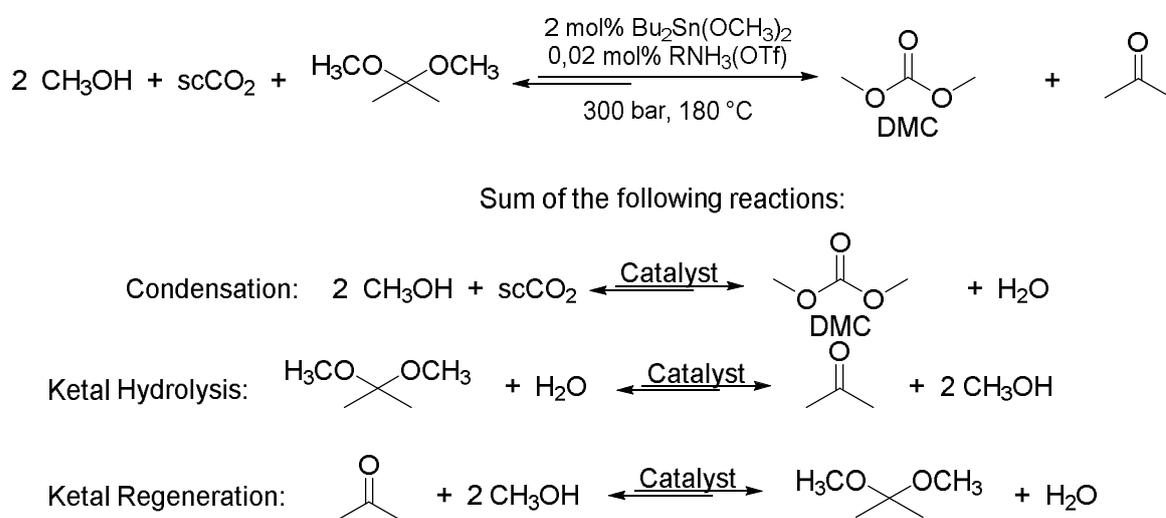
Scheme 1.28 Synthesis of dimethyl carbonate (DMC) using 2,2-dimethoxypropane as dehydrating agent.

Many hypothesis on the reaction mechanism in the presence of ketals and on the catalytic cycle based on mononuclear and multinuclear metal (tin) alkoxide as active species have been reported.[214,215,216]

Finally, nitriles have been investigated both as reaction solvents, able to increase the solubility of CO_2 in the alcoholic reaction mixture, and as dehydrating agents.

This is a promising route that allows to obtain higher yield in the desired carbonates.

Acetonitrile is one of the most investigated solvent and dehydrating agent to yield acetamide and acetic acid as the by-product.[217,218]

However, due to its low boiling point, high polarity and cost it seems not to be suitable for conditions generally employed in these reactions.

Other two promising nitriles successfully applied as dehydrating agents are benzonitrile and 2-cyanopyridine.

Benzonitrile is reported to enhance the solubility of CO_2 in several diols (like propylene glycol), at high temperature and pressure.[219]

However, the use of benzonitrile, although it increases the yield to the desired carbonate up to the 20% (18 h, T= 175°C and 100 bar), leads to the formation of several by-products, such as the esterification products of benzoic acid and propylene glycol (using different metal carbonates as catalysts).[220]

On the other hand, an outstanding result was obtained using 2-cyanopyridine as dehydrating agent, with an excellent yield of DMC (94% after 12 hour of reaction), in the presence of a simple heterogeneous catalyst made of CeO_2 under mild conditions.[221]

Indeed ceria is able to catalyze both the condensation reaction of methanol and carbon dioxide and the hydration of 2-cyanopyridine to 2-picolinamide.[222]

The overall reaction scheme is reported below (Scheme 1.29).
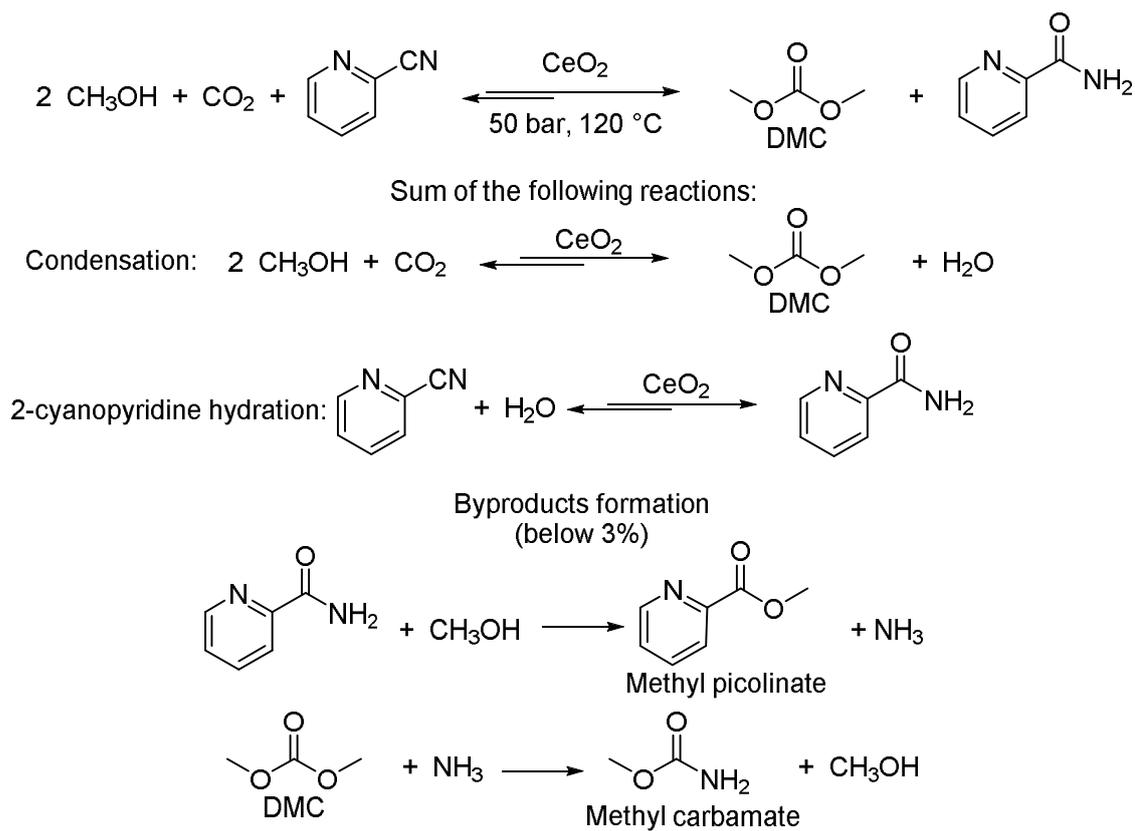
Scheme 1.29 Synthesis of dimethyl carbonate (DMC) in the presence of 2-cyanopiridine as the dehydrating agent.

1.3.5 The carbonates interchange reaction (CIR)

Similarly to a transesterification reaction between esters and alcohols,[223] the "transcarbonation" or "carbonates interchange reaction" (CIR) can be defined as follows:

"a process wherein one carbonate is converted to another one by which one or both the acyl oxygen parts of the parent carbonate are displaced by an appropriate alkoxide (or aryl oxide) to produce a different carbonate with the aid of a suitable catalyst"(Scheme 1.30).[149]
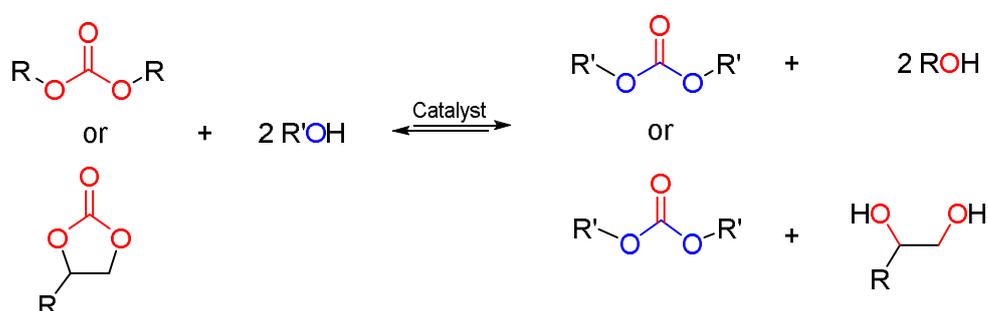
Scheme 1.30 Generic carbonates interchange reaction

Nevertheless:

"since CIRs are equilibrium reactions, it is possible to convert one carbonate into another; however, in practice, this may prove difficult, require special conditions, or even fail".[113]

The CIRs between alcohols or diols and organic carbonates adheres to the following rules:

   ➢ the less nucleophilic compound is displaced by the more nucleophilic in the formation of a new carbonate;
   ➢ with similar nucleophilicity, the heavier compound replaces the more volatile one (often removed by distillation).
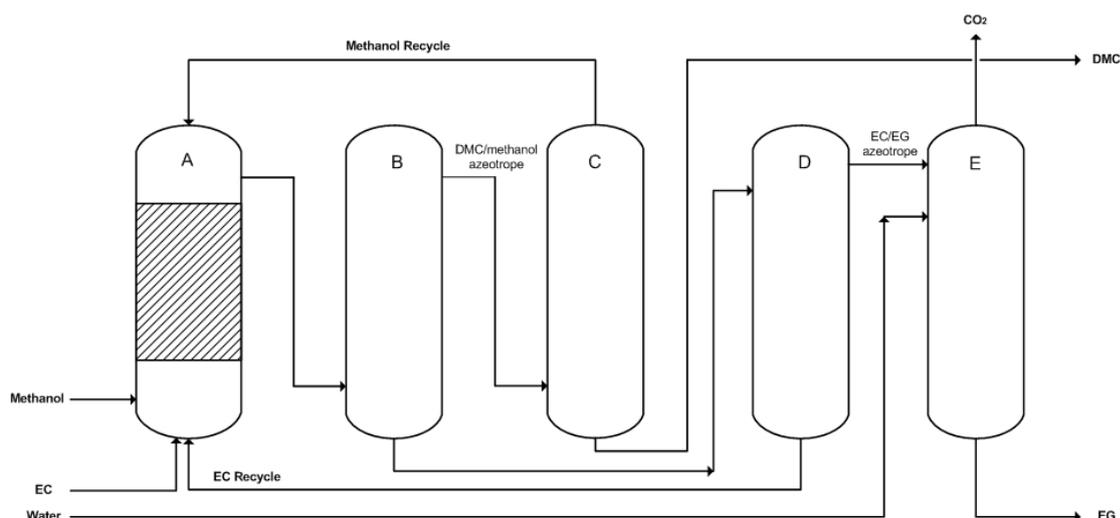
1.3.5.1 CIR of aliphatic alcohols and cyclic carbonate: the synthesis of linear carbonates

The most studied and applied carbonate interchange reactions are the ring opening to convert cyclic carbonates, like EC and PC, to linear organic carbonates, namely DMC and similar.

This is because cyclic carbonates are already successfully produced on industrial scale by the cycloaddition of CO_2 onto epoxides (see Chapter 1.3.4).

A wide variety of catalysts has been proposed for the CIR of cyclic carbonates and alcohols:[224]

- alkali and alkaline earth metals salts, oxides and ion exchangers;[225,226,227,228]
- N and P bases, including their quaternary salts anion exchangers;[229,230,231,232,233]
- Metal complex of Ti, Zr and Sn (especially Ti and Sn *n*-butoxide);[234,235,236]
- Combination of different metals and onium salts.[237]

In particular, the last two categories have been deeply investigated because are highly effective in catalyzing also the reaction between epoxides and CO_2 that lead to cyclic carbonates. In principle, using these catalytic systems it is possible to carry out both the synthesis of cyclic carbonates and their carbonate interchange reaction with alcohols at the same time.

In this way, EC reacts with methanol in a continuous multi-stage process to yield DMC (Scheme 1.31 and Fig. 1.6).[238]

Scheme 1.31 CIR between ethylene carbonate (EC) and methanol to yield DMC.

Fig. 1.6 Process diagram for the production of DMC and ethylene glycol (EG) by the CIR between ethylene carbonate (EC) and methanol.

In this process the reactant mixture is continually fed (methanol/EC mole ratio equal to 5), through a fixed bed reactor (A) filled with a weakly basic solid support catalyst (triphenylphosphine on poly-styrene-co-divinylbenzene), at 125°C and 7 bar.

The resulting mixture (containing around 20% by weight of DMC) is then distilled at atmospheric pressure to remove DMC as azeotropic mixture with methanol (column B).

The azeotrope is than processed at 10 bar in order to achieve the separation between methanol (recycled) and almost pure DMC (column C).

Another distillation column (D) is able to separate pure EC from the azeotropic mixture of EC and EG; finally this azeotrope undergoes hydrolysis of the organic carbonate to form CO_2 and ethylene glycol (EG).

However, with this (or similar) systems, where the reagents are fed together in a concurrent flow, the conversion in best conditions corresponds to the equilibrium one (often unfavorable).[239]

For this reason, new reactive distillation systems (RDS) have been developed in order to carry out the transesterification and separation of the products simultaneously, so to obtain a distillate that contains more DMC than the CH_3OH/DMC azeotrope (67/33 w/w) at the top of the column, and only EG at the bottom.[240,241]

These reactive distillation systems are promising approaches to overcome the unfavorable equilibrium limitation of the CIRs.

Moreover, the combination of reaction and distillation in a single vessel allows to exploit a number of specific advantages like improved selectivity, better heat control and effective utilization of the reaction heat, to name a few.

RDS has been successfully used and investigated in the past for several reactions: etherification, esterification, hydrogenation, hydrodesulfurisation and polymerization.

Various reviews have been published on this reaction and an increasing number of articles and patents (180 papers and 100 patents published only in 2002-2003), clearly reveals the increasing interest in this area.[242,243]

1.3.5.2 CIR of DMC and other aliphatic alcohols

The simplest symmetric linear carbonate, dimethyl carbonate (DMC), can be successfully used as starting point for the synthesis of a wide series of higher aliphatic carbonates by means of CIRs with the corresponding alcohols.

Noteworthy, symmetric organic carbonates, especially long-chain ones, find application in lubricants, cosmetics, plasticizers and fuel compositions.[244]

For these reasons, this reaction was investigated by many researchers, with a wide series of homogeneous and heterogeneous catalysts, similar to those presented in the previous chapter.[149]

However, since this reaction is reversible, depending on the experimental conditions, the reaction often needs long reaction time to achieve complete conversion of the reagent, and also leads to a mixture of symmetric and unsymmetrical products (Scheme 1.32).
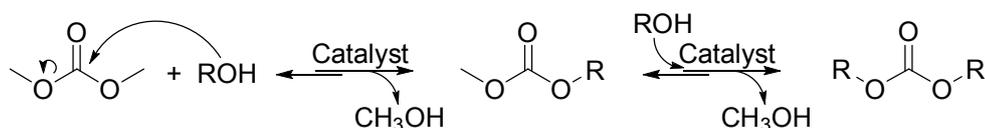
Scheme 1.32 CIR between DMC and a generic alcohol (ROH) to yield firstly the unsymmetric and then the symmetric products.

Recently, mainly basic (or bifunctional) catalytic systems have been investigated and claimed to be active for these reations, noteworthy ionic liquids,[245] 1,5,7-triaza-bicyclo[4.4.0]dec-5-ene (TBD)[246] and rather complicated heterogeneous catalysts systems (including MCM-41-TBD,[247] Mg/La/O,[248] CsF/α-Al$_2$O$_3$,[249] nano-crystalline MgO[250] and metal–organic frameworks[251]). Moreover, sophisticated procedures and high temperatures (>100 °C) have been applied to shift the equilibrium towards the desired products.

In particular, by conducting these reactions in the reactive distillation conditions, using an azeotropic distillation apparatus in order to continuously remove the mixture of DMC and co-formed methanol, can significantly improve yield and selectivity toward the symmetric (consecutive) product.

On the other hand, a great excess of DMC is needed in order to overcome the losses due to the distillation of the azeotrope.

Another possible approach is the use of gas-liquid phase-transfer catalysis conditions (GL-PTC), but the latter need high temperature (e.g 180°C), polymeric phase-transfer

catalyst (e.g. PEG-2000) and finally leads to yields of the symmetric carbonates below 50%.[252]

Some general rules affect the reaction and lead to a more favorable (or unfavorable) reaction equilibrium:

> ➤ An increase of the steric hindrance of the alkyl chain leads to a decrease in the conversion;[149]
> ➤ primary alcohols react better than secondary ones while tertiary are often almost inactive.[149]

The second rule is generally associated to the basicity strength of the conjugated alkoxides:

<div align="center">tertiary > secondary > primary.</div>

Indeed, the tertiary alkoxides are present at equilibrium in lower concentration than the others. Moreover, other competitive side reactions like elimination are more favored with tertiary alcohols.

Although equilibrium limited, CIRs of DMC and aliphatic alcohols don't suffer from severe thermodynamic limitations and are therefore more facile in comparison to the reactions described in the following chapter.

1.3.5.3 CIR of DMC with phenolics: the DPC synthesis and the reactive distillation method

The reactive distillation methodology is applied to another important category of CIRs: the reaction between phenolics and aliphatic carbonates, and in particular between DMC and phenol to yield diphenylcarbonate (DPC).

DPC is an important chemical intermediate, replacing phosgene in the reaction with Bisphenol A in the synthesis of high-performance aromatic polycarbonates in the so called "melt process" (with more than 350 patents that have appeared since 1995).

This process is possible because of the softer nucleophilicity of phenol anion, in which the negative charge can be delocalized on the aromatic ring, making phenol a better leaving group and helping the polymerization process.

Because of their high glass-transition temperature (T_g=140-155°C) and their outstanding properties such as high impact resistance, transparency, heat resistance and dimensional stability, polycarbonates have been widely employed as engineering plastic for vehicles and electrics and electronics appliance (eg, resins for optical disks CDs and DVDs), for a production of around 2.7 million tons per year.[253]

In 2002, Asahi-Kasei Corp. was the first to claim the development of a complete "phosgene-free" process for the synthesis of aromatic polycarbonates (and high-purity monoethylene glycol EG) starting from CO_2 and ethylene oxide (EO).[254]

The schematically representation of the whole process is reported in the figure below (Fig. 1.7).
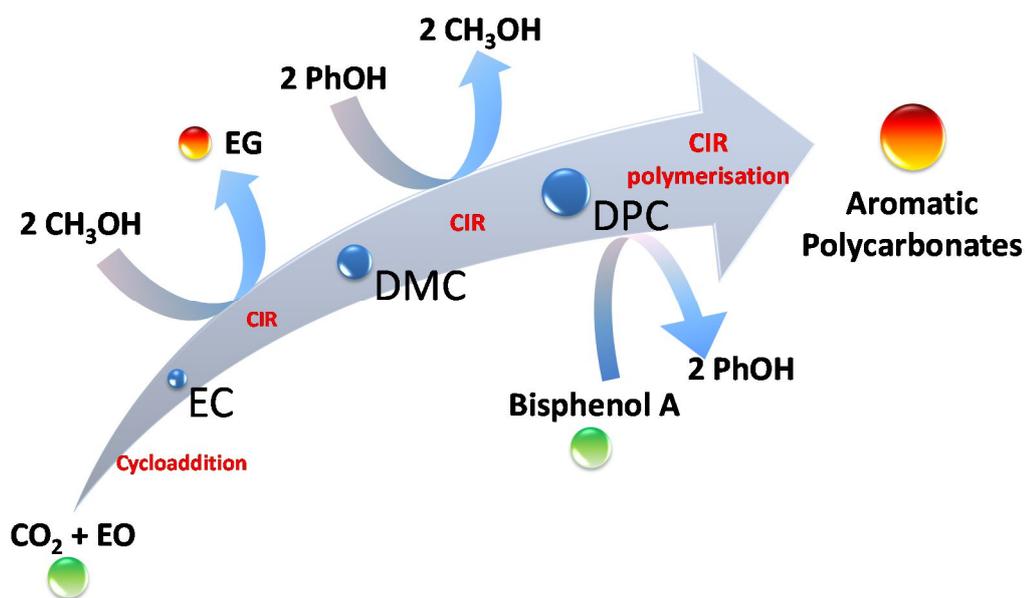

Fig. 1.7 Asahi Kasei's process for the synthesis of aromatic polycarbonates, starting from carbon dioxide, ethylene oxide (EO) and Bisphenol A (raw materials ●); through different reactions (mainly CIRs after the starting cycloaddition reaction) that lead to different intermediates ● and finally to the desired polycarbonates and mono ethylene glycol (products ●).

From the previous figure, it is clear the importance of the CIRs for the whole process. In particular we will focus our attention on the third step: the synthesis of DPC. This step (summarized in Scheme 1.33) is a combination of three different reactions.
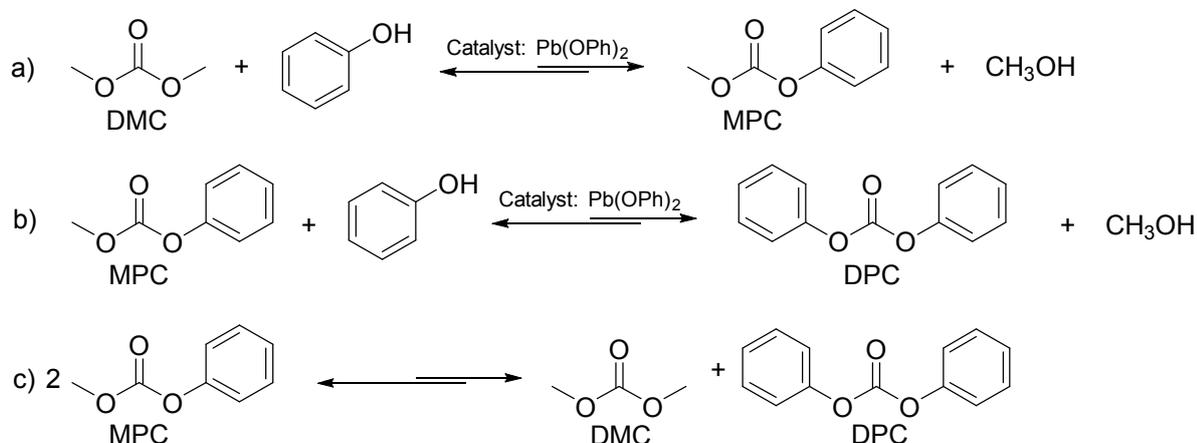
Scheme 1.33 Synthesis of diphenyl carbonate (DPC) through the CIR of dimethyl carbonate (DMC) and phenol, yielding firstly methylphenyl carbonate (MPC) intermediate of the reaction. MPC undergoes also a disproportion reaction yielding DMC and DPC.

All these reactions are equilibrium reactions having low equilibrium constants; in particular, reaction (a) is very slow with a thermodynamically unfavorable equilibrium constant (K_{eq}) equal to 3×10^{-4} at 180°C. Moreover, side reactions such as etherification and decarboxylation are favored and easily occur to give anisole and CO_2.[255]

The reasons behind this behavior are described in the chapter dealing with the general carbonates reactivity (Chapter 1.3.2).

Therefore, the transesterification of DMC and phenol belongs to a reaction of a soft nucleophile binding to a hard electrophile; on the contrary, O-methylation is the reaction of a soft nucleophile binding to a soft electrophile. According to the hard–soft principle, the O-methylation is much easier than the transesterification.

However, to overcome the thermodynamic limitation of this particular CIR, Asahi-Kesei Corp. has developed a process in which the reactions reported in Scheme 33 are conducted using two continuous multi-stage distillation columns at different pressures.

In this way, reactions and separation of the products are conducted simultaneously in the so-called "reactive distillation" system.[256]

This process is schematically represented in the following figure (Fig. 1.8).
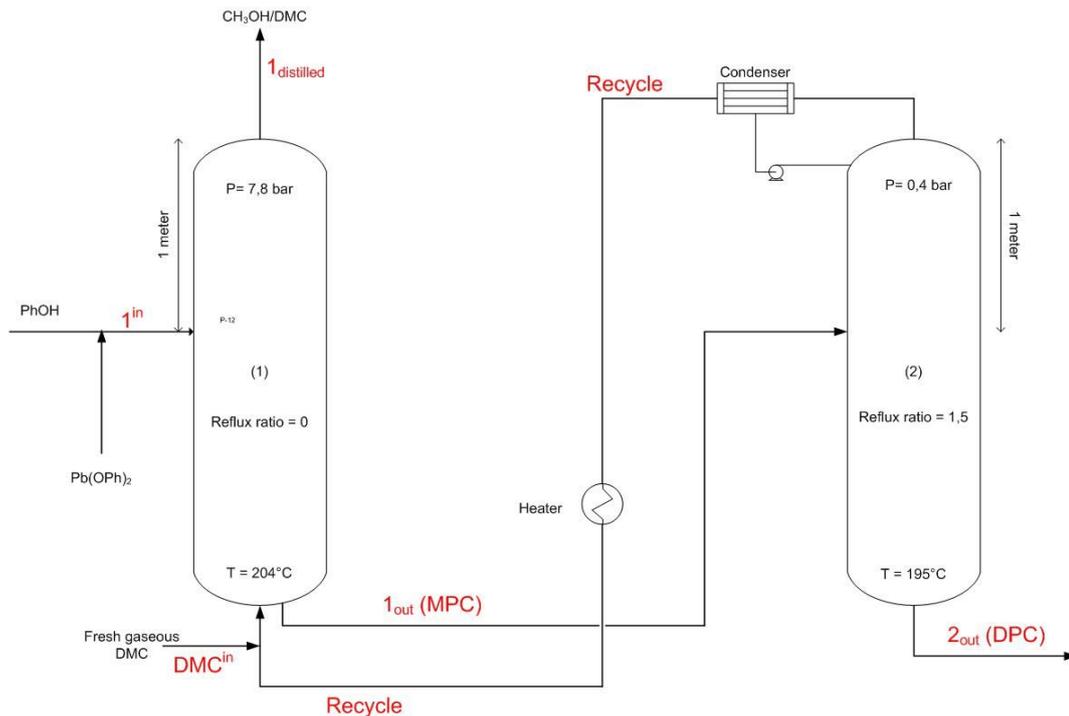
Fig. 1.8 Multi-column for the reactive distillation process for the synthesis of diphenyl carbonate (DPC) through the CIR of dimethyl carbonate (DMC) and phenol.

$In_{liquid}1 = 1^{in} + Recycle = 4,6$ Kg/h;

$1^{in} = 0,9$ Kg/h (3,8 wt% DMC + 92,8 wt% PhOH + 3,4 wt% $Pb(OPh)_2$);

$DMC_{gas}^{in} = 3$ Kg/h (pure DMC);

$1^{in} + DMC^{in} = $ (50,6 wt% DMC + 45,3 wt% PhOH + 3,3 wt% MPC + 0,8 wt% $Pb(OPh)_2$)

$1_{distilled} = 3,1$ Kg/h (mixture of methanol and DMC);

1_{out} (MPC) = 4,5 Kg/h (27,4% MPC + reagents and catalyst);

Recycle = 3,7 Kg/h;

2_{out} (DPC) = 0,8 Kg/h (92,6 wt% DPC and others).

(see example 3.3.3 of the reference)[254]

The major drawbacks of this process are its complexity and the high cost of the whole apparatus, consisting of two columns, the first one under pressure and the second one under vacuum.

Moreover, it is very difficult to reach the steady state and many tests are necessary, trying different conditions and spending a lot of money and time.[254]

Besides these aspects, also the toxicity of the phenate-lead catalyst contributes to the drawbacks of this process.

1.3.6 *Organic carbonates as reactive chemical intermediates*

In the following sections we will describe other possible reactive applications of organic carbonates, dividing them in function of the reactive centre involved.
The different reactive sites of organic carbonates are reported again for convenience (Fig. 1.9).
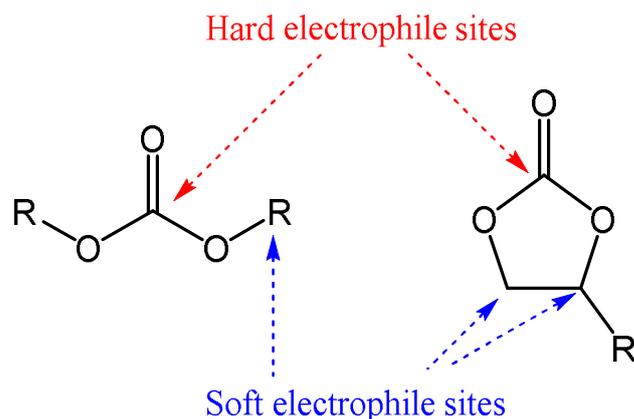

Fig. 1.9 Reactive electrophile sites on linear and cyclic organic carbonates

1.3.6.1 *Reaction on the hard-electrophile site*

In the previous Chapter on the Carbonate Interchange Reaction, we already discussed on how the reaction of alcohols with the carbonyl moiety of the carbonates, in the presence of an appropriate catalyst, leads to the formation of other carbonates.
However, other nucleophiles can be successfully used for the synthesis of other interesting products.
Of particular interest, aliphatic amines (primary or secondary) can be successfully used in the reaction with organic carbonates (Scheme 1.34).
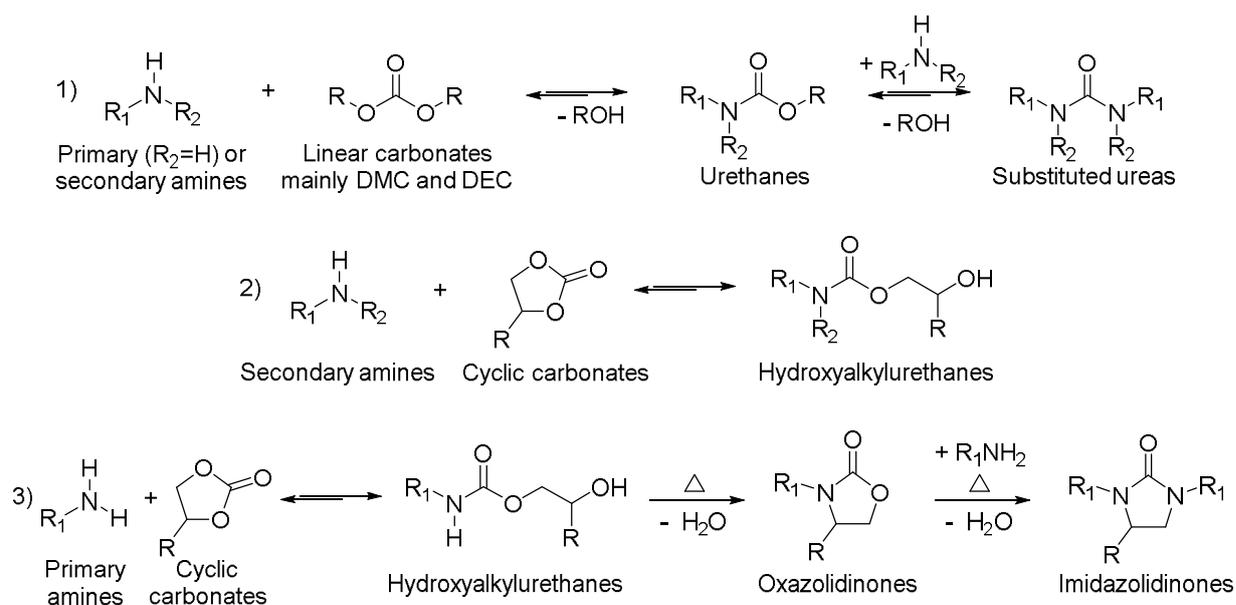
Scheme 1.34 Reaction of aliphatic amines with linear and cyclic organic carbonates.

Both cyclic and linear carbonates undergo attack at the carbonyl carbon atom by the nitrogen atom of the aliphatic amines, yielding urethanes.[257,258] If an excess of amines is used the reaction continues to yield substituted ureas.

However, unlike linear carbonates, the reaction of alkylene carbonates with amines yields a hydroxy-functional species useful as a reactive intermediate. Note that only one of the two possible isomers of the product obtained by ring-opening of cyclic carbonates is shown (Scheme 1.34, reaction 2).

Although similar products can be obtained via the reaction of diols and urea, such reactions generally require higher temperatures (120-170 °C) and produce ammonia as a by-product.[259]

Moreover, the hydroxyalkylurethanes produced usually do not undergo further reaction with a second mole of amine to produce urea or imidazolidinone, except at temperatures higher than 150 °C.[260]

If primary amines are used as starting materials (Scheme 1.34, reaction 3), the hydroxyalkylurethanes can undergo (at high temperatures) cyclisation to yield an oxazolidinone, with loss of water.

Although most of these reactions can be accomplished without the aid of a catalyst, alkali materials can be employed to increase the reaction rate.[261]

Finally, these are exothermic reactions, so the heat formed must be controlled by monitoring the addition rate of one component into the other.[262]

Another important reaction on the carbon of the carbonyl group is the synthesis of aliphatic polycarbonates.

This can be performed by the polymeric CIRs of organic carbonates with polyols (in particular with terminal diols spaced by three or more carbon atoms).

It is well know that carbonate linkages within a polymer chain introduce a spectrum of properties such as a reduced biodegradation time and enhanced mechanical performance.[263]

On the other hand, aliphatic polycarbonates in which the carbonate linkages are connected by two carbon atoms can be prepared by copolymerization of CO_2 and epoxides.[264,265,266]

Nowadays, these polymers are currently in the early stage of commercialization.[267,268]

1.3.6.2 *Reaction on the soft-electrophile site: organic carbonates as alkylating agents*

Organic carbonates are successfully employed as alkylating agents of aromatics, replacing more traditional, harmful and undesirable compounds.[269]

In particular, alkyl iodide are known carcinogens and dimethyl sulfate is an extremely hazardous liquid and vapor (may be fatal if inhaled).[270,271]

The most investigated organic carbonate for this kind of reaction is the lightest term of the series of linear carbonates: DMC. It is reported that DMC can react with a number of nucleophilic substrates, namely phenols, amines, sulfones, thiols and methylene-active derivatives of aryl and aroxy-acetic acids, under both batch and continuous flow conditions.[65]

The comparison between DMC and the more traditional methylating agents are reported in Table 1.7. In particular, the methylation of phenol with different methylating agents is also described in the following scheme (Scheme 1.35).

Property	Dimethylsulfate (DMS)	Methyl iodide (CH₃I)	Dimethylcarbonate (DMC)
Oral acute toxicity (rats)	LD_{50} 440 mg/kg	LD_{50} 76 mg/kg	LD_{50} 13.8 g/kg
Acute toxicity inhalation	LC_{50} 1.5 mg/L (4h)	LC_{50} 1.3 mg/L (4h)	LC_{50} 140 mg/L (4h)
Biodegradability (OECD-301C)	rapid hydrolysis	16% (28 days)	>90% (28 days)
Mutagenic properties	mutagenic	no data available	none
Carcinogenic properties	carcinogen	suspected carcinogen	none

Table 1.7 Comparison between different alkylating agents (toxicological and ecotoxicological properties).
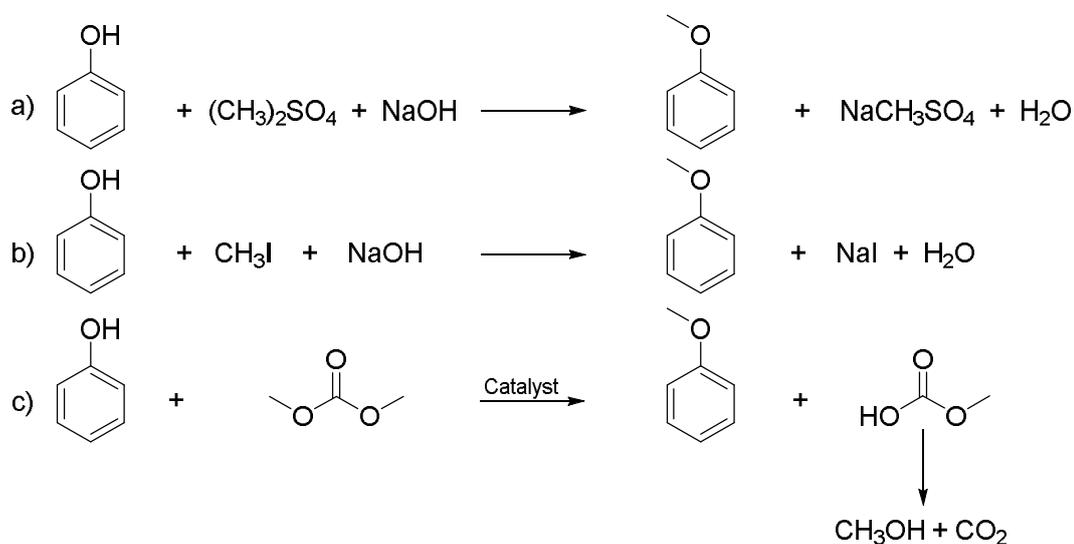
Scheme 1.35 Phenol methylation reaction with different alkylating agents.

DMC is a benign alkylating agent, that overcomes the problems due to the toxicity, corrosiveness, the need for stoichiometric amounts of the base, waste salt separation and disposal, all drawbacks associated to the use of alkyl halides and sulfates.

The possibility to use DMC and other aliphatic carbonates as alkylating agents is investigated in the corresponding chapter of this Thesis (Chapter 4.4).

On the other hand, also cyclic alkylene carbonates can be used for the alkylation of aromatic nucleophiles.

Of particular interest is the reaction between ethylene carbonate (EC) and phenol over heterogeneous catalytic systems (such as basic zeolites e.g. Na-mordenites), which permits a more selective synthesis of 2-phenoxyethanol compared to the industrial production using ethylene oxide.[272]

The two different reaction pathways are underlined in Scheme 1.36.
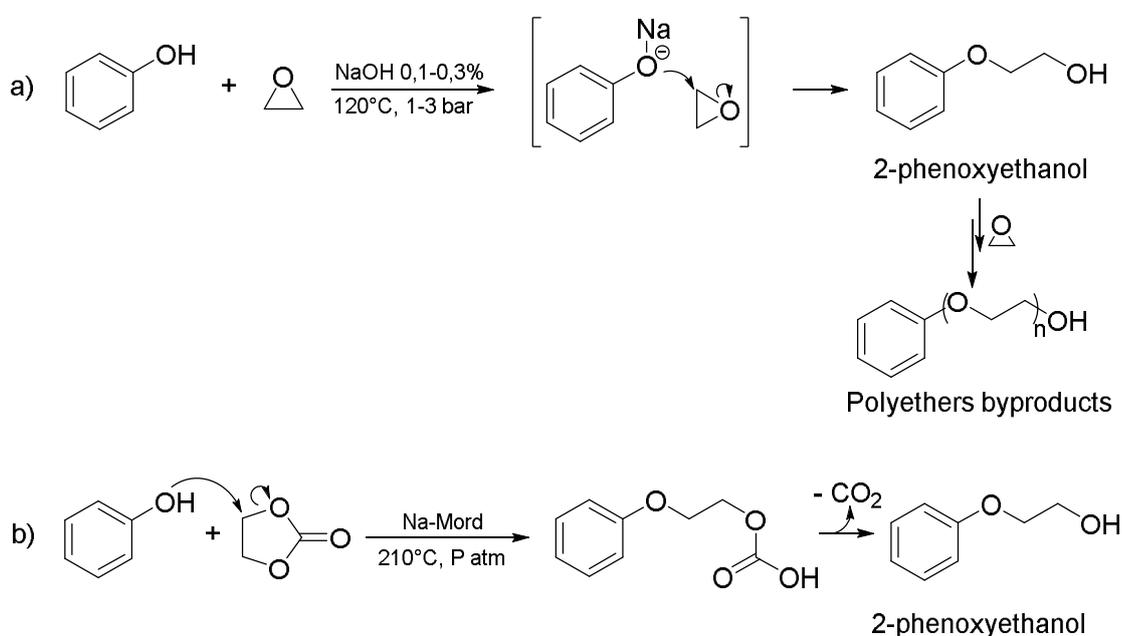
Scheme 1.36 Synthesis of 2-phenoxyethanol from phenol and ethylene oxide (a) or ethylene carbonate (b).

2-phenoxyethanol is an important synthetic intermediate in the production of plasticizers, pharmaceuticals, and fragrances with an annual global capacity around 170.000 tons.[273]

1.4 Bio-alcohols

A rapid overview on the main bio-alcohols investigated as described later in this Thesis is proposed in the following chapters.

1.4.1 Catechol

Catechol (1,2-dihydroxybenzene) is a crystalline phenolic compound that was discovered for the first time by Reinsch in 1839 by the distillation of the catechin.[274] Nowadays, it is industrially produced mainly by the hydroxylation of phenol with hydrogen peroxide in the presence of a catalyst such as:

- phosphoric and perchloric acid (Rhone-Poulenc process);[275]
- ferrocene and cobalt salts (Brichima process);[276]
- organic peroxides and acid (Ube process);[277]
- titanium silicalite (TS-1) (Enichem).[278]

Another possibility is the dehydrogenation of 1,2-cyclohexanediol at 300°C in the presence of a Pd/Te catalytic system.[279]

However, the current research is focused on the development and improvement of new synthetic pathways starting from lignin.

Lignin is one of the main components of the lignocellulosic biomass, with cellulose and hemicellulose. It constitutes from 15 to 35% of the typical dry lignocellulosic biomass and it is a rigid bio-polymer characterized by a complex structure of cross-linked phenolic compounds (including coniferyl, *p*-coumaryl and sinapyl alcohols): it represents the largest natural source of aromatics on the earth with an estimated production of 70 million tons per year.[280]

Many C–O–C bonds which exist either as ethers or as part of a furan ring are the most common bonding patterns in lignin; in particular there are 5 predominant types of linkages: β-O-4 ether bonds, β-5 phenylcoumaran bonds, β–β′ pinoresinol, diphenyl ether 4-O-5′, and β-1′ diphenyl methane. The relative abundance of these linkages depends on the specific plant.[281]

Bio-catechol can be obtained as by-product of different lignin treatments, in particular the pyrolysis and the hydrogenolysis.[280]

Noteworthy, the presence of a basic catalyst (namely NaOH) can improve the selectivity toward catechol although the yield is generally low (below 30%).[282,283]

Catechol finds many applications as chemical intermediate for the manufacture of insecticide, flavor and fragrance (e.g. vanillin) and others.[284]

1.4.2 *Glycerol*

Glycerol (1,2,3-trihydroxypropane) is a simple polyol compound.

It was accidentally discovered in 1779 by K.W. Scheele, the Swedish chemist, while he was heating a mixture of olive oil and litharge (lead monoxide). Scheele called glycerine the "sweet principle of fat".[285]

With fatty acids, it's a base component of triglycerides (found in fats and oils).

Indeed, nowadays it is mainly generated as a co-product in processes which involve the production of fatty acids by hydrolysis of triglycerides or by trans-esterification with methanol, which leads to the production of fatty acid methyl esters (FAME), also called biodiesel.[286]

Every year about 20 Mt of fats and oils are processed by the chemical industries; this leads to a great abundance of glycerol on the market; about 1.54 Mt in 2015 and it is expected to rise to 2.5 Mt in 2020.[287]

These data underline the importance of glycerol as a low-priced molecule with a ready availability and strong potential to become a primary building block for the biorefinery.

For these reasons, glycerol chemical and physical properties have been widely investigated and several technologies have emerged as candidates for the conversion of glycerol into other useful chemicals.[288]

Indeed, glycerol is an extremely versatile compound, which can be used as a feedstock for the synthesis of a high number of molecules (e.g. ethers, esters, carboxylic acids, ethylene glycol, epichlorohydrin, syngas, oligomers, polymers etc).[289]

On the other hand the conversion of glycerol into the corresponding organic carbonate (glycerol carbonate GlyC), offers interesting opportunities to the chemical industry, since it can be prepared directly and in high yield from glycerol.

We will discuss in further detail about the interesting properties and application of GlyC in chapter 4.3.2.1.

1.4.3 *Ethanol*

Ethanol is the simplest aliphatic alcohol after methanol with a wide range of applications ranging from solvent and chemical intermediate to the food industries (alcoholic beverages).

It is a bio-based chemical and nowadays more than 90% of the overall ethanol is produced by fermentation processes of sugar and biomass, the remaining 10% is produced by chemical transformation of ethylene or as a by-product of other processes.[290,291]

Moreover, ethanol represents the most important bio-fuel for vehicles, indeed it does not need special modification of the engines and it is already applied on a large scale in many countries, especially in Brazil.[292]

Recent technology developments and strategic commercial partnerships have positioned ethanol as a feedstock for chemical productions, improving its platform potential. Ethanol and related alcohols (propanol, butanol) are intermediates for the productions of the corresponding olefins via dehydration, providing a direct interface between the biorefinery and the conversion infrastructure of the petrochemical industry.[293]

In this way vapor phase dehydration of ethanol at 400°C over alumina catalyst affords a 99.9% selectivity to ethylene at 99.5% conversion.[294]

Moreover ethanol can also be oxidized to commodity chemicals like acetaldehyde (by dehydrogenation) and acetic acid.

For example ethanol oxidation over gold nano-particles supported on titania gives nearly 95% selectivity to acetic acid at >90% conversion.[295]

1.4.4 n-butanol

1-butanol (or *n*-butanol) is an aliphatic linear alcohol. It is liquid and colorless at room temperature.

1-butanol can be produced by means of various synthetic pathways:[296]

- by propylene hydroformylation (oxo synthesis) with subsequent hydrogenation of the aldehyde formed, that nowadays represents the most important industrial process;
- by hydroxycarbonylation of propylene into 1-butanol (Reppe process);
- by a multi-step process (Guerbet reaction), in which ethanol is firstly (oxi)dehydrogenated into acetaldehyde, then an aldol condensation occurs in basic conditions to yield acetaldol, that can be dehydrated to crotonaldehyde in the presence of an acid, and lastly hydrogenated into 1-butanol;[297,298]
- by catalytic hydrogenation of CO into higher alcohols (not applied on an industrial scale);
- by biomass fermentation based on *Clostridium acetobutylicum*, a bacterium leading to the formation of an ABE mixture (acetone, butanol, ethanol) which gives the name to the process.

The ABE process in particular was largely used during the first half of the last century for the production of acetone used in the manufacture of explosives for the war

industries; today there is a renewed interest in this process, especially with the aim of producing bio-1-butanol as a biofuel and as intermediate for bio-chemicals.[299, 300]

Nowadays, various companies supply 1-butanol produced by fermentation and the research is focused on the improvement of the overall efficiency of the process by means of genetic modification of the bacteria in order to decrease the sensibility to alcohol concentration and replacing the starting materials (generally sugars) with cheaper ones, like lignocellulosic waste and algae.

Finally, the availability and relatively low cost of 1-butanol makes this compound an interesting bio-platform molecule for the synthesis of chemicals. Its versatile reactivity makes it a good starting material for the synthesis of aldehydes and ketones (mainly butyraldehyde by dehydrogenation at high temperatures), and alkenes (by dehydration). [301,302]

These are useful intermediates for the synthesis of a wide range of chemicals. For example butyraldehyde undergo reactions such as Tishchenko dimerisation, to form butylbutyrate.

Moreover 1-butanol can be successfully used as reactant in the gas-phase oxydehydration to yield other important chemical intermediates, such as maleic anhydride[303].

2 AIM OF THE WORK

The aim of the three-year work presented and discussed in this Thesis was to investigate on the synthesis and application of organic carbonates as reactive chemical intermediates.

More specifically, the main goals of this work were:

> ➤ To investigate the direct condensation between alcohols or diols and CO_2 in order to obtain organic carbonates and water, over heterogeneous catalytic systems based on mesoporous nanosilicas (MCMs) and functionalized zeolites (Cs-BEA$_{RIPP}$);
> ➤ To study the synthesis of DMC by the carbonate interchange reaction of ethylene carbonate (EC) and methanol with the former catalysts;
> ➤ To achieve the synthesis of pyrocatechol carbonate (PCC), target molecule of the PRIN project, by the carbonate interchange reaction of DMC with catechol, improving a reactive distillation system in order to optimize yield and selectivity toward the desired products;
> ➤ To investigate the peculiar reactivity of PCC for the synthesis of other organic carbonates (in particular symmetric aliphatic carbonates and glycerol carbonate), polycarbonates and polyureas;
> ➤ To achieve the synthesis of 2-hydroxymethyl-1,4-benzodioxane, an interesting intermediates for the pharmaceuticals industries;
> ➤ To study the reactivity of some of the organic carbonates as gas-phase alkylating agents of phenolics.

The reactions considered in this work follow the cascade pathway proposed in the scheme below (Scheme 2.1), in which the reagent of a reaction is the product of the previous one.
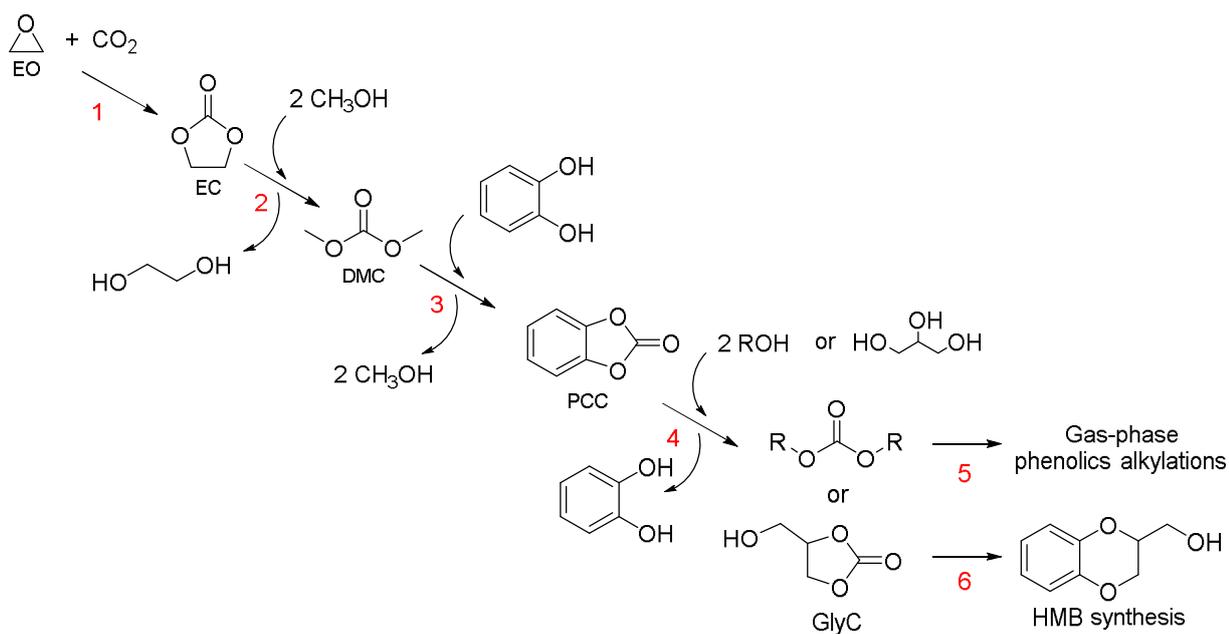
Scheme 2.1 Considered reactions: 1) cycloaddition of carbon dioxide and epoxide leading to the formation of cyclic carbonates (EC); 2) Carbonate Interchange Reaction (CIR) of EC and methanol to form DMC; 3) CIRs of DMC and alcohols or diols (e.g. catechol) to yield other carbonate (e.g pyro catechol carbonate, PCC); 4) CIRs of PCC and aliphatic alcohols or glycerol to yield symmetric carbonates or glycerol carbonate; 5) study of symmetric carbonates as alkylating agents for phenol; 6) reaction of GlyC and catechol to yield 2-hydroxymethyl-benzodioxane (HMB).

Each one of these reactions will be discussed in details in the following chapters.

Noteworthy, in many case (reaction 3 and 4) the co-products of the reactions (methanol and catechol) are the reagent of the previous step and theoretically they can be recycled to synthetize again the precursor (DMC and PCC).

3   MATERIALS AND METHODS

3.1 Compounds analysis and quantification

3.1.1 Gas-Chromatograph

The compounds of interest were analysed and quantified using a gas-chromatograph Thermo Focus GC model equipped with a non-polar capillary column Agilent HP-5 (5% phenyl – 95% methylsiloxane) having these dimensions: 25m x 320µm x 1.05µm.
The injector was maintained at a temperature of 280°C in the split mode (30:1), the carrier gas was nitrogen (1.2 mL/min in column).
The volume of solution injected for each analysis was 0.5 µL.
The standard programmed temperature used is described below:
the oven remains in the isotherm at 50 ° C for two minutes, then starts the ramp of 20 °C/min to reach 280 ° C where it stays isothermally for five minutes.

Each compounds was calibrated in an appropriate range of concentrations, in order to obtain a response factor, using an appropriate internal standard (decane or octane) according to the formula:

$$\frac{A}{Astd} = f * \frac{mol}{mol\text{std}}$$

3.1.2 GC-MS and ESI-MS

The unknown products were also analysed by means of electrospray ionization mass spectroscopy (ESI-MS) and GC-MS.
The GC-MS used was a Agilent Technologies 6890 GC coupled with a mass spectrometer Agilent Technologies 5973 equipped with a non-polar column (5% Phenyl - 95% methylsiloxane), 30m x 250 µm x 1.05 µm.
Helium was used as carrier gas at a flow rate in the column equal to 1ml/min; the injector was maintained at a temperature of 250 ° C in the split mode (50:1); total flow was 23.9 mL/min. The volume of solution injected was 0.5 µL and the standard temperature program was the same as that used for products analyses: isothermal step at 50 ° C for two minutes, then the ramp of 20 °C/min until reach 280 ° C, final isothermal step for 5 minutes.

3.2 Catalysts

3.2.1 Commercial catalysts

Some of the catalysts used in this thesis were purchased from commercial suppliers. In particular:

- sodium methoxide ($NaOCH_3$, Sigma-Aldrich, reagent grade 95%), chosen as homogeneous basic catalyst for the CIRs;
- "low surface area" magnesium oxide (MgO, Acros organics) that was calcined again at 450°C for 5 hours in order to clean the surface from carbonates;
- alumina (γ-Al_2O_3 98%, Puralox SCF140, SASOL germany GmbH), chosen as heterogeneous acid catalyst.

3.2.2 "High area" MgO and Mg/Al/O synthesis

Magnesium oxide has been synthesized by means of a well-known precipitation method in which $Mg(NO_3)_2*6H_2O$ dissolved in water was used as metal precursor (1 mol/L in distilled water), and the solution was then added dropwise to a second solution of $Na_2CO_3*10H_2O$ (1 mol/L in distilled water), under magnetic stirring, at 60°C.

The pH was maintained between 9.8 and 10.2 during all the synthesis and monitored with an Amel Instrument 380, calibrated with two buffers at pH 7 and 13.

The obtained magnesium hydroxide was filtered, washed with distilled water and dried overnight at 110°C. The material was then crushed and calcined at 450°C for 5 hours.

The Mg/Al mixed oxide with a metal ratio of Mg:Al=3:1 was synthesized by a co-precipitation procedure typically used for hydrotalcites synthesis.

This method consists in a simultaneous precipitation of the metals hydroxides at controlled pH and temperature.

In this way, a solution of $Mg(NO_3)_2*6H_2O$ and $Al(NO_3)_3*9H_2O$ (in a molar ratio of 3 to 1, cations concentration 1 mol/L in distilled water) was added dropwise under stirring to a solution containing $Na_2CO_3*10H_2O$ (1 mol/L in distilled water).

Sodium carbonate was used in excess compared to the stoichiometric amount required for the formation of the hydrotalcite.

The pH was maintained between 9.8 and 10.2 during all the synthesis and monitored with an Amel Instrument 380, calibrated with two buffers at pH 7 and 13.

The obtained hydrotalcite $Mg_6Al_2CO_3(OH)_{16} \cdot 4(H_2O)$, was filtered and washed with distilled water (in order to remove the nitrates), and dried overnight at 110°C.

The precursor was then crushed and calcined at 450°C for 4 hours in order to produce the desired mixed oxide.

3.3 Catalysts characterisation

3.3.1 X-ray diffraction analyses (XRD).

XRD powder patterns of the catalysts were recorded with a Ni-filtered Cu Kα radiation (λ = 1.54178 Å) on a Philips X'Pert vertical diffractometer equipped with a pulse height analyzer and a secondary curved graphite-crystal monochromator.
The analysis of the phases present in the patterns were performed using the Bragg's Law:

$$n\lambda = 2d \sin\theta$$

in order to calculate the crystalline d values, and compare them with those reported in the literature and collected in the ICDD database (International Centre for Diffraction Data).

3.3.2 BET: specific surface area analysis.

The BET surface area of the catalysts was determined by N_2 absorption–desorption at liquid N_2 temperature using a Sorpty 1750 Fison instrument.
0.2 g of the sample was typically used for the measurement, and the sample was outgassed at 150 °C before N_2 absorption.

3.3.3 Thermogravimetric/differential thermal analyses (TGA/DTA).

TG/DT analyses of the molecular sieves were performed with a SDT Q 600 instrument, in order to evaluate their methanol adsorption capacity. 30 mg of the sample was typically employed for the measurement, at temperatures from room temperature up to 220 °C, with a heating rate of 2 °C/min, in a nitrogen flux.

3.4 In-situ Infrared spectroscopy

The reagents adsorption on the catalytic systems has been investigated by means of in-situ IR spectroscopy.

The spectroscopy study on the direct condensation of carbon dioxide and alcohols reported in Chapter 4.1 has been performed as described below in collaboration with the University of Torino.

FT-IR spectra were collected at 2 cm^{-1} resolution on a Bruker Vertex 70 spectrophotometer, equipped with a MCT cryodetector, at "beam temperature" (BT), *i.e.* the temperature reached by samples under the IR beam. The samples were examined in the form of self-supporting pellets mechanically protected with a pure gold frame. The experiment were performed using a home-made quartz IR cell, equipped with KBr windows and characterized by a very small optical path (2 mm). The cell can be connected to a conventional high-vacuum glass line, equipped with mechanical and turbo molecular pumps (capable of a residual pressure p < 10^{-4} mbar), that allows to work in a controlled atmosphere.

The reported in-situ FT-IR experiment were obtained following this procedure (IR spectra were collected at each step):

1) Before reagents adsorption, all samples were activated in vacuum at 150°C for 2 hours inside the IR cell using a dedicated vacuum glass line.

2) The IR cell was connected to the instrument glass line.

3) Vapours of ethylene carbonate were put in contact with the catalyst by melting the solid reagent inserted in a special glass balloon connected to the IR cell.

4) Methanol vapours (40 mbar) were introduced inside the cell after the stabilization of the IR signals of ethylene carbonate. Liquid methanol was inserted in a special container connected to the glass line.

5) The reaction was followed by collecting spectra every minute.

The adsorption of catechol over MgO, described in Chapter 4.2 has been investigated by means of infra-red spectroscopy and the IR range investigated was between 4000 and 200 cm^{-1} (NIR Near Infra-Red); a Perkin Elmer Spectrum One FT-IR spectrometer was used.

Moreover, phenol adsorption over MgO has been investigated between 4000 and 200 cm^{-1} (NIR Near Infra-Red), using a Perkin Elmer Spectrum One FT-IR spectrometer.

In particular the IR spectra discussed in Chapter 4.4 were recorded using a sample of catalyst placed inside an apparatus maintained under vacuum, in order to pretreat the sample and facilitate the desorption of light impurities and water adsorbed on the

surface; subsequently, the probe molecule (phenol in our case) was adsorbed and desorption was then performed. The instrumentation used is shown in Fig. 3.1.

Fig. 3.1 The in-situ infrared apparatus used to study the adsorption of reactants on catalysts in vacuum

The spectra were recorded following the steps reported below:

1) The catalyst to be examined, in powder form, was pressed in the form of a thin rectangular tablet and placed in a "slide" of quartz;

2) Such "slide" was placed in a cylindrical tube of quartz, wrapped in a heating band to its central part and terminating with a window consisting of two tablets of KBr, through which the beam of the incident radiation passed. The "slide" was skated appropriately in such a way to allow the catalyst to intercept the optical path, or positioned at the level of the heating bands;

3) Such a cylindrical tube of quartz was an extreme of the vacuum line, which by means of suitable fittings and taps glass seal, was provided with ampoules in which the reagents to be adsorbed were introduced. There were also two glass traps immersed in liquid nitrogen, which protected the pump from the diffusive contact with the chemical species that were progressively desorbed from the catalyst;

4) The vacuum line as a whole was placed on a cart that allows you to properly place the sample within the instrument so as to intercept the optical path of the IR source. The vacuum line was connected upstream with two vacuum pumps: a mechanical pump that serves to push the vacuum until values around 10^{-3} mbar and a diffusive pump which allows to reach the high vacuum until 10^{-6} mbar .

5) After a vacuum between 10^{-5} and 10^{-6} mbar was reached, and after suitably positioning the trolley with the vacuum line on the optical path, the pre-treatment of the sample was started by heating it while checking, by means of IR, that all the impurities deposited on the surface had been removed.

6) Afterwards, the sample was cooled and processed by adsorption of the molecule of interest.

7) When the IR spectra confirmed the adsorption of a significant amount of the probe molecule, the desorption step was started, by heating the sample and recording the IR spectra at regular temperature intervals.

4 RESULTS AND DISCUSSION

4.1 Condensation of alcohols and CO_2

4.1.1 Introduction

This Chapter deals with the investigation on the possibility to replace the cycloaddition between the highly reactive epoxides and CO_2 with the direct condensation between different alcohols and CO_2 in relatively mild conditions (below the supercritical point), using various catalytic systems.

First, we decided to investigate the possibility to use a well-known low-temperature solid sorbent already used in the carbon capture and storage (CCS): amino functionalized mesoporous nanosilicas, SBA-15.

These systems are of particular interest because they are characterized by the presence of large pores; both porosity and basic groups density on the surface are critical features for the effectiveness of CO_2 sequestration.

Moreover, the possibility to use the same systems for both CO_2 capture and its conversion to high added-value chemicals, represents the obvious advantage in the aim to simplify the whole process, opening the possibility to perform the capture and the reaction in the same plant.

Another heterogeneous catalyst based on a cesium zeolite (described in Chapter 4.1.5) has been investigated for the same reactions.

This study was performed in collaboration with other Italian Universities, in particular:

- The University of Alessandria for the synthesis and characterization of ammino-functionalized mesoporous nanosilicas;
- The University of Torino for the synthesis and characterisation of the Cs-modified zeolite;
- The University of Torino, for the in-situ IR reactivity study of CO_2 and carbonates over nanosilicas.

In our Department, we have carried out the reactivity study of the direct condensation between alcohols and CO_2 and for the carbonate interchange reactions (CIRs) between EC and methanol to yield DMC.

4.1.2 The high-pressure reaction vessel

The reactions described in this chapter were carried out at high pressures in a batch reactor: a stainless steel autoclave (internal volume 50ml).
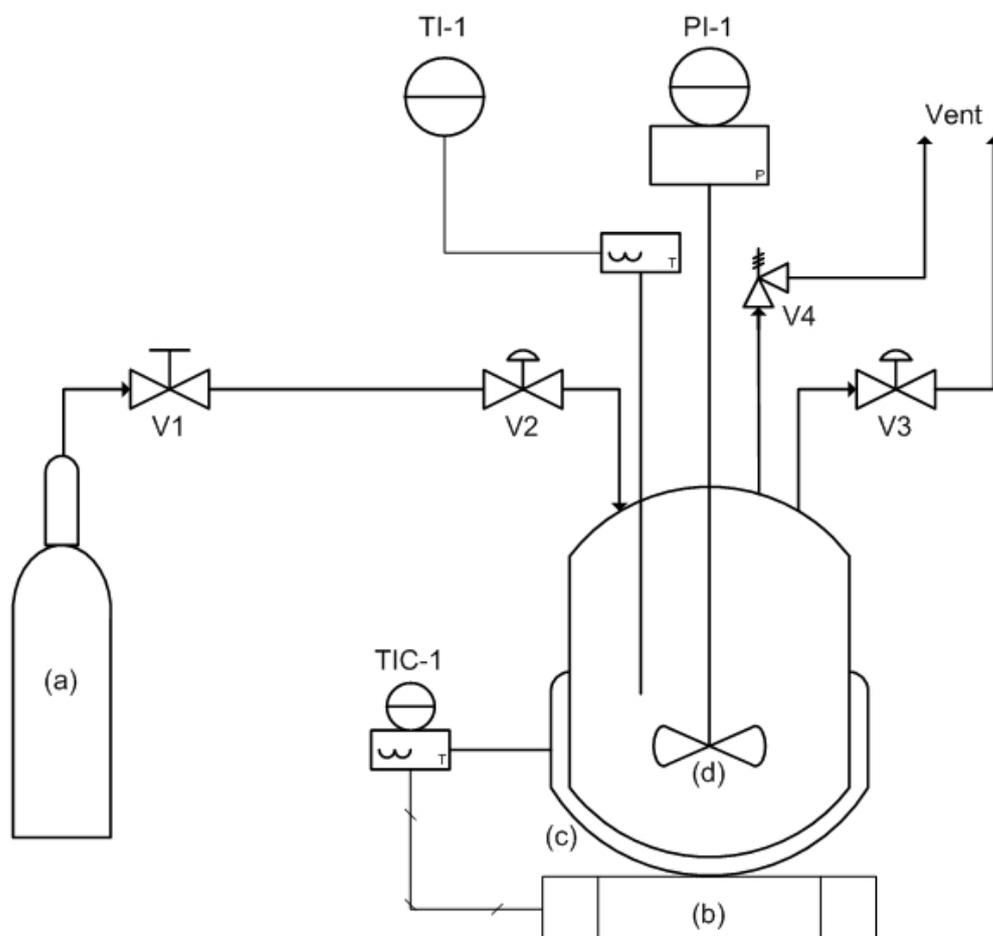The reaction apparatus is shown in the following scheme.

Fig. 4.1 High-pressure batch reactor system, stainless steel autoclave schematization: a) CO_2 cylinder or in some cases N_2 cylinder, V1 shut-off valve, V2 high-pressure needle valve (IN), b) heating plate controlled by a thermocouple (TIC-1), in order to obtain the desired reaction temperature of the c) aluminum heating block, and d) magnetic stirring; V3 high-pressure needle valve (OUT) and V4 safety relief valve.

In a standard reaction procedure the reagents and the catalyst are charged inside the autoclave, then the system is sealed and purged with the desired gas (CO_2 or N_2), finally the reactor is pressurized at the desired starting pressure with the same gas and the heating is started.
The time zero of the reaction is taken when the reactor reaches the desired reaction temperature.

4.1.3 Functionalized mesoporous nanosilicas (SBA-15) synthesis

The mesoporous silicas SBA-15 (Santa Barbara Amorphous number 15) were synthesized for the first time in 1998 in the Santa Barbara University (California).[304] These are materials characterized by an highly ordered structure with large cylindrical channels (from 6,5 to 15 nm), that is the right size to allow the diffusion and adsorption of big molecules, and a thickness of the wall from 3,1 to 4,8 nm. Finally, a series of smaller pores (ca. 2 nm sized) link together the bigger channels.[305,306,307]

This peculiar structure makes possible to obtain materials with high surface area (690-1040 m^2/g).

In particular, we have studied three different SBA-15 functionalized with different organic silanes, as shown in Fig. 4.2:

a) 3-aminopropyltrimethoxysilane (APTS);
b) 3-(2-aminoethyl) aminopropyltrimethoxysilane (EAPTS);
c) 3-[2-(2-aminoethyl)aminoethyl] aminopropyltrimethoxysilane (PAPTS).
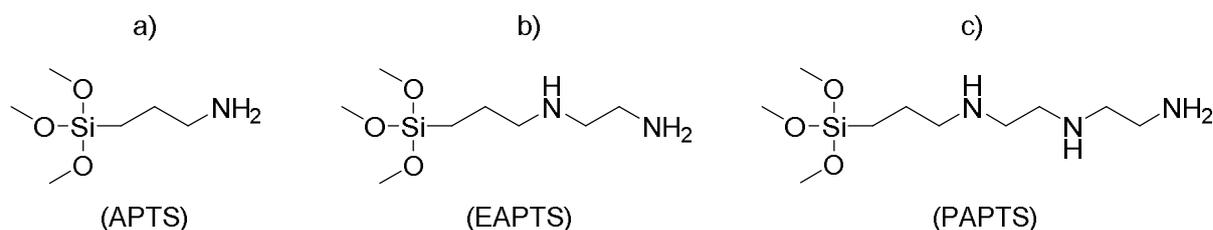
Fig. 4.2 Organic silanes used for the synthesis of functionalized SBA-15.

These materials were synthesized by means of two different methods:

➢ post-synthesis surface grafting;
➢ one-pot synthesis.

In the first case, the SBA-15 was synthesized as described by Zhao et al. using a sol-gel methodology.[304]

The commercial block copolymer Pluronic P123 (8 grams), used as the template, was dissolved in 60 mL of deionized water at 308K for 24 hours.

The gel obtained was acidified with 240 mL of a HCl 2M solution and then tetraethyl orthosilicate (TEOS, 17g) was added and stirred for 24 hours.

The obtained gel underwent a hydrothermal treatment (24 h at 373K), then it was filtered, washed with deionized water and dried at 393K for 36 hours.

Finally the material was calcined at 823K for 5 hours in an air flow (100 mL/min) in order to remove the organic template and obtain the SBA-15 structure.

The grafting methodology used was the same for the synthesis of all samples investigated (APTS, EAPTS, PAPTS); it is schematically shown in Scheme 4.1.
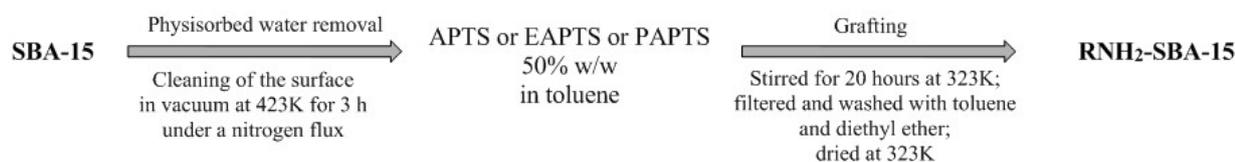

Scheme 4.1 Grafting procedure for the synthesis of amino-functionalized mesoporous nanosilicas.

The main drawbacks of the post-synthesis grafting method are the decrease of the channel dimension (and porosity), and the inhomogeneous distribution of the amino silanes on the catalyst surface.[308]

Another methodology for the production of amino-functionalized SBA-15 is the one-pot synthesis.
In this synthetic pathway the organic silanes are added to the organic mixture before the drying and calcination steps, as reported in the following scheme (Scheme 4.2).
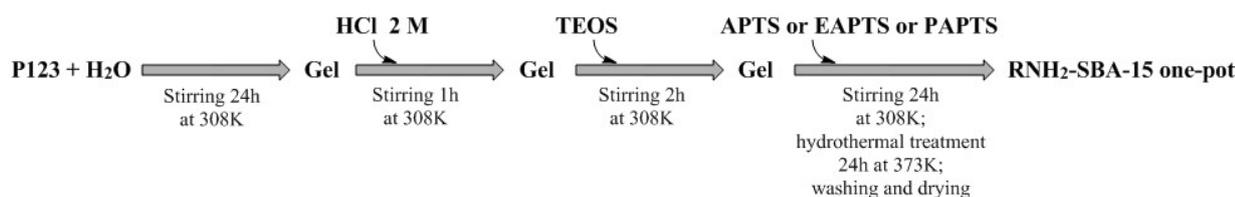
Scheme 4.2 One-pot synthesis of amino-functionalized mesoporous nanosilicas.

The commercial block copolymer Pluronic P123, used as the template, was dissolved in 15 mL of deionized water at 308K for 24 hours.
The gel obtained was acidified with 60 mL of a HCl 2M solution, stirred for one hour and then tetraethyl orthosilicate (TEOS, 3.8g) was added, and the sol ws stirred for 2 hours more.
A 10 mol% of the desired organo silane was added to the gel and stirred for 24 hours. Then the mixture underwent a hydrothermal treatment (24 h at 373K), it was filtered, washed with deionized water and dried at 393K for 36 hours.
Finally, the material was extracted with ethanol in order to remove the excess of organic template and dried again at 393K for 36 hours.

Many papers report that, with this method, the introduction of the organic amino silanes leads to a decrease of the overall structural order of the nanosilicas.[309]
However, this problem can be limited by allowing the TEOS hydrolysis for longer time and by changing the temperature and growing time of the gel mixture.[310,311]

4.1.4 Mesoporous nanosilicas (SBA-15) characterisation

All the catalytic systems synthesized as described in the previous chapter were characterized by means of XRD, TEM, IR, porosimetry and thermogravimetric analysis.

The pristine SBA-15 obtained with the first synthesis method (before grafting) were characterized as reference material for the modified SBA-15 materials.

Both the TEM and the powder X-ray diffraction (XRD) analysis (Fig. 4.3) show the typical regular hexagonal structure of SBA-15 silicas.
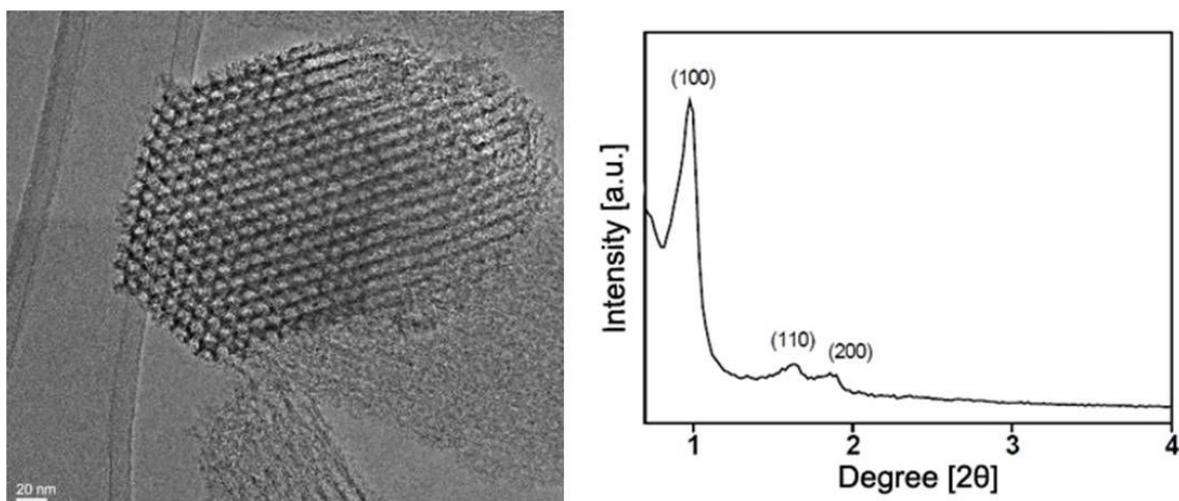
Fig. 4.3 TEM image of the pristine SBA-15 (left) and the corresponding XRD pattern (right).

In particular, the XRD analysis shows the three typical reflections at 0.9, 1.5 and 1.8 °2θ related to the crystal plane (100), (110) and (200) of SBA-15.[312]

Moreover, the TEM images better shows the porous structure with an average particle dimension of 150 nm and a regular pattern of hexagonal channel with an inner diameter of 5-10 nm.

The porosimetry analysis was performed in order to achieve information on the surface area and a more precise value of pore volume and diameter (Fig. 4.4, Table 4.1). The materials were pretreated at 220°C for 6 hours under an He flow, before performing the measurements using N_2 at 77K.
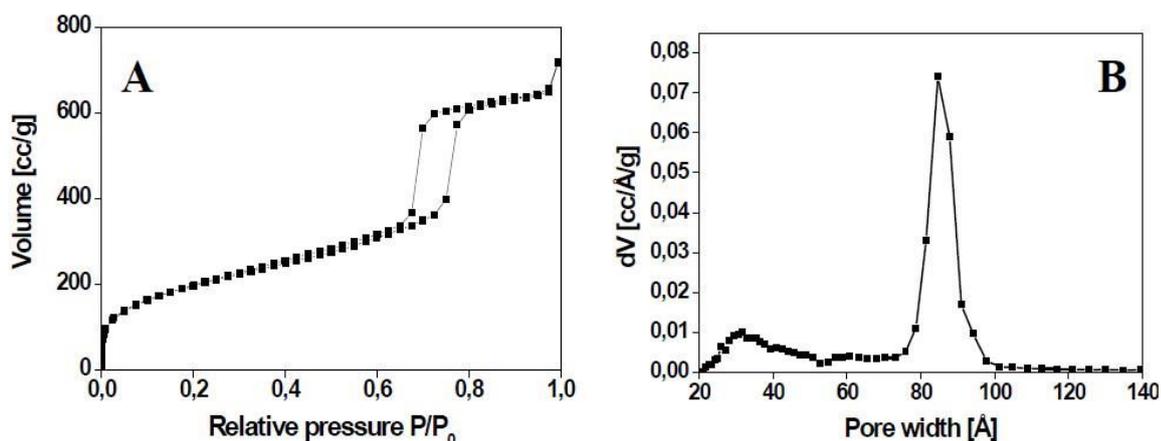
Fig. 4.4 Porosimetry analysis adsorption-desorption curves of nitrogen at 77K related to the relative pressure (P/P$_0$) from 1x10^{-6} to 1 (A, left); pores distribution obtained with the Montecarlo DFT method (B, right).

Catalyst	Surface area (m²/g)	Channel diameters (nm)	Secondary pores diameters (nm)	Pores volume (cc/g)
SBA-15	720	8.5	1-4	0.98

Table 4.1 Surface area and pore dimensions of pristine SBA-15.

The SBA-15 were then characterized by means of both infrared spectroscopy and thermogravimetric analysis (Fig. 4.5).
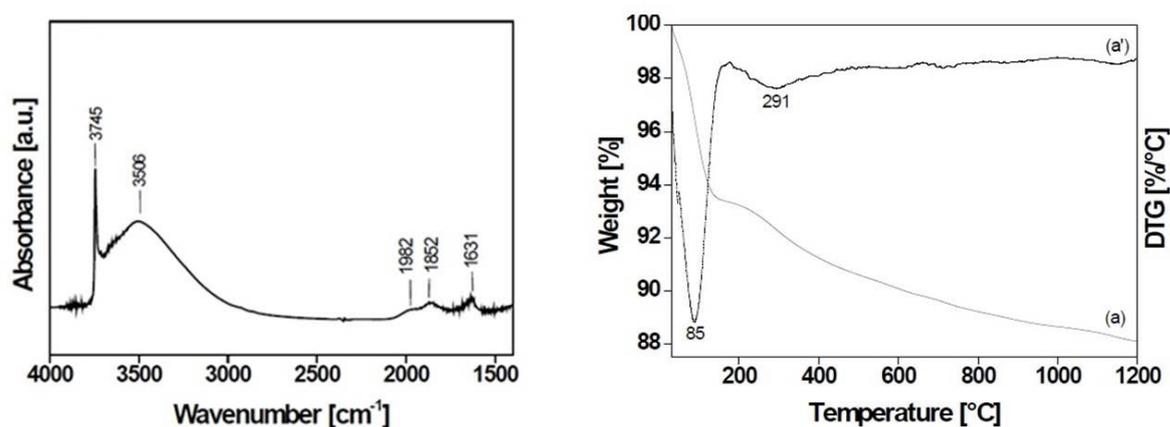
Fig. 4.5 Infra-red spectra of SBA-15 after pretreatment in vacuum in order to remove the physisorbed water (left); SBA-15 TGA analysis (a) and the related derivative (a'), obtained in an Argon flow of 20ml/min, 5°C/min from 30 to 1200°C.

Both analysis are important in order to check for the presence (IR) of silanol groups (Si-O-H) and to estimate their amount (TGA).

These sinalos are very important because are the active site for the "grafting" (condensation) reaction with the organic silanes.

In particular, the narrow IR band at 3745 cm^{-1} is assigned to the isolated silanol groups on the surface, while the broad band with a maximum at 3506 cm^{-1} is related to the perturbed Si-O-H close enough to each other so to develop an interaction via hydrogen bonding. Finally the broad bands at lower wavenumbers are related to the Si-O-Si overtones.[304]

On the other hand, the thermogravimetric analysis allowed us to quantify the physisorbed water (around 7% w/w at 85°C) and the overall weigh loss due to the condensation of the silanol groups (5% w/w from 180 and 1200°C).

With the following equation:

$$ n\left(\frac{OH}{g}\right) = \frac{\frac{\%OH}{100}}{M.W.(H2O)} * NAvogadro * 2 $$

it is possible to estimate the number of silanol groups (ca. $3{,}67*10^{21}$) per gram of silica and by dividing it for the surface area (720 m^2/g), we find an average of 5,1 Si-OH/nm^2.

4.1.4.1 Characterisation of functionalized mesoporous nanosilicas (RNH$_2$-SBA-15): grafting

The materials functionalized by the post-synthesis grafting method were characterized and compared with the starting (non-functionalized) SBA-15.

In particular we will consider the following amino-modified materials:

- SBA-15/APTS;
- SBA-15/EAPTS;
- SBA-15/PAPTS.

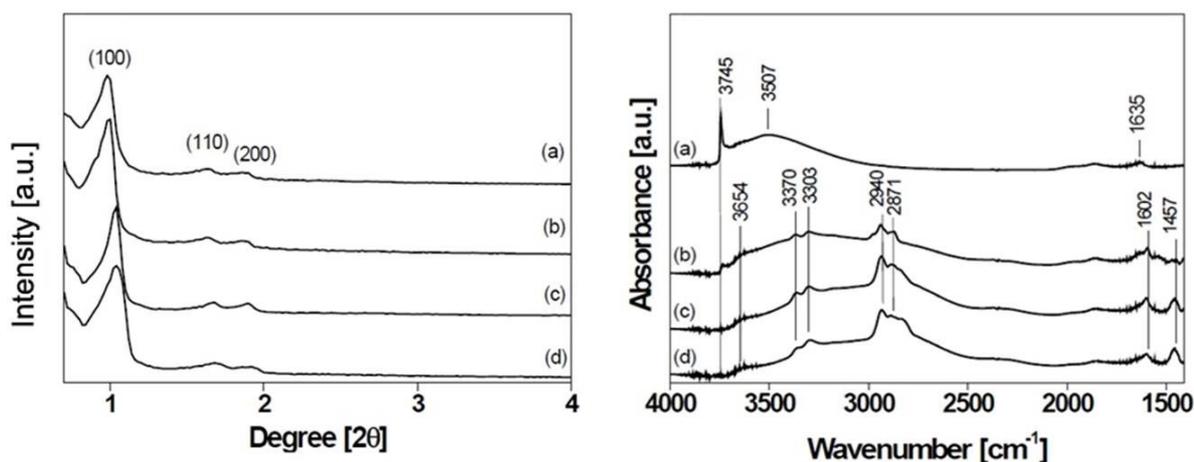The corresponding powder XRD and IR analysis are reported in the next page.

Fig. 4.6 Powder XRD analysis (left) and IR spectra (right) of the different nanosilicas: a) SBA-15 (reference); b) SBA-15/APTS; c) SBA-15/EAPTS; d) SBA-15/PAPTS.

From the similarity between the XRD patterns of the functionalized silicas and the reference starting material (SBA-15), we can assume that the grafting process did not affect the structure order.

Moreover, the effectiveness of the grafting process is demonstrated by IR spectra.

Indeed, the intensity of both the sharp band at 3745 cm^{-1} and the broad band centred at 3507 cm^{-1} related to the reactive Si-OH groups, were significantly decreased, an event which demonstrates the occurrence of the condensation with the silanes.

Furthermore, bands at 3370, 3303 and 1602 cm^{-1} are related to the asymmetric, symmetric stretching and bending vibrations of the NH$_2$ groups, respectively; the 2940, 2871 and 1457 cm^{-1} bands are attributable to the asymmetric and symmetric stretching and bending vibrations of the aliphatic chains CH$_2$ groups, respectively.[309]

All the above described features prove that the grafting process was successful.

Of course, we are modifying the catalytic surface by functionalising the organic chains with the desired reactive amino groups; therefore we can expect a modification of both the surface area and the porosity features of the material.

The results of the porosimetry analysis, conducted in the same way as reported in Fig. 4.4, are shown in the following table.

Catalyst	Surface area (m²/g)	Channel diameters (nm)	Secondary pores diameters (nm)	Pores volume (cc/g)
SBA-15	720	8.5	1-4	0.98
SBA-15/APTS	563	8.0	/	0.94
SBA-15/EAPTS	360	7.8	/	0.57
SBA-15/PAPTS	236	7.0	/	0.41

Table 4.2 Surface area and pore dimensions of SBA-15, pre and post functionalization by grafting with different organic silanes.

As expected, both the surface area and the pores volume decreased with the corresponding increase of the silane length, in the order APTS<EAPTS<PAPTS.

Of course, also the channel diameters followed the same trend, while the secondary pores with size between 1 and 4 nm disappeared in the grafted systems probably due to an occlusion of these smaller cavities.

Again, the TGA analysis is fundamental in order to quantify the number of the amino groups with which we have functionalized the materials surface.

In the following figures, the TGA analysis of the three functionalised systems are reported and compared with that one of the non-functionalized SBA-15 as reference material.
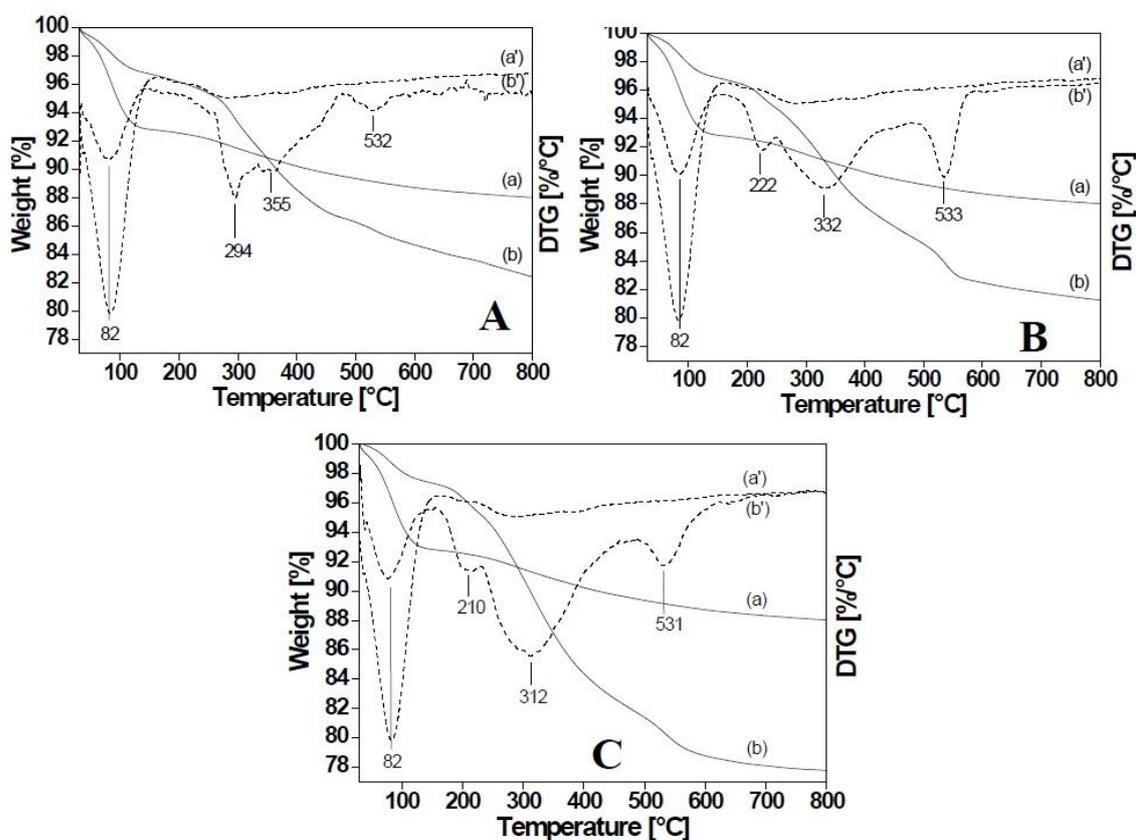
Fig. 4.7 TGA analysis of the functionalized SBA-15 nanosilicas.
A: SBA-15/APTS. B: SBA-15/EAPTS. C: SBA-15/PAPTS.
The grafted silicas are reported both as such (b) and as derivative curve (b'); pristine SBA-15 is reported as reference material, named (a) and its derivative curve (a').
All the analysis were carried in an oxygen flow of 100ml/min, temperature ramp 10°C/min, from 30 to 800°C.

All the samples showed similar trends:

first, it is possible to observe a weight loss centred at 82°C, due to physisorbed water desorption; then, the weight loss seen in the 180-600°C range is due to the decomposition of the silanes, starting from the final part of the aliphatic chain (around

300°C) and ending with the silane part covalently bonded to the support (around 530°C).

Starting from the molecular weight of the organic silanes used for SBA-15 functionalisation, and from the surface area analysis, we were able to calculate the concentration and distribution of silanes and amino groups on grafted materials (Table 4.3).

Catalyst	Surface area (m²/g)	Silanes concentration (mmol/g)	Number of amino groups/nm²
SBA-15/APTS	563	2.4	0.88
SBA-15/EAPTS	360	1.7	2.17
SBA-15/PAPTS	236	1.6	2.93

Table 4.3 Silanes concentration and amino groups number per square nanometer of the grafted nanosilicas surface.

It is worth noting that the increase of length of the silanes aliphatic chain corresponds to a decrease of their concentration on the catalyst surface.

This is probably due to the steric hindrance that limits the diffusion of silanes, that cannot reach all the reactive silanols on the catalyst surface.

4.1.4.2 *Characterisation of functionalized mesoporous nanosilicas (RNH₂-SBA-15): one-pot synthesis*

The nanosilicas obtained by the one-pot synthesis were characterized by means of the same techniques used for the grafted materials.

Although this method is an easier synthetic pathway for the preparation of amino-functionalized SBA-15, it shows two problems:

- the inclusion of silanes during SBA-15 structure formation that led to a loss of the structural order; this is evident from the powder XRD pattern (Table 4.8, left);
- the use of acid conditions during the synthesis (in order to make the TEOS hydrolysis easier) led to the formation of several protonated amino groups (NH_3+), as proven by the appearance of IR bands at 1618 and 1508 cm^{-1} (NH_3+ asymmetric and symmetric stretching, respectively); this implied a considerable loss of the number of basic sites needed for our reactions (Fig. 4.8, right).
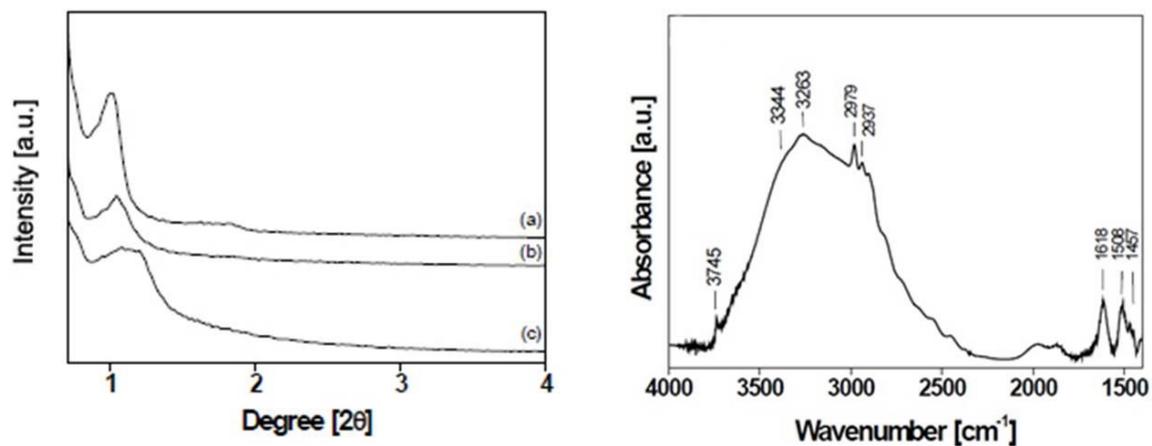
Fig. 4.8 XRD pattern (left) and FT-IR spectra (right) of the functionalized silicas obtained by the one-pot synthesis

Because of these reasons, we decided to focus our research work on the materials functionalized by the post-synthesis grafting method.

4.1.5 Cs-BEA synthesis and characterization

This material was synthesized and characterized by Dott. Maria Botavina and Prof. Gianmario Martra (Torino University).

They started from an acid form of the zeolite (H-BEA with Si/Al ratio of 16,5); this zeolite is characterized by a three-dimensional 12-membered-ring channel structure with pores diameter of around 7 Å (Fig 4.9), large enough to allow the easy diffusion of a wide range of organic molecules.
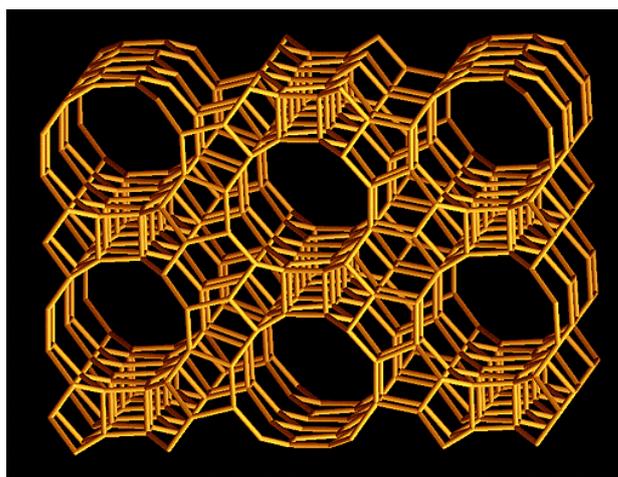
Fig. 4.9 H-BEA 3D structure.

In particular, they decided to add basic properties to this material by adding Cs+ atoms inside the porous structure by means of ion exchange, and then by adding caesium oxide nanoparticles by means of wet impregnation of the zeolites.

The ion exchange procedure was conducted by treating the H-BEA under stirring in a solution of 0,5M CsCl (three times, 1 hour at 50°C). After that, the solid was filtered, washed several times with water and dried at 100°C for 8 hours.

From elemental analysis, a Cs/Al molar ratio equal to 0.92 was obtained (sample named $Cs_{0,92}$-BEA).

The catalyst obtained was then impregnated with a CsOH solution (Wet Impregnation), under stirring at 80°C, obtaining a catalyst with an increased Cs/Al molar ratio equal to 1.6 (sample named $Cs_{1,6}$-BEA).

4.1.6 Condensation of alcohols and CO_2

4.1.6.1 High-pressure catalytic tests

The materials described in the previous chapters were investigated as catalysts for the direct condensation between alcohols and CO_2.

This is a strictly thermodynamically-limited reaction that usually needs harsh conditions, active catalysts and efficient dehydrating agents, as described in the introduction part of this Thesis (Chapter 1.3.4.2).

Moreover, we decided to test these reactions in relatively mild conditions, below the supercritical point of CO_2.

However, although the reactivity of several substrates (methanol, ethanol, 1-butanol, phenol, catechol, 1,2-propandiol and glycerol) was investigated with all the catalysts described in the previous chapters (functionalized nano-silicas SBA-15/EAPTS, SBA-15/PAPTS, SBA-15/APTS and zeolite $Cs_{1,6}$-BEA), under a wide range of reaction conditions (by changing the reaction temperature from 80 to 100°C, and loading the autoclave with a starting pressure ranging from 20 to 50 bar of CO_2), no products were formed.

It is evident that CO_2 needs harsher conditions in order to be activated for these reactions. Furthermore, aware of the strict thermodynamic limitations, the catalytic tests were repeated in the presence of different drying agents, both inorganic (Na_2SO_4) and organic (nitriles and 2,2-dimethoxypropane), however without recording any appreciable improvement.

In order to better understand the completely lack of reactivity observed with these catalysts, a complete in-situ IR analysis of the reaction between methanol and CO_2 over the functionalized SBA-15 was undertaken; results are described in the following chapter.

4.1.6.2 *In-situ IR spectroscopy analysis of the condensation between* CO_2 *and alcohols*

In situ FT-IR spectroscopy was employed to study the reaction between carbon dioxide and methanol, aimed at the direct synthesis of dimethyl carbonate in the presence of SBA-15/APTS. The FT-IR spectra collected during each reaction step are reported in Fig. 4.10, recorded in the 1800-1300 cm^{-1} spectral range.
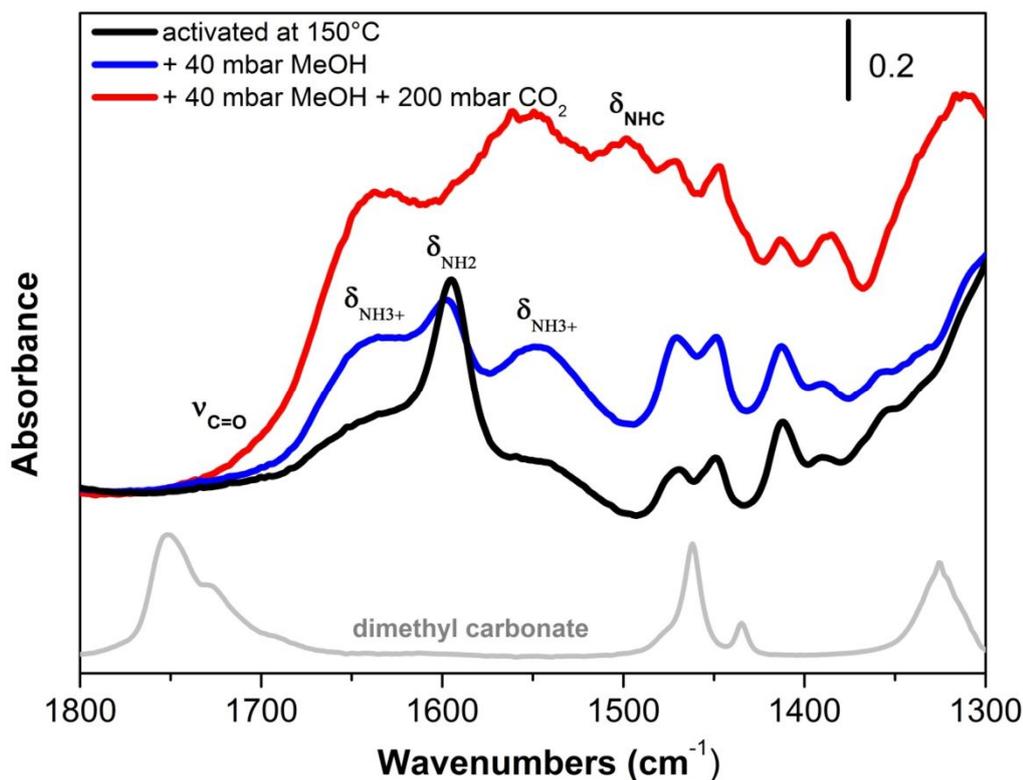

Fig. 4.10 Absorbance FT-IR spectra of SBA-15/APTS, in the 1800-1300 cm^{-1} spectral range after activation in vacuo at 150°C (black), after contact with 40 mbar of methanol (blue) and after contact with 40 mbar of methanol and 200 mbar of CO_2 (red). The spectrum of liquid dimethyl carbonate is reported in light grey.

The spectrum collected after the activation of the material is reported in black, recorded in the 1800-1300 cm^{-1} spectral range. The spectrum is dominated by a band located at ~ 1600 cm^{-1} attributable to the NH_2 deformation (δ_{NH2}) of the amino group grafted to the silica surface. On the contrary, the absorption bands at 1630 and 1550 cm^{-1} are attributed to the asymmetric and symmetric δ_{NH3+} vibrations, respectively, indicating the presence of a small fraction of amino groups in the protonated form. Bands falling between 1500 and 1400 cm^{-1} can be eventually attributed to the CH_2 bending vibrations of the amino-propyl chain.

The dimethyl carbonate synthesis was carried out starting from the pre-adsorption of methanol vapors on the catalyst (see the blue spectrum). The admission of 40 mbar of

methanol led to the perturbation of the band at ~ 1600 cm^{-1} (NH$_2$ deformation) and to the parallel increase of intensity of bands ascribed to NH$_3^+$ bending vibrations (1630 and 1550 cm^{-1}). These spectral modifications are indicative of the dissociative adsorption of methanol to form the alcoholate species (R-O$^-$), proving an efficient activation of methanol on catalyst basic sites.

After the contact with 200 mbar of CO$_2$, multiple overlapped absorptions appeared in the 1700-1400 cm^{-1} region, a proof for the formation of the carbamate species (see the red spectrum in Fig. 4.10), as a result of the interaction of carbon dioxide with the amine-grafted SBA-15.

In any case, no bands due to the formation of dimethyl carbonate were shown, even after a prolonged contact (till 24 hours) between methanol and carbon dioxide and/or after the increase of the reaction temperature (till 140°C). Therefore, although the material is able to activate both methanol (forming the corresponding alcoholate) and CO$_2$ (forming the more reactive carbamate), the direct synthesis of the linear organic carbonate did not occur, confirming the scarce catalytic results reported in the previous chapter.

4.1.7 Synthesis of DMC by CIR of Ethylene Carbonate (EC) and methanol

Dimethyl carbonate (DMC) can be synthesized by a two-step reaction, in which the first step is carried out starting from ethane epoxide and CO_2 in order to obtain a cyclic carbonate (cycloaddition reaction); then the cyclic carbonate is separated and it can undergo two consecutive CIRs with methanol in order to yield firstly the 2-hydroxyethyl methyl carbonate (from here onwards referred to as "intermediate"), and finally the desired DMC and ethylene glycol (EG) as the co-product.

The overall synthesis is reported in the following scheme (Scheme 4.3).
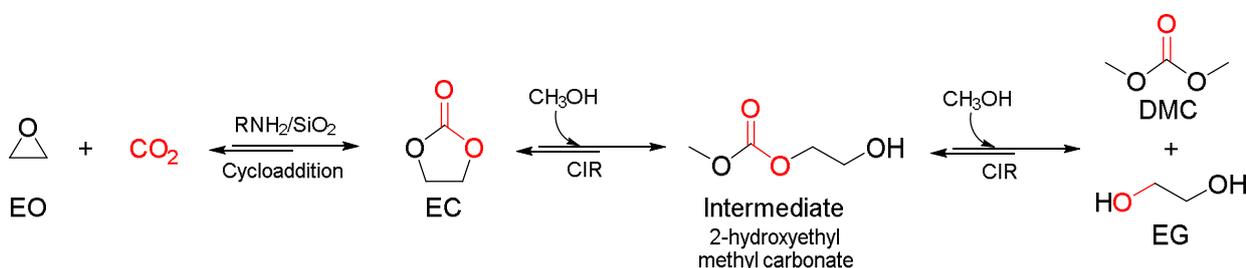
Scheme 4.3 Cycloaddition reaction of CO_2 and ethylene oxide (EO) to yield ethylene carbonate (EC); EC can undergo further carbonate interchange reaction with methanol to yield DMC and ethylene glycol.

Nowadays, this process is conducted in a two, separated steps after the cyclic carbonate separation and purification.

Amino-functionalized silica catalyst has been investigated by Zhang et al for the synthesis of cyclic carbonates by reacting CO_2 (20 bar) and epoxide at 150°C in the first step of this process (also described in the introduction Chapter 1.3.4.1).[313]

From in-situ IR spectroscopy experiments, reported in the previous chapter, the efficient activation of methanol over the basic sites of the catalyst to yield a methoxy species was demonstrated.

Therefore we decided to investigate our RNH_2-SBA-15 catalyst for the second step of DMC synthesis: the CIRs between EC and the activated, deprotonated, methanol.

Theoretically, the use of a catalytic system able to promote both steps, opens the possibility to investigate the one-pot synthesis of DMC in a single reactor.

First, we tested the catalytic behavior of the three different RNH_2-SBA-15 samples obtained by the post-synthesis grafting method, performing the reaction with a molar ratio of methanol to EC equal to 10, in a simple two-necked flask equipped with two reflux condensers, at the reflux temperature of methanol (reaction temperature 65°C), and at atmospheric pressure.

The catalysts have been "activated" by removal of physisorbed water, putting the catalyst for one night in oven at 120°C before each reactivity test.

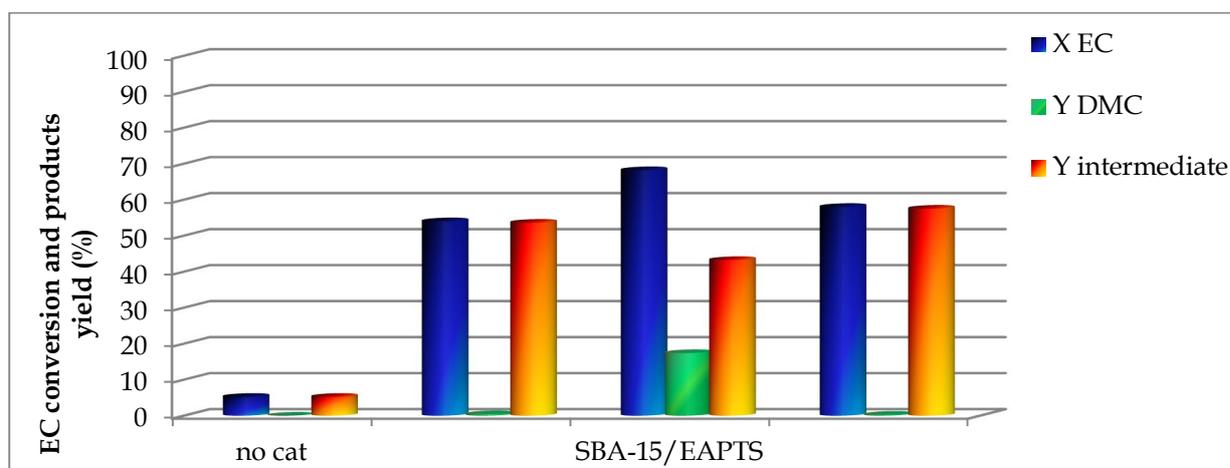The results are shown in the graph below (Fig 4.11).

Fig. 4.11 Catalytic results, $CH_3OH:EC=10:1$, $T=65°C$, $t=6$ h, catalyst 5% w/w with respect to EC.

SBA-15/EAPTS showed the highest catalytic activity, with a relatively high yield to dimethyl carbonate (around 17%).

The other catalysts, SBA-15/PAPTS and SBA-15/APTS, showed similar conversion of EC, 58 and 54% respectively, but very high selectivity to the intermediate, 2-hydroxyethyl methyl carbonate.

In some cases there was a minor contribute of the hydrolysis of EC due to the presence of water, that slightly increased EC conversion compared to the sum of yields to products.

Because of these reasons, we decided to study the SBA-15/EAPTS catalyst more in detail, by carrying out the reaction in a stainless steel autoclave reactor (described in Chapter 4.1.2), by feeding the reagents mixture and the catalyst (with the same ratio as for the previous test), and pressurizing the system with 10 bar of nitrogen.

In this way, we have investigated the influence of the reaction temperature on the catalytic behavior.

The catalytic results obtained with grafted SBA-15/EAPTS, for an increase of the reaction temperature from 70 up to 140°C, are shown in Fig. 4.12.

At higher temperatures, the yield to DMC showed a rapid increase up to ca. 58%.

In concomitance, the yield to the asymmetric intermediate rapidly decreased, demonstrating that higher temperatures are necessary (with these heterogeneous systems) in order to proceed with the second CIR between methanol and the intermediate to yield DMC.
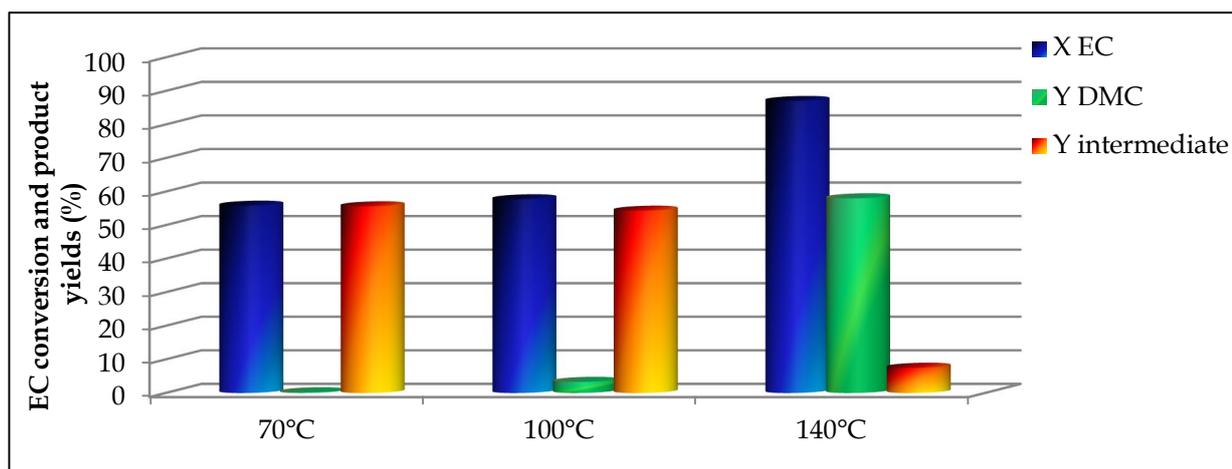
Fig. 4.12 Catalytic results in function of the reaction temperatures, $CH_3OH:EC=10:1$, t=6 h, autoclave reactor purged with 10 bars of nitrogen, catalyst grafted SBA-15/EAPTS, 5% w/w with respect to EC.

On the other hand, at higher temperature the contribution of EC decomposition to EG was relevant, with an increase of the gap between the conversion of this reagent and the sum of yields to products.

The complete comparison at 140°C between the three heterogeneous mesoporous nanosilicas investigated is reported below (Fig. 4.13).
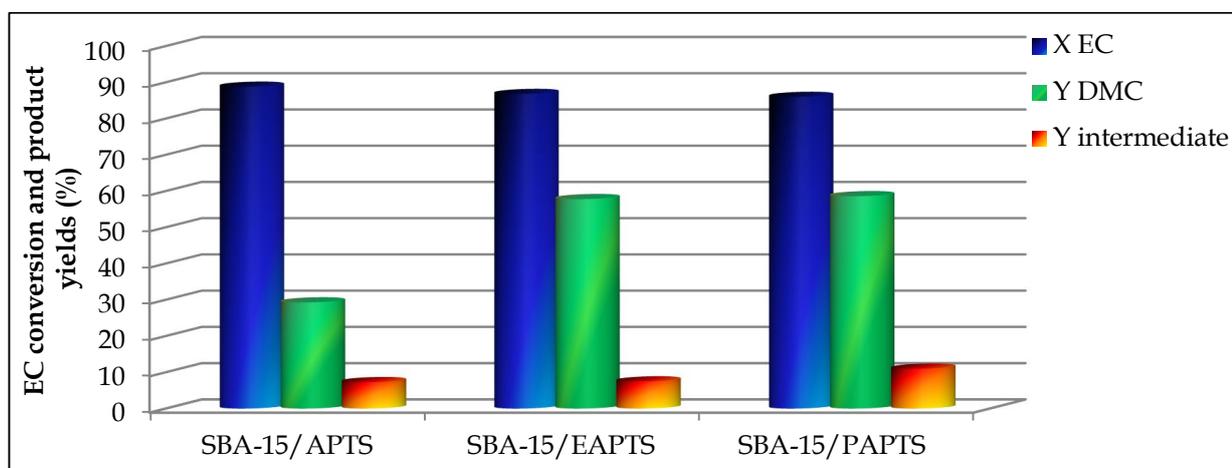
Fig. 4.13 Catalytic results, $CH_3OH:EC=10:1$, T=140°C, t=6 h, autoclave reactor purged with 10 bars of nitrogen, catalyst 5% w/w on the respect of EC.

Noteworthy, the EC conversion was the same (around 87%) for all catalysts.

This is probably due to the equilibrium limitation at the reaction conditions used.

Moreover, the APTS catalyst showed higher degradation of the reagent and lower yield to the products, whereas the other two catalysts led to similar behaviors with lower decomposition of EC to EG.

From these results, we can confirm that the increase of the number and density of the amino groups led to an increased catalytic activity.

Moreover, results obtained at higher temperatures highlight the importance of preventing the direct decomposition of EC to EG by either decarbonylation (or decarboxylation) or hydrolysis.

Therefore, we decided to perform one test by pressurizing the autoclave with 10 bar of carbon dioxide at the beginning of the reaction.

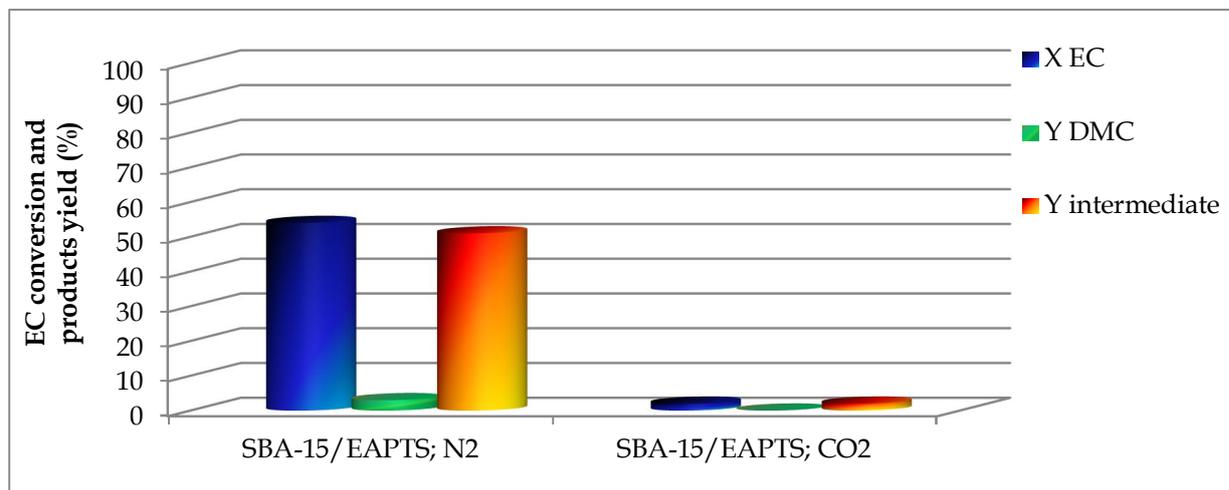The results obtained with SBA-15/EAPTS are shown below (Fig. 4.14).

Fig. 4.14 Catalytic results, $CH_3OH:EC=10:1$, T=65°C, t=6h, autoclave reactor pressurized with 10 bars of nitrogen (left) or of carbon dioxide (right), catalyst 5% w/w with respect to EC.

Performing the test under the same conditions but in the presence of CO_2 led to a dramatic decrease of activity.

This can be easily explained by a competitive mechanism for the adsorption of CO_2 and methanol on the basic active sites; on the other hand, this result confirms the capability of these systems to capture CO_2 forming carbammate bonds.

The catalysts tested so far were synthesized using the "grafting" method; we also tested the SBA-15/EAPTS obtained by the "one-pot" synthesis.

In this way, we performed the test by reacting a molar ratio of methanol to EC equal to 10, in a simple two-necked flask equipped with two reflux condensers, at the reflux temperature of methanol (65°C) and at atmospheric pressure (Fig. 4.15).
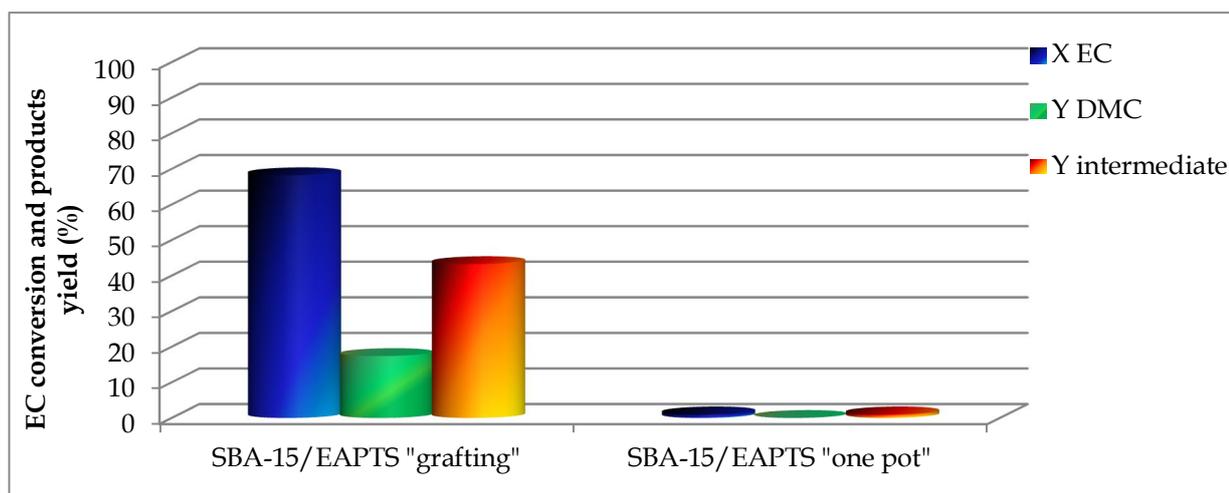
Fig. 4.15 Comparison test between the "grafting" and the "one-pot" synthesis, $CH_3OH:EC=10:1$, T=65°C, t=6 h, catalyst SBA-15/EAPTS 5% w/w with respect to EC.

This behavior, similar to that one observed by co-feeding CO_2 in the autoclave (Fig 4.14) is easily explained because of the peculiarity of the one-pot synthesis.

Indeed, the acidic conditions used in the synthesis leads to a protonation of the basic amino groups needed for the activation of the alcohol at the beginning of the reaction. For this reason, the materials obtained by the one-pot systems were completely inactive in the reaction.

The interesting behavior of these catalytic systems for the CIR between methanol and EC was investigated by means of in-situ IR spectroscopy as reported in the following chapter.

4.1.7.1 *In-situ IR spectroscopy study of the CIR of EC with methanol*

In-situ FT-IR spectroscopy was employed in order to study the reaction between ethylene carbonate and methanol aimed at the synthesis of DMC in presence of SBA-15/EAPTS, at room temperature. The FT-IR spectra collected at the various reaction steps are reported in Fig 4.16 in the 1800-1600 cm^{-1} spectral range.
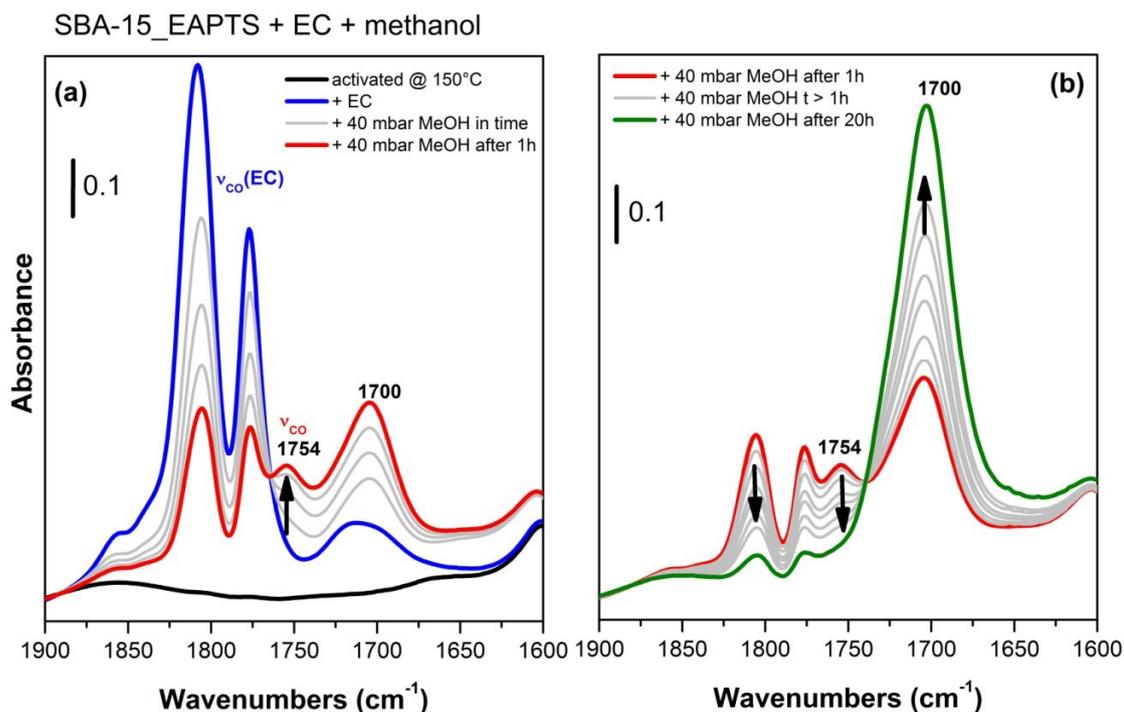

Fig. 4.16 Absorbance FT-IR spectra of SBA-15/EAPTS, in the 1900-1600 cm^{-1} spectral range. Section (a): activation in vacuo at 150°C (black spectrum), contact with ethylene carbonate (blue spectrum) and contact with 40 mbar of methanol till to 1 hour (red spectrum). Section (b): 1 hour contact with 40 mbar of methanol (red spectrum) and 20 hours contact with 40 mbar of methanol (green spectrum). Grey light spectra represent intermediate contact times with 40 mbar of methanol.

After activation in vacuum (see the black spectrum of section (a)), ethylene carbonate was put in contact with the catalyst (section (a)- blue curve). The presence of adsorbed ethylene carbonate was highlighted by the appearance in the spectrum of a doublet of bands at 1807 cm^{-1} and 1777 cm^{-1} attributed to the combined carbonyl stretching modes (v_{CO}). When methanol vapors were introduced into the cell, the signals of ethylene carbonate immediately started to change and, at the same time, two new bands appeared at 1754 and 1700 cm^{-1} and gradually increased (see the light grey and red curves in section (a) of Fig. 4.16). In particular, the signal located at 1754 cm^{-1} reached the highest intensity just after 1 hour of reaction (see the red spectrum). After this period, this spectral component started to decrease together with the bands of residual ethylene carbonate at 1807 cm^{-1} and 1777 cm^{-1}, whereas the new band at 1700

cm^{-1} dramatically increased. After 20 hours of reaction (see the green spectrum in section (b) of Fig. 4.16) the band at 1754 cm^{-1} totally disappeared and the signal at lower frequency dominated the spectrum.

The spectral behavior of the 1754 cm^{-1} component (that appeared after few minutes and then totally disappeared) allows to ascribe it to the carbonyl stretching mode (ν_{CO}) of the 2-hydroxyethylmethyl carbonate species, which is the intermediate of the reaction between ethylene carbonate and methanol. Unfortunately, no signal ascribable to the carbonyl stretching mode of the reaction product (DMC) could be identified in the spectrum even after the total disappearance of the intermediate spectral features (the C=O stretching of dimethyl carbonate, in fact, should appear very close (or even superimposed) to the $\square_{CO}$ of the intermediate species, at around 1750 cm^{-1}). The impossibility to observe the spectral features of DMC is probably due to the reaction environment of this particular *in-situ* experiment that was deeply different from the reaction conditions achieved inside the reactor, in which the reaction occurs in liquid phase. Inside the IR cell, in fact, both reagents are in vapour phase and therefore, in these reaction conditions, the just formed dimethyl carbonate is probably able to react with the residual ethylene carbonate that, in basic environment, undergoes ring opening polymerization producing a polycarbonate species.[314,315]

The appearance in the spectrum of the intense band at 1700 cm^{-1} (almost totally irreversible) is a proof for the formation of a polymeric by-product (probably a poly-ether-carbonate).

The above described *in situ* FT-IR experiment was carried out also on the other two amino-modified SBA-15 (SBA-15/APTS and SBA-15/PAPTS). In the presence of these two catalysts the reaction followed the same pathway, as reported in the following figures (Fig. 4.17 and Fig. 4.18).
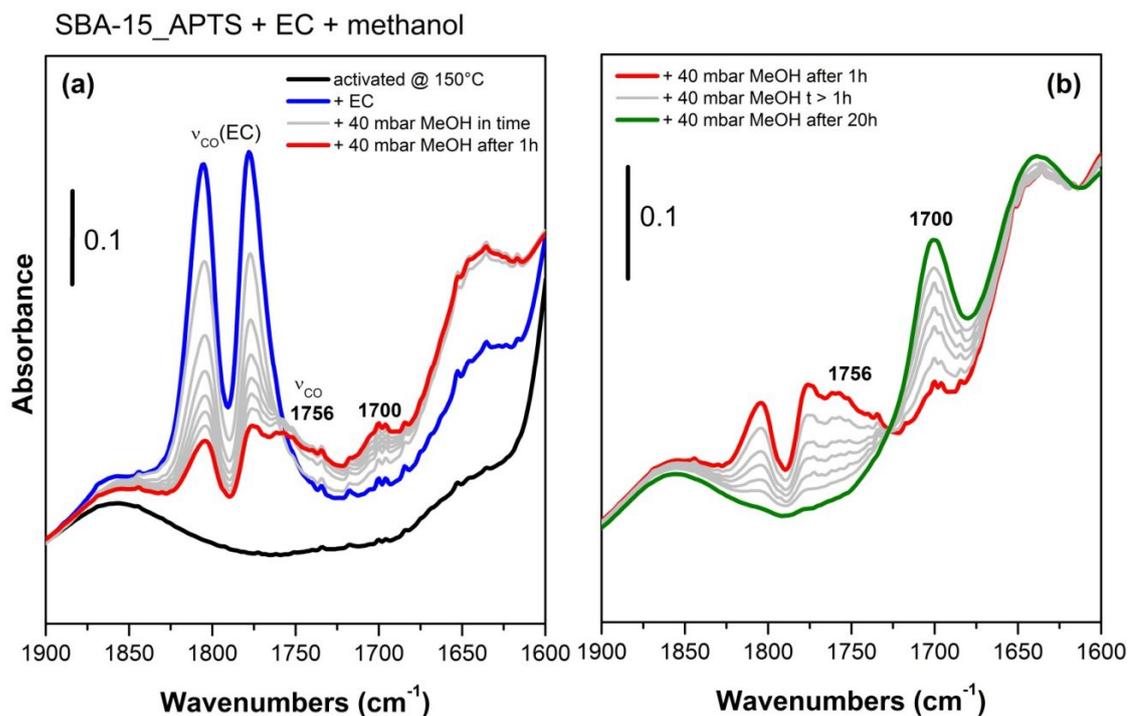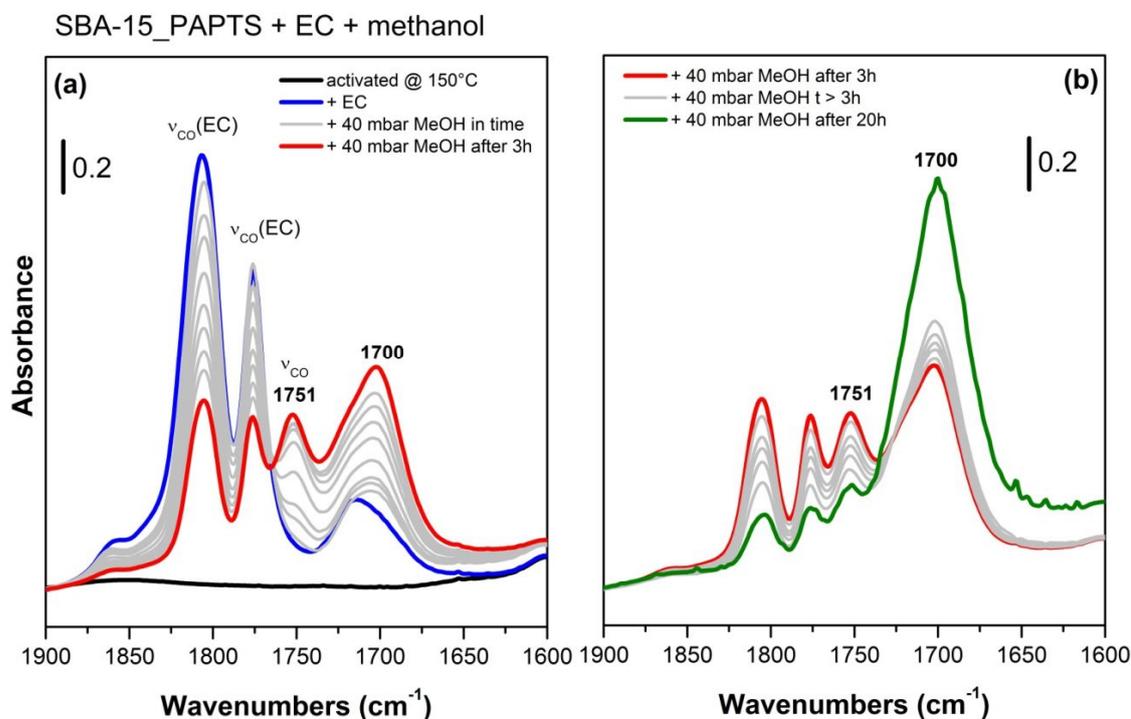
Fig. 4.17 Absorbance FT-IR spectra of SBA-15/APTS, in the 1900-1600 cm^{-1} spectral range. Section (a): activation in vacuo at 150°C (black spectrum), contact with ethylene carbonate (blue spectrum) and contact with 40 mbar of methanol till to 1 hour (red spectrum). Section (b): 1 hour contact with 40 mbar of methanol (red spectrum) and 20 hours contact with 40 mbar of methanol (green spectrum). Grey light spectra represent intermediate contact times with 40 mbar of methanol.

Fig. 4.18 Absorbance FT-IR spectra of SBA-15/PAPTS, in the 1900-1600 cm^{-1} spectral range. Section (a): activation in vacuo at 150°C (black spectrum), contact with ethylene carbonate (blue spectrum) and contact with 40 mbar of methanol till to 3 hour (red spectrum). Section (b): 3 hour contact with 40 mbar of methanol (red spectrum) and 20 hours contact with 40 mbar of methanol (green spectrum). Grey light spectra represent intermediate contact times with 40 mbar of methanol.

One of the more evident differences concerns the catalytic activity of the material grafted with the propylamine. The SBA-15/APTS seems to be less reactive with respect to catalysts grafted with alkylamine chains containing more than one amino-group.

Worth of being noted is also the higher stability of the 2-hydroxyethylmethyl carbonate species (the reaction intermediate), in the presence of the material grafted with the tri-amine (SBA-15/PAPTS). In fact, in this case, the reaction intermediate began to react with another methanol molecule thus being converted into DMC just after 3 hour of reaction. The higher length of the alkylamine chain provided a higher mobility so allowing a stronger stabilization of the intermediate species.

4.2 Optimized reactive distillation system for the CIR with DMC

4.2.1 Introduction

The carbonate interchange reaction (CIR) of DMC with a wide series of alcohols and diols aimed at the synthesis of the corresponding organic carbonates, have been investigated using both homogeneous (Na methoxide) and heterogeneous (MgO) basic catalysts.

As described in the Introduction part of this Thesis, DMC represents an environmental benign reagent showing a low toxicity and a high biodegradability, and it is a well-known solvent for a wide series of organic compounds.

Indeed, in these reactions DMC was used both as a green and efficient carbonylating agent and as reaction solvent, so avoiding the needs for other volatile organic compounds.

As widely explained in the corresponding chapter (Chapter 1.3.5), the main problem typically met in CIRs is that these reactions are equilibrium-limited, often with unfavorable equilibrium constants.

The most successful and widely applied method used to overcome this problem is the continuous removal of the co-product, methanol, using a reactive distillation apparatus and, in this way, shifting the reaction toward the formation of the desired product.

Nevertheless, the formation of an azeotrope between methanol and DMC greatly complicates these processes.

In fact, once the reaction has started, the concentration of methanol in the reaction mixture increases progressively until the azeotrope composition.

This is a homogeneous pressure-maximum azeotrope in a completely miscible system, with a boiling point of about 64°C (lower than the boiling point of the two pure compounds) at 102,52 kPa (slight overpressure) and containing 85 mol% of methanol and 15 mol% of DMC at atmospheric pressure.[254,316]

Several papers and patents report complex distillation systems, often in vacuum or adding a third component, in the attempt to remove methanol from the reaction mixture, or in general to break the azeotrope.[317]

In this chapter we report about a new and simple implemented reactive distillation system that we have developed for the continuous in-situ removal of methanol from the reaction mixture, with a negligible loss of DMC.

This new procedure was firstly used with the aim to overcome the strict thermodynamic limitation encountered in the synthesis of the pyrocatechol carbonate

(PCC), the target of the PRIN project, as a possible intermediate in the synthesis of methylenedioxibenzene (MDB).

However, this new and efficient reactive distillation procedure was used to synthesize several carbonates by means of the CIR with DMC, achieving yields considerably higher than the equilibrium values or than those reported in the literature for some of the carbonates described later.

4.2.2 Synthesis of PCC: backgrounds

Pyrocatechol carbonate (PCC) represents the simplest five-membered aromatic cyclic carbonate (Fig. 4.19).
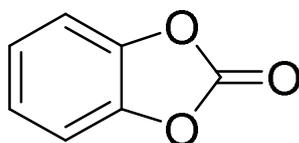

Fig. 4.19 Pyrocatechol carbonate (PCC).

The PCC synthesis with a basic-catalyzed carbonate interchange reaction (CIR) of catechol and dimethyl carbonate (DMC) appeared for the first time in a German Patent in 1976.[318]

However, in that paper, the CIR was carried out by the azeotropic distillation of the mixture of DMC and methanol (co-product of the reaction), that leads to the loss of part of the DMC and finally is detrimental for the reaction (maximum reported catechol conversion equal to 45% after 15 hours of reaction).

A more recent literature survey disclosed relatively few methods available for the preparation of PCC (Scheme 4.4), despite its high potential as a chemical intermediate. Starting from catechol, these methods included different reactions such as:

- reactions with phosgene and ethyl chloroformate,[319]
- oxidative cleavage of a bis-dichloroacetate compound,[320]
- cyclocarbonylation processes catalyzed by La- and Pd-based systems,[321]
- CIRs with bis-methyl salicyl carbonate (BMSC) or DMC, catalyzed by Et$_3$N or alumina loaded with cesium hydroxide, respectively.[322]

Yield, %

31-85

40

74-89

50

n.a.
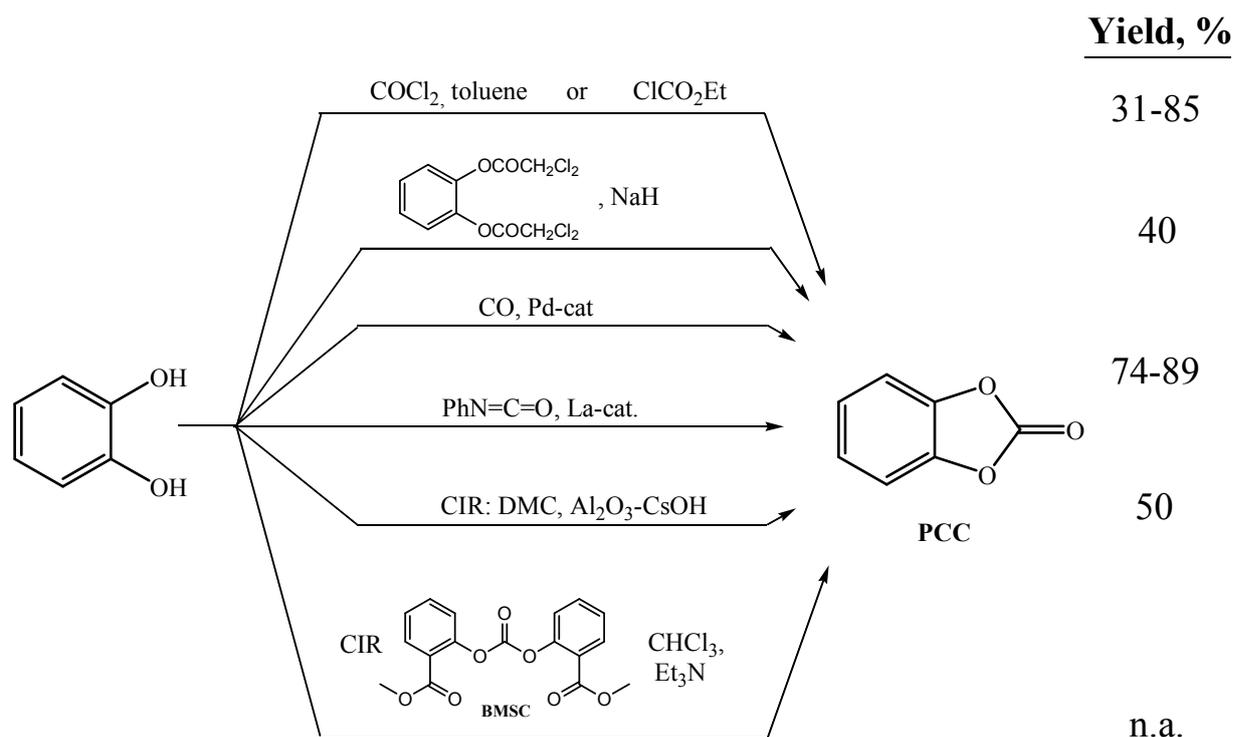
Scheme 4.4 Synthetic routes to PCC with the corresponding yields (show on the right of each processes)

However, many of these procedures, were either directly or indirectly phosgene-dependent since they used phosgene or its derivatives such as alkylchloroformates, BSMC, and phenylisocyanate.[323]

Other methods also posed safety concerns because they involved stoichiometric amounts of toxic chlorinated compounds, or noxious CO at high pressures (up to 30 bar).

For all these reasons, the most attractive preparation method of PCC is from the CIR of DMC and catechol, although the moderate yield of the product reported (50%), indicates that there is large room for improvement.

Furthermore, one of the most active homogeneous catalysts studied for the CIR of DMC and alcohols, namely di-*n*-butyltin oxide (Bu$_2$SnO) and other similar complexes, is completely inactive with *o*-substituted phenols, like catechol. This is probably due to the formation of a stable cyclic tin ester which is inert toward further reaction (Fig. 4.20).[324]
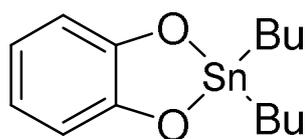

Fig. 4.20 Stable complex between catechol and the tin catalyst.

## 4.2.3 Synthesis of PCC: traditional reaction systems

Firstly, we investigated the synthesis of PCC by means of the CIR of DMC and catechol using a reagent ratio equal to 10.

All the reactions were carried in mild conditions, at atmospheric pressure and at the reflux temperature of DMC ($T_{b\ (DMC)}$=90°C) in a double-necked round bottom flask, under reflux of the carbonate.

This excess of DMC permitted us to avoid the use of any other solvent.

DMC, indeed, acts properly both as the reagent and as a green solvent.

Moreover, we decided to use a simple and cheap basic homogeneous catalyst such as sodium methoxide ($NaOCH_3$). The reaction mechanism is shown in the following scheme (Scheme 4.5).
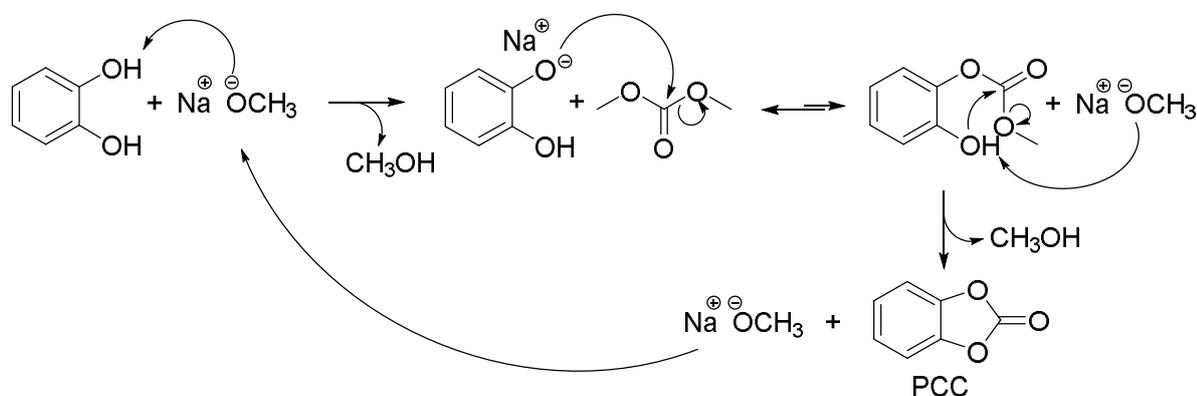
Scheme 4.5 Reaction mechanism of the CIR between catechol and DMC, catalyzed by sodium methoxide.

Firstly catechol is deprotonated by the catalyst, then the generated catecholate anion is a more active nucleophile able to attack the carbonyl of the carbonate moiety (slow and unfavored step); finally the asymmetric intermediate undergoes the intra-molecular cyclisation that leads to PCC.

The overall reaction produces two molecules of methanol for each molecule of PCC formed.

Like phenol, also catechol (once activated by deprotonation in the presence of a catalyst) is able to delocalize the negative charge on the aromatic ring.

This leads to a decrease of the electronic density on the oxygen atom and makes catechol a "softer" nucleophile.

For this reason the nucleophilic attack on the carbonyl carbon of the DMC is thermodynamically unfavoured compared to other reactions (e.g alkylations).

As a matter of fact, conducting the reaction without any method to remove the co-product methanol leads to very low PCC yield even after 24 hours of reaction.
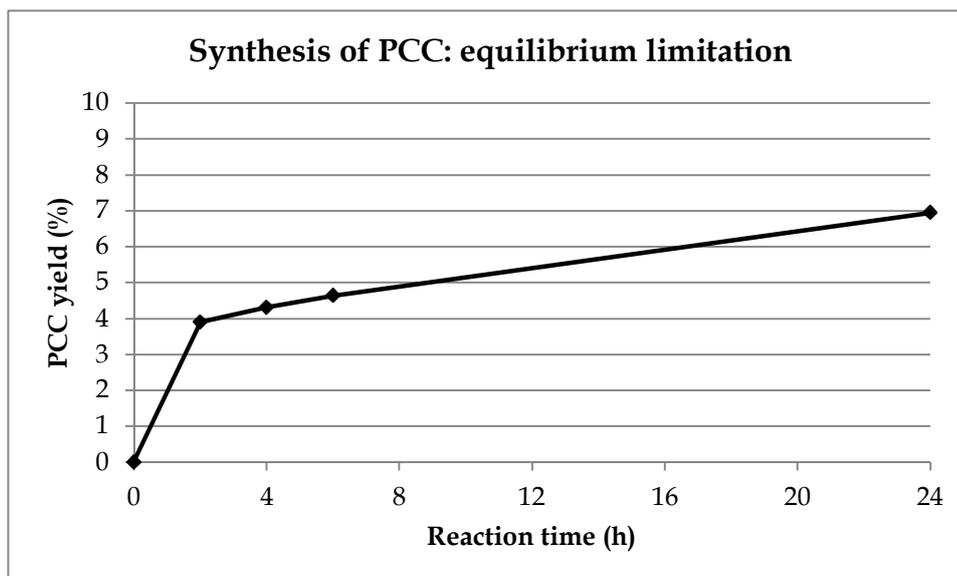
Fig. 4.21 PCC synthesis in a round bottom flask with simple reflux condensers; DMC:Catehol:NaOCH$_3$=10:1:0.033; Tr=90°C, T$_{oil\ bath}$=120°C.

From the graph above it is clear that the reaction quickly reaches an almost steady equilibrium state with a PCC yield that increases to only the 7% after 24 hours of reaction.

Therefore, it is crucial to use a reaction system able to remove the co-product methanol, shifting the equilibrium toward the products side and increasing the yield into PCC according to the Le Châtelier principle.

The most interesting way to overcome this problem is to perform the reaction in a reactive distillation system (RDS), as described in the Introduction part of this Thesis (Chapter 1.3.5).

Although the use of a "traditional" RDS system allows to greatly improve the yield to PCC (Fig. 4.22), this is generally a complex system. Moreover, in this way the reaction is performed in a distillation column, distilling away from the top the azeotropic mixture between DMC and methanol, and thus losing at least the 15 mol% of the starting reagent. This means that a great excess of DMC is needed to overcome an excessive concentration of the mixture and a detrimental pauperization of DMC.

Furthermore, few degrees of difference in the temperature can accelerate too much the distillation giving not enough time to the reaction to proceed.
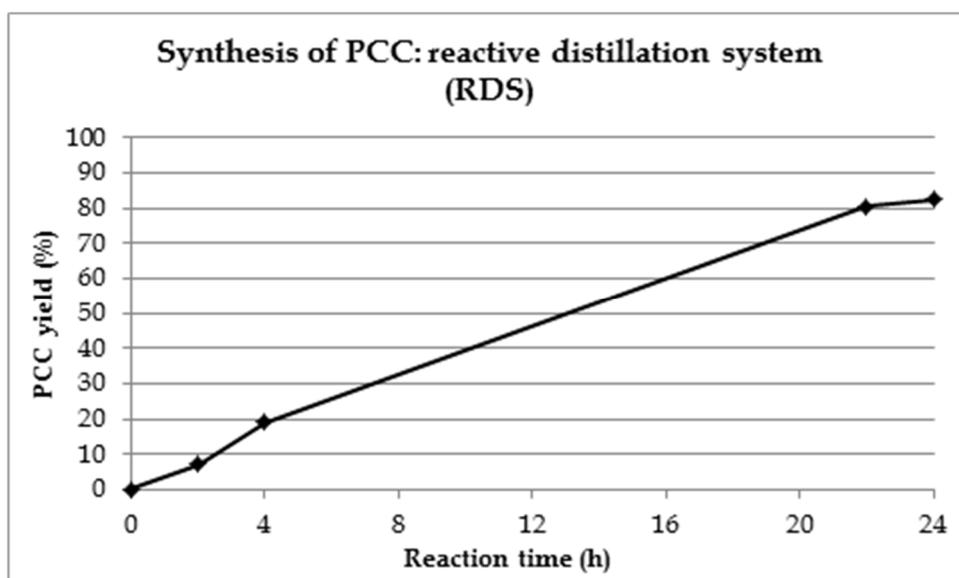
Fig. 4.22 PCC synthesis in two necked round bottom flask connected to a Vigreux column; DMC:Catehol:NaOCH$_3$=10:1:0.033; Tr=90°C; T$_{oil\ bath}$=120°C.

4.2.4 Synthesis of PCC: the "implemented" RDS

Once we had understood the problems deriving from the use of the traditional systems, we decided to developed a new, simpler and more efficient RDS.

The idea behind this "implemented" distillation system was to add the contribution of a selective adsorption of methanol by means of appropriate molecular sieves, taking advantage of the different molecular size of this simplest alcohol compared to DMC.

The shape and size of the zeolite channels were decided after an adsorption test carried out with a mixture of DMC and methanol at room temperature, in which the 3 and 4 Å zeolite showed the best adsorption capability compared to 5Å and other molecular sieves with larger cavities.

The molecular sieves tested were the follow:

3Å sodium potassium alumino silicate, CE Instruments Thermo Quest Italia SPA, $K_3Na[(AlO_2)_{12}(SiO_2)_{12}]xH2O$;

4Å sodium alumino silicate, Sigma Aldrich, $Na_{12}[(AlO_2)_{12}(SiO_2)_{12}]xH2O$;

5Å sodium calcium alumino silicate, UOP type 5Å, $Ca_{4,5}Na_3[(AlO_2)_{12}(SiO_2)_{12}]xH_2O$.

In our "implemented" reactive distillation system (Fig. 4.23), we have used the same two-necked round bottom flask and the reflux condenser as in the first test (Fig. 4.21), but between the vertical column and the flask a porous glass support was added in order to hold up about six grams of molecular sieve. On the second neck, another condenser was needed both for liquid sampling and in order to avoid a possible over-pressure inside the flask.
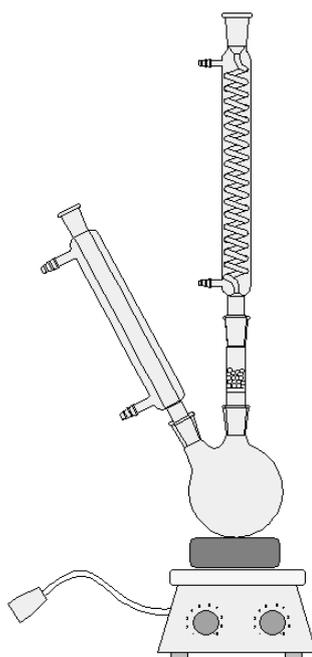
Fig. 4.23 Schematically representation of the "implemented" reactive distillation system (RDS) with the selective adsorption of methanol inside molecular sieves.

At the beginning of the reaction, the distilled mixture, containing almost pure DMC, is condensed and can fall back again into the reaction mixture, because it is not retained by the molecular sieves.

However, during the proceeding of the reaction, methanol forms as co-product, and although it is maintained in low concentration inside the batch, the distilled mixture collected above the porous glass progressively becomes richer in this alcohol, as shown in the following table (Table 4.4).

Reaction time (h)	Reactive mixture molar composition	Distilled (above sieves) mixture molar composition
6	DMC = 90,4% ; CH_3OH =9,6%	DMC = 81,9% ; CH_3OH =18.1%
24	DMC = 86,2% ; CH_3OH =13,8%	DMC = 39,8% ; CH_3OH =60,2%

Table 4.4 Composition of the lightest compound (DMC and methanol) in the mixtures inside the batch and the distilled one above the sieves.

In this way, the sieves placed over the support get wet by the distilled mixture of methanol and DMC; the former is preferentially hold by the zeolites, the latter can fall again into the reaction batch, shifting the reaction equilibrium toward the desired product.

Noteworthy, there is a T gradient on the vertical column, since the temperature the boiling reaction mixture is around 90°C,whereas that one of the reflux condenser is about 25°C. As a matter of fact, the temperature of the support and of the sieves depend on the composition of the distilled mixture. It reaches a

maximum at the beginning of the reaction and then it decreases down to ca 60 °C.

This is a stable system, not critically dependent on the bath temperature because the mixture is condensed by the condenser, then falls on the sieves and finally returns to the flask, so avoiding the continuous removal of the azeotropic mixture of DMC and methanol.

After each reaction, the molecular sieves are restored in a stove at 190°C overnight.

No signs of a real "deactivation" of the adsorption capability of the zeolites were observed (for more than 10 cycles).

Surprisingly, this operation does not work when the same molecular sieves are directly placed inside the reaction mixture. This is probably because the zeolite acts as a sieve only at low temperatures (below 90°C), and probably also some detrimental interaction with the basic catalyst may occur. Moreover, the magnetic stirrer crushed the zeolites into smaller partciles and made their recycle impossible.

Finally, with our system, we were able to reach almost total conversion of catechol in 24 hours of reaction with a total selectivity into the desired product (Fig. 4.24); moreover the ratio between the DMC and methanol did not decrease during reaction, which demonstrates the efficiency of our system.
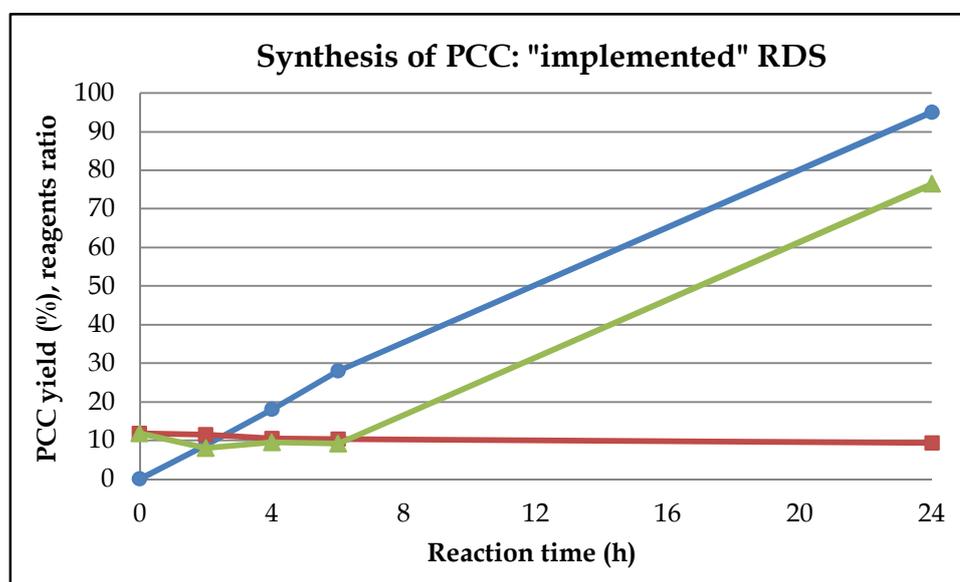

Fig. 4.24 PCC yield and the reagents ratio with our "implemented" RDS in the optimized condition (DMC:Catechol:NaOCH$_3$=10:1:0.033; Tr≈90°C, T$_{oil\ bath}$=120°C). ● PCC yield (blue), ■ DMC/Methanol ratio (brown), ▲ DMC/Catechol ratio (green).

We have also optimized the separation and purification steps of PCC. Indeed, we were able to recover from the 40% to the 60% of the starting DMC (which can be

recycled in order to synthesize more PCC) by means of distillation in mild vacuum conditions (rotary evaporator). Thereafter, the solid obtained was washed with mildly acidic water (pH=4) in order to remove the catalyst and traces of unreacted catechol.

In this simple way, we were able to obtain 90% of isolated PCC yield (purity >99%). This is an outstanding result, with no comparison in the literature.

The adsorption capacity of the 4Å molecular sieves was calculated by a thermogravimetric analysis (TGA). The conditions used for the analysis are explained in the corresponding Chapter 3.3.3.

We found that this zeolite has an adsorption capacity of about 10% of their weight, so the 6 grams of zeolites loaded in the column were able to hold about 0.6g of methanol. This amount represents about the 50% of the methanol theoretically formed from the reaction (starting with 2 grams of catechol), but it is enough to shift the reaction equilibrium.

## 4.2.5 "Implemented" RDS: extension of the concept

The system described in the previous Chapter is a versatile device that can be applied for the synthesis of several different organic carbonates.

Theoretically, every CIR starting from DMC can be improved by the selective continuous removal of methanol using our method.

4.2.5.1 Synthesis of diphenyl carbonate (DPC)

As discussed in the introduction (Chapter 1.3.5), another important carbonate with a commercial relevance is DPC, as a key intermediate for the production of polycarbonates.

Unfortunately, because of the "softer" nucleophilicity of phenol, the reaction is strictly limited and has a very low equilibrium constant (K_{eq} = 3x10^{-4} at 180°C for the synthesis of the intermediate MPC).
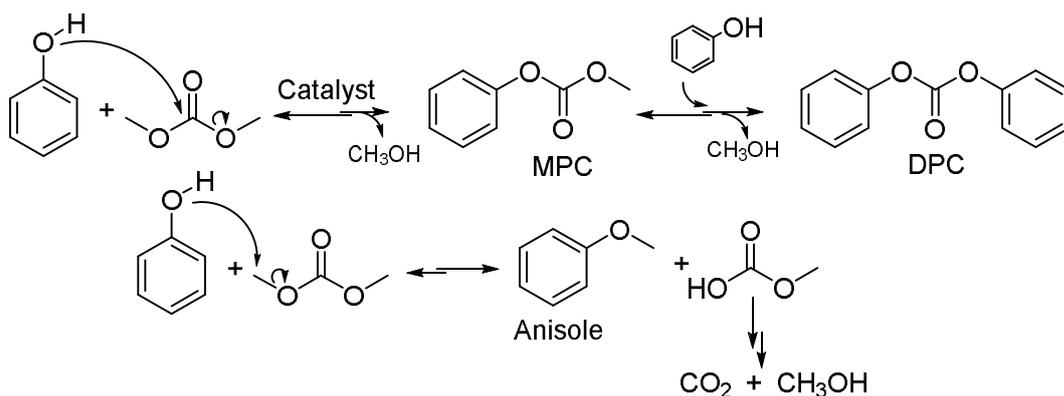
Scheme 4.6 Synthesis of DPC by CIR of phenol and DMC and the preferred side reaction of methylation to yield anisole.

Therefore we decided to apply our system, working in the same mild conditions as those used for PCC synthesis; results are reported in the following section.
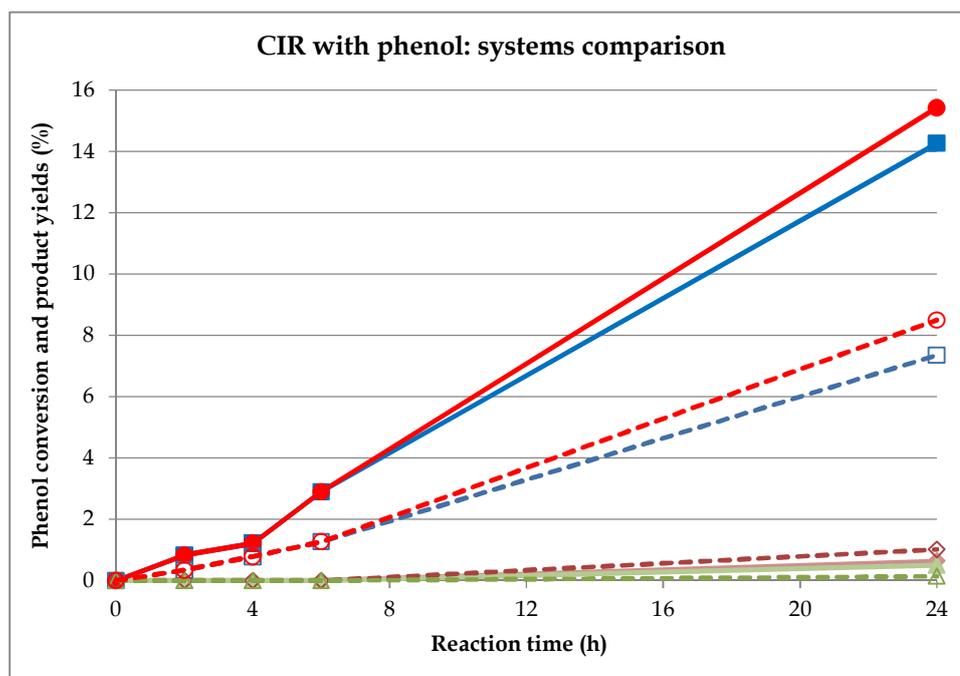

Fig. 4.25 CIR between phenol and DMC.
Comparison between the "implemented" RDS and a simple reflux condenser (dashed lines). (DMC:Phenol:NaOCH$_3$=10:1:0.067; Tr≈90°C, T$_{oil\ bath}$=120°C).● Phenol conversion (red), ■ MPC (blue), ▲ DPC (green) and ♦ anisole (brown) yields.

Fig. 4.25Fig 4.25 compares phenol reactivity with and without our implemented method. It is clear that, with our method, the reaction rate was about twice as much that one achieved with the simple reflux of the mixture. Moreover we were able to achieve higher selectivity toward the desired products (MPC and DPC).

However, still the reaction was very slow and led to a MPC yield of ca 14% only.

The big difference of reactivity between catechol and phenol can be explained by taking into account the different intermediates formed. Indeed, PCC formation passes through only one slow step, the formation of the asymmetric intermediate, which then undergoes a rapid intra-molecular cyclisation; conversely, the formation of DPC needs two slow and unfavored steps: the formation of MPC and then the attack of another phenol molecule to yield DPC.

As a matter of fact, also the reactivity of aliphatic diols confirm this trend, as described in the next pages.

4.2.5.2 *Synthesis of cyclic aliphatic carbonates: PC, BC, GlyC*

Aliphatic alcoholates are "harder" nucleophiles compared to the aromatic anion, so the CIR with DMC is by far more favored.

Indeed, 1,2-butanediol and 1,2-propanediol show similar reactivity, and the use of the "implemented" RDS allowed us to reach almost complete conversion of reagents in only two hours of reaction, with total selectivity to the corresponding cyclic carbonate: propylene carbonate (PC) and butylene carbonate (BC) respectively.
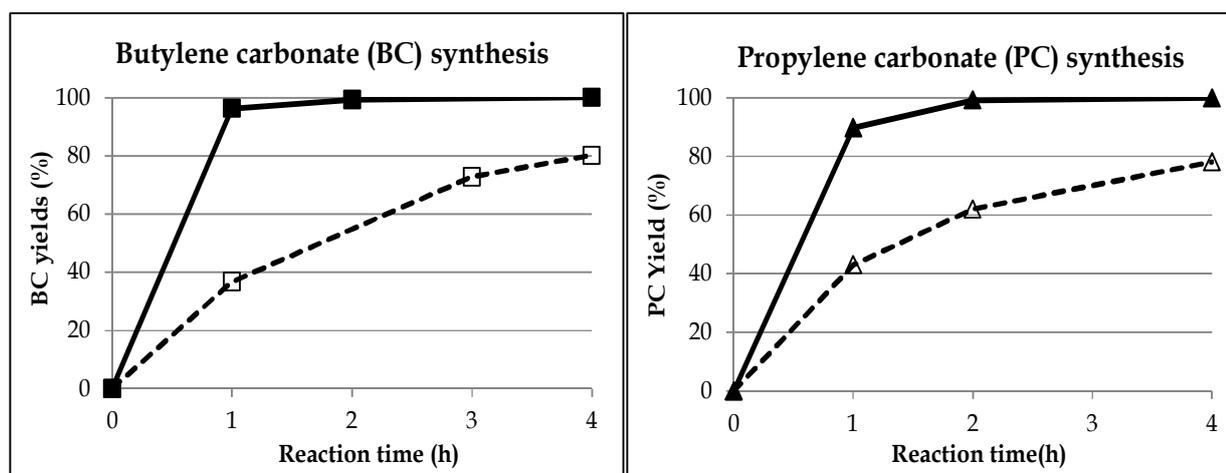

Fig. 4.26 CIR of 1,2 butanediol (left) and 1,2 propanediol (right) with DMC. Comparison between the "implemented" RDS and a simple reflux condenser (dashed lines). (DMC:diol:NaOCH$_3$=10:1:0.033; Tr≈90°C, T$_{oil\ bath}$=120°C). ■ BC yield "implemented" RDS, □ BC yield with reflux condenser; ▲ PC yield "implemented" RDS, △ PC yield with reflux condenser.

Interestingly, the use of vicinal diols le to a fast reaction with always 100% selectivity toward the corresponding five-membered cyclic carbonate.

This was not the case, for example, when the reaction was carried out with 1,3 diols, for example 1,3-butanediol.

In fact, conducting the reaction in the same conditions as those reported above, but with 1,3-butanediol, a mixture of products was obtained in which the yield to the six-membered cyclic carbonate was only a few points % greater than yield to dimers and other heavier compounds.

An interesting, intermediate behaviour, was shown by glycerol.

Indeed, the CIR between glycerol and DMC is a well-studied reaction because of the importance of the product: glycerol carbonate (GlyC).

We will better explain the GlyC importance, synthetic pathways and applications in the corresponding chapter (Chapter 4.3.2.1).

Although the reaction was fast, the presence of three reactive hydroxyl groups in the molecule, made the overall process of CIR with DMC unselective to the desired cyclic product (GlyC).

Indeed, the low solubility of glycerol in DMC caused either the need for an excess of DMC, or high reaction temperatures, in order to obtain an homogeneous solution. However, both parameters pushed the consecutive reactions toward the formation of other dimers and heavier by-products (Scheme 4.7).
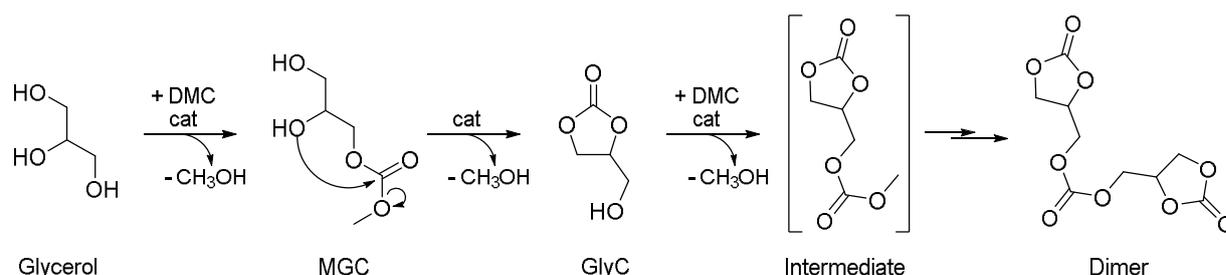
Scheme 4.7 Glycerol carbonate (GlyC) synthesis by means of CIR of glycerol and DMC. Also two possible consecutive products ("intermediate" and "dimer") are shown.

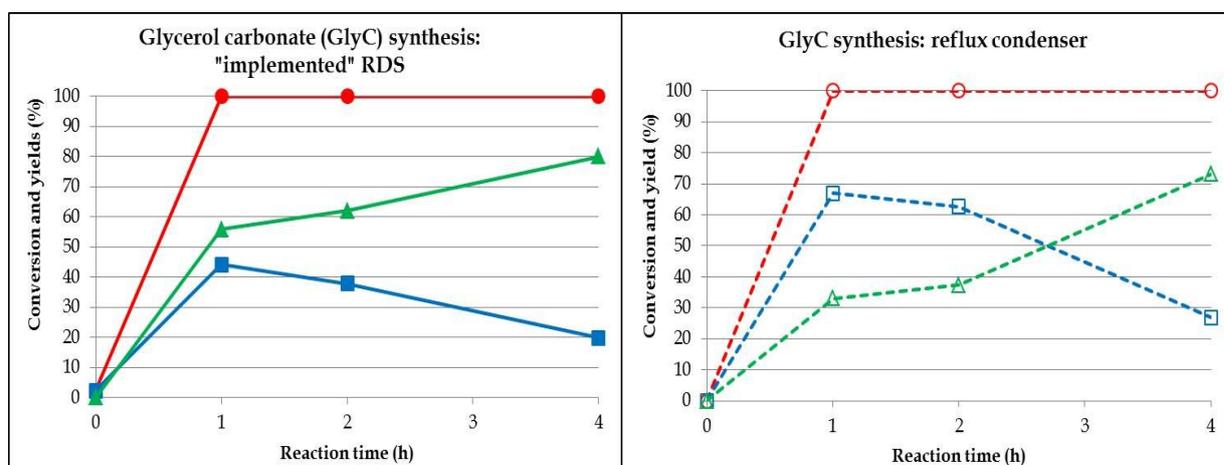The experimental results are shown in the following figure (Fig. 4.27).

Fig. 4.27 CIR between glycerol and DMC with (left) and without (right) the "implemented" RDS. (DMC:glycerol:NaOCH$_3$=10:1:0.033; Tr≈90°C, T$_{oil\ bath}$=120°C). ● and ○ glycerol conversion (red); ■ and □ GlyC yield (blue); ▲ and Δ consecutive by-products yields (intermediate+dimer+heavier; green).

As expected, our system favoured the consecutive reaction by subtracting the co-produced methanol from the reaction medium; however, finally, in this particular case this was detrimental for GlyC selectivity.

Although glycerol conversion was complete after 1 hour of reaction, the selectivity to the desired product was always below 70%.

We have found the way to overcome this problem and developed a selective synthesis of GlyC as described later in this Thesis (Chapter 4.3.3.1).

4.2.5.3 Synthesis of linear aliphatic carbonates

Thereafter, we have studied the synthesis of linear carbonates using the carbonate interchange reaction between DMC and linear and cyclic alcohols. Firstly, we studied the synthesis of methylbutyl carbonate (MBC) and dibutyl carbonate (DBC) reacting *n*-butanol with DMC in the presence of Na methoxide (homogeneous catalyst). The reaction mechanism is reported in Scheme 4.8.
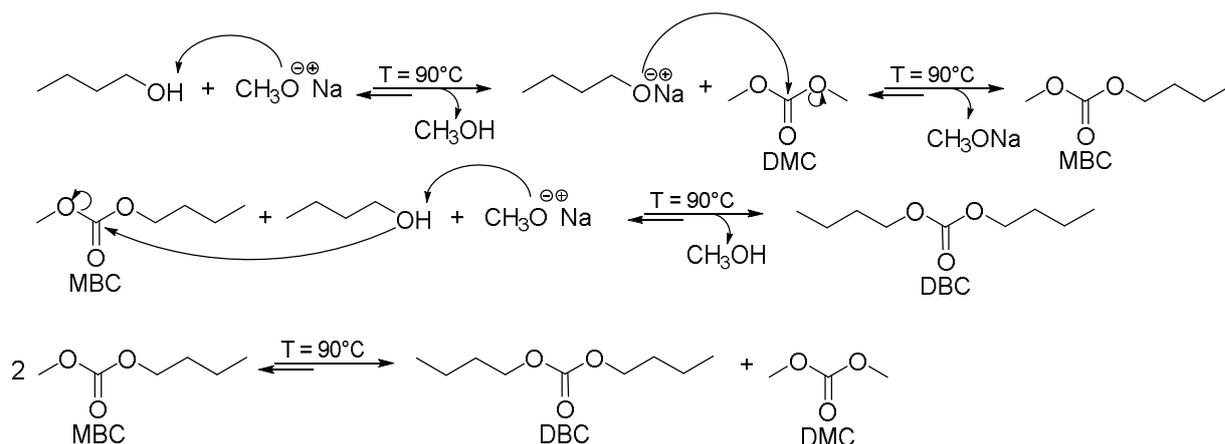
Scheme 4.8 Synthesis of MBC and DBC by means of CIR between DMC and *n*-butanol, catalyzed by sodium methoxide.

DBC, in particular, is an important alkyl carbonate, extensively used for the production of various organic and polymeric materials, mainly for the synthesis of polycarbonates. DBC is also considered an excellent environmental heritage protection lubricant material because of its good lubricity and wearability, corrosion resistance, high thermal oxidative stability, and outstanding solubility. The synthesis of DBC therefore has been growing fast during latest years due to a continual market demand.[325,326,327,328]

However, the CIR between *n*-butanol and DMC, when no method for methanol removal is applied, reaches in one hour a stable, almost equilibrium-limited state, with only a further slight increase of the yield during the following hours of reaction (Fig 4.28).
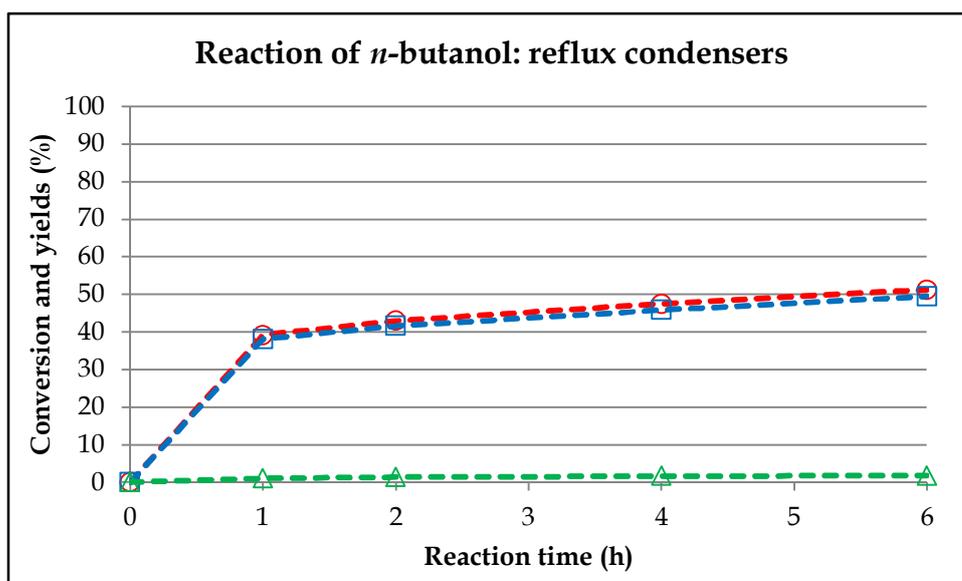
Fig. 4.28 CIR of *n*-butanol and DMC with simple reflux condenser.
(DMC:*n*-butanol:NaOCH$_3$=5:1:1/30; Tr≈90°C, T$_{oil\ bath}$=120°C). ○ *n*-butanol conversion (red), □ MBC yield (blue), Δ DBC yield (green).

We have also discovered that the selectivity to both the symmetric product (dibutyl carbonate) and the unsymmetric one (methylbutyl carbonate), is strictly dependent on the feed ratio of the reagents. Indeed, by feeding a high DMC/*n*-butanol ratio, combined with our "implemented" RDS, the formation of the asymmetric product (MBC) was promoted (Fig. 4.29). Conversely, a lower ratio and higher reaction temperatures, facilitated the formation of the symmetric carbonate (DBC) (Fig. 4.30).
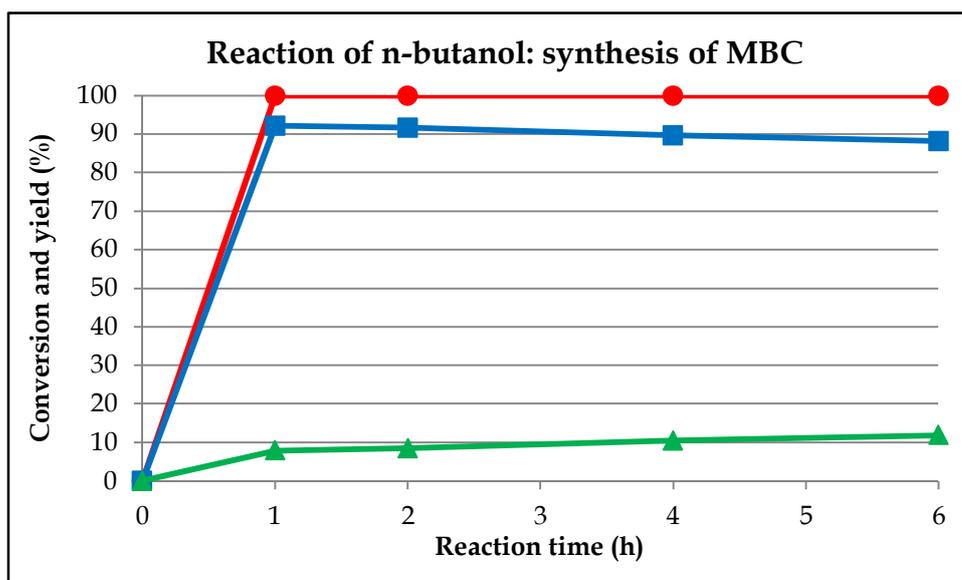

Fig. 4.29 MBC synthesis by means of CIR between *n*-butanol and DMC, "implemented" RDS.
(DMC:*n*-butanol:NaOCH$_3$=5:1:1/30; Tr≈90°C, T$_{oil\ bath}$=120°C). ● *n*-butanol conversion (red), ■ MBC yield (blue), ▲ DBC yield (green).
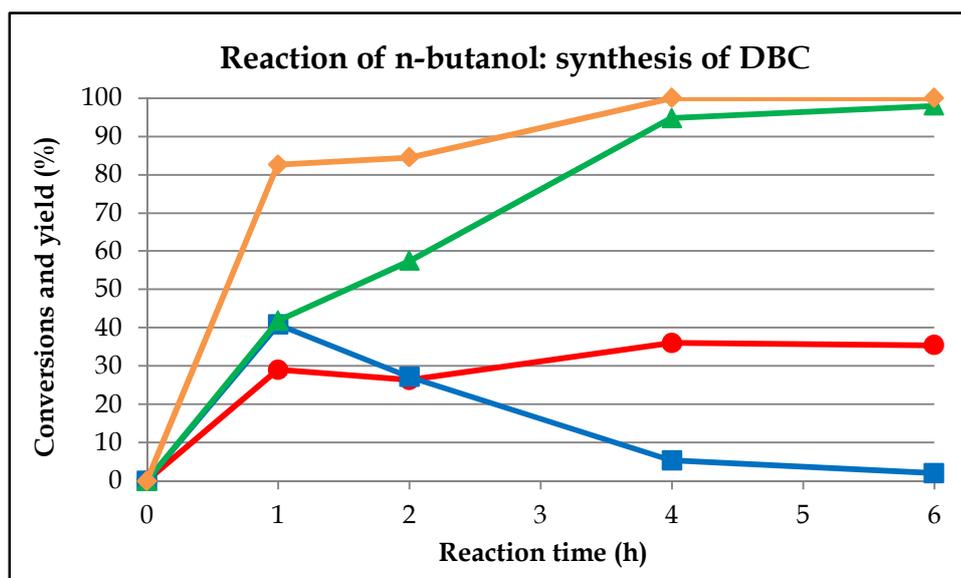
Fig. 4.30 DBC synthesis by means of CIR between *n*-butanol and DMC, "implemented" RDS. (DMC:*n*-butanol:NaOCH$_3$=1:5:1/30; Tr≈118°C, T$_{oil\ bath}$=120°C). ● *n*-butanol conversion (red), ♦ DMC conversion (orange), ■ MBC yield (blue), ▲ DBC yield (green).

Furthermore, we compared the reactivity of aliphatic and aromatic cyclic alcohols. In particular, Fig. 4.31 shows the reactivity of cyclohexanol, which can be taken as a probe molecule to demonstrate the importance of alcohol nucleophilicity in the CIR. Indeed, the feed of an excess DMC led to a fast reaction with complete conversion of cyclohexanol after 2 hours of reaction, with almost complete selectivity to the asymmetric carbonate (methylcyclohexyl carbonate, MCC), with only 1% of the symmetric carbonate (dicyclohexyl carbonate, DCC) after 4 hours of reaction.
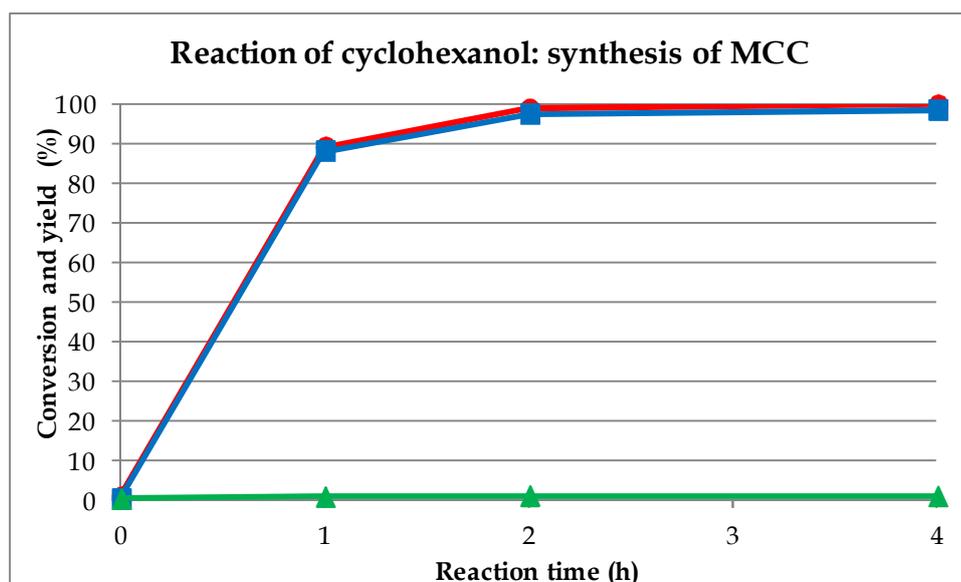

Fig. 4.31 CIR between cyclohexanol and DMC, "implemented" RDS. (DMC:cyclohexanol:NaOCH$_3$=10:1:1/30; Tr≈90°C, T$_{oil\ bath}$=120°C). ● cyclohexanol conversion (red), ■ MCC yield (blue), ▲ DCC yield (green).

The increase of the steric hindrance of the alcohols led to a slower reactivity and higher selectivity to the asymmetric products.

Finally, we have investigated the reactivity of menthol in order to confirm this trend.

The (-)menthol structure is reported in the following figure (Fig. 4.32)
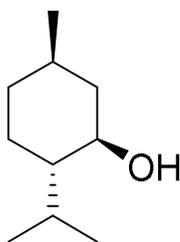
Fig. 4.32 (-) menthol structure: (1R,2S,5R)-2-Isopropyl-5-methylcyclohexanol

The carbonates derived from menthol are interesting products because of their potential use for the formulation of cooling sensation agents and sensory stimulation compositions.[329]

The results of the CIR between menthol and DMC are reported below (Fig. 4.33).

The reaction led to complete conversion of the alcohol after 5 hours of reaction with the selective formation of the asymmetric product methylmenthyl carbonate (MMeC); the symmetric product dimenthyl carbonate (DMeC) did not form.

Fig. 4.33 CIR between (-) menthol and DMC, "implemented" RDS.
(DMC:menthol:NaOCH₃=10:1:1/30; Tr≈90°C, T_oil bath=120°C). ■ MMeC yield.

4.2.6 "Implemented" RDS: heterogeneous catalysis

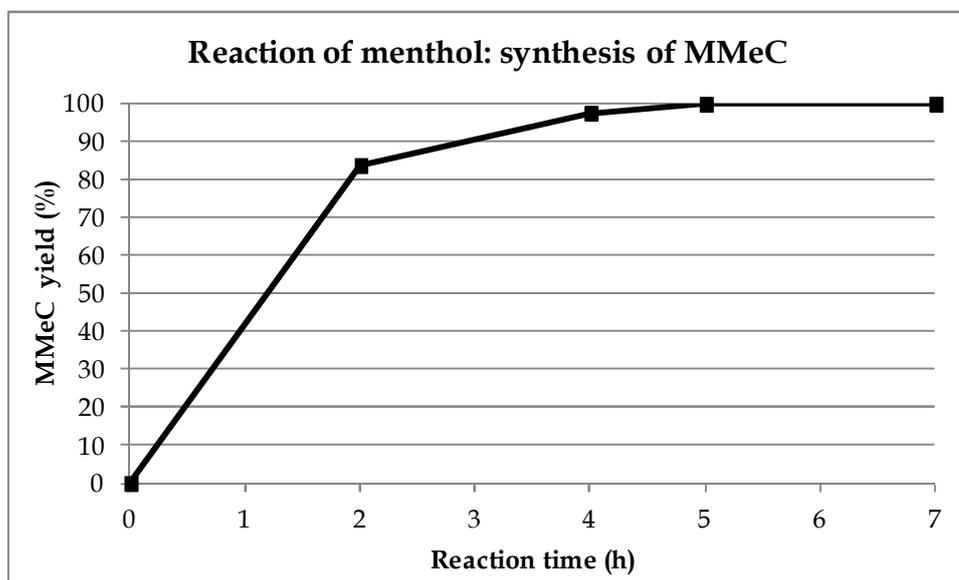After having optimized the RDS by using a simple and cheap homogeneous catalytic system (NaOCH$_3$), we started to investigate the possibility to use an heterogeneous catalytic.

The obvious advantages of this choice regards the easier recovery of the catalyst after reaction, that facilitates both products purification and catalyst recycle.

We decided to study a simple, cheap and well-known basic heterogeneous catalyst such as magnesium oxide (MgO).

This was synthesized by a precipitation method described in the experimental part of this Thesis (Chapter 3.2.2), and had a surface area of 200 m^2/g.

Surprisingly, at the lower reaction temperature (90°C), MgO showed good reactivity, although slower compared to that shown by the homogeneous catalyst, and very good conversion and selectivity to the desired products were achieved with all the aliphatic alcohols and diols tested.

Moreover, a leaching test was performed in order to control if part of MgO had dissolved in the reaction mixture.

In order to carry out this test, the reaction was started with a *n*-butanol:DMC reagent ratio equal to 5, and with a 5% w/w of MgO (with respect to DMC) as the catalyst.

Then, after 2 hours of reaction, the catalyst was filtered and the liquid mixture was made react again under the same conditions.

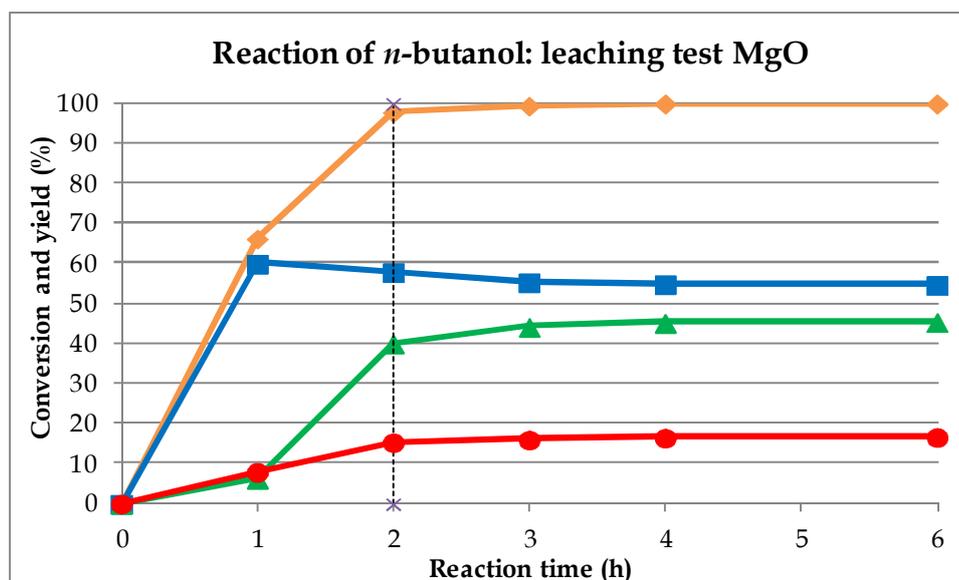The result of this experiment is shown in the graph below (Fig. 4.34).

Fig. 4.34 DBC synthesis by means of CIR between *n*-butanol and DMC, "implemented" RDS: leaching test.
(DMC:*n*-butanol =1:5; MgO 5% w/w on respect to DMC Tr≈118°C, T$_{oil\ bath}$=120°C). ● *n*-butanol conversion (red), ♦ DMC conversion (orange), ■ MBC yield (blue), ▲ DBC yield (green).

It is shown that both yield of products and butanol conversion stopped after MgO removal, with a steady value which was shown for more than 4 hours of reaction; this demonstrates that MgO did not dissolve in the reaction mixture.

The comparison between the catalytic results obtained using both homogeneous and heterogeneous catalysts is summarized in Table 4.5.

CIRs with DMC										
Alcohol (A)	Ratio A:DMC	Asymmetric carbonate (AC)	Symmetric carbonate (SC)	Implemented RDS	Catalyst	T (°C)	t (h)	X_A (%)	Y_{AC} (%)	Y_{SC} (%)
n-butanol	1 : 5	MethylButyl Carbonate (MBC)	DiButyl Carbonate (DBC)	NO	NaOCH₃ (1/30 mol)	90	1	39	39	0
n-butanol	1 : 5	MethylButyl Carbonate (MBC)	DiButyl Carbonate (DBC)	YES	NaOCH₃ (1/30 mol)	90	1	100	92,1	7,9
n-butanol	1 : 5	MethylButyl Carbonate (MBC)	DiButyl Carbonate (DBC)	YES	MgO 5% w/w	90	1	98,3	91,7	6,6
n-butanol	5 : 1	MethylButyl Carbonate (MBC)	DiButyl Carbonate (DBC)	YES	NaOCH₃ (1/30 mol)	118	4	36	5,3	94,7
n-butanol	5 : 1	MethylButyl Carbonate (MBC)	DiButyl Carbonate (DBC)	YES	MgO 5% w/w	118	4	17,8	38,4	60,7
1,2 propanediol	1 :10	five-membered cyclic carbonate: Propylene Carbonate (PC)		YES	NaOCH₃ (1/30 mol)	90	2	99	Y_{PC} = 99	
1,2 propanediol	1 :10	five-membered cyclic carbonate: Propylene Carbonate (PC)		YES	MgO 5% w/w	90	2	58	Y_{PC} = 58	
1,2 butanediol	1 :10	five-membered cyclic carbonate: Butylene Carbonate (BC)		YES	NaOCH₃ (1/30 mol)	90	2	99	Y_{BC} = 99	
1,2 butanediol	1 :10	five-membered cyclic carbonate: Butylene Carbonate (BC)		YES	MgO 5% w/w	90	2	57	Y_{BC} = 57	
Glycerol	1 :10	Glycerol carbonate (GlyC)	Heavier by-products	NO	NaOCH₃ (1/30 mol)	90	1	100	Y_{GlyC} =66,9	Y_{by-p} = 33,1
Glycerol	1 :10	Glycerol carbonate (GlyC)	Heavier by-products	YES	NaOCH₃ (1/30 mol)	90	1	100	Y_{GlyC} = 44,1	Y_{by-p}= 55,9
Cyclohexanol	1 :10	MethylCyclohexyl Carbonate (MCC)	DiCyclohexyl Carbonate (DCC)	YES	NaOCH₃ (1/30 mol)	90	2	98,8	97,6	1,2
Cyclohexanol	1 :10	MethylCyclohexyl Carbonate (MCC)	DiCyclohexyl Carbonate (DCC)	YES	MgO 5% w/w	90	2	85,8	85,3	0,5
(-)Menthol	1 :10	MethylMenthyl Carbonate(MMeC)	DiMenthyl Carbonate (DMeC)	NO	NaOCH₃ (1/30 mol)	90	2	19,7	19,7	0
(-)Menthol	1 :10	MethylMenthyl Carbonate(MMeC)	DiMenthyl Carbonate (DMeC)	YES	NaOCH₃ (1/30 mol)	90	2	83,7	83,7	0
Catechol	1 :10	five-membered cyclic carbonate: PyroCatechol Carbonate (PCC)		NO	NaOCH₃ (1/30 mol)	90	24	7	Y_{PCC} = 7	
Catechol	1 :10	five-membered cyclic carbonate: PyroCatechol Carbonate (PCC)		YES	NaOCH₃ (1/30 mol)	90	24	95,5	Y_{PC} = 95,5	
Catechol	1 :10	five-membered cyclic carbonate: PyroCatechol Carbonate (PCC)		YES	MgO 5% w/w	90	24	5,4	Y_{PC} = 5,4	
Phenol	1 :10	MethylPhenyl Carbonate (MPC)	DiPhenyl Carbonate (DPC)	NO	NaOCH₃ (1/30 mol)	90	24	8,5	7,3	0,1
Phenol	1 :10	MethylPhenyl Carbonate (MPC)	DiPhenyl Carbonate (DPC)	YES	NaOCH₃ (1/15 mol)	90	24	15,4	14,2	0,6
Phenol	1 :10	MethylPhenyl Carbonate (MPC)	DiPhenyl Carbonate (DPC)	YES	MgO 5% w/w	90	24	1,5	0,8	0,3

Table 4.5 Summary table on the CIRs of DMC with several alcohols and diols, both with and without the implemented distillation system and with homogeneous (NaOCH₃) and heterogeneous (MgO) catalysis.

On the other hand, the reaction of aromatic alcohols (phenol) and diols (catechol) did not proceed with MgO. This is due to the stronger interaction between these more acidic alcohols and the catalytic surface, with the formation of a strong adsorbed magnesium salt of the corresponding alcoholate.

This hypothesis was confirmed by means of infrared spectroscopy characterisation.

Firstly, the catechol spectra was registered (Fig. 4.35) and the main bands were attributed to the vibrational mode of the molecule by matching experimental and calculated wavenumbers (Table 4.6).
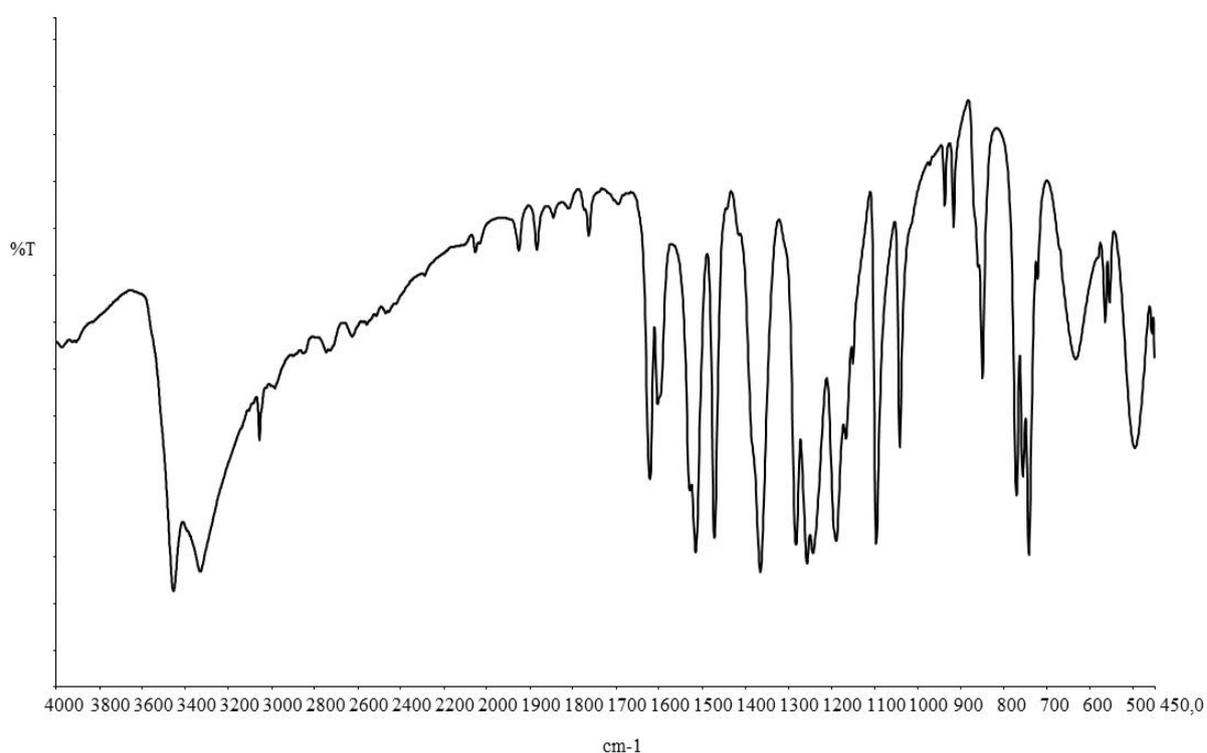

Fig. 4.35 Catechol infra-red spectrum between 4000 and 450 cm-1 (transmittance mode)

Calculated Wavenumbers (cm⁻¹)	Experimental Wavenumbers (cm⁻¹)	Vibrational mode description
3898	3451	ν OH
3838	3327	ν OH
3239	3100	ν sym CH
3229	3080	ν asym CH
3216	3052	ν asym CH
3194	3043	ν asym CH
1668	1620	ν aromatic CC + δ OH
1664	1600	ν aromatic CC
1554	1596	ν aromatic CC + δ OH
1507	1528	ν aromatic CC
1482	1514	ν aromatic CC
1382	1470	ν aromatic CC + δ OH + δ CH
1324	1364	δ CH + δ OH + ν CO
1285	1281	ν CO (both) + δ OH
1231	1255	δ OH (both)
1184	1241	δ OH + ν CO + δ CH
1108	1187	δ CH + δ OH
1050	1165	δ CH
861	1149	δ CH
781	1096	δ CH
729	1040	δ CH

Table 4.6 Catechol main vibrational mode and related bands wavenumbers

Then, MgO was recovered after the reaction test with catechol, filtered and washed with dichloromethane in order to remove the weakly adsorbed organic molecule. Then the catalyst was dried and its IR spectrum was taken.

The catechol spectrum and that one of the used catalyst are compared in the following figure (Fig. 4.36).
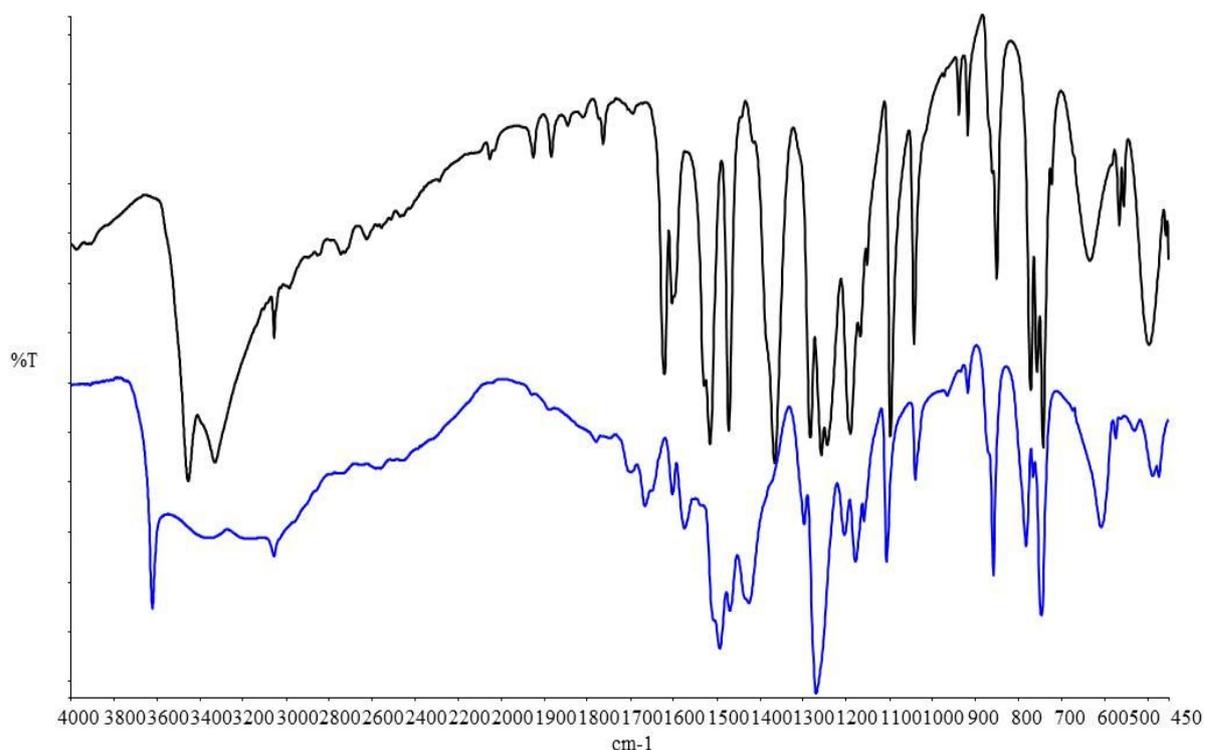
Fig. 4.36 FT-IR spectra of catechol moiety (black) and of the used MgO after the reaction with catechol and DMC (blue). Spectra collected in transmittance mode between 4000 and 450 cm^{-1}.

Spectra clearly show that the aromatic species was adsorbed, and that the main bands were perturbed due to the formation of the catecholate magnesium salts. In particular, the –OH stretching bands at 3451 and 3327 cm^{-1} disappeared with the concomitant formation of the Mg-OH moiety vibrating at 3618 cm^{-1}.

Moreover, the band at 1363 cm^{-1} completely disappeared demonstrating the deprotonation of both–OH groups; in the CO stretching region (around 1200 cm^{-1}), the shift of the bands toward higher wavenumber and the corresponding formation of a strong band centred at 1268 cm^{-1} can be attributed to the CO stretching in the dissociated alcoholate.

Furthermore the bands at 1620 and 1596 cm^{-1} attributed to the C-C stretching bands, with a minor component of –OH bending were strongly perturbed and shifted toward 1663 and 1572 cm^{-1}, respectively, while the band centred at 1601 cm^{-1} was almost unperturbed.

A further proof for the formation of magnesium catecholate was achieved by reacting catechol with magnesium hydroxide (Mg(OH)$_2$), and comparing the spectrum of the obtained salt with that one of used MgO (Fig. 4.37).
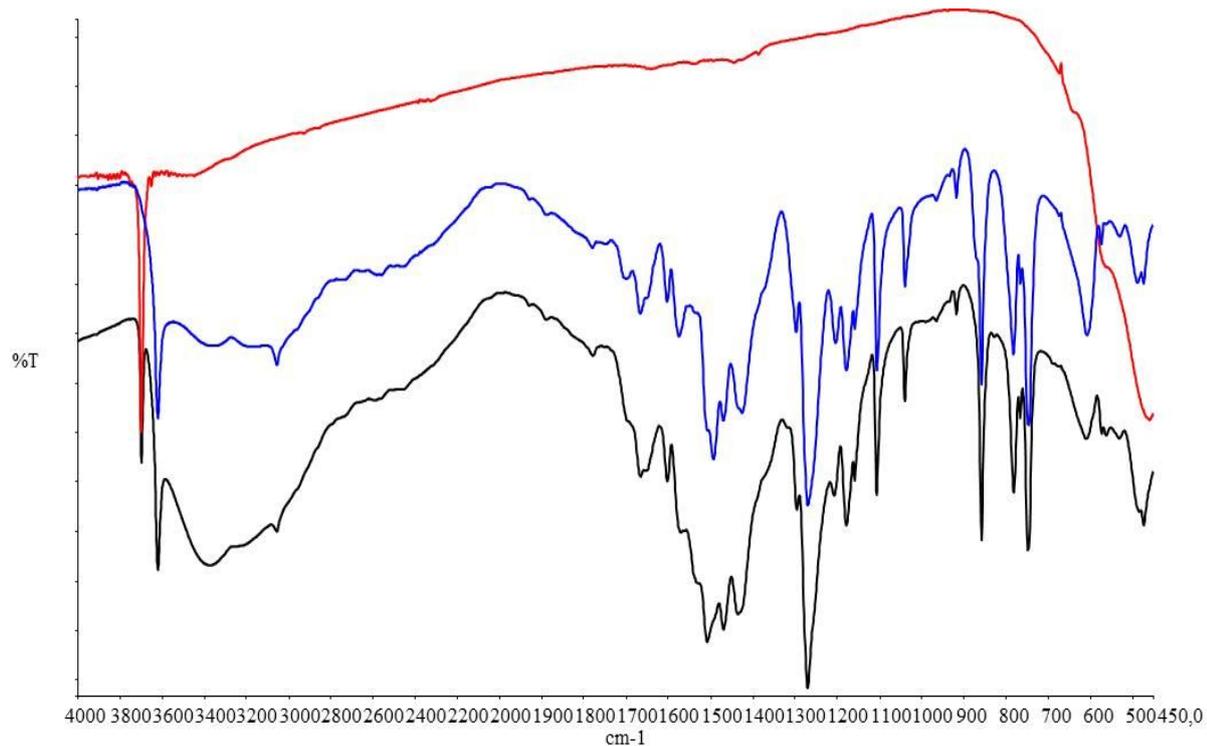
Fig. 4.37 FT-IR spectra of the used MgO after the reaction with catechol and DMC (blue), of the catechol magnesium salt (black) and of the pure magnesium hydroxide (red). Spectra registered in the transmittance mode between 4000 and 450 cm^{-1}.

The spectra clearly show the similarity between the magnesium salt, obtained reacting catechol and Mg(OH)$_2$, and the used MgO catalyst; the same bands were shown, which proved the formation of strongly adsorbed catecholate on MgO surface.

4.2.7 *Final considerations*

The CIR between DMC and alcohols or diols was optimized by developing an "implemented" reactive distillation set-up, in which the selective adsorption of methanol inside molecular sieves was combined with the removal of methanol from the reaction medium by distillation.

This system allowed us to greatly increase the yield and the selectivity to the desired products; in particular, PCC was synthesized with yield > 90% and complete selectivity.

However, this was not true for glycerol carbonate (GlyC) synthesis. In fact, glycerol, with its three reactive hydroxyl groups, underwent many consecutive reactions, which were favoured by the selective removal of methanol, and that finally led to the formation of oligomers and heavier by-products.

These reactions were firstly optimized using an homogeneous catalytic system ($NaOCH_3$), and then implemented with an heterogeneous catalyst based on MgO.

This is a cheap basic catalyst able to catalyse the CIR of DMC with all the aliphatic alcohols and diols investigated, also in mild conditions (90°C and atmospheric pressure).

On the other hand, the reaction with phenol and catechol led to a stronger and detrimental interaction of these alcohols with MgO, with formation of the corresponding magnesium salt that did not react further.

4.3 A study of PCC reactivity

4.3.1 Introduction

PCC (pyrocatechol carbonate, benzo-1,3-dioxolan-2-one) was synthesized with very high yield and selectivity (90% and 99%, respectively) using our "implemented" reactive distillation system, as described in the previous chapters.

PCC represents a so far scarcely investigated molecule; to the best of our knowledge, no author ever reported on the use of this organic carbonate as a chemical intermediate for the synthesis of other high added-value products.

This prompted us to further investigate the potential of PCC as a highly active electrophilic species, by reacting it with nucleophilic reagents.

In particular, we have investigated the reactivity of PCC with alcohols and polyols in the CIR, in order to obtain other interesting carbonates (or polycarbonates), and with amines in order to obtain substituted ureas and polyureas.

The main goal of this work was to obtain the highly efficient and selective synthesis of symmetric aliphatic carbonates and of glycerol carbonate.

As reported in the previous chapter, the synthesis of symmetric carbonates by CIR with the traditional carbonate sources (DMC or EC) includes two consecutive (equilibrium-limited) reactions, in which during the second step the asymmetric carbonate either reacts with another alcohol molecule, or undergoes disproportionation, in both cases finally producing the symmetric carbonate.

This means that we need to wait long reaction time in order to achieve high yield of the symmetric product, and also we need to operate with a large excess of the alcohol in order to modulate selectivity and shift reaction equilibria.

On the other hand, with a polyol reagent like glycerol, it is very difficult to achieve high selectivity toward the desired 5-membered cyclic glycerol carbonate (GlyC), because of the formation of different oligomers and heavier by-products with carbonate-type bond between different the glycerol moieties.

As discussed in the introduction (Chapter 1.3.6), it is known that the CIRs follow the rule that the more nucleophilic compound displaces the less nucleophilic one, thus giving rise to the formation of a new carbonate.

In this way, PCC should show an easier ring opening due to the simultaneous contribution of both its steric strain[330] and the properties of the catechol anion as a softer nucleophile and a better leaving group (in analogy to the above mentioned case of diphenyl carbonate for the formation of polycarbonates, Chapter 1.3.5.3).

The generic reaction pathway for the CIR of PCC and alcohols to yield symmetric carbonates is reported below.
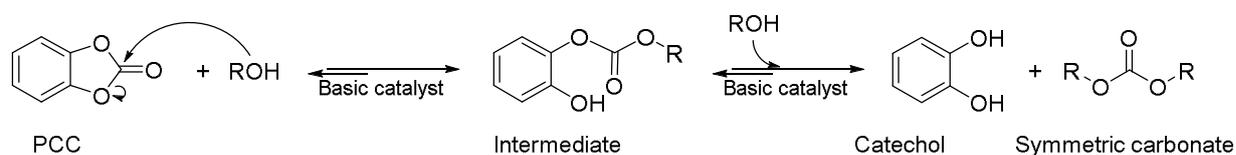
Scheme 4.9 CIR of PCC and a generic alcohol (ROH).

The characteristics of the desired products, the results of reactivity experiments and details about reaction mechanisms, as well as the problem of PCC sensitivity toward hydrolysis, are described in the following chapters.

4.3.2 CIR of PCC: products of interest

The main synthetic targets obtained by the CIR of PCC with several alcohols are reported below.

4.3.2.1 Glycerol carbonate (GlyC)

Glycerol carbonate (GlyC, 4-hydroxymethyl-2-oxo-1,3-dioxolane) is a polyfunctional carbonate, bearing both a carbonate moiety and a hydroxyl group.
This small molecule (molar weight 118.09 g/mol) has gained importance over the latest 20 years because of two main reasons:

- as a possible method for the valorisation of glycerol, which is becoming widely available as a major bio-based by-product, from the manufacture of biodiesel (as described in the Introduction part of this Thesis, Chapter 1.4.2);
- for its multifaceted reactivity, which implies numerous applications.

The combination of its bio-based origin and reactivity has made GlyC to be elected as a versatile and renewable building block for a more sustainable chemistry.
Moreover, GlyC can be synthesized by means of various synthetic pathways, as shown below (Scheme 4.10).
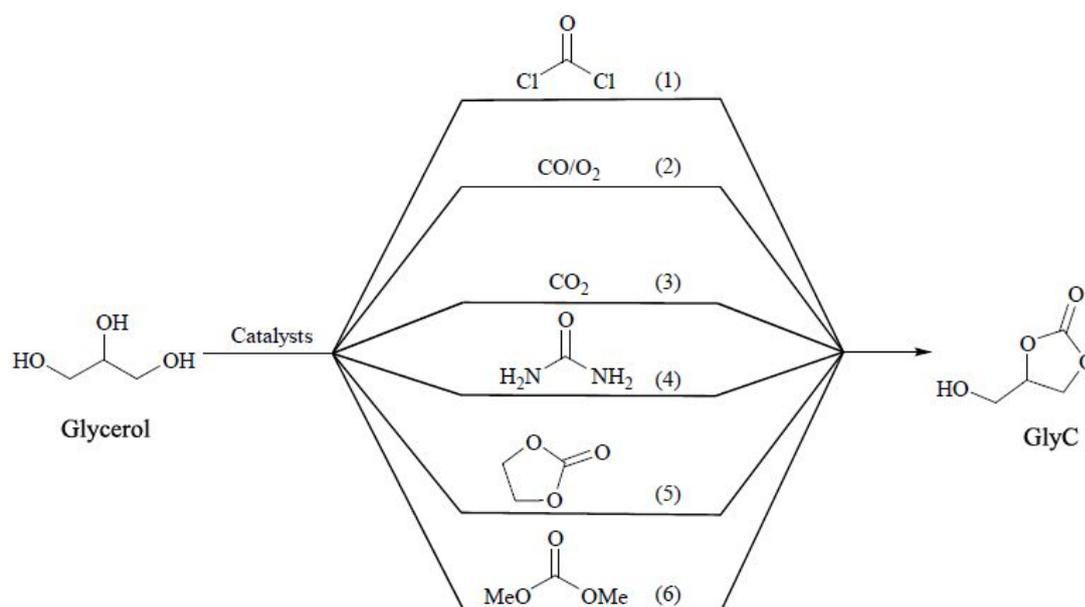
Scheme 4.10 Different routes for GlyC synthesis starting from glycerol.

Among these synthetic pathways, (1), (2) and (3) are referred to as phosgenation, oxidative carbonylation and direct carboxylation of glycerol, respectively; these routes are problematic and hold several drawbacks.

For example, route (1) uses a dangerous, toxic and corrosive starting material (phosgene); route (2) uses a dangerous inflammable mixture of CO (also toxic), oxygen and glycerol over a metallic catalyst.[331]

On the other hand, route (3) is limited by strict thermodynamic constraints, needs high pressure of CO_2 and, in the optimized conditions, in the presence of a homogeneous tin catalyst (n-Bu$_2$Sn(OCH$_3$)$_2$), it gives a maximum conversion of about 7-10%.[332,333]

Route (4) is the glycerolysis of urea; it is carried out at relative high temperature (T>130°C) and reduced pressure, in order to remove ammonia and shift the equilibrium toward GlyC formation.[334,335]

Noteworthy, this pathway leads to the production of high quantity of ammonia as a co-product, which is limiting its industrial implementation. A possible solution would be to combine the production of glycerol carbonate and the synthesis of urea from ammonia in the same plant.

The last synthetic routes (5) and (6), represent the CIR of glycerol with cyclic and linear carbonates, respectively.

These reactions, widely studied and described in several interesting reviews, generally allows to achieve better results, but often leads to a mixture of the desired product with by-products and oligomers.[288,335,336]

GlyC is a promising intermediate for several applications. Because of its high boiling point (110–115 °C at 0.1 mmHg), high flash point (190 °C) and low volatility

(vapor pressure is 8 mbar at 177 °C), GlyC and its esters are solvents with lower vapour pressure compared to Volatile Organic Compounds (VOC), useful for many applications, as a bio-based alternative to organic solvents.

Moreover, GlyC has been investigated as a component in gas separation membranes, polyurethane foams and surfactants, as a nonvolatile reactive solvent, as a component in coatings, and as a source of new hyperbranched polymers.[288]

Finally, GlyC has a chance to become a major chemical intermediate, for instance it can be converted into either glycidol (by decarboxylation) or epichlorohydrin, a product widely applied industrially, under mild conditions.[337]

A schematic overview of the direct and indirect applications of GlyC is summarized below (Scheme 4.11).
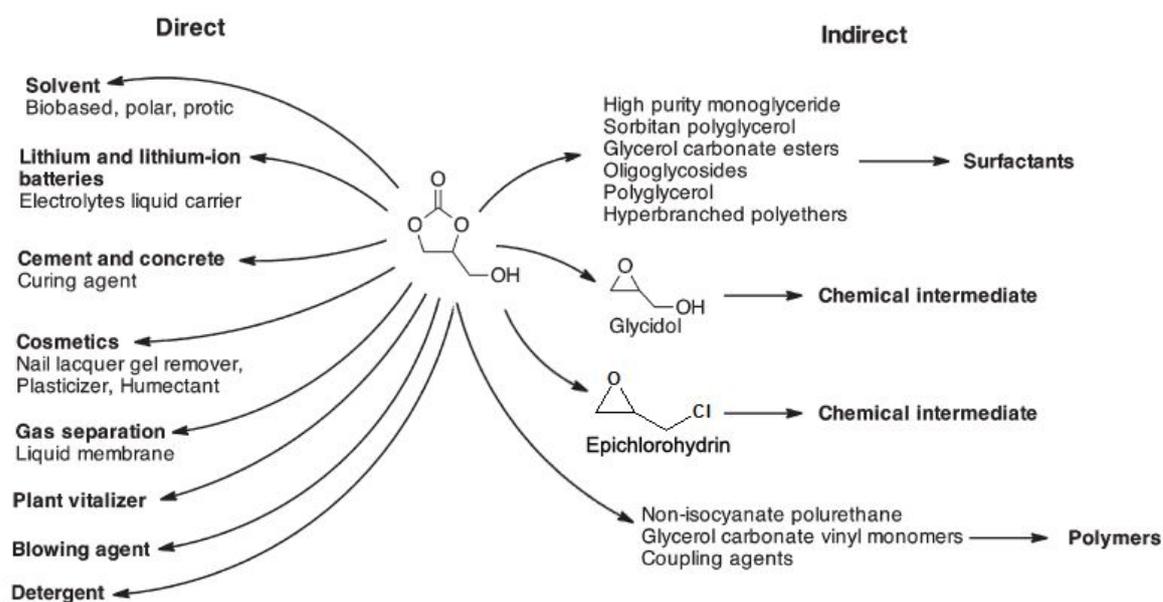
Scheme 4.11 GlyC applications, adapted from ref. [335]

4.3.2.2 Solketal and solketal carbonate (SC)

Isopropylidene glycerol (solketal) is a commercially available glycerol derivative.

It represents the protected form of glycerol prepared by reaction between glycerol and acetone, whereby, an isopropylene group is covalently linked to two vicinal hydroxyl groups.

It finds use as a solvent, plasticizer and starting material for the preparation of speciality monoglycerides and chemicals.[338,339]

Because it holds only one reactive hydroxyl group is a selective reactant (for example, by means of CIR) for the synthesis of the corresponding carbonate (Solketal carbonate, SC). The molecular structures are reported below (Fig. 4.38).
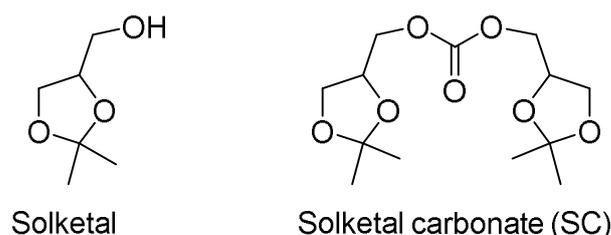
Fig. 4.38 Solketal and Solketal carbonate (SC).

Kenar et al. reported the synthesis of SC, and used it as an intermediate for the synthesis of polyol carbonate (after the removal of acetone by de-protection of the diol) and for carbonate based polymers.

In particular, they claim the synthesis of SC by CIR of solketal and diethyl carbonate (DEC) (solketal:DEC=2,4:1), in the presence of sodium methoxide as catalyst, by using an azeotropic distillation system at 90°C for 20 hours and then increasing the temperature up to 120°C in order to distill away the azeotrope (ethanol/DEC).

After distillation and extraction with CH_2Cl_2 they were able to obtain a SC isolated yield as high as 65%.[340]

4.3.2.3 *Linear carbonates: Diethyl carbonate (DEC), Dibutyl carbonate (DBC), Diallyl carbonate (DAC)*

Diethyl carbonate (DEC, Fig. 4.39) finds many applications as solvent and reactant in the manufacture of pharmaceuticals, fertilizers, pesticides, dyes and polymers.[341,149]
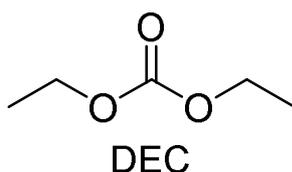

Fig. 4.39 Diethyl carbonate structure.

Nowadays, it is mainly produced by the reversible consecutive, second order CIR of DMC and ethanol by means of reactive distillation systems that lead to the synthesis of both the symmetric (DEC) and asymmetric methylethyl carbonate.[342,343,344]

As described before in this work, dibutyl carbonate (DBC, Fig. 4.40) is an important long-chain alkyl carbonate for the petrochemical industry; it is used for the production of various organic and polymeric materials, mainly for the synthesis of polycarbonates. DBC is also considered an excellent environmental protection lubricant material because of its good lubricity and wearability, corrosion resistance,

high thermal oxidative stability, and outstanding solubility. The synthesis of DBC therefore has been growing fast in latest years due to a continual increase of market demand.[325,326,327,328]
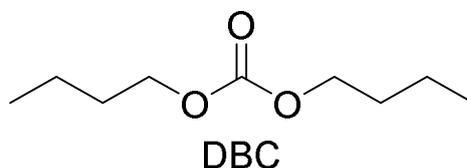

Fig. 4.40 Dibutyl carbonate.

Diallyl carbonate (DAC, Fig. 4.41) is a very important polyfunctional carbonate. Allyl and vynil carbonates are used for the synthesis of optical plastics with outstanding properties.[345]

It has been also widely investigated as highly efficient allylating reagent.[346,347,348]
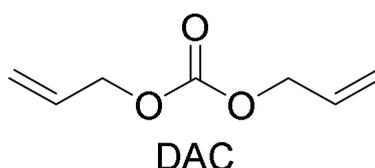
Fig. 4.41 Diallyl carbonate.

4.3.2.4 *Dicyclohexyl carbonate (DCC) and Diisopropyl carbonate (DIPC)*

Secondary alcohols are reported to be much less reactive in the CIR for the synthesis of the corresponding carbonates.

This is mainly due to the increase of the steric hindrance and, to a lesser extent, to the lower stability of their deprotonated active form compared to the primary one.

For these reasons, we decided to investigate the synthesis of two organic carbonates, scarcely studied before in the literature, derived from two different secondary alcohols,.

The first one, derived from cyclohexanol, is dicyclohexyl carbonate (DCC, Fig. 4.42).
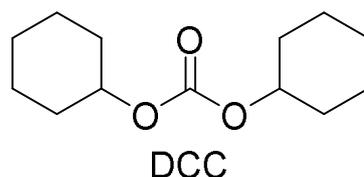
Fig. 4.42 Dicyclohexyl carbonate

This carbonate was chosen because it is a possible intermediate for diphenyl carbonate (DPC) synthesis by means of dehydrogenation and aromatisation.
The catalytic tests of this latter reaction are not reported in this Thesis.

The second one, derived from isopropyl alcohol, is diisopropyl carbonate (DIPC, Fig. 4.43).
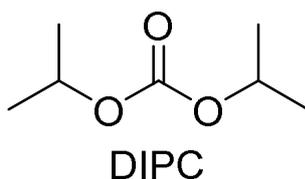
Fig. 4.43 Diisopropyl-carbonate

This carbonate can be successfully used as solvent, due to its lower reactivity compared to DMC.

4.3.3 The CIRs of PCC: results and comparisons

The same homogeneous and heterogeneous catalysts used in the CIR between DMC and alcohols were also tested for the CIR of PCC: sodium methoxide ($NaOCH_3$) and MgO (200 m^2/g), respectively.

All reactions were performed in a simple round bottom flask equipped with reflux condenser or in a close screw cap vial equipped with a magnetic stirrer.

4.3.3.1 Synthesis of glycerol carbonate (GlyC)

As described in the corresponding chapter (Chapter 4.3.2.1), GlyC is widely recognized as an important bio-based intermediate and solvent.

However, due to the three reactive hydroxyl groups present in glycerol, to obtain a fast and selective synthesis by means of the traditional synthetic routes is not an easy task.

Because of these reasons, we decided to test the reactivity of PCC in the CIR with glycerol using $NaOCH_3$ as homogeneous basic catalyst.

The reaction follows the mechanism reported below (Scheme 4.12).
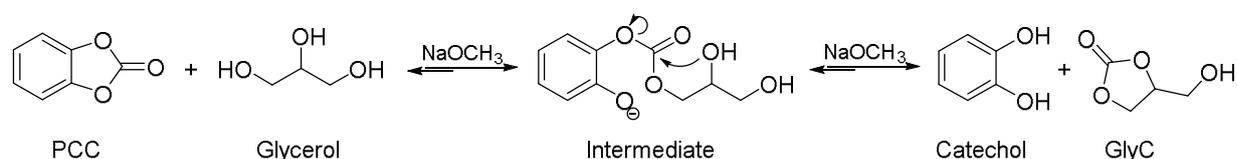
Scheme 4.12 CIR between PCC and glycerol

Indeed, by loading PCC and glycerol in a stoichiometric ratio (1:1), at low temperature (T=60°C), we were able to obtain the selective formation of the desired product (no by-products were detected) (Fig. 4.44).

Fig. 4.44 PCC:Glycerol:NaOCH$_3$=1:1:1/30; round bottom flask with reflux condenser. T = 60°C. ● PCC conversion (red), ■ GC yield (brown) and ▲ Glycerol conversion (green).

The surprising reactivity of PCC leads to an easy and fast reaction free from equilibrium limitations; moreover, the instability of the intermediate, that undergoes a rapid intramolecular ring-closure, allows the selective formation of GlyC with a yield of 88% in only 30 minutes reaction. Noteworthy, PCC conversion was higher than that of glycerol. This was due to both PCC decomposition and hydrolysis back to catechol, because of both the atmospheric humidity and the water contaminant in the reagents. However, conducting the reaction in a double-necked round bottom flask under an inert nitrogen flow, which removed the humidity from the reactor vessel, allowed us to overcome this problem in part (Fig. 4.45).
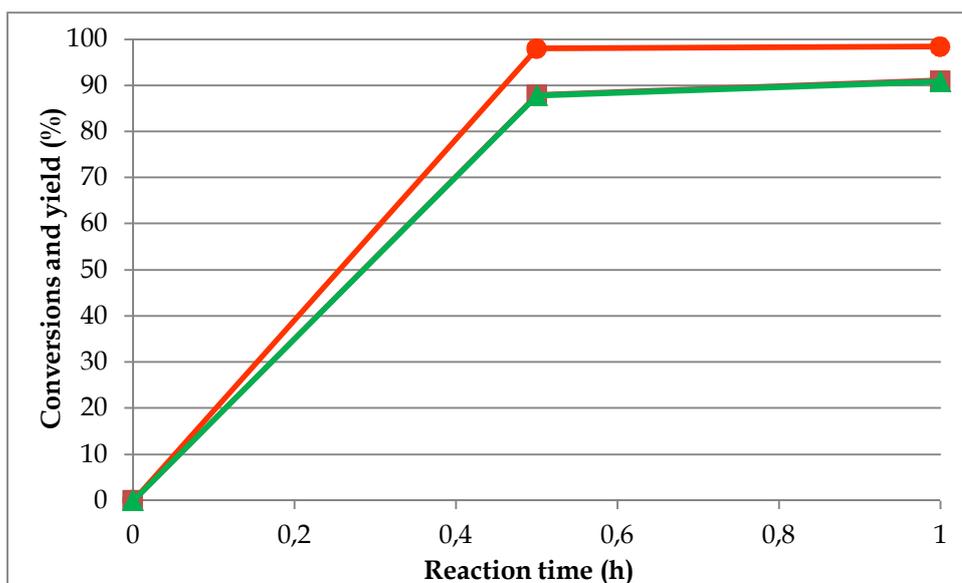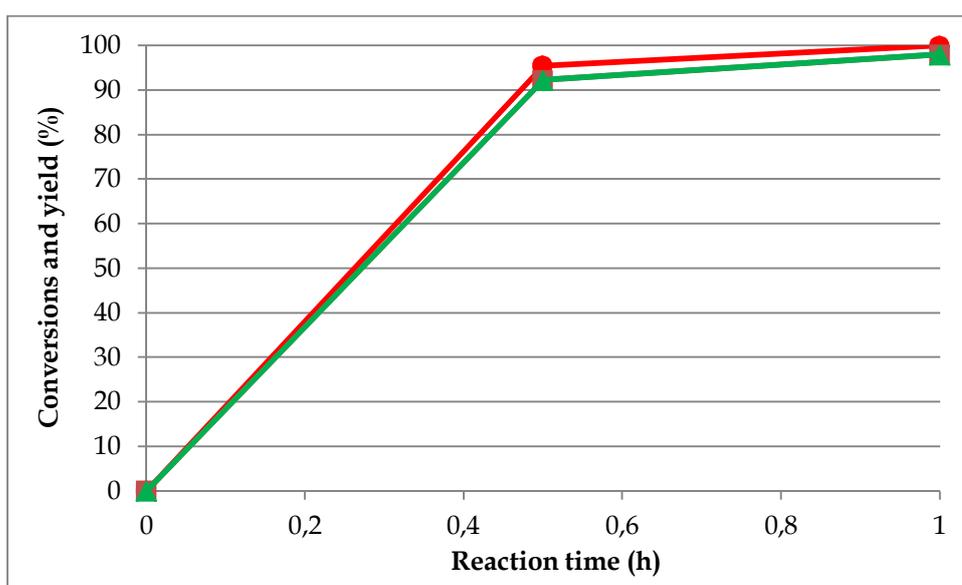

Fig. 4.45 PCC:Glycerol:NaOCH$_3$=1:1:1/30; round bottom flask with reflux condenser, N$_2$ flow. T = 60°C. ● PCC conversion (red), ■ GC yield (brown) and ▲ Glycerol conversion (green).

In this way, after one hour reaction we are able to obtain almost quantitative yield of GlyC (ca 98%) with an outstanding selectivity (>99%), while limiting the extent of PCC decomposition to negligible values.

After the encouraging results obtained, we decided to study the possibility to move from an homogeneous (NaOCH₃) to an heterogeneous (MgO) catalytic system.

We started to perform the reaction in a very simple system made up of a screw-cap vial equipped with a magnetic stirrer and purged with a nitrogen atmosphere before the start of the reactions.

We decide to add a small amount (1 ml) of anhydrous THF as reaction solvent in order to overcome the material transfer problems due to the high density of the mixture of PCC and glycerol at the beginning of the reaction.

Indeed, we also discovered that the GlyC formed during the reaction, helps to better solubilize the yet unconverted reagents.

All the results obtained with the screw-cap vial, with both homogeneous and heterogeneous catalysis, and the comparison of reactivity with DMC and EC as carbonyl source in the same conditions, are reported in the following table (Table 4.7).

GlyC synthesis									
Homogeneous catalysis: Sodium methoxide									
Carbonyl source (A)	Alcohol (B)	Molar ratio	N_2	Catalyst NaOCH₃	T (°C)	t(h)	X_A (%)	X_B (%)	Y GlyC
PCC	Glycerol	1:1	yes	1/30mol	40	1	98,4	99,8	92
PCC	Glycerol	1:1	yes	1/30mol	60	0,5	95,5	94	94
PCC	Glycerol	1:1	yes	1/30mol	60	1	98,6	99	95,5
EC	Glycerol	1:1	yes	1/30mol	60	1	73	80	69
DMC	Glycerol	1:1	yes	1/30mol	60	1	27	30	26
Heterogeneous catalysis: MgO, anhydrous THF as solvent									
Carbonyl source (A)	Alcohol (B)	Molar ratio	N_2	Catalyst NaOCH₃	T (°C)	t(h)	X_A (%)	X_B (%)	Y GlyC
PCC	Glycerol	1:1	yes	MgO 5% w/w	60	1	99	96	96
EC	Glycerol	1:1	yes	MgO 5% w/w	60	1	60	95	69
DMC	Glycerol	1:1	yes	MgO 5% w/w	60	1	20	11	1

Table 4.7 Synthesis of GlyC, both with homogeneous and heterogeneous catalysts (X: conversion; Y: yield).

From results summarized above, the benefit of the CIR starting from PCC, in comparison with the more conventional reagents for these reactions (EC and DMC), are evident.

PCC allowed us to obtain better yield and selectivity using both the homogeneous and the heterogeneous catalyst.

In particular, using the cheap and simple MgO, we were able to obtain 96% GlyC yield at 60°C in only 1 hour of reaction, with no appreciable by-products (adding only the minimum amount of anhydrous THF in order to solubilize PCC and facilitate mass transfer).

The use of a heterogeneous system facilitates the further product purification and separation steps. In this way, we have performed the separation of the product with a chromatographic column obtaining an isolated yield of GlyC equal to **77%** with a purity grade **> 99%**.

Furthermore, both EC and DMC showed worse reactivity and selectivity in the end leading, especially in the case of EC, to the formation of oligomers which were insoluble in acetone (the solvent used for the gas-cromatographic analysis). This caused a considerable loss in the carbon balance for these reactions.

4.3.3.2 *Changing reaction conditions: synthesis of 2-hydroxymethyl-1,4-benzodioxane (HMB)*

The reaction of an equimolar amount of PCC and glycerol led to the fast and selective synthesis of GlyC with almost quantitative conversion of reagents.

In other words, after one hour reaction time at low temperature (60°C) we were able to obtain a mixture containing GlyC and catechol with a 1:1 molar ratio.

Catechol is formed as the only co-product of the reaction starting from PCC.

Noteworthy, except for the mixture with GlyC, the hydroxyl groups and hydrophilicity of catechol made easier its separation from the aprotic organic carbonates by solvent extraction (this concept will be discussed in detail in the following chapter).

On the other hand, GlyC with its free –OH group showed a solubility similar to that of catechol with the solvents tested. Moreover, the high boiling point of GlyC and thermal instability made the distillation an unwise choice. These characteristics made the separation of catechol and GlyC a tricky problem, solved by the liquid chromatographic separation.

Because of these reasons, we decided to turn this problem into an advantage, converting GlyC from a reaction product into a reactive chemical intermediate, in order to synthesize 2-hydroxymethyl-1,4-benzodioxane (Fig. 4.46).
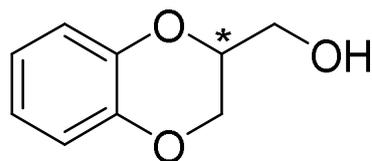
Fig. 4.46 2-hydroxymethyl-1,4-benzodioxane (HMB).

1,4-benzodioxane derivatives, characterized by a chiral centre (*), are interesting molecules, that can be found in a variety of natural products and therapeutic agents possessing important biological activities.

The interest for these molecules has been arising during the latest years due to the discovery of their interesting biological properties, such as:

calcium antagonist, α-adrenergic blocking, spasmolytic, antigastric, antidepressant anxiolytic and antipsychotic, and hepatoprotective to name a few. These activities are influenced by the absolute configuration of the 1,4-benzodioxane unit. In particular, enantiomerically pure HMB and the corresponding carboxylic acid are important intermediates of various drug molecules (doxasozin, prosympal, piperoxan and dibozane, to name some commercial products, Fig. 4.47). These compounds could also be used as intermediates for very useful synthetic transformations.[349,350,351,352,353,354]

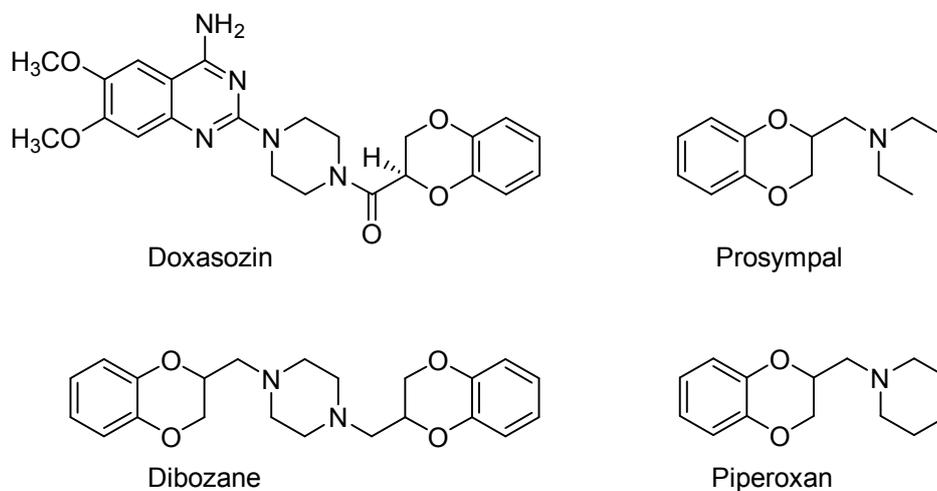
Doxasozin

Prosympal

Dibozane

Piperoxan

Fig. 4.47 Active principle structures of many commercial drugs.

From the literature we know that GlyC at high temperature (and low pressure) in the presence of a catalyst undergoes decarboxylation to glycidol (Scheme 4.13).[355]
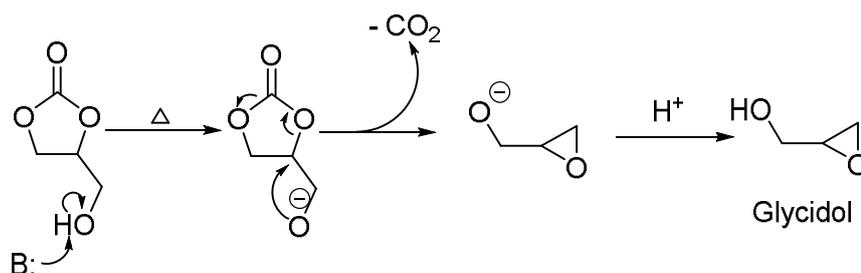
Scheme 4.13 Glycerol carbonate decarboxylation to glycidol

In 2013, R. Bai et Al. have reported the one-pot synthesis of glycidol reacting DMC and glycerol in mild conditions in the presence of solid $NaAlO_2$ as the catalyst.[356]
So we decided to perform the synthesis of 2-hydroxymethyl-1,4-benzodioxane in two steps:

1. CIR of PCC and glycerol (1:1) at 60 °C for 1 hour in the presence of the homogeneous catalyst (6.6 mol.%) and an inert flow of nitrogen (open system, double-necked round bottom flask with condenser);
2. To increase the temperature in order to promote the decarboxylation of GlyC to glycidol; and carry out the in-situ condensation of the so-formed glycidol with catechol to yield the desired product.

This synthetic pathway is summarized below (Scheme 4.14).
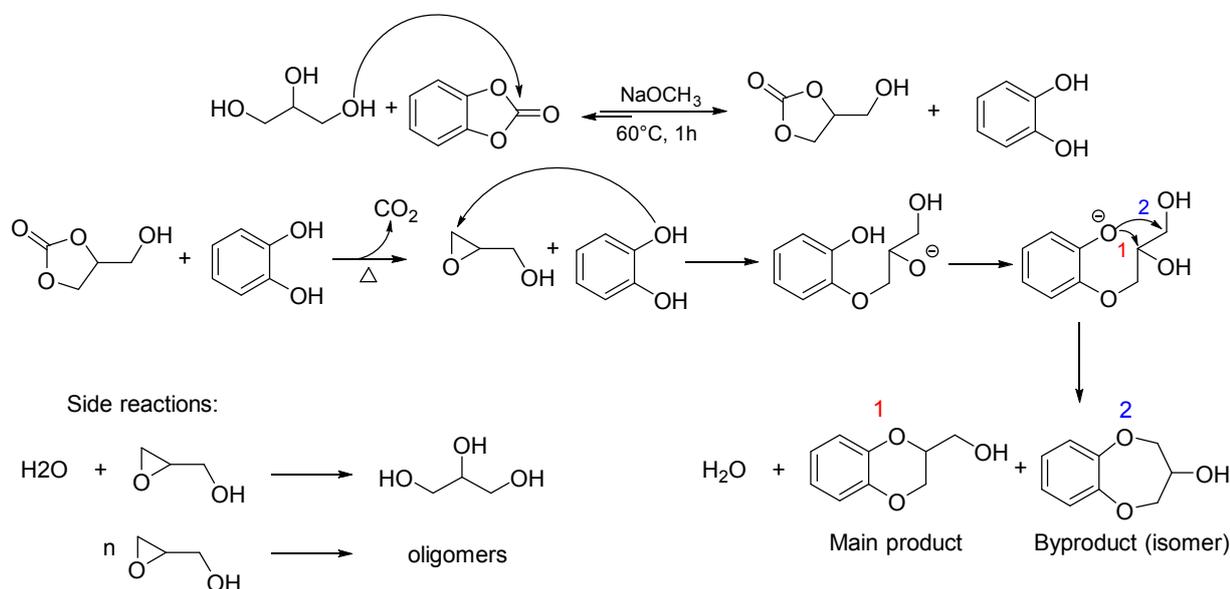
Scheme 4.14 Reaction pathway from PCC and glycerol to HMB

The first step (CIR of PCC and glycerol) was already discussed and optimized in the previous chapter; we will now focus our attention on the other steps.

In particular, starting from a mixture of catechol:GlyC=1:1, we first investigated the influence of the reaction temperature at atmospheric pressure on the decarboxylation of GlyC (Fig. 4.48).

Fig. 4.48 Catechol:GlyC:NaOCH$_3$=1:1:1/15; round bottom flask with reflux condenser, N$_2$ flow, 4h of reaction. T influence study. Catechol conversion (blue), GlyC conversion (red), HMB yield (green), glycerol yield (light blue) and others yield (grey).

From these results, the relevant influence of temperature on both the decarboxylation of GlyC and the subsequent formation of the desired HMB is evident.

With the term "others", we consider mainly the structural isomer of HMB (called "by-product" in the scheme above), and few other heavier by-products.

Noteworthy, at 170°C we were able to obtain complete conversion of GlyC (100%) but catechol conversion was exactly half as much of this value (around 50%), with a HMB yield around 44%.

This can be explained by the reaction mechanism shown in Scheme 4.14. Indeed, each condensation between catechol and glycidol produces one molecule of HMB and one molecule of water. Unfortunately, water can readily react with another molecule of glycidol, opening the oxirane ring and yielding glycerol that is inert for the desired reaction.

In order to prove this we decided to perform one test by feeding a double amount of GlyC in the optimized conditions (170°C) and shortening the reaction time to one hour only; the results obtained are shown in Fig. 4.49.
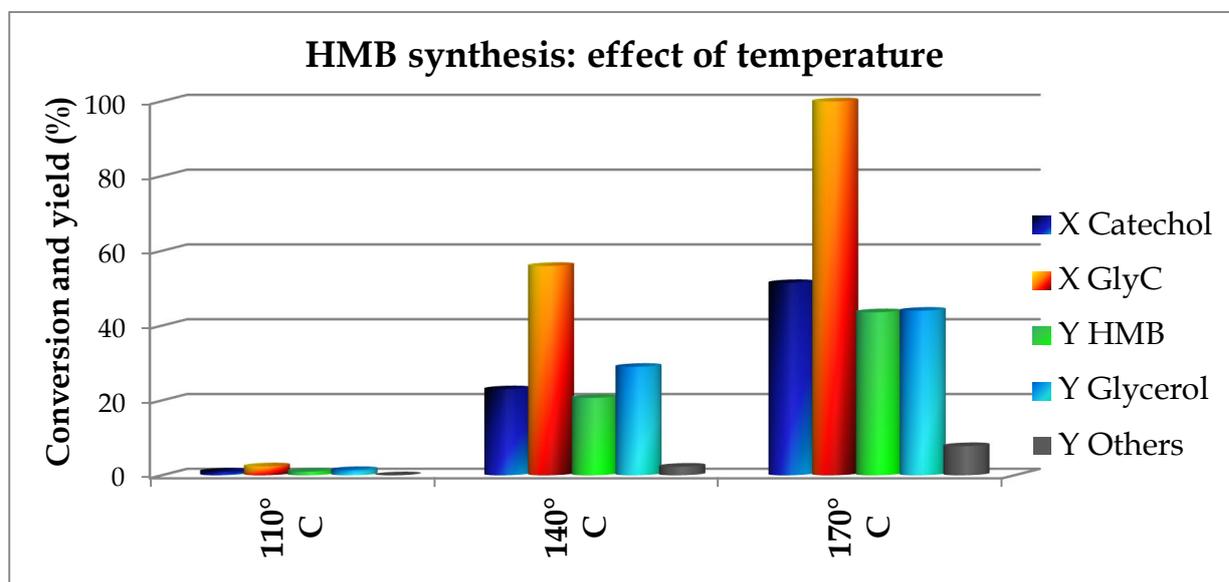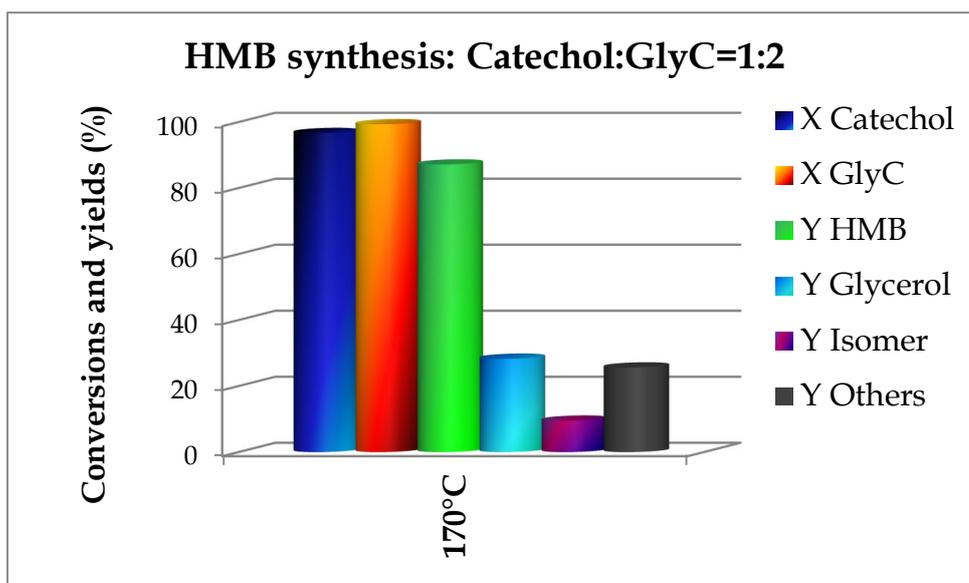
Fig. 4.49 Catechol:GlyC:NaOCH$_3$=1:2:1/15; round bottom flask with reflux condenser, N$_2$ flow, 1h of reaction. T influence study. Catechol conversion (blue), GlyC conversion (red), HMB yield (green), glycerol yield (light blue), isomer yield (purple) and others, heavier by-products yield (grey). HMB and isomer yield based on catechol; glycerol and others based on GlyC.

In this way, the feed of an excess GlyC allowed us to obtain the complete conversion of catechol and a remarkable increase of the yield to the desired product (up to 90%).

On the other hand, the greater excess of GlyC gave rise to the formation of heavier polymer-like by-products, insoluble in acetone (but soluble in water), with losses in the carbon balance for the aliphatics reagent.

Interestingly, when the reaction was performed in the same reaction conditions but in the absence of catalyst (NaOCH$_3$), a complete lack of reactivity was shown, with no reactants conversion and products formation. Interestingly, GlyC showed to be stable toward the thermal decomposition/decarboxylation, and the sodium salt proved to be the catalyst for both decarboxylation and condensation.

At the best of our knowledge, we are the first to perform the synthesis of HMB through this pathway.

4.3.3.3 Reaction with primary alcohols: synthesis of DEC, DBC, DAC and SC

PCC shows a wonderful reactivity in very mild reaction conditions with glycerol, so we decided to test it for the selective synthesis of a wide series of symmetric carbonates, in particular starting from primary aliphatic alcohols.

We will consider as starting material the following alcohols: ethanol, *n*-butanol, allyl alcohol and solketal; the corresponding carbonates are shown in Scheme 4.15.
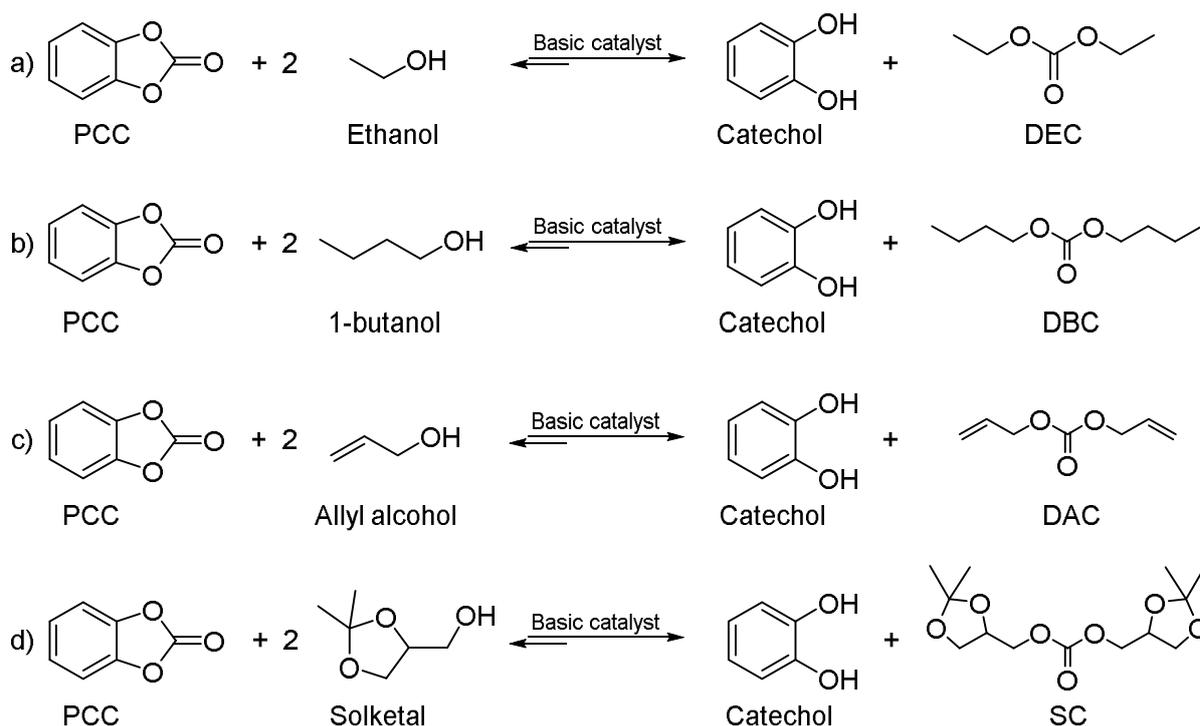
Scheme 4.15 CIRs of PCC and primary alcohols.

From a preliminary study we discovered that by flowing nitrogen to the reactor dome, the PCC decomposition due to atmospheric humidity was considerably reduced. However, we chose to use commercial reagents and not anhydrous ones, so some PCC hydrolysis was anyway expected.

At the beginning, we studied the PCC reactivity with alcohols at the same mild conditions previously used with glycerol: with an inert atmosphere of nitrogen, temperature 60 °C, one hour of reaction time.

For example, let's take into account the reactivity of PCC and ethanol, with the two reactants being fed in a stoichiometric ratio (molar ratio 1:2), at 60 and 80°C (Fig. 4.50).

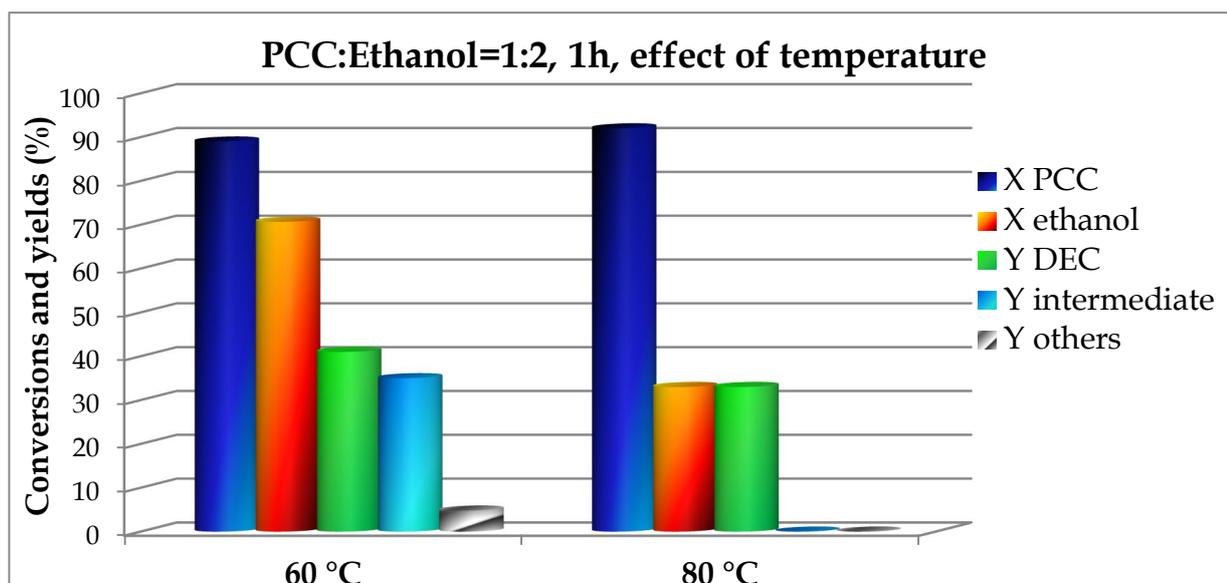**Fig. 4.50** Catalytic results obtained feeding the stoichiometric amount of PCC and ethanol at different temperatures: 60°C (left) and 80°C (right) respectively.

Unfortunately, we rapidly discovered that aliphatic alcohols show slower reactivity compared to polyols like glycerol.

Indeed, when a stoichiometric amount of reagents was used at 60°C, a complex mixture containing the desired product (DEC), the asymmetric carbonate ("intermediate") and one heavier compound (probably the ethylated product of the intermediate) was obtained.

Therefore, we decided to increase the reaction temperature up to 80°C; results obtained with different alcohols are reported in the following table (Table 4.8).

Symmetric carbonates synthesis									
Homogeneous catalysis: Sodium methoxide									
Carbonyl source (A)	Alcohol (B)	Molar ratio	N_2	Catalyst NaOCH$_3$	T (°C)	t(h)	X_A (%)	X_B (%)	$Y_{Symm.\ Carb.}$	$Y_{intermediate}$
PCC	Ethanol	1:2	yes	1/30mol	80	1	92	33	33	0
PCC	1-butanol	1:2	yes	1/30mol	80	1	89	48,1	48	0,1
PCC	Allylic alcohol	1:2	yes	1/30mol	80	1	100	53	52,7	0,3
PCC	Solketal	1:2	yes	1/30mol	80	1	97,3	82,7	73,5	1,9

Table 4.8 CIR of PCC with aliphatic alcohols (X: conversion; Y: yield based on the limiting reagent).

When the temperature was increased of twenty degrees C only, the reaction rate was fastened and complete conversion of the asymmetric carbonates to the desired products was achieved.

Unfortunately, at 80°C also PCC decomposition was faster and in competition with the desired reaction; this led to a large difference between PCC conversion and symmetric carbonate yield.

This problem was solved by feeding a slight excess of the alcohol, in particular three times as much than the stoichiometric requirement (alcohol:PCC molar ratio equal to 6).

Therefore, the molar ratio of reagents is a crucial parameter to obtain higher selectivity while working at lower temperatures.

The following table compares the reactivity of different carbonates, namely PCC, EC and DMC, at 60°C (Table 4.9).

DEC synthesis									
Homogeneous catalysis: Sodium methoxide									
Carbonyl source (A)	Alcohol (B)	Molar ratio	N_2	Catalyst $NaOCH_3$	T (°C)	t(h)	X_A (%)	X_B (%)	$Y_{Symm. Carb.}$	$Y_{intermediate}$
PCC	Ethanol	1:6	yes	1/30mol	60	1	100	29	93	0
EC	Ethanol	1:6	yes	1/30mol	60	1	64	33	8	43
DMC	Ethanol	1:6	yes	1/30mol	60	1	78	18	21	57
DBC synthesis									
Homogeneous catalysis: Sodium methoxide									
Carbonyl source (A)	Alcohol (B)	Molar ratio	N_2	Catalyst $NaOCH_3$	T (°C)	t(h)	X_A (%)	X_B (%)	$Y_{Symm. Carb.}$	$Y_{intermediate}$
PCC	1-butanol	1:6	yes	1/30mol	60	1	100	28	71	0
EC	1-butanol	1:6	yes	1/30mol	60	1	59	10	4	9
DMC	1-butanol	1:6	yes	1/30mol	60	1	5	1	0	5
DAC synthesis									
Homogeneous catalysis: Sodium methoxide									
Carbonyl source (A)	Alcohol (B)	Molar ratio	N_2	Catalyst $NaOCH_3$	T (°C)	t(h)	X_A (%)	X_B (%)	$Y_{Symm. Carb.}$	$Y_{intermediate}$
PCC	Allylic alcohol	1:6	yes	1/30mol	60	1	100	36	73	0
EC	Allylic alcohol	1:6	yes	1/30mol	60	1	61	48	2	5
DMC	Allylic alcohol	1:6	yes	1/30mol	60	1	34	7	2	32
SC synthesis									
Homogeneous catalysis: Sodium methoxide									
Carbonyl source (A)	Alcohol (B)	Molar ratio	N_2	Catalyst $NaOCH_3$	T (°C)	t(h)	X_A (%)	X_B (%)	$Y_{Symm. Carb.}$	$Y_{intermediate}$
PCC	Solketal	1:6	yes	1/30mol	60	1	100	39,6	98	2
EC	Solketal	1:6	yes	1/30mol	60	1	28,7	14,4	1,6	24,6
DMC	Solketal	1:6	yes	1/30mol	60	1	74	21,8	14,6	34,2

Table 4.9 Reactivity comparison in the CIRs of PCC, EC and DMC with several alcohols in order to obtain diethyl carbonate (DEC), dibutyl carbonate (DBC), diallyl carbonate (DAC) and solketal carbonate (SC). (X: conversion, Y: yield based on the limiting reagent).

From the results, it is clear that PCC showed an outstanding reactivity, with no comparison with the carbonate sources traditionally used in CIRs. Indeed, while using DMC and EC led to a mixture of products, with very low yields to the desired

products, the use of PCC allowed us to obtain high yield (> 70% for DAC and DBC and > 90% for DEC and SC), with complete selectivity to the symmetric carbonates with almost all the alcohols.

Both the alcohol chain length and the content of water affected reactivity; as a matter of fact, longer chain alcohols reacted ore slowly and gave lower yield to the desired carbonates.

However, considering the mild reaction conditions used (60°C for 1 hour of reaction) and the simplicity of the reaction apparatus (screw-cap vial), these are very interesting results.

On the other hand, the only side reaction was the decomposition of PCC back to catechol (that is also the co-product of the reaction), but it could be limited by the use of an inert atmosphere of nitrogen and by the low reaction temperature.

Furthermore, another advantage of using PCC regards products separation. Indeed, while the longer-chain symmetric carbonates are characterized by a very low solubility in water, catechol and the unreacted alcohols can be rapidly solubilized in an aqueous medium thus facilitating the separation and purification of products.

To further improve these reactions, we decided to shift from an homogenous to an heterogeneous (MgO) catalytic system, in order to make easier the separation of the catalyst from the reaction mixture and the purification of products.

Unlike the tests with glycerol, a slight excess of alcohols allowed us to avoid the need for other solvents.

The results obtained from tests under the optimized reaction conditions are reported in the following table (Table 4.10).

Symmetric carbonates synthesis									
Heterogeneous catalysis: magnesium oxide (MgO) No solvent									
Carbonyl source (A)	Alcohol (B)	Molar ratio	N_2	Catalyst MgO	T (°C)	t(h)	X_A (%)	X_B (%)	Y Symm. Carb.	Y intermediate
PCC	Ethanol	1:6	yes	5% w/w	80	1	94	23	65	9
PCC	1-butanol	1:6	yes	5% w/w	80	1	83	21	60	0
PCC	Allylic alcohol	1:6	yes	5% w/w	80	1	95	24	72	0
PCC	Solketal	1:6	yes	5% w/w	80	1	46	27	31,5	0,5

Table 4.10 CIR of PCC catalyzed by MgO, no solvent, 80°C for 1 hour

As expected, the reaction rates obtained were slower compared to those with sodium methoxide; so, we decided to increase the reaction temperature up to 80°C in order to achieve a product mixture almost free from the asymmetric carbonate ("intermediate").

However, we found that, again, a simple and cheap system like MgO is active for the reactions investigated under the mild reaction conditions used.

4.3.3.4 Reaction with secondary alcohols: synthesis of DIPC and DCC

It is known that secondary and tertiary alcohols undergo the CIR with difficulty.

This is due to the increasing steric hindrance of the alcohols which limits their reactivity.

So we decided to exploit the peculiar reactivity of PCC also for the synthesis of organic carbonates derived from secondary alcohols, and, in particular:

iso-propanol for the synthesis of diisopropyl carbonate (DIPC) and cyclohexanol for the synthesis of dicyclohexyl carbonate (DCC).

The catalytic results obtained by feeding different PCC/alcohols molar ratios are summarized in the table reported below (Table 4.11).

Symmetric carbonates synthesis: secondary alcohols									
Homogeneous catalyst: Sodium methoxide									
Carbonyl source (A)	Alcohol (B)	Molar ratio	N_2	Catalyst $NaOCH_3$	T (°C)	t(h)	X_A (%)	X_B (%)	$Y_{Symm.\ Carb.}$	$Y_{intermediate}$
PCC	2-propanol	1:4	yes	1/15mol	80	1	86	-	10,3	43,3
PCC	2-propanol	1:10	yes	1/15mol	80	1	86,3	-	56,8	14,5
PCC	2-propanol	1:30	yes	1/15mol	100*	5	100	-	90	0
PCC	Ciclohexanol	1:4	yes	1/15mol	80	1	89,6	25,6	47,6	14,3
PCC	Ciclohexanol	1:10	yes	1/15mol	80	1	97,2	14,8	93,9	1,3
PCC	Ciclohexanol	1:30	yes	1/15mol	80	2	98,5	5,9	98,5	0

Table 4.11 CIRs of PCC and *i*-propanol or cyclohexanol using different reagents ratio. (X: conversion; Y:yield based on the limiting reagent). * reaction performed in autoclave with autogenic pressure.

The results confirmed that with secondary alcohols a greater excess of these reagents is needed in order to obtain high yield and selectivity toward the desired products.

In particular, with *i*-propanol a 15 times alcohol excess compared to the stoichiometric amount was needed in order to obtain 90% yield to the desired symmetric carbonate (DIPC). Cyclohexanol was more reactive and a DCC yield of about 94% was obtained with a 5 times excess of the alcohol.

4.3.4 *PCC and amines: synthesis of substituted ureas*

Substituted ureas are important compounds because of their wide range of applications: as antioxidants in gasoline, agricultural chemicals, dyes and intermediates, or additives in polymers synthesis.[357]

Moreover, some of them exhibit useful biological activities as structural components of drug candidates for HIV protease inhibitors, CCK-B receptor and endothelin antagonists.[358,359,360]

A preliminary study was carried out in order to investigate the possibility to synthesize these molecules by reaction between PCC and amines.

In particular, the reactivity of PCC with isopropylamine to yield 1,3-diisopropylurea was investigated at room temperature under stirring in a simple screw-cap vial.

Interestingly, using an excess of amine (10 times) and without any basic catalyst, the PCC conversion was complete within one hour of reaction at 25°C.

Moreover, during the reaction the formation of a solid precipitate was observed. The solid was filtered, washed with isopropylamine and analysed; it was found to correspond to the desired product (isolated yield equal to 61%). Indeed, the obtained urea showed low solubility in the amine phase. In this way, an easier product isolation and purification was possible.

On the other hand, catechol remained preferentially in the organic phase and a red solution was obtained, containing the intermediate and a lower amount of the desired product.

Furthermore, isopropylamine has a low boiling point (33°C), so it can be easily removed by distillation, while the catechol could be recycled in order to synthesize new PCC.

The reaction investigated is shown in the following scheme (Scheme 4.16).
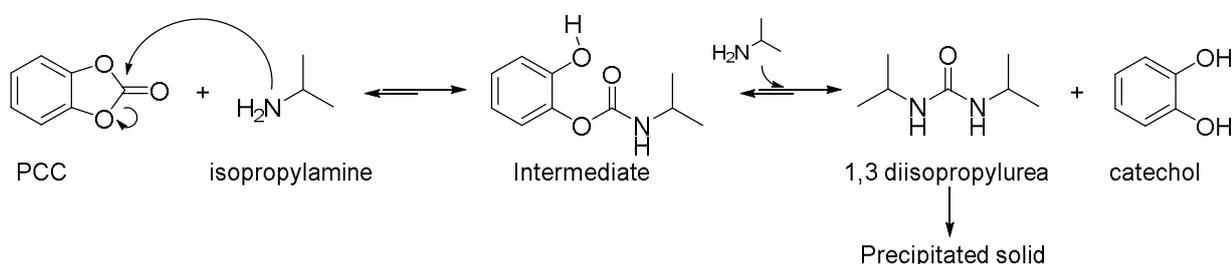
Scheme 4.16 Reaction mechanism between PCC and isopropylamine to 1,3-diisopropylurea.

4.3.5 Final considerations

PCC demonstrated to possess an outstanding reactivity for the CIR with aliphatic alcohols, by far superior to that one of other carbonate sources (e.g. DMC and EC).

The reaction takes place in very mild conditions (low temperature and reaction time), with no solvent (as written in the green chemistry principles, "no solvent" is the best solvent) and, finally, show outstanding selectivity toward the desired products.

In particular, starting from the alcohols, the symmetric carbonates are selectively produced feeding only a slight excess of the alcohol, while with polyols, like glycerol, the reaction is faster and extremely selective toward the desired glycerol carbonate (GlyC), with no formation of heavier compounds (polyols or polycarbonates).

Furthermore, also the purification of the products is easier in the case of PCC, indeed symmetric carbonates generally show very low solubility in water while both catechol and the unreacted alcohols are readily soluble in the aqueous medium. This leads to an easy separation by means of extraction.

On the other hand, GlyC and catechol have shown similar solubility with a wide range of solvents.

To overcome these separation problems, we have discovered a new and interesting reactivity using GlyC as a precursor for the safe, in-situ, generation of glycidol (by means of decarboxylation) that readily reacts with catechol by condensation leading to the formation of 2-hydroxymethyl-benzodioxane (HMB), an interesting high-added value compound.

Finally, the reactivity of PCC and amines was investigated, in particular with isopropylamine the reaction is fast and does not need a basic catalyst to occur; in this case, complete conversion was achieved after only one hour of reaction at room temperature. Moreover, the di-substituted urea shows low solubility in the amine and start to form a precipitate during the reaction, thus helping to shift the equilibrium toward the formation of the desired product.

4.4 Gas-phase alkylations with organic carbonates

4.4.1 Introduction

The alkylation of various functional groups, namely carboxylic acids, phenols, acidic enols, amines and thiols, is an important reaction for the synthesis of intermediates and derivatives, and in the preparation of protecting groups.[361]

There are many different procedures to alkylate these groups using "traditional" reagents,[362] but recently the search for greener and improved alkylating agents has provided several alternatives.
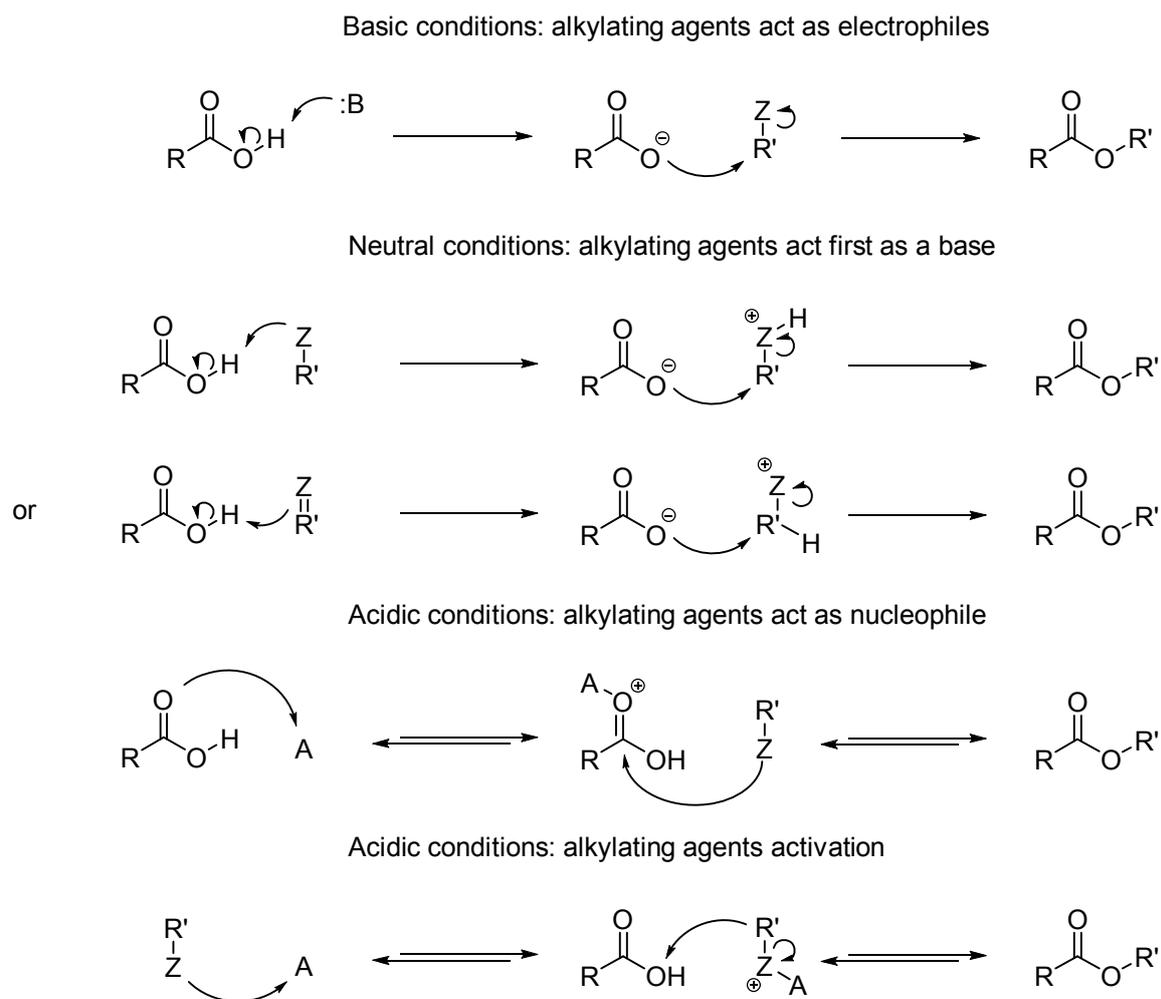
Because of their peculiar properties, organic carbonates represent one of the most promising and reactive compounds in the aim of replacing conventional alkylating agents (as discussed in the introduction part of this Thesis, Chapter 1.3.6.2).

Alkylating agents can be classified into three different categories, depending on reaction conditions or catalyst type: basic, neutral and acidic (
Table **4.12**).

Basic conditions	Neutral conditions	Acidic conditions
Alkyl halides (CH$_3$I)	Diazomethane (CH$_2$N$_2$)	Alcohols CH$_3$OH/H+
Tosylates CH$_3$OTs;	TMSCHN$_2$	CH$_3$OH/BF$_3$
Mesylates CH$_3$OMs	Triazene: Ph-NH-N=NCH$_3$	
Meerwein salts: (CH$_3$)$_3$O-BF$_4$	DMF Acetal: (CH$_3$O)$_2$CHNCH$_3$	
Sulfates (CH$_3$)$_2$SO$_4$	Isourea: RNHC(OCH$_3$)NR	
Organic carbonates (DMC)	Orthoacetal: (CH$_3$O)CR	
Tetralkylammonium salts (CH$_3$)$_4$NX		

Table 4.12 Alkylating agents classification, adapted from reference.[363]

Associated with the reaction conditions or catalysis type, different mechanisms have been proposed; some examples for a generic carboxylic acid alkylation are reported in the following scheme (Scheme 4.17).

Basic conditions: alkylating agents act as electrophiles

Neutral conditions: alkylating agents act first as a base

or

Acidic conditions: alkylating agents act as nucleophile

Acidic conditions: alkylating agents activation

Scheme 4.17 Mechanism for alkylation of acid substrates in function of the reaction conditions used, adapted from reference.[363]

As shown above, in the alkylation of acidic substrates, the alkylating agent displays different behaviours depending on the reaction conditions.

For instance, basic conditions usually promote the activation of the substrate that readily reacts with the alkylating compound, the latter acting as an electrophilic species (first line of the scheme); in neutral conditions, the alkylating agent usually acts as a base, forming an activated species for the alkylation.

Finally, in acid conditions (Lewis or Brønsted), the alkylating agent usually behaves as a nucleophile, either reacting with the activated substrate, or being itself activated to form an intermediate which readily continues the alkylation.

Noteworthy, alcohols and in particular methanol, represent a cheaper alternative for these reactions but generally show low activities.

Cavani et al. demonstrated that in the gas-phase methylation of phenol with methanol on different catalysts (in particular basic oxides and mixed oxides), methanol is activated in a different manner compared to the conventionally accepted mechanism.

In particular, at high temperature, methanol undergoes a dissociative dehydrogenation on the catalyst producing formaldehyde, that is the real active specie for the methylation.

This reaction is extremely chemo-selective toward the methylation of the aromatic ring producing cresols and xylenols.[364,365]

In general, alkylations usually require small functional groups in order to reduce steric hindrance and avoid kinetic limitations; therefore, methylations are the most investigated reactions. Moreover, it is reported that basic or neutral conditions are more effective and selective, and occur under milder conditions compared to acid-type alkylations.[363]

In this way, organic carbonates can be effectively used in basic conditions as alkylating agents and, within the class of carbonates, dimethyl carbonate (DMC) is the most investigated for the methylation of a wide range of substrates (Scheme 4.18).
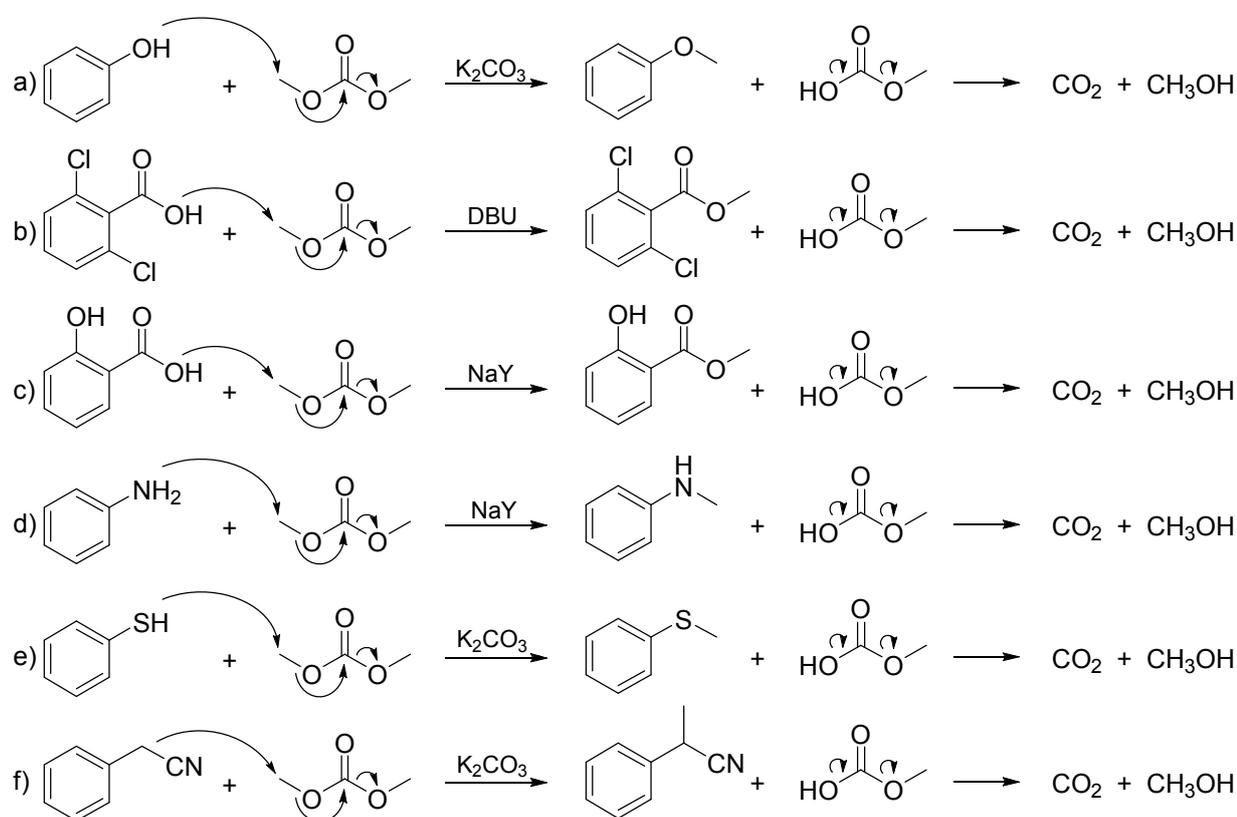
Scheme 4.18 Alkylation of different substrates with dimethyl carbonate (DMC).

It is important to underline that using carbonates as alkylating agents leads to an irreversible reaction because of the formation of the instable alkoxy-carbonate anion that rapidly decomposes to CO_2 and alcohol (methanol in the case of DMC), shifting the reaction toward the products and finally contributing to increase yields.

Moreover, this reaction shows a high and specific chemoselectivity.

For example, if we consider phenols, the reaction is highly specific in O-alkylation, with formation of anisole (phenylmethyl ether, Scheme 4.18, a)).[366]

However, in the co-presence of both hydroxyl and carboxylic acid functional groups on the phenyl ring, the reaction with DMC gives rise to the formation of the corresponding ester with very high selectivity (Scheme 4.18, b) c)).[367,368]

Finally DMC is highly efficient also for other heteroatoms selective methylation, in particular it is highly selective in the mono-N-methylation of primary aromatic amines,[369,370] in S-methylation of thiophenols and in methylation of activated carbon atoms like in arylacetonitriles (Scheme 4.18; d) e) f)).[371]

The list of catalysts for methylation with DMC includes:
alkali metals halides, hydroxides, alkoxides and carbonates (e.g. $CsCO_3$); phosphines and phosphoniumhalides, tertiary amines, hydrotalcites, basic zeolites etc.[99]

Also acidic systems, especially $AlPO_4$ (supported on Al_2O_3) and some acidic commercial zeolites are reported to be active catalysts, for example for the selective O-methylation of catechol to guaiacol and veratrole.[372]

Despite the methylation with DMC is already a well-studied reaction, only few works reported about the alkylation with longer chain carbonates.

For example, Li et al. described the ethylation of benzene with DEC over different acid zeolites (HZSM-5).[373]

Moreover, diethyl carbonate (DEC) was investigated for the high temperature (360°C) ethylation of phenol over mesoporous nano-silicas (MCM-41).

Over these systems, the alkylation is not fully selective to O-alkylation, and a mixture of products (in particular phenylethyl ether and 2-ethyl phenol in a molar ratio of 2:1) is typically obtained; moreover, the impregnation with TiO_2 is reported to increase both phenol conversion and C-alkylation selectivity. [374]

Another group reported similar behaviours with Al incorporated in the silicate structure of MCM-41, and described an increase of poly-alkylated products while decreasing the Si/Al ratios.[375]

It is worth noting that only the reactivity of symmetric carbonates has been considered so far.

Indeed, few papers report the reactivity of asymmetric carbonates for alkylations.

Perosa et al reported the selective methylation of different aromatic substrates with various methyl alkyl carbonates in the liquid phase.[376]

## 4.4.2 *Phenol and products of interest*

Phenol is a white, amorphous compound at ambient temperature. It has a melting point of 40,9°C and, in the molten state, it is a clear and colorless liquid.

Phenol is soluble in aromatic hydrocarbons, alcohols, ketones, ethers, acids, and halogenated hydrocarbons.[377]

Likewise catechol, it can be derived from lignin by different treatments, namely pyrolysis and hydrogenolysis (see Chapter 1.4.1).

The chemical properties of phenol are unique. They are due to the presence of a hydroxyl group and an aromatic ring which show complementary behavior in facilitating both electrophilic and nucleophilic type of reactions. The unshared electron pair located on the hydroxyl group is delocalized over the aromatic ring leading to an electron excess at the ortho and para positions.[378,379]

For all these reasons, phenol is the starting material for the synthesis of a wide series of commercially relevant compounds (Scheme 4.19).
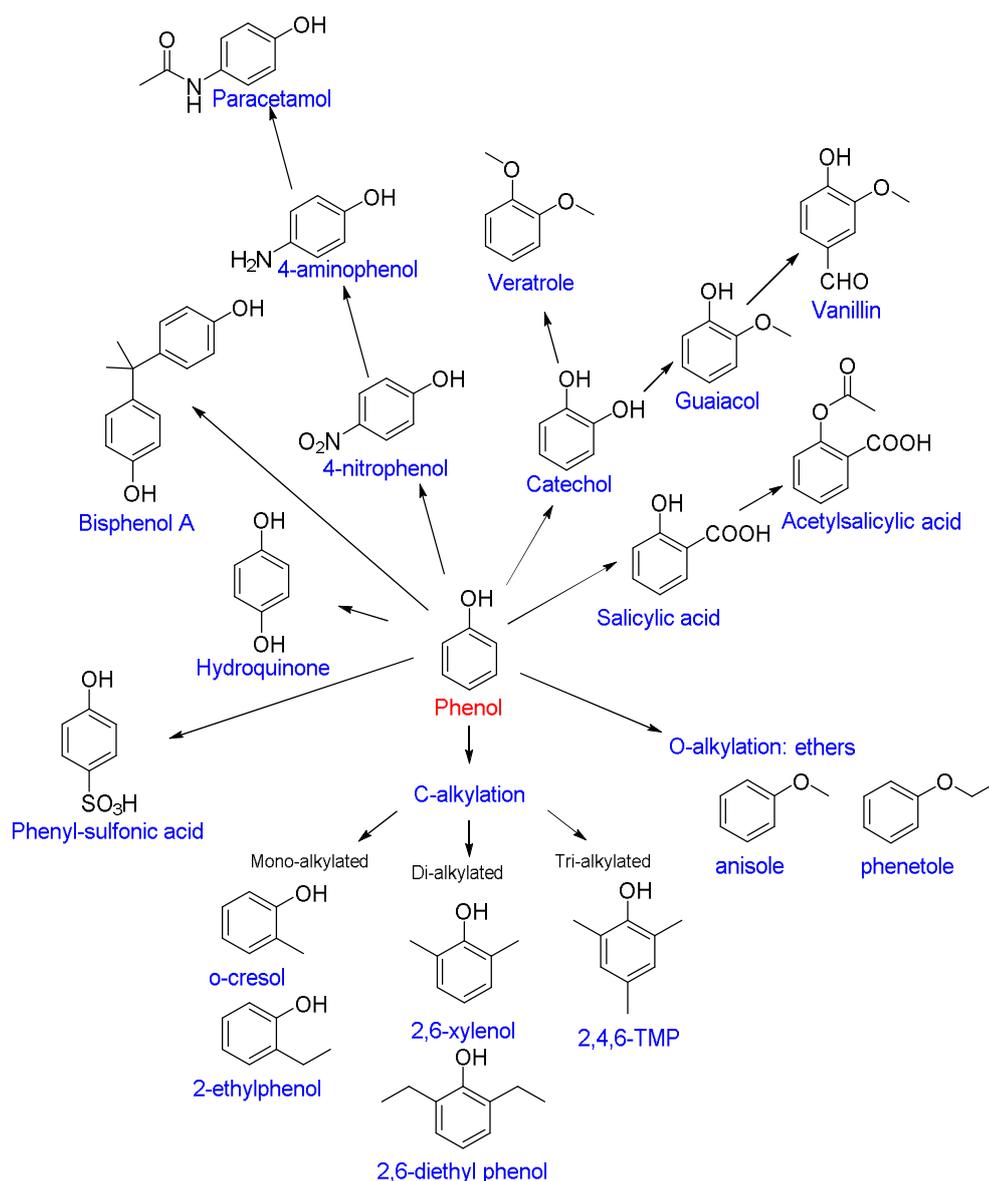
Scheme 4.19 The phenol "tree" of the most important derivatives produced from phenol.

Of particular interest are the products derived from phenol alkylation, which can be divided into two main classes in function of the chemo-selectivity achieved:

the products derived from the alkylation of the phenol hydroxyl oxygen atom (O-alkylated) and the products derived from the alkylation of the aromatic ring (C-alkylated).

The main products belonging to these classes are:

- anisole (methylphenyl ether) and phenetole (ethylphenyl ether); both are important intermediates in the synthesis of pharmaceutical and fragrances and as octane boosters for gasoline;[380]

- *o*-cresol (*ortho*-methyl phenol) is used for the synthesis of polymers and resins, especially for the synthesis of epoxy-*o*-cresol novolak resins; moreover it is also

an important precursor of various dyes, pharmaceuticals (e.g. carvacrol) and antioxidants;[381]

- *p*-cresol (*para*-methyl phenol) is an important intermediate in the synthesis of antioxidants and preservatives for foods and plastics;[382]

- monoethyl phenols are used in the production of phenolic resins and varnish products, in particular 2-ethylphenol is used as a precursor of indene-coumarone resins and for some pharmaceuticals;[383]

- 2,6-xylenol (2,6-dimethyl phenol) is used to produce poly(phenylene oxide) resins, which are distinguished by their high thermal stability, impact and fire resistance and dimensional stability;[381]

- 2,3,6 and 2,4,6 trimethyl phenol (TMP) are important precursors in the synthesis of vitamin E and other pharma.[381]

4.4.3 Aim of this chapter

We investigated organic carbonates as reactive and selective alkylating agents for the synthesis of high-value phenolic compounds.

In particular, the reactivity of dimethyl carbonate (DMC), diethyl carbonate (DEC), methylbutyl carbonate (MBC) and dibutyl carbonate (DBC) with phenol have been investigated using the same cheap heterogeneous catalyst, magnesium oxide (MgO), used also in the previous chapters for the synthesis of the carbonates.

At the best of our knowledge, nobody has ever reported about phenol alkylation with organic carbonates using this simple catalytic system.

In particular, the reactivity of DEC was investigated over different catalysts, namely MgO, alumina (Al_2O_3) and a Mg/Al mixed oxide; a complete study on the effect of the main reaction parameters (temperature, residence time, reagents feed molar ratio) on phenol conversion and products yield is here reported.

4.4.4 *Experimental*

4.4.4.1 *Gas-phase continuous flow reactor*

The alkylation reactions described in this Chapter were performed in a continuous flow reactor, shown below (Fig. 4.51).
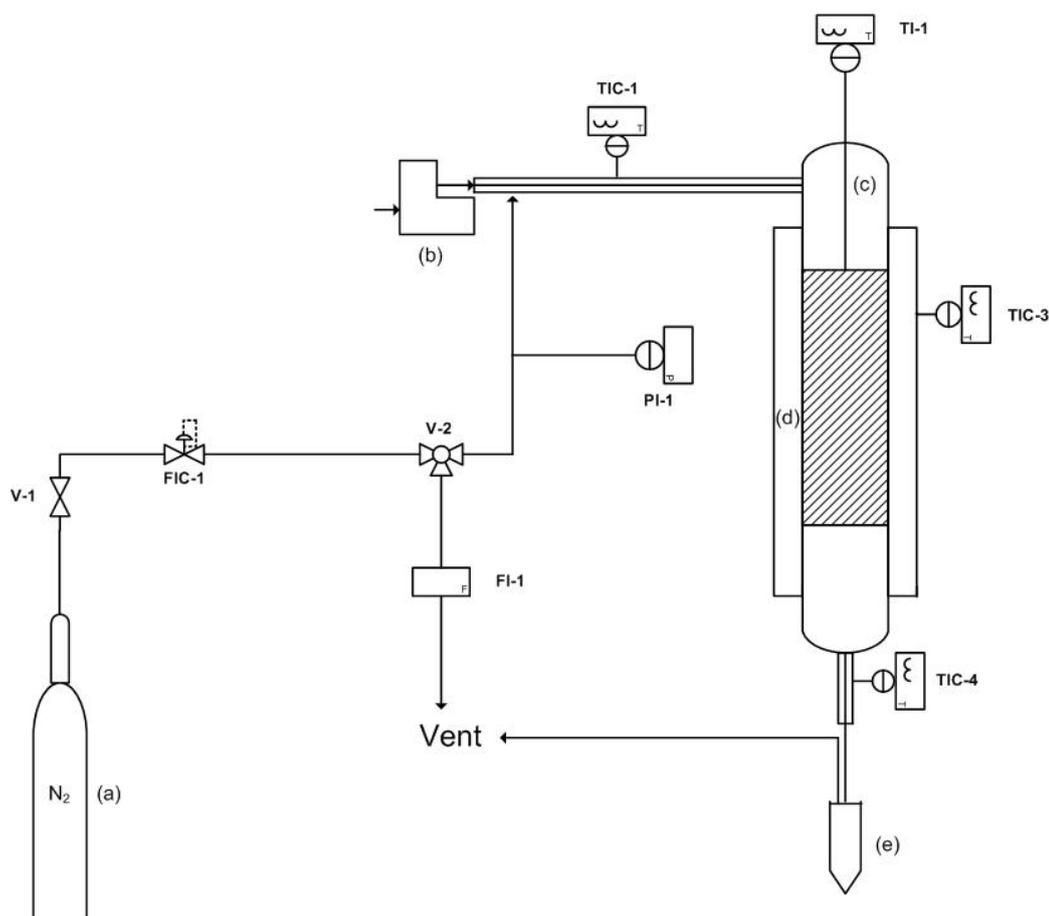

Fig. 4.51 Gas-phase continuous flow reactor used for alkylation experiments.

The rig can be divided into three zones:
1.   feeding area of the reactants;
2.   reaction zone;
3.   sampling zone.

The feeding zone is made of devices able to set and control both the inert gas and the liquid reagents mixture flow. In particular, it is made of the following elements.
Mass flow meter (FIC-1), which regulates and maintains a constant flow rate of the inert, carrier gas (nitrogen) from the cylinder (a). Bubble flowmeter (FI-1), in order to further control the flow of the inert gas pre-set to match the flow actually delivered. High precision infusion pump (b), Kd Scientific 100, used to adjust the input flow rate

to the reactor of the reaction mixture placed in the syringe fixed appropriately on that pump. Pressure gauge (PI-1), in order to rapidly detect any increase in pressure within the system. The feeding pipe consists of a steel tube that connects the point of reagents mixing with the inert gas to the input line of the reactor, maintained at a constant temperature of 250°C by means of heating bands controlled by a thermocouple (TIC-1).

The reaction zone is made of a glass reactor (c) with a diameter of 1.5cm and length 46.5cm; inside the reactor is inserted a thermocouple (TI-1) in order to measure the real temperature of the catalytic bed; the catalytic bed is made of $1cm^3$ of catalyst in the form of pellets of particle size between 30 to 60 mesh, and is positioned approximately 20cm from the reactor bottom, in the isothermal zone. The reactor is in turn inserted inside a tubular heating furnace, model Carbolite MTF 12/25/250 (d).

The output flow from the reactor is maintained at a temperature of 250 ° C by a band heater to prevent condensation of high-boiling products prior to the collection area and sampling (TIC-4). The sampling area (e) is made of a glass bubbler containing iso-propyl alcohol (2-propanol) in which the reaction products are solubilized; the solution can then be periodically analyzed by gas chromatography. The bubbler is kept cold by means of an ice bath.

4.4.4.2 Catalytic test procedure

Catalytic tests were carried out in a downstream tubular glass reactor. The liquid reagents solution was fed using a syringe pump, vaporized and carried over by a nitrogen flow. The reactor temperature was maintained at the desired temperature by an electric furnace (MFT122525/301 Carbolite), surrounding the reactor whose temperature was controlled by means of a controller connected to a thermocouple placed within the catalyst bed. In a typical reaction, the pelletized catalyst was loaded into the reactor tube to form a catalyst bed with volume of 1 ml. The reactor was purged with flowing N_2 and then heated to the reaction temperature. After the system stabilization, the liquid organic feed (mix of alkylating agent and phenol) was introduced through the inlet pipeline. Condensable compounds in the downstream flow were collected in a bubbler containing pure iso-propanol.

The accumulation of the liquid products took ca 30-40 min. After this, the bubbler was removed and another one was immediately repositioned in order to restart the reaction. The solution contained in the flask was poured into a 25mL volumetric flask, brought to volume and finally added with 20 μL of octane or decane as an internal standard. At this point the solution was ready for GC analysis.

The optimal residence time for phenol methylation was assumed to be equal to 1s; residence time was calculated by taking into account the following parameters:

catalyst volume, temperature, inert flux, syringe flux and weight percentage of phenol.

4.4.4.3 Catalysts synthesis and characterisation

The synthesis of the "high surface area" MgO and of the Mg/Al mixed oxide was carried out following the procedures described in the experimental section of this Thesis (Chapter 3.2.2).

All the heterogeneous catalysts used for the gas-phase phenol alkylation were characterized by means of BET surface area analysis as described in chapter 3.3.2.

The results of the surface area analysis of catalysts are reported below (Table 4.13).

Commercial MgO	Synthesized MgO	Mg/Al mixed oxide	γ-Al$_2$O$_3$
20 m^2/g	200 m^2/g	160 m^2/g	140 m^2/g

Table 4.13 BET surface area analysis of the catalysts

The catalysts were also analysed by means of powder-XRD as described in chapter 3.3.1. The XRD patterns are reported below.

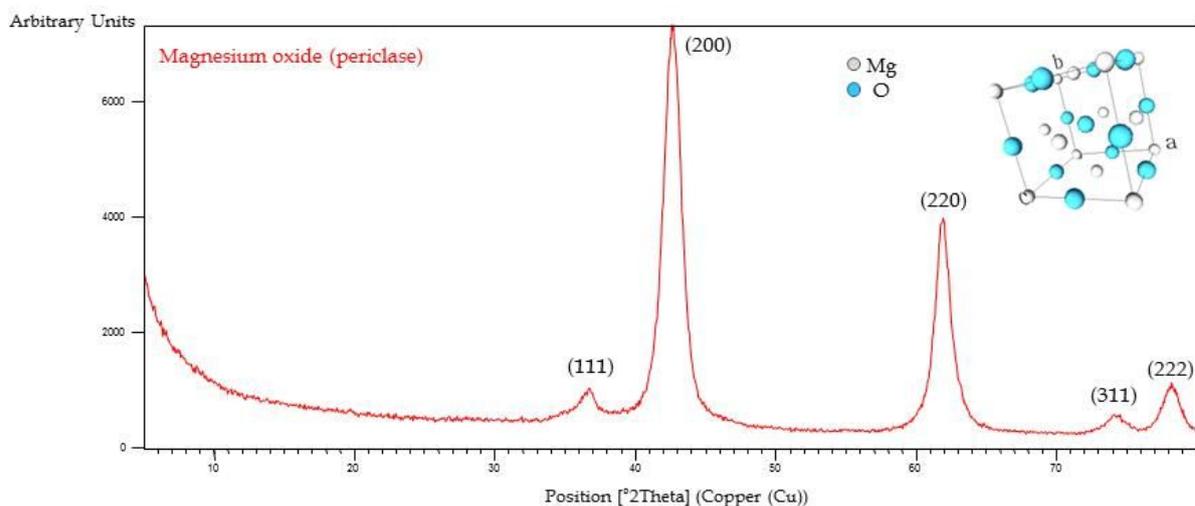MgO (periclase-like structure) formation was confirmed by the pattern shown below.

Fig. 4.52 MgO X-ray diffraction pattern, with Miller index and a representation of its unit cell.

The formation of the hydrotalcite, precursor of the Mg/Al mixed oxide, was confirmed by means of XRD. After the treatment at high temperature (calcination), the XRD analysis was repeated and the pattern did correspond to that one of a MgO-like pattern. The broader and less intense reflections are due to the lower crystallinity, consequence of the incorporation of the Al atoms inside the MgO structure (Fig 4.53).
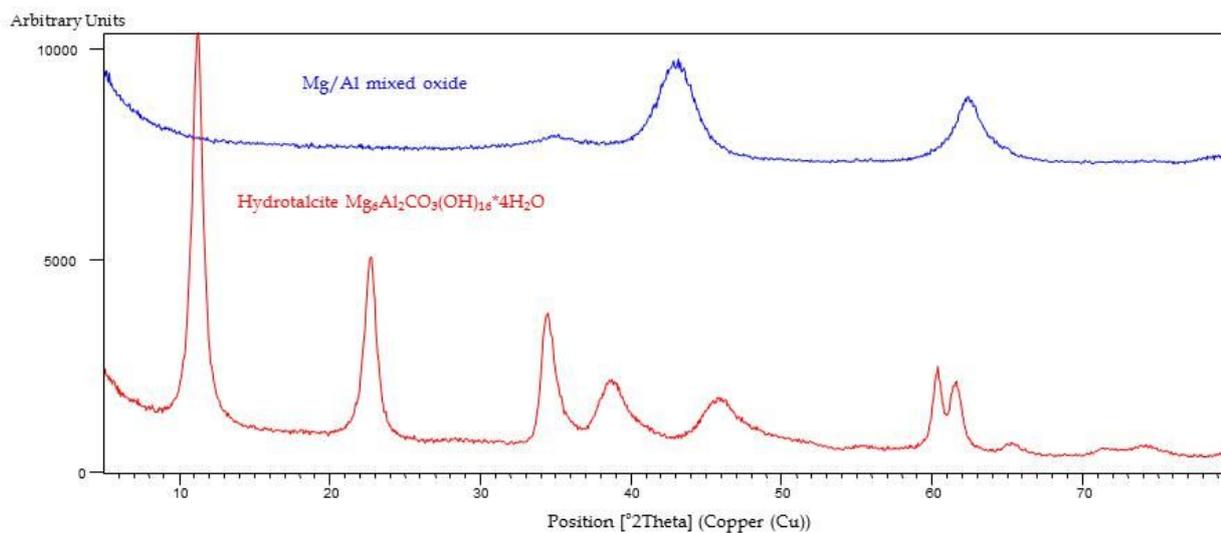
Fig. 4.53 Hydrotalcite (red) and Mg/Al (3/1) mixed oxide (blue) X-ray diffraction pattern.

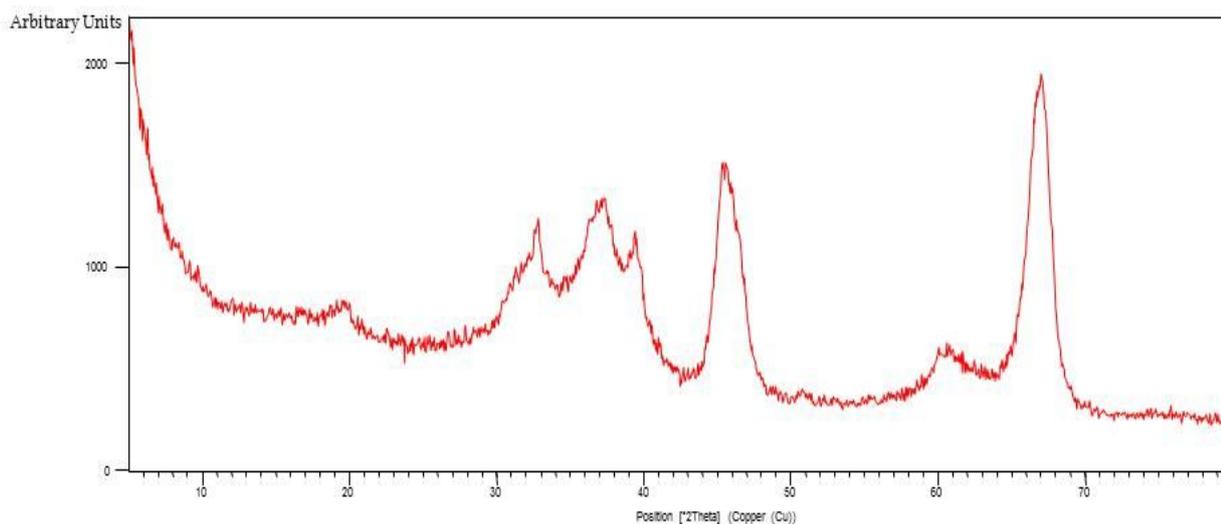The XRD pattern of γ-Al$_2$O$_3$ is reported below.

Fig. 4.54 γ-Al$_2$O$_3$ X-ray dffraction pattern.

4.4.5 Gas-phase phenol methylation: DMC and methanol as alkylating agents with MgO catalyst

Firstly, we decided to test the catalytic activity of MgO synthesized by means of the precipitation method and characterized by an high surface area (around 200 m²/g), in the gas-phase methylation of phenol, comparing the reactivity of DMC and methanol.

In Fig. 4.55, results obtained by feeding a molar ratio of alkylating agent-to-phenol equal to 10, with a residence time (τ) of 1 s are reported in function of temperature.
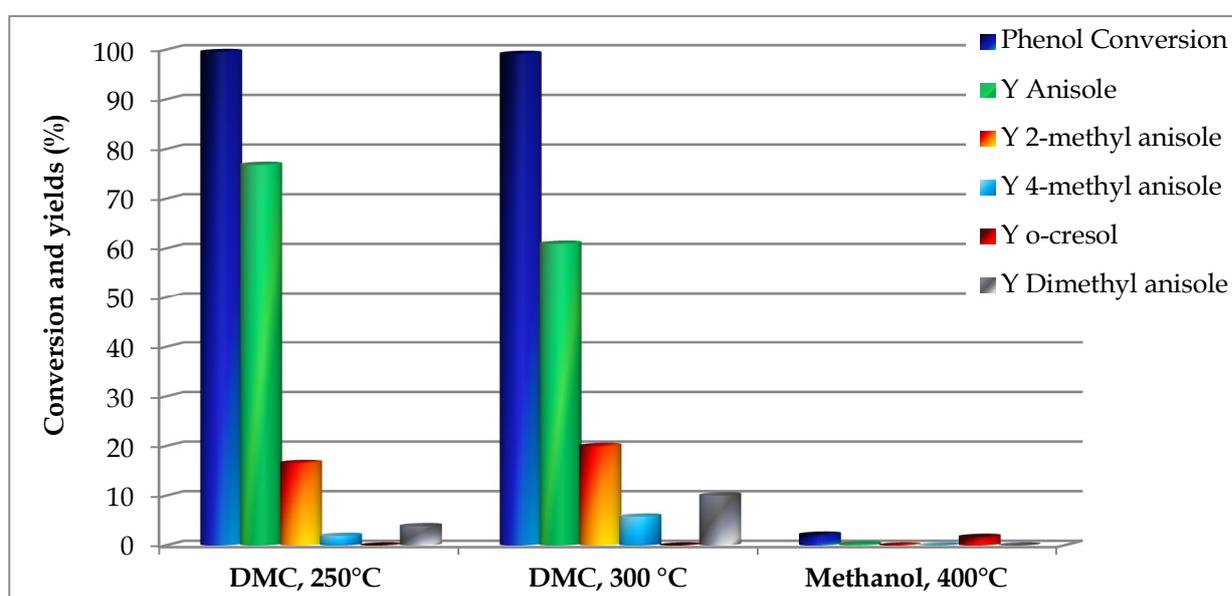

Fig. 4.55 Catalytic results over MgO (200 m²/g), Alkylating agent:Phenol=10:1, τ = 1 s.

Over a simple basic system like MgO, phenol was activated and generated the phenate species; the latter is a softer nucleophile compared to other aliphatic alcoholates, and readily reacts with the methyl C atoms of DMC (soft electrophile). Furthermore, the reaction led to the formation of an unstable intermediate (methoxy carbonate anion), that rapidly decomposed to CO_2 and methanol. Complete phenol conversion was achieved already at relatively mild temperature (250°C), with very high selectivity to the O-alkylated product: anisole. The main by-products were 2-methyl anisole and 2,6-dimethyl anisole. These products probably form from the alkyl rearrangement of the methyl group that undergoes internal rearrangement from the oxygen atom to the activated position on the aromatic ring.

The selectivity to anisole could be optimized by limiting the excess DMC and lowering the reaction temperature; indeed, an increase of temperature from 250

to 300°C led to both an enhanced formation of these consecutive polyalkylated products and a lower selectivity to anisole.

This particular aspect was deeply investigated for the gas-phase ethylation of phenol with DEC, and will be described in the following chapters.

On the other hand, methanol needs high reaction temperature on basic systems in order to be activated via in-situ dehydrogenation (endothermal reaction) to formaldehyde, the latter being the real (hydroxy)alkylating agent. However, even at 400°C the use of methanol with MgO led to very low phenol conversion. Noteworthy, organic carbonates and alcohols (or their activated forms: aldehydes) show opposite chemo-selectivity. Indeed, while carbonates show specific selectivity to O-alkylation, methanol shows higher selectivity to C-alkylation on the aromatic ring.

4.4.6 Diethyl carbonate (DEC) for the gas-phase phenol ethylation over basic catalysts

Because of the interesting results obtained with DMC, we decided to study the reactivity of diethyl carbonate (DEC), a compound which has been much less investigated in literature than DMC, for the gas-phase ethylation of phenol.

It is known that carbonates reactivity decreases with the increase of the alkyl chain length, therefore DEC would probably need higher temperatures compared to DMC.

Firstly, a commercial MgO characterized by low surface area (around 20 m²/g) was used in order to draw an overview of the influence of the main parameters such as residence time (τ), temperature (T) and molar feed ratio between the reagents.

Indeed, from a preliminary test carried out at 350°C by feeding a molar ratio DEC:PhOH=10:1 with a τ equal to 1 s, the "low surface area" MgO showed an interesting reactivity with a phenol conversion of about 77% (Fig. 4.56).
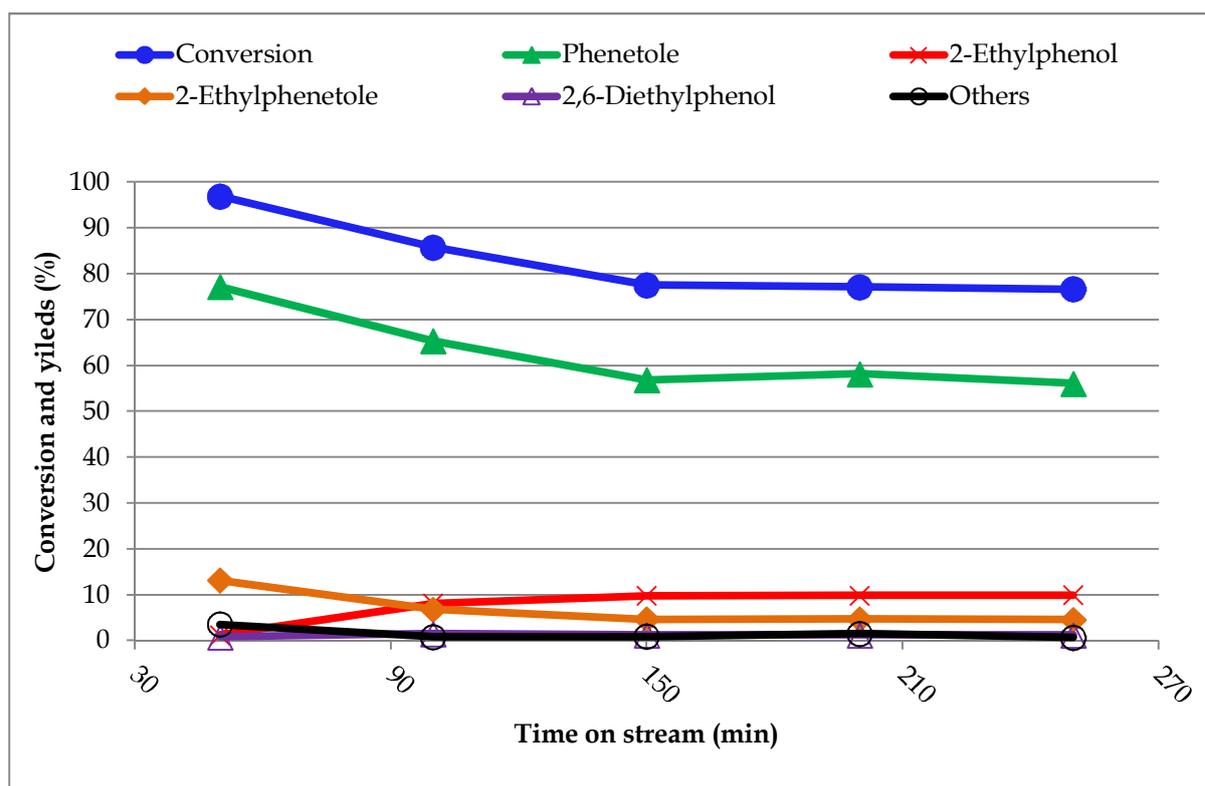

Fig. 4.56 Catalytic results over MgO (20 m²/g) in function of time on stream, DEC:Phenol=10:1, T = 350°C, τ = 1 s.

The results obtained confirmed both the great reactivity of organic carbonates as alkylating agents for phenol, and the chemo-selectivity of this reaction toward O-alkylation.

Interestingly, also one product of C-alkylation, 2-ethylphenol, formed with yield around 10%.

This compound probably formed from the intra-molecular rearrangement of phenetole at high temperature, with migration of the ethyl group from the oxygen atom to the activated ortho position on the aromatic ring. Then, 2-ethylphenol underwent further alkylation on the hydroxyl group with formation of the major by-product, 2-ethyl-phenetole.

This behaviour was confirmed by performing the same test with a different MgO, synthesized by a well-known precipitation method and characterized by a high surface area (around 200 m²/g) (Fig. 4.57).

The increase of surface area led to the expected increase of activity, with a stable and complete conversion of phenol.

Furthermore, an higher surface area facilitated the consecutive reactions increasing the yield to polyalkylated compounds ("Other" in the following figure) and to the consecutive product 2-ethylphenetole, with a corresponding decrease of the yield to the intermediate, 2-ethylphenol.
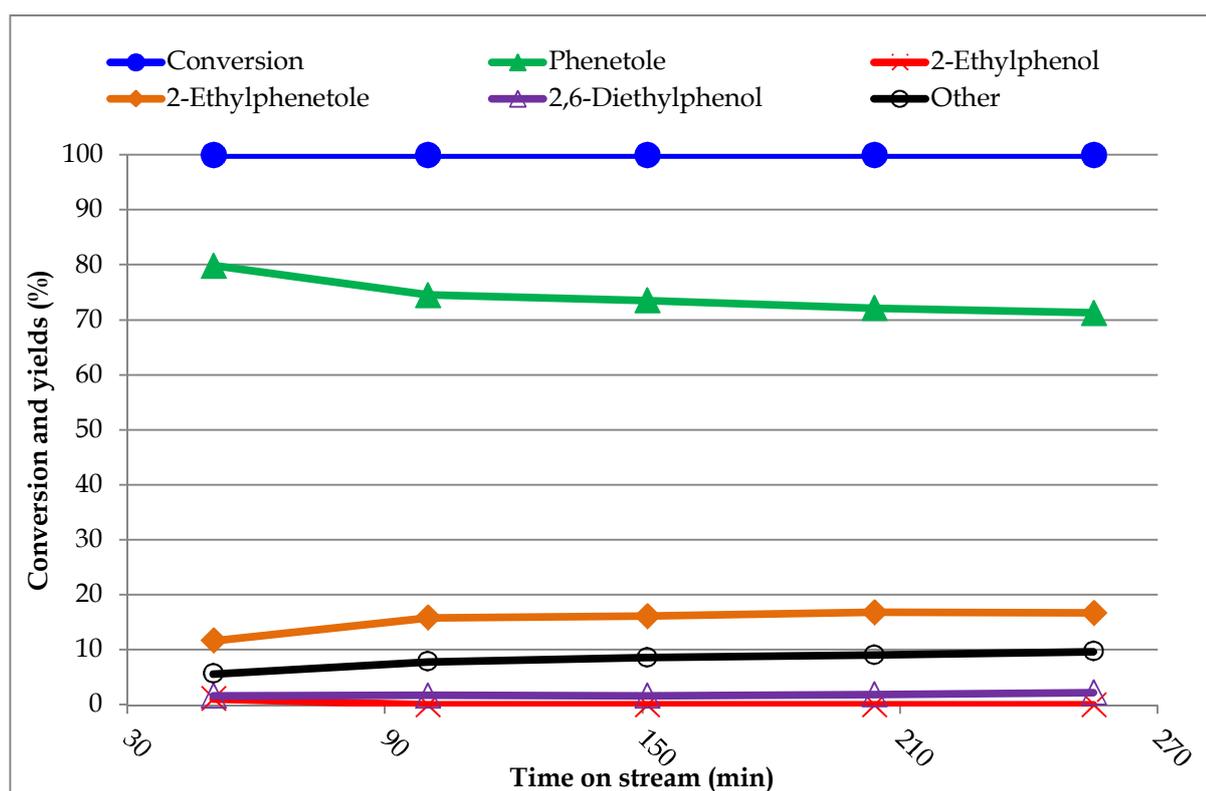

Fig. 4.57 Catalytic results over MgO (200 m²/g) in function of time on stream, DEC:Phenol=10:1, T=350°C, τ = 1 s.

4.4.6.1 *Study of the effect of residence time*

Because of the interesting results obtained with MgO, we decided to focus on commercial MgO in order to investigate the influence of different parameters on conversion and products distribution.

As expected, we found that in the same conditions as those used for the previous tests (350°C, DEC:PhOH=10:1, MgO "low surface area") the increase of the residence time led to a steady increase of phenol conversion value with no changes in products distribution; only a slightly increase in selectivity to the O-alkylated products (phenetole and 2-ethylphenetole) was observed.
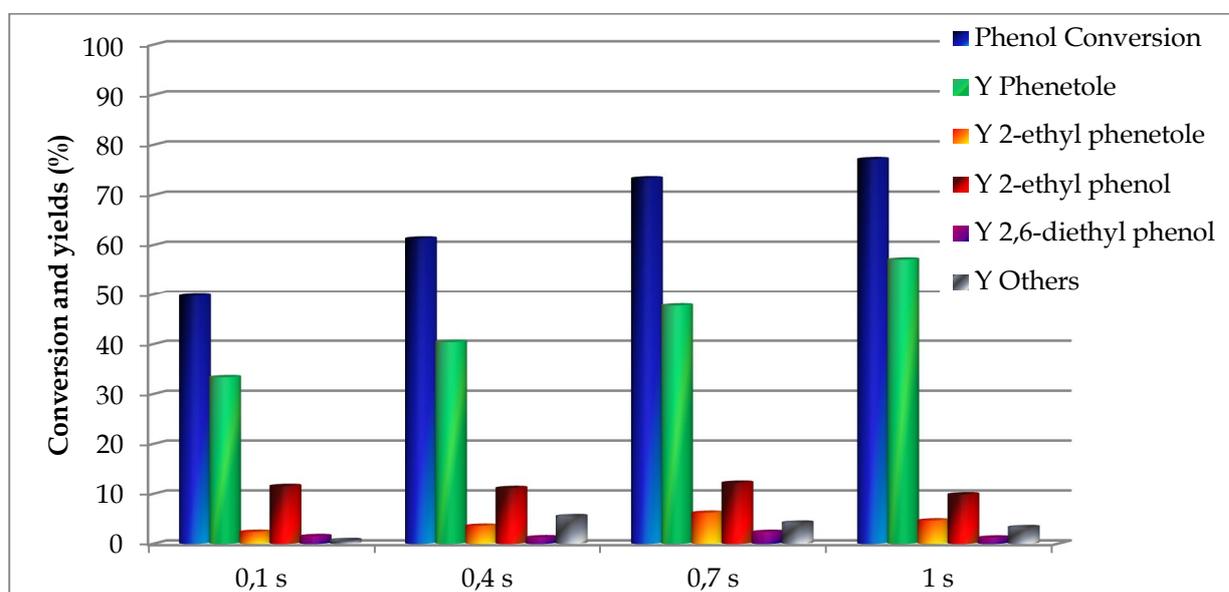

Fig. 4.58 Catalytic results over MgO (20 m^2/g), DEC:Phenol=10:1, T= 350°C, τ = variable from 0,1 to 1 s.

4.4.6.2 *Study of the effect of the inlet molar ratio*

The study of the influence of the inlet feed composition was performed by feeding different molar ratios between DEC and phenol, in particular DEC:phenol ratio equal to 4 and 10, in order to investigate the possibility to increase the selectivity to phenetole.

Again, a greater excess of the alkylating agent led to an increase of the aromatic conversion with a negligible change in products distribution.

This behaviour confirms the great chemo-selectivity of DEC in O-alkylation with the formation of phenetole, while the other by-products derived mainly by consecutive reactions occurring on phenetole.
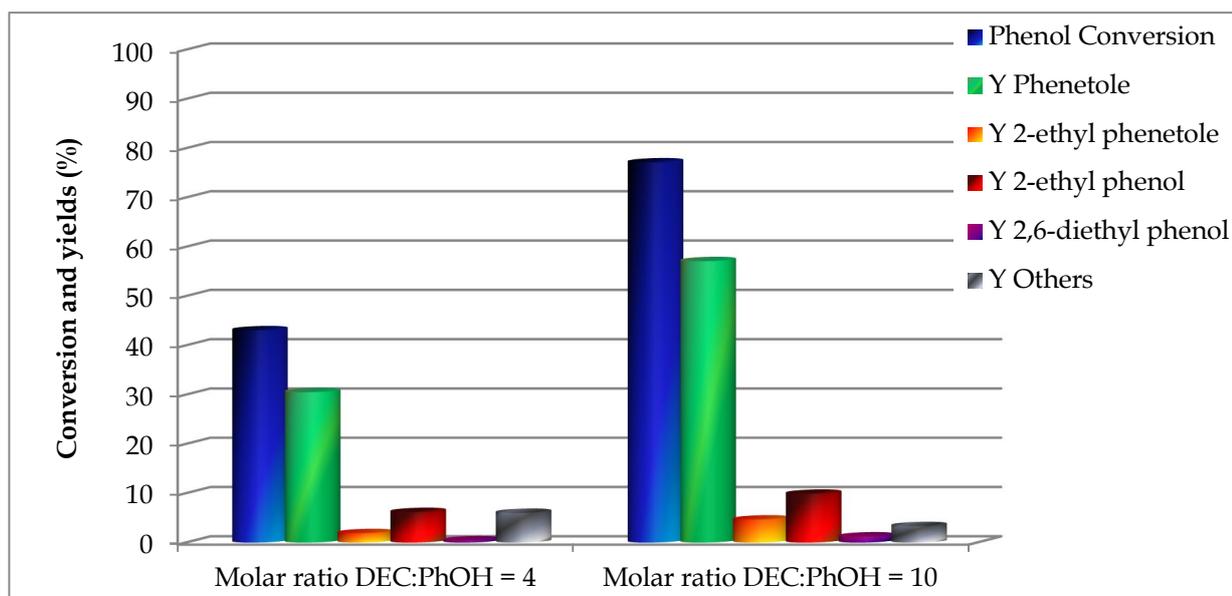
Fig. 4.59 Catalytic results over MgO (20 m^2/g), DEC:Phenol variable ratio, T= 350°C, τ = 1 s.

4.4.6.3 *Study of the effect of temperature*

Finally, a study of the temperature influence between 300°C and 400°C was performed.

Also in this case, phenol conversion increased along with temperature, increasing reaction rates and promoting the consecutive reactions.

An interesting example was 2-ethylphenol (2-EP) behaviour. Indeed, 2-EP probably formed as a consecutive product of the thermal transposition of phenetole, in which the ethoxy group migrates toward the most available and activated ortho position of the aromatic ring.

Moreover, 2-EP selectivity progressively decreased with the rise of temperature and disappeared at 400°C, in favour of the consecutive poly-alkylated products, such as 2-ethyl phenetole, 2,6-diethyl phenol and others (Fig. 4.60).
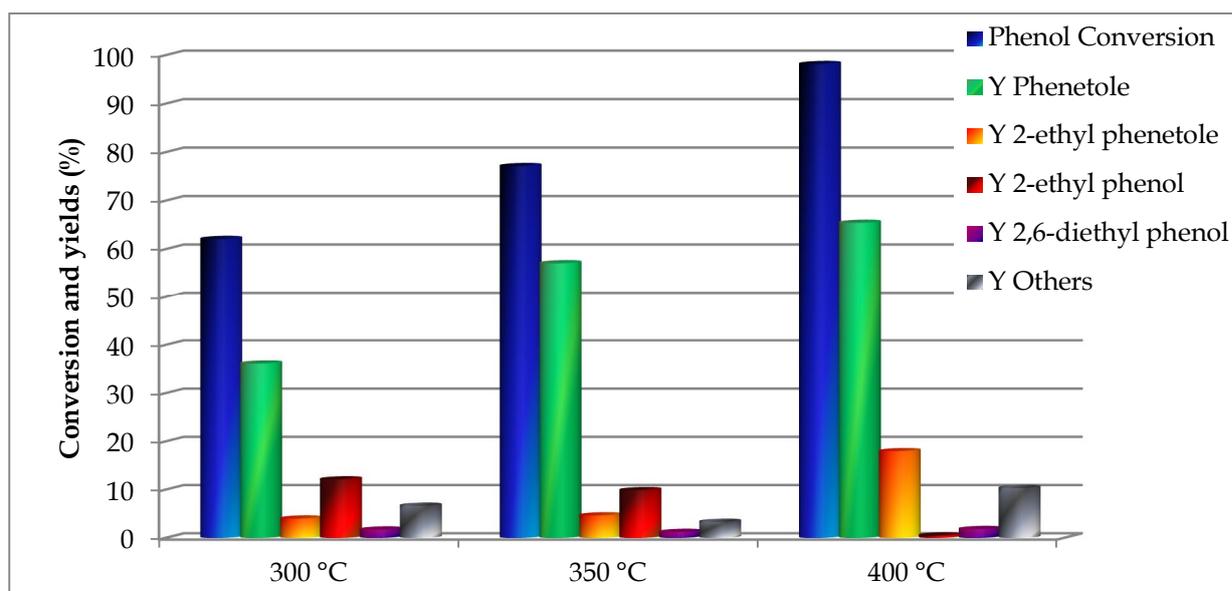
Fig. 4.60 Catalytic results over MgO (20 m²/g), DEC:Phenol=10:1, variable T, τ = 1 s.

The results show that even though the alkylation with DEC remained highly chemo-specific and oriented to the phenol oxygen atom (O-alkylation) in all the temperature range, higher temperatures made easier both the alkyl rearrangement in phenetole with formation of 2-ethylphenol, and the consecutive ethylation of this intermediate to 2-ethyl phenetole. This rearrangement was favoured at high temperature on the MgO surface. Interestingly, when pure phenetole was fed over the low surface area MgO in the same range of temperatures, neither the disproportionation nor the alkyl rearrangement took place until 400°C. At this temperature only phenol was detected (yield<1%).

This behaviour can be explained by considering that phenetole is hardly adsorbed on the basic catalyst, whereas starting from phenol a concerted mechanism with DEC is possible.

4.4.6.4 *Gas-phase phenol ethylation over basic systems: comparison of alkylating agents*

In order to better highlight the peculiar reactivity of DEC in gas-phase phenol ethylation, a complete comparison with more traditional alkylating agents, such as ethanol and diethyl ether (DEE), was performed.

In particular, the reactivity of these reagents with phenol was investigated using the "low surface area" MgO in the same range of temperature (300-350-400°C) and feeding the same excess of the alkylating agent (10 times the amount of phenol) previously used.

Interestingly, DEE was completely un-reactive with phenol and no alkylated products were detected in the whole temperature range investigated.

Furthermore, ethanol showed very low reactivity with 5% phenol conversion only at 400°C.

As expected, a similar behavior compared to methanol was obtained (Fig. 4.61). In fact, the reaction was selective in C-alkylation at the ortho-position of the aromatic ring, with formation of 2-ethylphenol as the main product of the reaction.
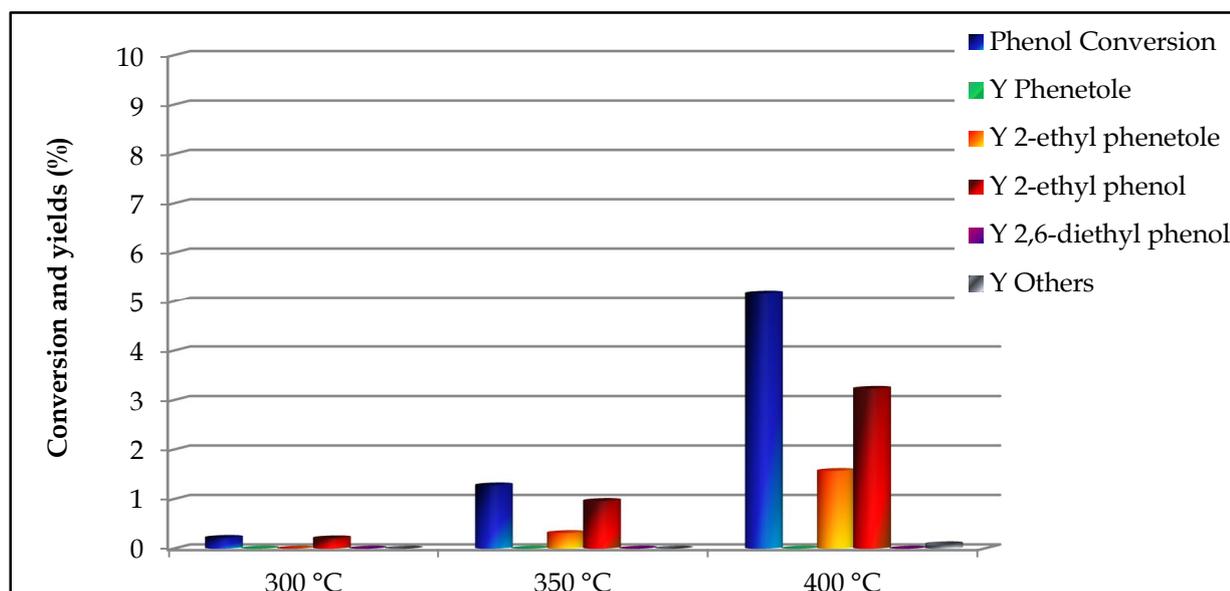

Fig. 4.61 Catalytic results over MgO (20 m²/g), Ethanol:Phenol=10:1, variable T, τ = 1 s.

Results clearly show the superiority of DEC as ethylating agent with an heterogeneous basic catalyst, in which the latter plays the role of phenol activation and formation of the phenate species.

4.4.6.5 *Decomposition of the alkylating agents on MgO*

With the aim of better understanding the behavior of the alkylating agents on MgO catalytic surface, a few decomposition tests were performed by feeding only pure DEC or ethanol (350°C, τ=1s).
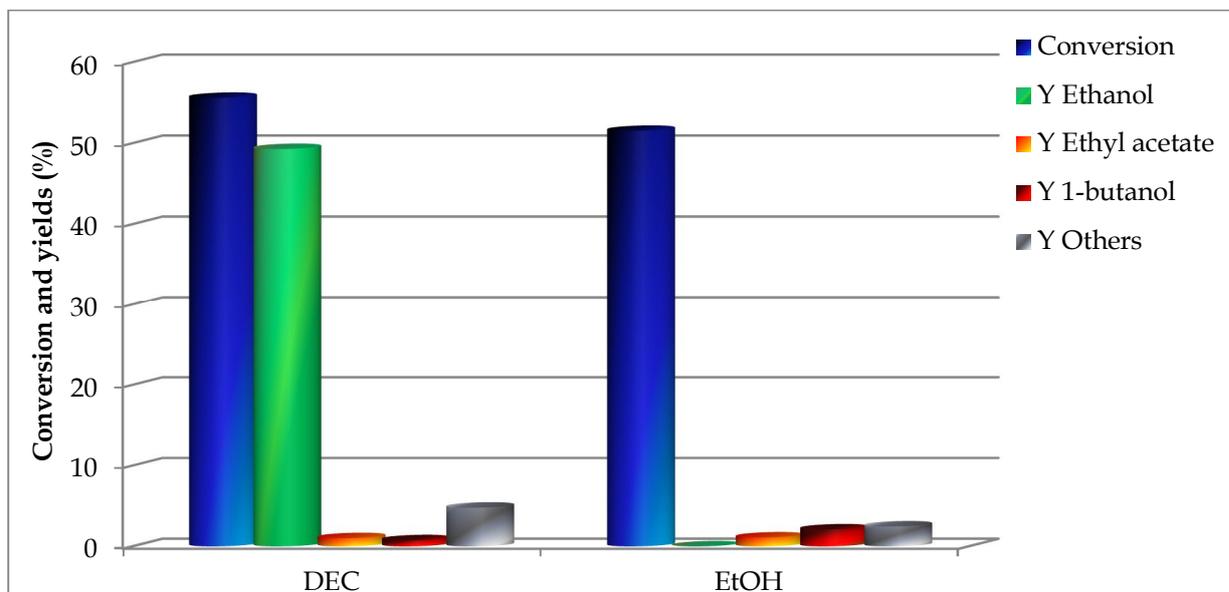The results are shown in the figure below (Fig. 4.62).

Fig. 4.62 Results of the decomposition of the alkylating agents in the reaction conditions, MgO (200m^2/g), T=350°C, τ=1s.

The picture shows the conversion of DEC and ethanol, and yields to the main condensable products (1-butanol, ethylacetate and heavier condensation products), while the gaseous components, ethylene and CO_2, were not quantified.
On MgO, DEC was much more reactive than ethanol and easily decomposed to yield ethylene, CO_2 and ethanol, as reported in the scheme below (Scheme 4.20).
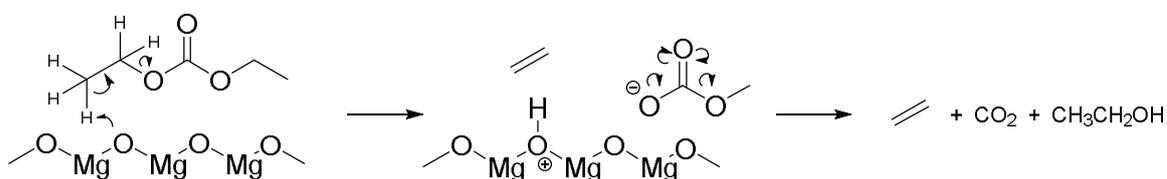
Scheme 4.20 DEC decomposition over MgO surface leading to the formation of ethylene, carbon dioxide and ethanol

Afterwards, ethanol further reacted with formation of same products obtained when ethanol is made react directly.

Ethanol, although more stable than DEC, underwent a dissociative adsorption over MgO leading to the formation of acetaldehyde and hydrogen.

Over basic systems, acetaldehyde can follow different reaction pathways and be transformed into 1-butanol (Guerbet reaction) and ethyl acetate (Tishchenko reaction), as summarised in the scheme below (Scheme 4.21).
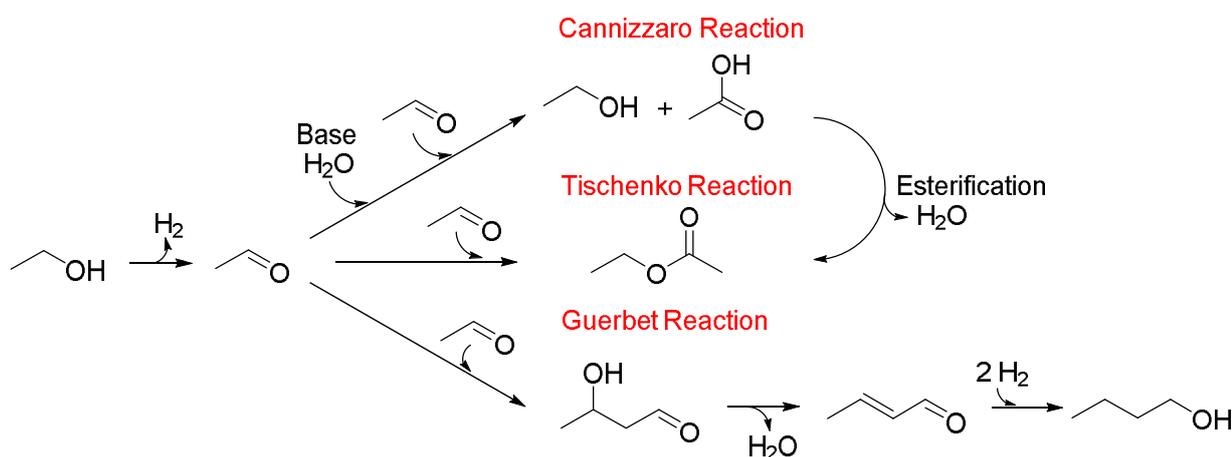
Scheme 4.21 Ethanol reactions pathways over basic systems. Ethanol dehydrogenation to acetaldehyde, a reactive intermediate for disproportionation reaction (Cannizzaro), Tishchenko reaction to ethylacetate and Guerbet reaction to 1-butanol.

Indeed, with both DEC and ethanol, both 1-butanol and ethylacetate were produced.

4.4.7 Infrared spectroscopy in vacuum: phenol adsorption on MgO

Catalytic tests highlighted the role of the basic catalyst in the in-situ activation of the adsorbed phenol to phenate and the preferred formation of the ortho-alkylated products; this behavior was investigated more in detail.

In particular, phenol adsorption on MgO was studied by means of IR spectroscopy in vacuum, investigating also the influence of temperature on the desorption of adsorbed species.

The attribution of free molecules vibrations were interpreted by matching experimental (Fig. 4.63), calculation and literature data.
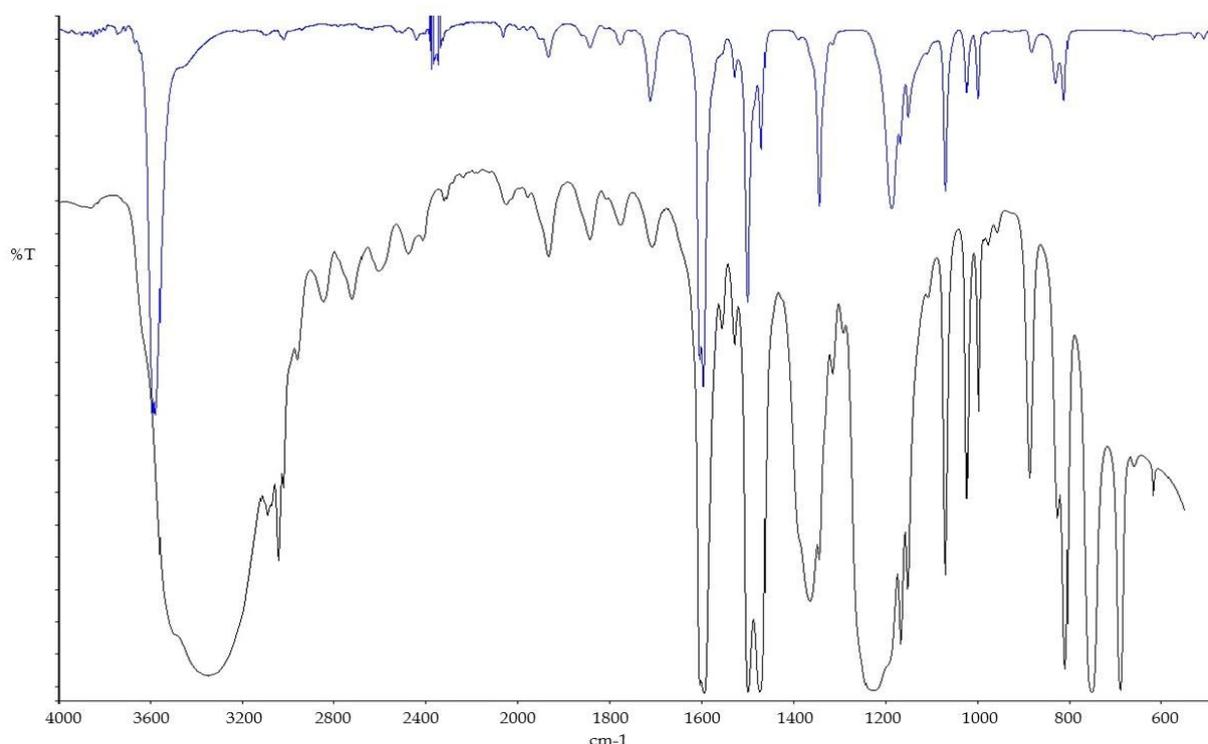
Fig. 4.63 Phenol infra-red spectra between 4000 and 600 cm-1 acquired in transmittance, obtained by dropping melt phenol on a KBr tablet (black) and by dissolving it in a 0,1M solution of DCM.

The main FT-IR bands related to the free phenol are reported in Table 4.14. The comparison of the experimental frequencies with the calculated ones made possible the description of the vibrational modes, that are essential for understanding the spectra of phenol adsorbed on MgO.

Calculated Wavenumbers (cm⁻¹)	Experimental Wavenumbers (cm⁻¹)	Vibrational mode description
4196	3583	ν OH
3379	3108	ν sym CH
3370	3094	ν asym CH
3353	3076	ν asym CH
3343	3045	ν asym CH
3326	3024	ν asym CH
1810	1605	ν aromatic CC
1797	1579	ν aromatic CC
1671	1500	ν aromatic CC + δ CH + ν CO
1635	1470	ν aromatic CC + δ CH
1488	1343	δ CH + δ OH
1404	1185	ν CO + δ CH
1370	1167	δ CH + δ OH
1291	1149	δ OH + δ CH
1197	1070	ν asym aromatic CC
1176	1023	δ CH
1122	1000	δ CH

Table 4.14 Phenol main vibrational mode and related bands wavenumbers

Fig. 4.64 displays the spectra of the catalyst after the pretreatment in vacuum at 450°C (black), of phenol adsorbed on MgO at room temperature (blue) and of the compound obtained by performing the desorption at increasing temperatures under vacuum (from room temperature up to 450°C).
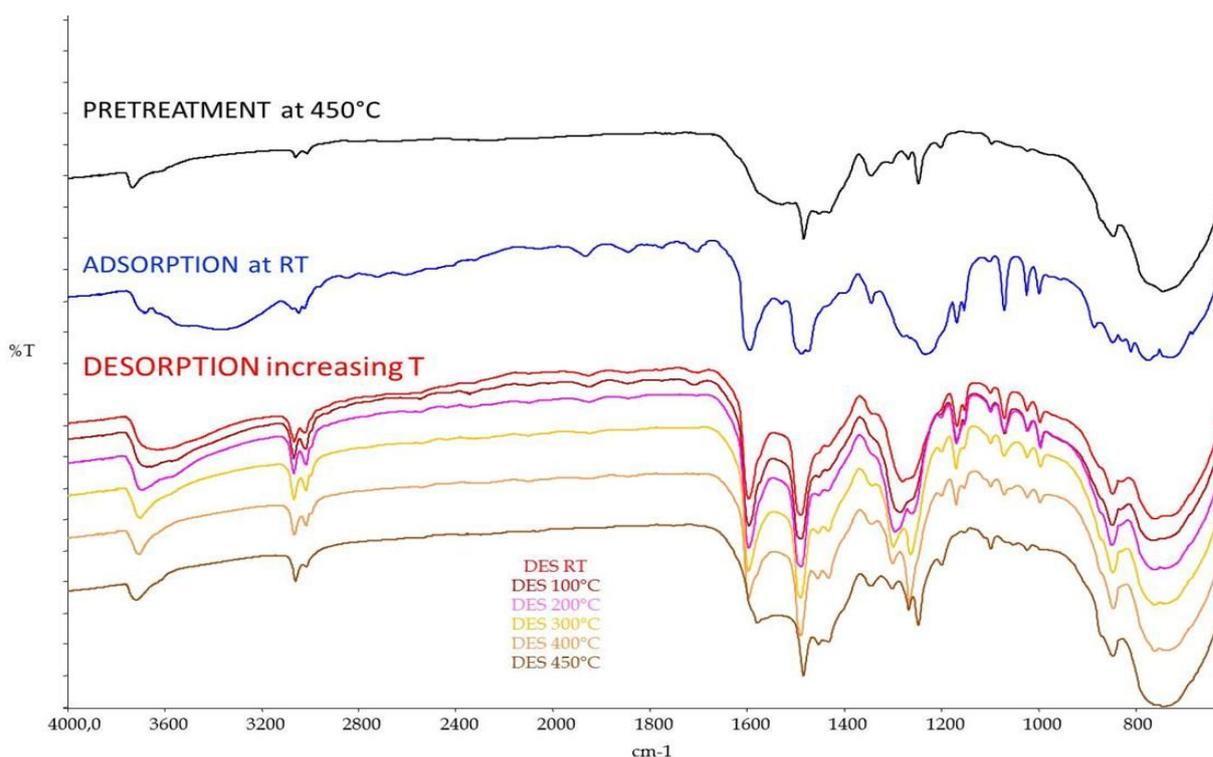
Fig. 4.64 Infra-red spectra in vacuum of phenol adsorbed over a tablet of MgO and after desorption at increasing temperatures.

From spectra recorded (after subtraction of the pretreated catalyst spectrum), the following results are worth of being mentioned.

I. **The OH stretching region:** the interaction of phenol with the catalytic surface resulted in a perturbation of catalysts hydroxyl group, confirmed by a shift of the band from 3736 to 3700 cm^{-1}; moreover, the vibration of phenol OH group at 3558 cm^{-1} remained still noticeable after adsorption on the dry catalyst, however with a small shift toward lower wavenumber;

II. **The aromatic CH stretching region:** C-H aromatic stretching were shifted to lower wavenumbers, and after adsorption the two most intense bands at 3094 and 3045 cm^{-1} of the aromatic CH stretching mode of the free phenol were shifted to 3068 and 3016 cm^{-1}, respectively; however, the evident broadening hindered the identification of less intense bands at 3108, 3076 and 3024 cm^{-1}.

III. **The aromatic CC stretching region:** the two pairs of original bands attributed to the phenol aromatic CC stretching (1605-1596 cm^{-1} and 1499-1470 cm^{-1}) were perturbed. In particular, the first pair of bands gathered together, but the most important difference concerned the behavior of the band at 1470 cm^{-1}. During the thermal treatment, the intensity of this band gradually decreased and shifted toward higher wavenumber, until it became completely enveloped in the band at 1499 cm^{-1}, already shifted to 1492 cm^{-1}.

IV. **The OH bending region:** the band related to the OH bending mode of phenol remained unperturbed at 1343 cm^{-1} after phenol adsorption; however, during the desorption this band rapidly disappeared in favor of the band at 1289 cm^{-1}, attributed to the CO stretching of the phenate species.

V. **The CO stretching region:** we observed the concomitant presence of phenate and phenol species (1289 and 1259 cm^{-1} respectively).

VI. **The aromatic CH bending:** the band at 1167 and 1149 cm^{-1} attributed to the bending of aromatic CH and OH groups, remained almost unperturbed; the same behavior was observed for the bands at 1070, 1023 and 1000 cm^{-1}, attributed to the bending mode of the aromatic CH.

The FT-IR spectrum of chemisorbed phenol demonstrates that phenol is adsorbed as phenate, following the orthogonal mode of adsorption proposed by Tanabe, resulting in a perturbation of vibration modes in ortho and para positions.[384,385]

Moreover, the phenate species was strongly adsorbed on the catalyst surface and desorbed only at high temperature.

4.4.8 Diethyl carbonate (DEC) in the gas-phase phenol ethylation over acid catalysts

The gas-phase ethylation of phenol with DEC has been investigated also with a commercial γ-Al_2O_3 (140 m²/g), in order to study the performance with an acid catalyst.

In particular, the carbonate could be adsorbed on catalyst acid sites with generation of more reactive species for ethylation.

Two possible mechanisms for the reaction over MgO and γ-Al_2O_3 are reported below (Scheme 4.22); note that with alumina also O-alkylation, leading to the formation of phenetole, is a feasible reaction.

Basic systems: phenol activation

Acid systems: DEC activation
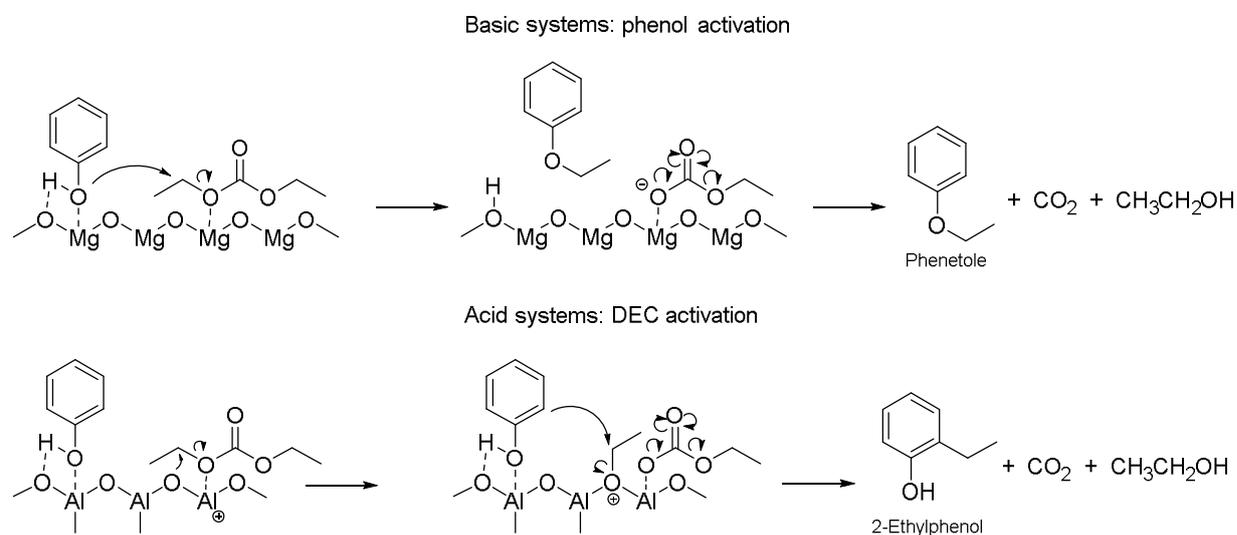
Scheme 4.22 Possible reaction mechanisms over MgO and γ-Al_2O_3.

Because of these reasons, we studied the influence of feed composition by comparing results obtained at different inlet DEC/Phenol molar ratios, equal to 4 (excess of DEC), 1 (stoichiometric ratio) and 0.5 (excess of phenol), at 300°C. Results are reported below (Fig. 4.65).
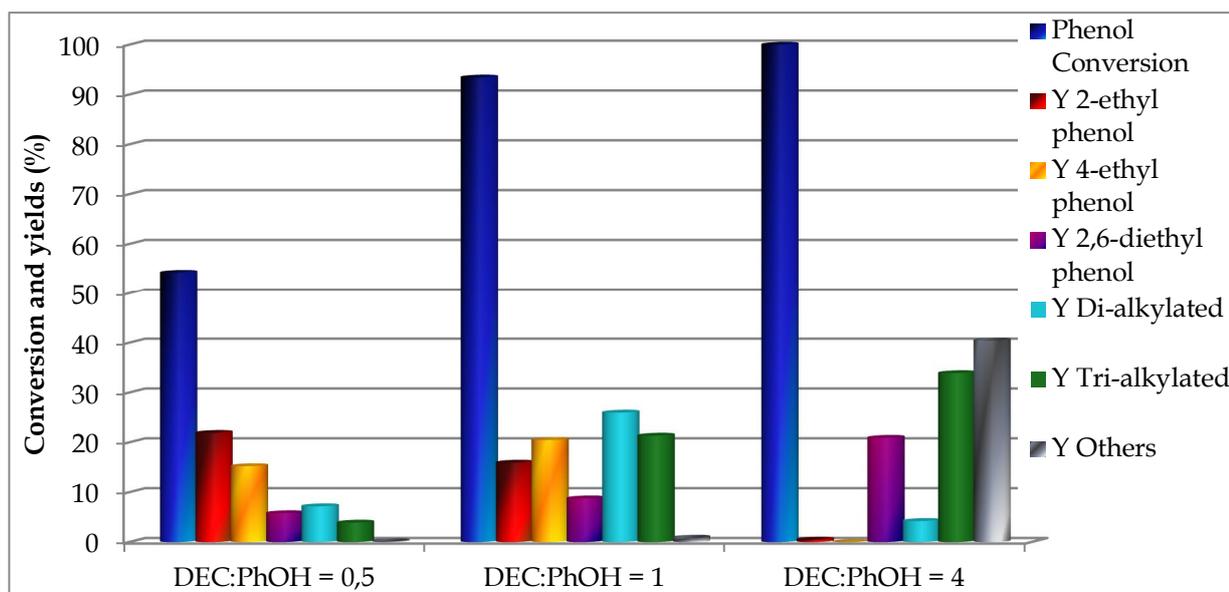
Fig. 4.65 Catalytic results over Al_2O_3 (140 m^2/g), feed ratio variable, T=300°C, τ = 1 s.

Interestingly, alumina showed an outstanding activity, since it was able to catalyze the reaction and provide high phenol conversion even with a stoichiometric feed ratio.

Moreover, the reaction showed very high chemo-selectivity toward C-alkylation; indeed only few poly-alkylated, heavier compounds ("Trialkylated" and "Others" in Fig. 4.65) had the ethoxy moiety.

On the other hand, no control on products distribution was possible; inasmuch also when low DEC/phenol ratios were used, a complex mixture of polyalkylated compounds was produced, whose yield obviously increased when a large excess of DEC was used.

Moreover, no mono-ethyl phenols formed as long as an excess of DEC was fed.

Noteworthy, when a sub-stoichiometric amount of DEC was fed, the phenol conversion decreased down to the theoretical limit (50%), but again both di- and tri-alkylated compounds were also produced.

This can be explained only by taking into account of the several reactions that are catalyzed by the acid sites of alumina.

In 2011, Strassberger et al reported a study on the dealkylation of anisole and phenetole, chosen as lignin model compounds, over Al_2O_3 and Mg/Al mixed oxides.[386]

Indeed, they found that phenetole and anisole can undergo a dissociative adsorption, and alkyl rearrangement and disproportionation over acid sites as well, as shown in the following scheme.

Dissociative adsorption of phenetole over acid site and alkyl rearrangment

Possible side reactions:
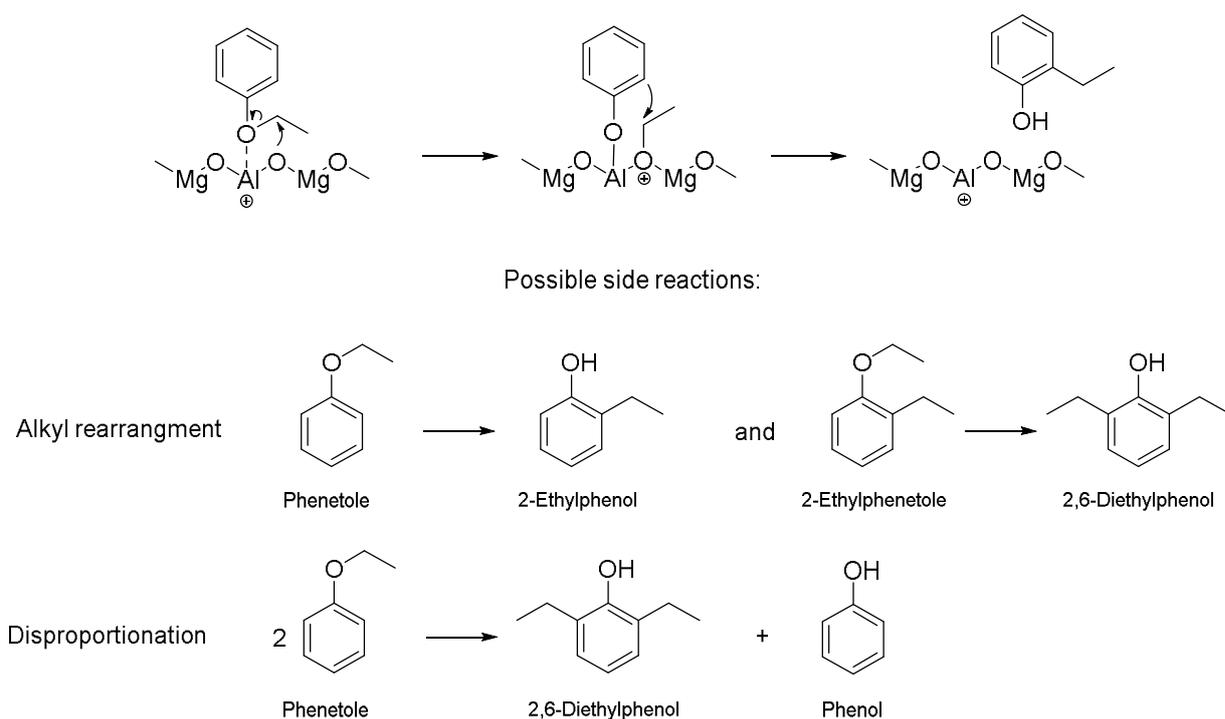
Scheme 4.23 Dissociative adsorption of phenetole over acid sites and possible side reactions. Adapted from reference.[386]

The remarkable selectivity toward C-alkylated products shown with an acid system like γ-Al$_2$O$_3$ suggests that alkyl rearrangements are faster compared to O-alkylation. Indeed, no phenetole-derived products lighter than the tetraethylated compounds were found.

4.4.9 Diethyl carbonate (DEC) in the gas-phase phenol ethylation over Mg/Al mixed oxide

With the aim of investigating the synergic effect of basic and acid sites in a single bifunctional catalyst and limit the unselective alkylations shown with γ-Al_2O_3, a Mg/Al mixed oxide (atomic ratio 3 to 1) was synthesized as described in chapter 4.4.4.3.

With the Mg/Al/O catalyst, when the reaction was carried out at 350°C with a great excess of DEC (DEC/phenol 10:1), phenol conversion was lower than 90%, while in the same conditions with MgO we were able to obtain a complete and stable conversion.

Moreover, a complex mixture of products was obtained, with a phenetole yield lower than 40%. Interestingly, an increase of the C-alkylated products (2-ethylphenol, 2,6-diethylphenol) and polyalkylated compounds was also observed (Fig. 4.66).
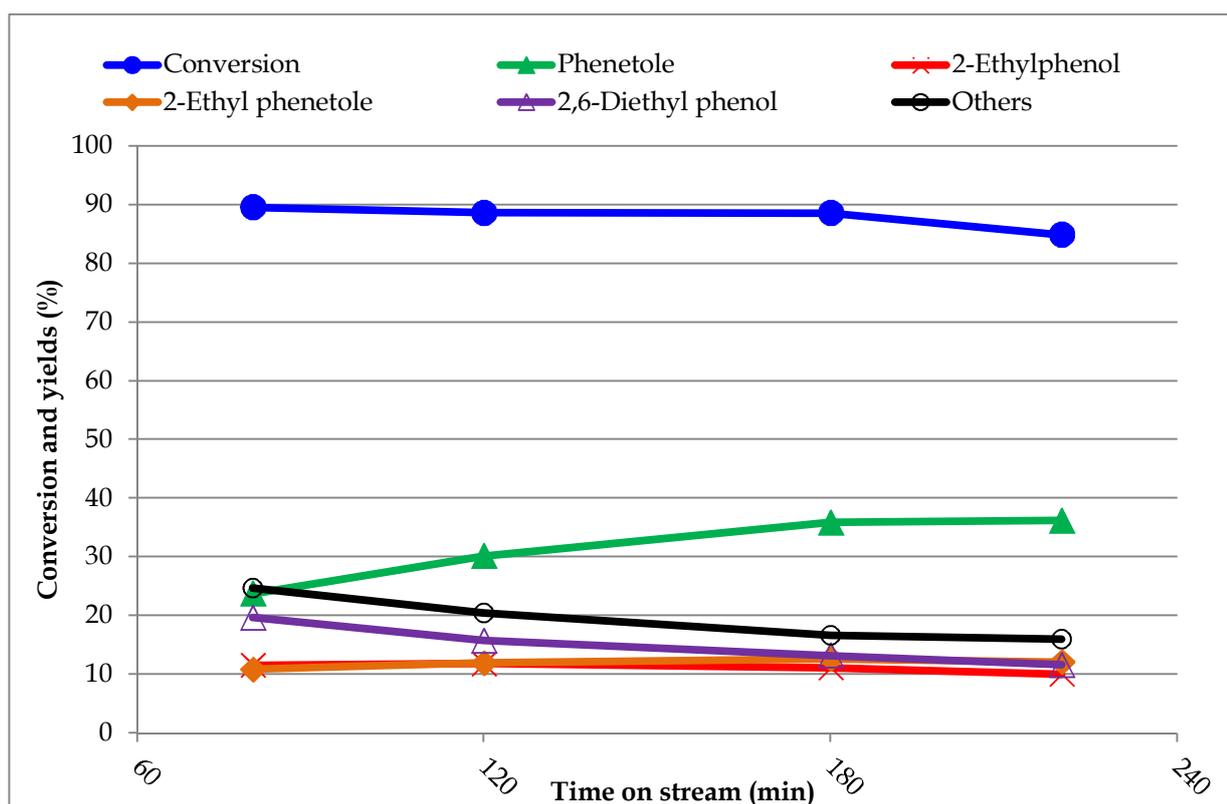

Fig. 4.66 Catalytic results over Mg/Al/O (160 m²/g) in function of time on stream, DEC:Phenol=10:1, T=350°C, τ = 1 s.

This behavior can be explained by taking into account the contribution of side reactions, as explained in the previous Chapter. In particular, basic sites catalyze the selective O-alkylation of the phenate species with DEC, but the so-formed phenetole

can be adsorbed again over a neighbouring acid site that promotes its dissociation with formation of adsorbed phenol and an ethyl species, thus promoting both alkyl rearrangements and disproportionation reactions.

The mechanism proposed is reported in the following scheme (Scheme 4.24).
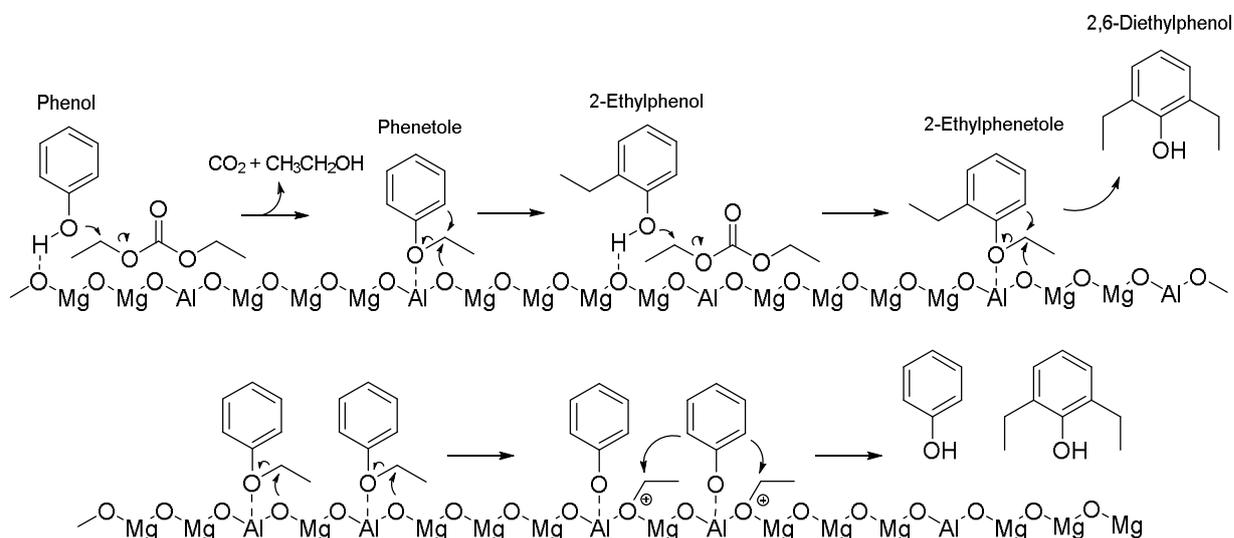
Scheme 4.24 Proposed mechanism for the consecutive O-alkylation and alkyl rearrangement over Mg/Al/O (top) and disproportionation reaction (bottom).

In order to both confirm this mechanism and better understand the influence of the reaction temperature, we decided to perform a test, limiting the DEC excess (DEC/phenol 4), at three different temperatures: 300, 350 and 400°C.

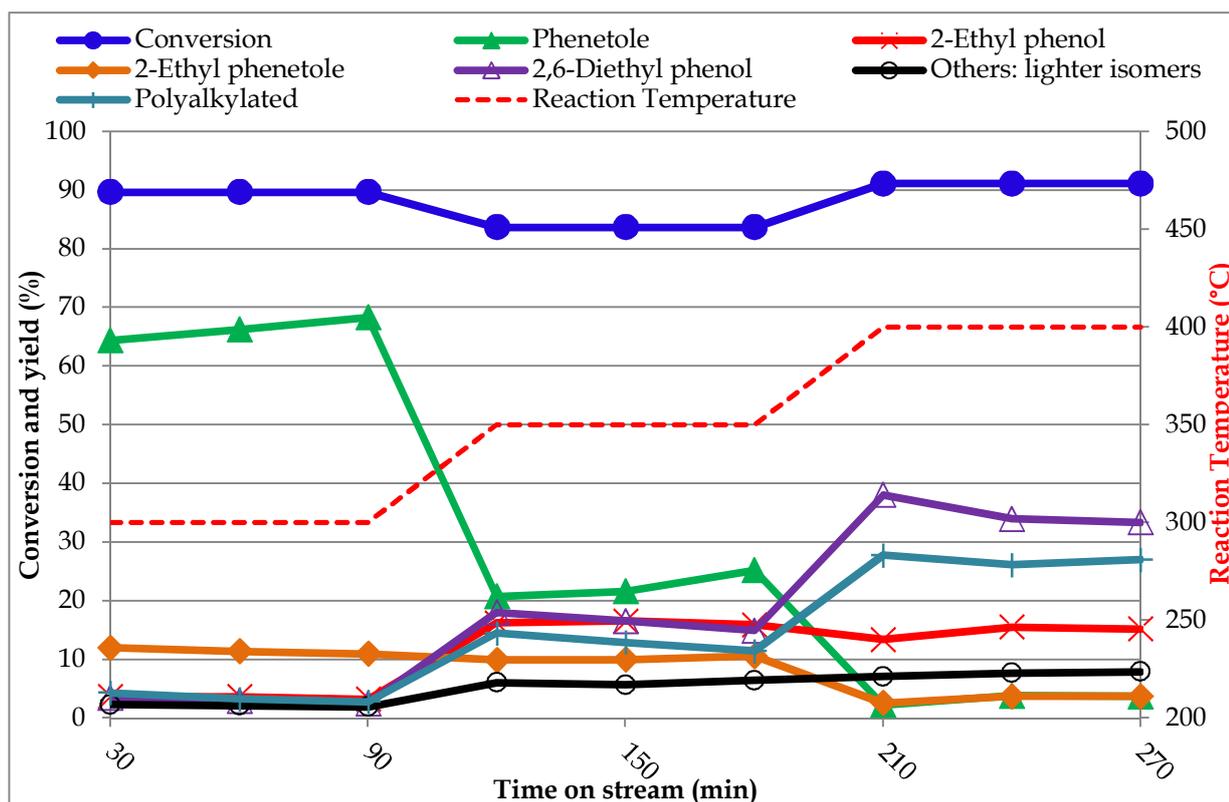The results obtained are shown below (Fig. 4.67).

Fig. 4.67 Catalytic results over Mg/Al/O (160 m²/g) in function of time on stream, DEC:Phenol=4:1, T variable: 300-350 and 400°C, τ = 1 s.

In this way, we have found the great influence of the reaction temperature on products distribution.

In particular, at low temperature (300°C) the behavior of Mg/Al/O was not much different from that shown by MgO; phenetole was quite stable and only a minor part of it underwent dissociative adsorption with formation of "unconverted" phenol and ethylphenol.

The great excess of DEC favored the consecutive conversion of ethylphenol to 2-ethylphenetole.

On the other hand, an increase of the reaction temperature led to a rapid decrease of both phenetole and 2-ethylphenetole yields, and favoured the formation of 2-ethylphenol, 2,6-diethylphenol and polyalkylated compounds. This behavior is more typical of the acid catalyst alumina, but one major difference between the latter and Mg/Al/O is the higher selectivity to mono and dimethylated compounds achieved with the latter catalyst.

It is clear that the reaction temperature and the smart design of the acid sites in the bifunctional catalyst allows to progressively shift the organic carbonate reactivity with phenol from a high selectivity in O-alkylation to the selective formation of C-alkylated compounds. This is an interesting result that will deserve further investigation.

4.4.9.1 DEC decomposition with Mg/Al/O

The results obtained by feeding only DEC over the Mg/Al mixed oxide at 350°C are reported below.
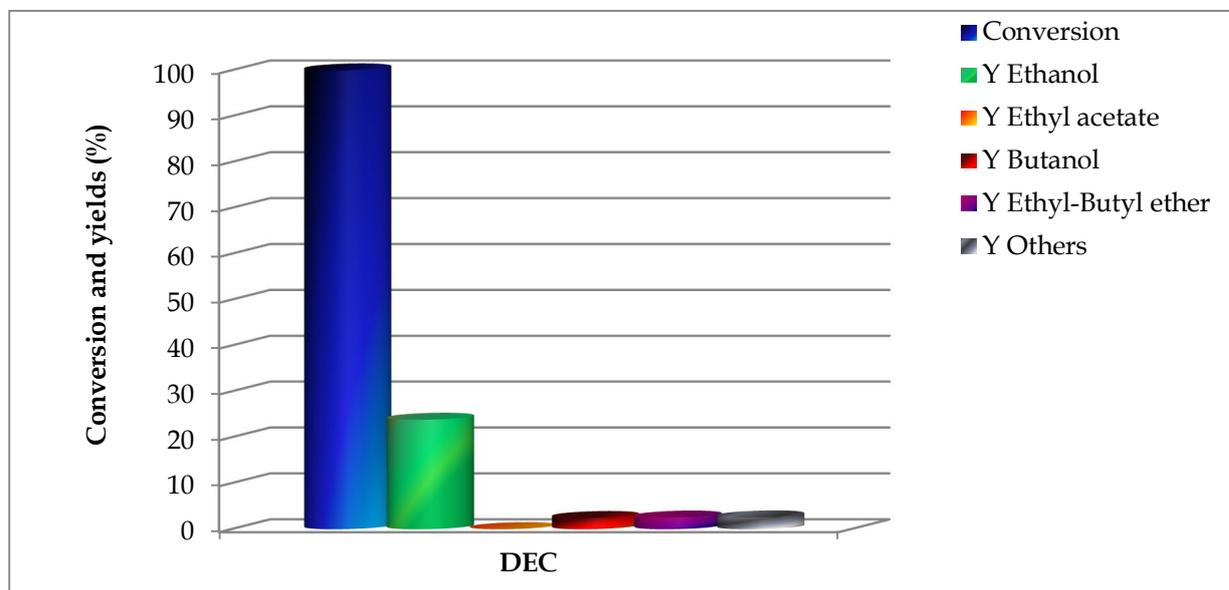
Fig. 4.68 DEC decomposition over Mg/Al/O at 350°C, τ=1s.

Noteworthy, with the mixed oxide the conversion of DEC was complete, while with MgO it was around 50%.

Moreover, the overall amount of condensable compounds produced (mainly ethanol, ethyl acetate, 1-butanol and ethyl-butyl ether) was not high enough to justify for such an high conversion. This carbon-loss had not observed previously with MgO, and we discovered it to be due to the formation of a great amount of diethylether (DEE). DEE was not analysed with our standard GC analytical procedure, and its presence was confirmed by means of GC-MS analysis.

Interestingly, a new product, ethylbutyl ether, was also detected. This product probably formed by decarboxylation of the asymmetric carbonate (ethylbutyl carbonate), the product of the nucleophilic attack of an activated butanol molecule on the DEC carbonyl carbon atom, or by reaction of 1-butanol with a chemi-sorbed ethyl group.

4.4.9.2 Gas-phase phenol ethylation over Mg/Al mixed oxide: comparison of alkylating agents

With the aim of better understanding the role that DEE, formed by DEC decomposition, might have during phenol ethylation, we carried out a comparison by feeding a mixture of DEE and phenol (10:1), at 350°C. Results are shown in the following figure (Fig. 4.69).
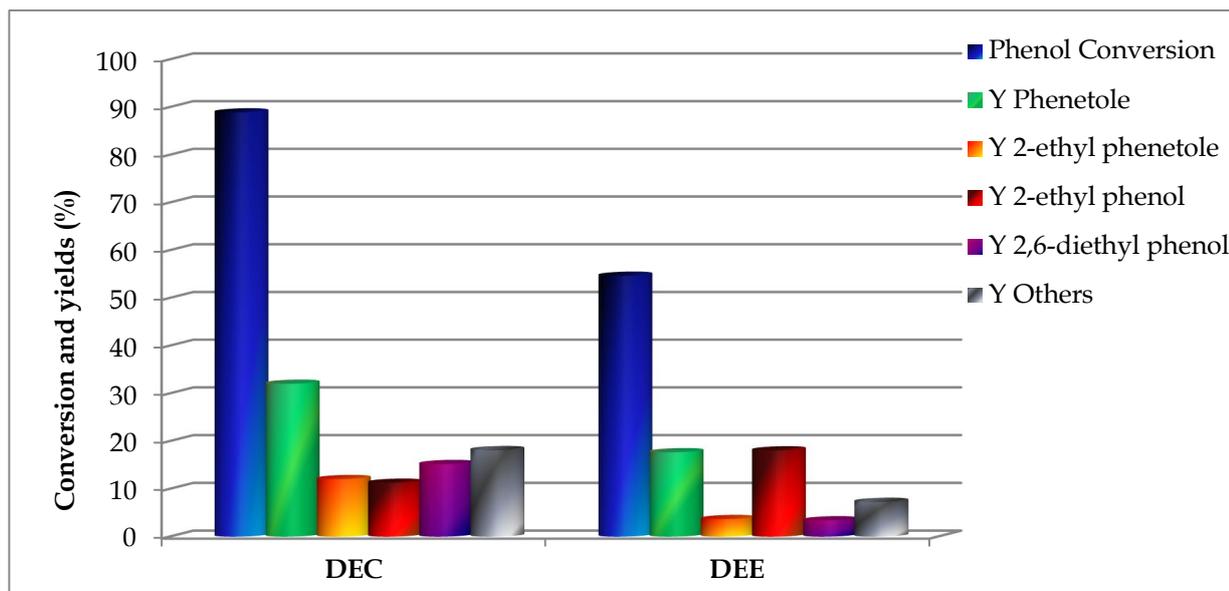
Fig. 4.69 Catalytic results with Mg/Al/O (160 m²/g), DEC or DEE:Phenol=10:1, T= 350°C, τ = 1 s.

Although the previous tests with DEE over MgO had shown a complete inertness of this reagent toward phenol alkylation, with the Mg/Al mixed oxide DEE reacted with phenol, and a phenol conversion of about 55% was achieved. However, DEC showed a greater reactivity (phenol conversion 88%) and higher yields to 2,6-diethylphenol and other polyalkylated compounds were also obtained.

Nevertheless, the similar products distribution suggests that similar ethyl species probably form over the acid sites starting from both alkylating agents.

4.4.10 Asymmetric carbonates in the gas-phase alkylation of phenol: the example of methylbutyl carbonate (MBC)

4.4.10.1 MBC decomposition over basic systems

Considered the interesting results obtained so far with the lighter symmetric linear aliphatic carbonates, DMC and DEC, we decided to investigate the reactivity of other heavier carbonates.

In particular, we decided to study the reactivity of an asymmetric carbonate: methylbutyl carbonate (MBC), synthesized as reported in chapter 4.2.6, Table 4.5 (row 3).

The mixture obtained after the synthesis, composed mainly of MBC and DMC, was distilled and MBC was obtained with 92% purity.

First, the decomposition of MBC was investigated by feeding MBC only over the high-surface-area MgO (200 m²/g), at 300°C. Results are reported below (Fig. 4.70).
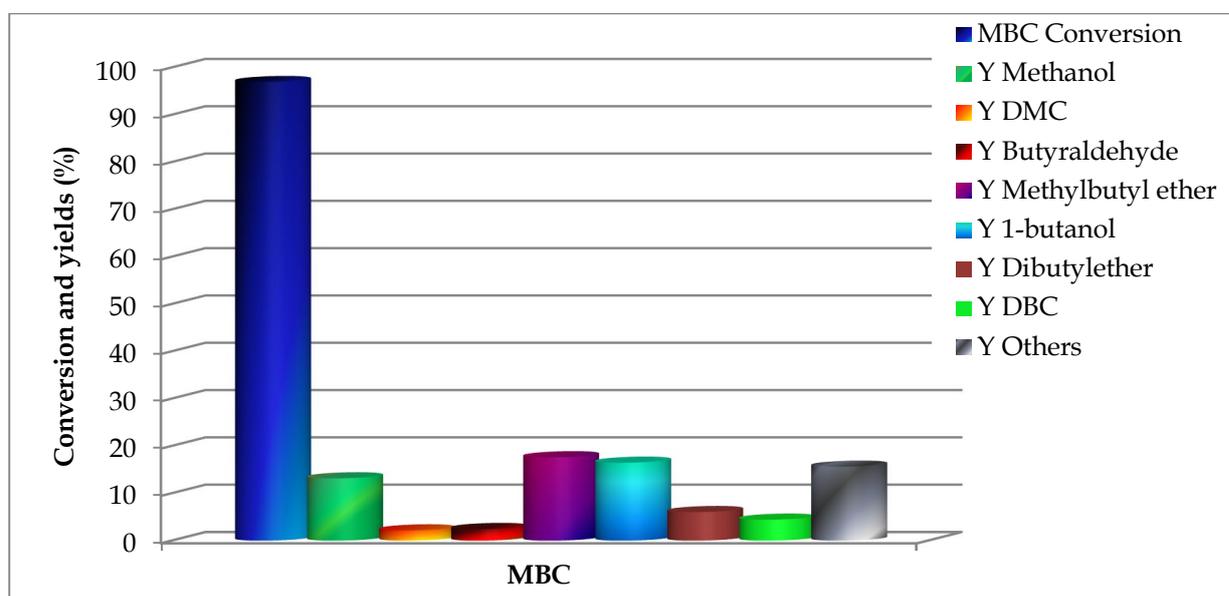

Fig. 4.70 MBC decomposition over MgO, T=300°C, τ=1s.

Noteworthy, the reactivity of the asymmetric carbonate was much higher compared to that, for example, of DEC.

Indeed, the conversion was almost complete at 300°C; conversely, with the same catalyst DEC decomposed by the 50% only, at 350°C.

Moreover, many reactions occurred at the same time leading to the formation of a complex mixture of products.

The main condensable products were: methanol, 1-butanol, butyraldehyde, methylbutyl ether and dibutyl ether.

Interestingly, also a disproportionation reaction occurred, that gave rise to the formation of both DMC and DBC as co-products.

The hypothesized reactions for MBC decomposition are shown in the following scheme.
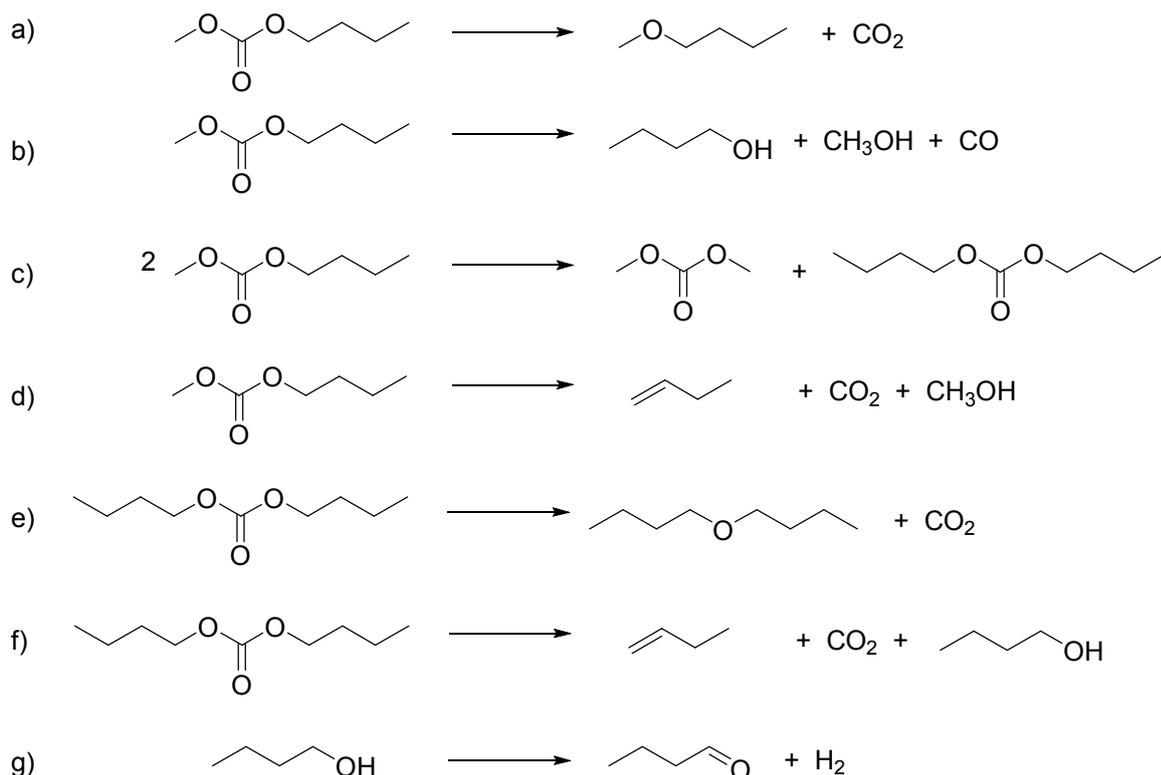
Scheme 4.25 Hypothesized reactions for MBC decomposition with MgO at 300°C: a) MBC decarboxylation, b) MBC decarbonylation, c) MBC disproportionation to DMC and DBC, d) MBC decomposition after β-hydrogen extraction with the formation of butane, CO_2 and methanol, e) DBC decarboxylation, f) DBC decomposition, g) 1-butanol dehydrogenation.

4.4.10.2 The gas-phase phenol alkylation with MBC on MgO catalyst

The reactivity of MBC in the gas-phase alkylation of phenol was tested in similar conditions as for the decomposition test described in the previous chapter.

A 4:1 MBC:phenol mixture was fed at the temperature of 300°C, with the MgO catalyst; results are reported below.

Fig. 4.71 Catalytic results with MgO (200 m²/g) in function of time on stream, MBC:Phenol=4:1, T=300°C, τ = 1 s. Continuous line: yield and conversion of phenolic compounds, dotted lines: MBC conversion and DBC yield, calculated with respect to MBC.
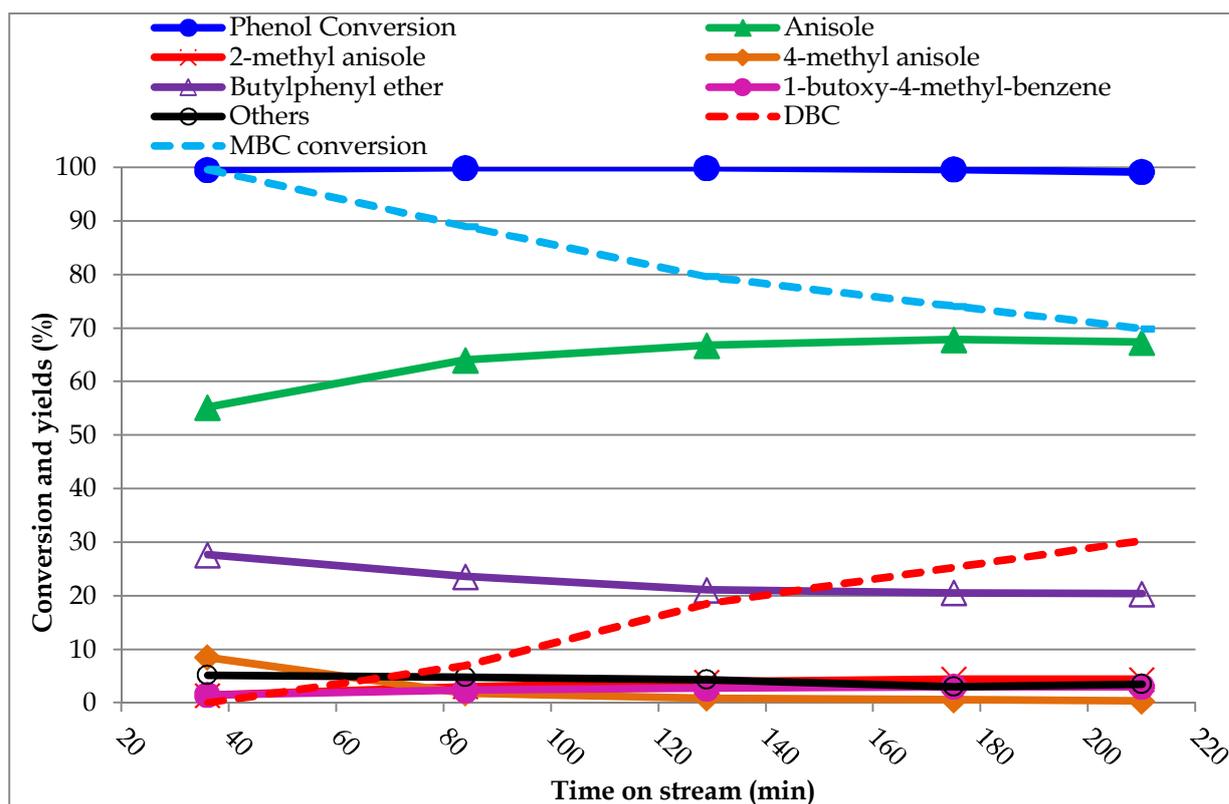
Surprisingly, by feeding a low excess of the asymmetric carbonate at relatively mild conditions (300°C), a complete conversion of phenol was obtained.

As expected, the main products were the two O-alkylated products: anisole and butylphenyl ether, respectively.

However, anisole formed with greater yield ($Y_{anisole}$ = 67%) than butylphenyl ether ($Y_{butylphenylether}$ = 20%).

This was due to the major steric hindrance of the butyl chain that limited its reactivity and availability for the nucleophilic attack of the activated phenolic oxygen.

A further proof for this hypothesis was the progressive increase of the yield to dibutyl carbonate (DBC) during the reaction. DBC was probably almost unreactive under the conditions used, because it is known that heavier carbonates generally need harsher conditions to react compared to lighter carbonates. Indeed, the yield to this product increased to 30% despite the conversion of the alkylating agent was decreasing at the same time; note that the conversion of phenol was stable, suggesting that even a lower excess of MBC is enough to obtain complete conversion of the aromatic.

Interestingly, the reaction of the MBC methyl group with phenol favored the formation of butyl species more active for the further reaction with MBC to

generate DBC; in fact, in the previous test carried out with MBC alone, only a 4% DBC was formed.

Furthermore, DMC (the other product of MBC disproportionation) was not detected; because of its high reactivity as methylating agent (Chapter 4.4.5), it contributed to increase the selectivity to anisole.

Again, organic carbonates showed a very high selectivity in O-alkylation.

The possible reaction mechanisms are shown in the following scheme (Scheme 4.26).
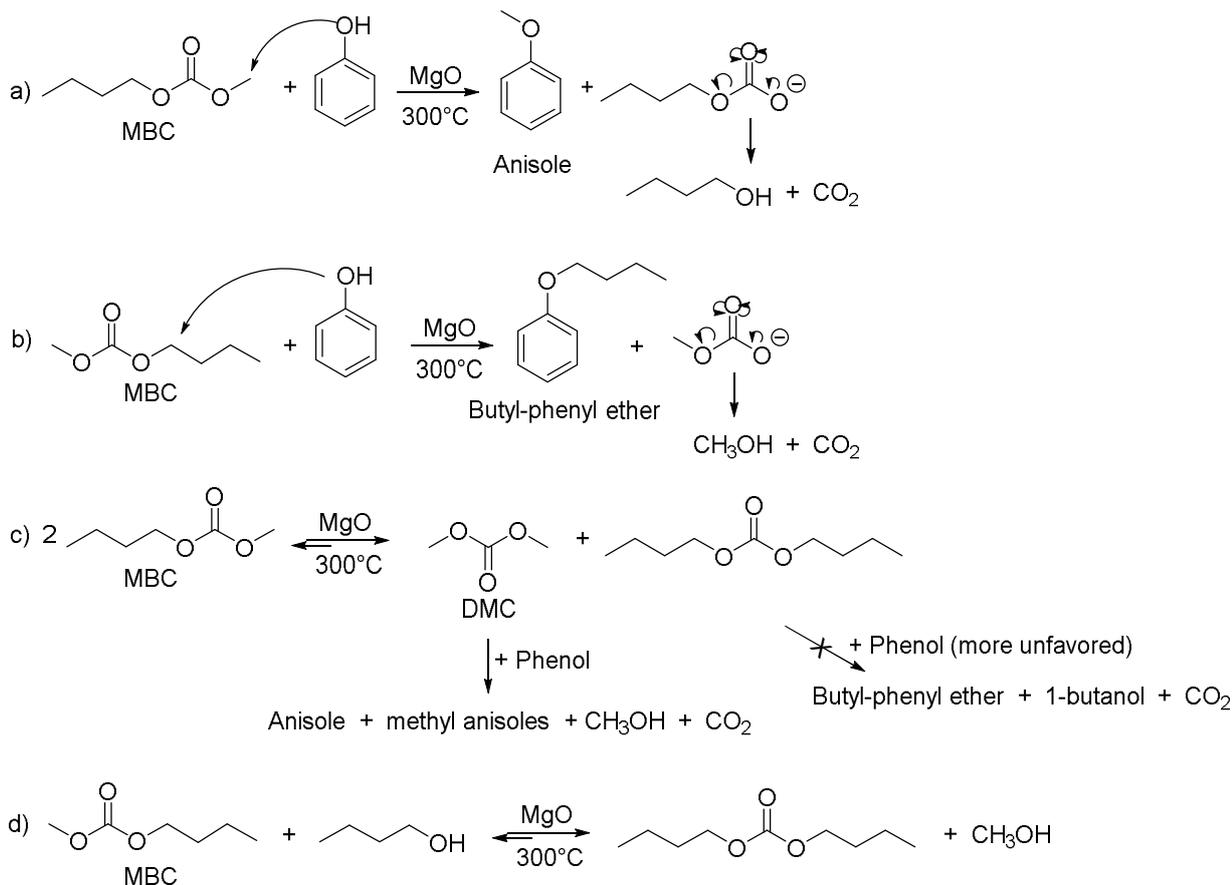
Scheme 4.26 Reaction pathways toward the formation of the main reaction products: anisole, butylphenyl ether and DBC.

In order to obtain a further proof of the lower reactivity of the symmetric carbonate compared to the asymmetric one, a mixture richer of DBC was fed to the reactor, with the MgO catalyst at 300°C.

The feeding had the following molar composition:

DBC: 44.6%; MBC:13.3%; Butanol:21.7%; Phenol:20.4%.

The catalytic results are shown below.
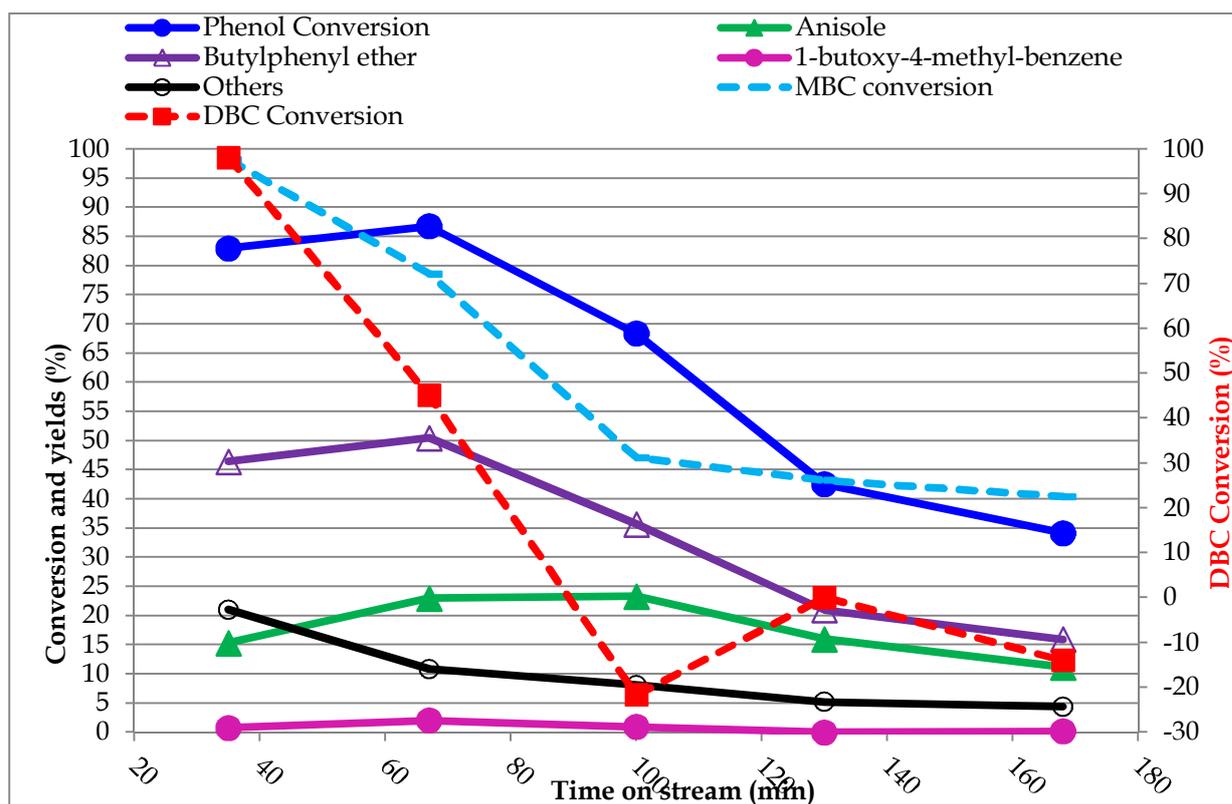
Fig. 4.72 Catalytic results with MgO (200 m^2/g) in function of time on stream, DBC:Phenol=2:1, T=300°C, τ = 1 s. Continuous line: yield and conversion of phenolic compounds, dotted lines: DBC and MBC conversion.

Noteworthy, phenol conversion rapidly dropped from 80 down to 35%, showing a strong catalyst deactivation.

Although the butylphenyl ether selectivity was higher, anisole derived from the MBC contained in the mixture still remained the major by-product.

Interestingly, at the beginning of the reaction, DBC was strongly adsorbed over the catalyst surface; this caused a very high degree of conversion. However, increasing the reaction time, DBC desorption led to the fast drop of its conversion down to values formally lower than 0%. Therefore, the system required long time to reach the steady state.

Finally, in order to better understand the possible contribution of the 1-butanol contained in the feeding mixture, a complete comparison with this alcohol has been performed, as described in the following chapter.

4.4.10.3 Gas-phase phenol alkylation, comparison of alkylating agents: 1-butanol

Finally, the reactivity of MBC was compared with that one of the corresponding alcohol, in this case 1-butanol.

Again the alcohol showed a much lower reactivity and needed higher temperature in order to promote the dehydrogenation to the more active aldehyde. The results obtained are shown below.
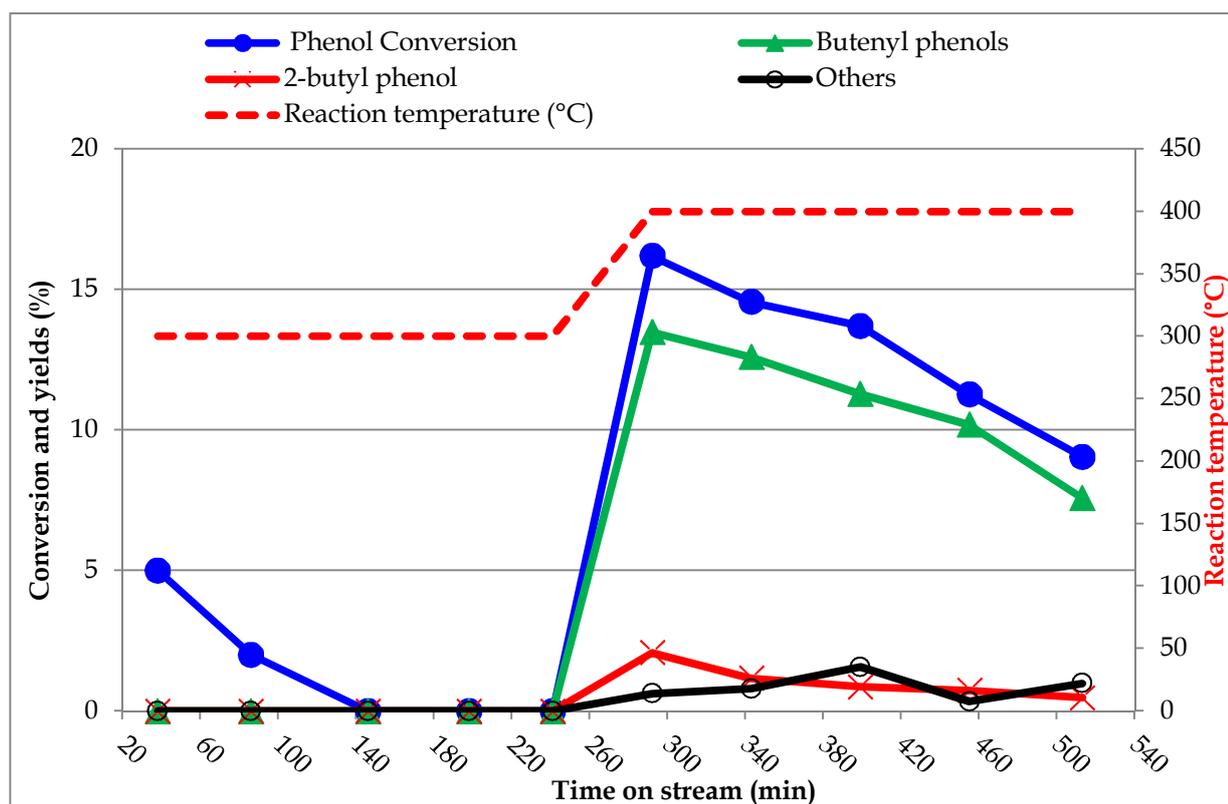
Fig. 4.73 Catalytic results with MgO (200 m²/g) in function of time on stream, 1-butanol:phenol=4:1, T variable from 300 to 400°C, τ = 1 s.

In particular, 1-butanol was totally unreactive at 300°C (the starting phenol conversion value was due to its strong adsorption on the catalyst surface), and only increasing the reaction temperature up to 400°C allowed us to measure a phenol conversion close to 15%, that however then rapidly declined down to less than 10%.

Moreover, the products were completely different from those obtained with the carbonate.

Indeed, with 1-butanol at high temperature a complex mixture of different isomers of unsaturated butyl phenolic compounds was produced, and only a minor fraction of the expected 2-butylphenol formed.

A possible reaction mechanism for the generation of this product is proposed below.
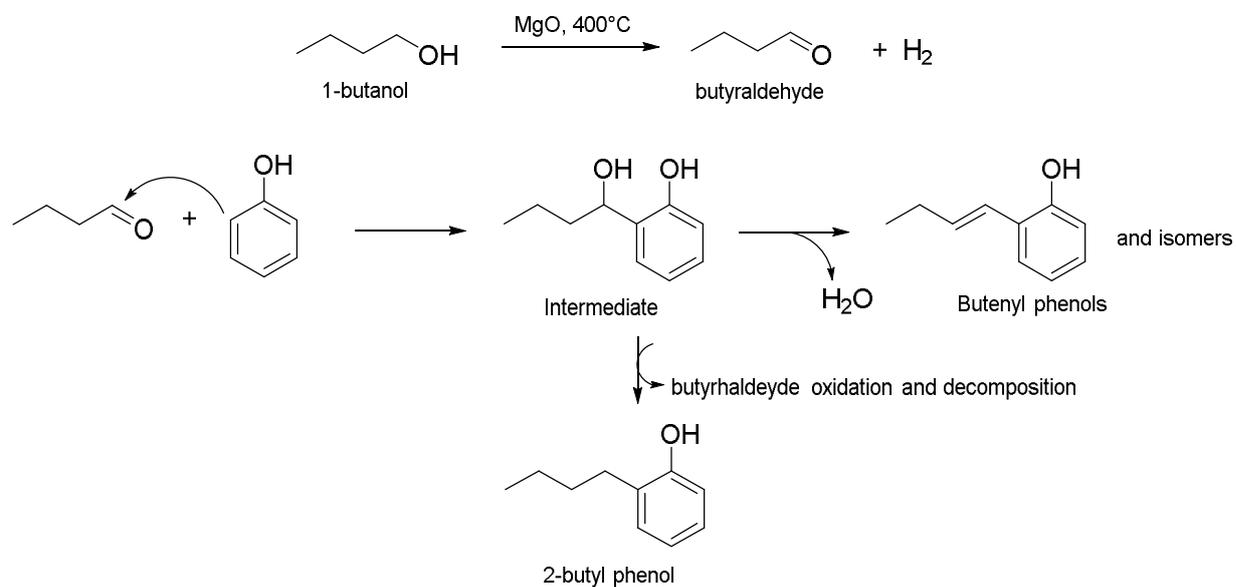
Scheme 4.27 Gas-phase phenol alkylation with 1-butanol, through its dehydrogenation to butyraldehyde leading to the formation of saturated and unsaturated butyl phenols.

4.4.11   *Final considerations*

Many organic carbonates have been tested for the gas-phase continuous-flow phenol alkylation.

It was found that using a simple heterogeneous catalyst (MgO), organic carbonates showed very high chemo-selectivity in O-alkylation forming the corresponding phenyl ethers, with a reactivity that has no analogy with other "green" alternative alkylating agents like alcohols and ethers.

Moreover, the symmetric carbonates tested showed a reactivity trend that followed the alkyl chain length:

$$DMC > DEC > DBC$$

in which DMC was the more active reagent in methylation and in formation of anisole.

Moreover, it was found that the reaction temperature and the presence of acid sites strongly influence the stability of the asymmetric phenyl ether formed, leading to an increase of the contribution of other side reactions, such as alkyl rearrangements and disproportionation.

Indeed, when an acid system (γ-Al$_2$O$_3$) was used, no control on phenol alkylation rate was possible, and a complex mixture of polyalkylated products formed.

However, the tuning of the acid sites strength by means of the design of a mixed catalytic system (Mg/Al, 3:1 mixed oxide), led to a better activity while avoiding the need for a large excess of the alkylating agent. Furthermore, an increase of the reaction temperature favoured the alkyl rearrangements on acid sites, and allowed to completely change the chemo-selectivity of the alkylated products. Indeed at 400°C we observed a 35% yield to 2,6-diethylphenol, while phenetole and ethylphenetole (the O-alkylated compounds) yields were both below 5%.

This is an interesting result, in which the greater reactivity of organic carbonates can be properly used so to obtain either O-alkylated or C-alkylated phenolics through a tuning of catalyst composition and of reaction temperature as well.

5 CONCLUSIONS

The three years of my PhD work, described in the present Thesis, have been devoted to the study of organic carbonates both as "greener" solvents and reactive chemical intermediates.

In particular, although the direct condensation reaction between alcohols and CO_2 requires harsher catalytic conditions than those reported here, enhanced catalytic systems and efficient dehydration strategies aimed at overcoming the strict thermodynamic limitations, nevertheless new synthetic strategies for the selective and efficient synthesis of organic carbonates have been developed.

In particular:

- ✓ We have developed an efficient and versatile reactive distillation system for the CIR of DMC with alcohols or diols, in which molecular sieves are arranged in the reactor in order to shift the equilibrium toward the formation of the desired products by means of the selective adsorption of methanol;

- ✓ In this way, we have obtained the almost quantitative yield of pyrocatechol carbonate (PCC), a new and previously not investigated organic carbonate;

- ✓ We have found the outstanding reactivity of PCC in the CIR with alcohols and polyols obtaining the selective synthesis of a variety of organic carbonates in very mild conditions: glycerol carbonate (GlyC), diethylcarbonate (DEC), dibutyl carbonate (DBC) and diallylcarbonate (DAC), to name a few.

Moreover, the reactivity of some of the carbonates synthesized has been investigated.

In particular:

- ✓ GlyC have been investigated as glycidol precursor in the condensation reaction with catechol to synthesize 2-hydromethyl-benzodioxane (HMB);

And:

- ✓ DMC, DEC, MBC, and DBC have been investigated as highly reactive and safer alkylating agent for the gas-phase alkylation of phenol, showing very high chemo-selectivity in O-alkylation;

✓ On the other hand, by modulating the acid strength of the catalyst and increasing the reaction temperature, the reaction selectivity could be completely shifted toward the C-alkylated products, an interesting and original behavior if the literature on the reactivity of organic carbonates is taken into account.

6 REFERENCES

[1] P. T. Anastas; M.M. Kirchhoff Acc. Chem. Res. 2002, 35, 686-694.

[2] European Commission, A Resource-Efficient Europe –Flagship Initiative Under the Europe 2020 Strategy,COM(2011) 21 (Brussels, 26.1.2011).

[3] P. T. Anastas; J. C. Warner, Green Chemistry: Theory and Practice, Oxford University, 1998, 30.

[4] P. T. Anastas, Green Chem., 2003, 5, 29.

[5] M.P. Vukalovich, V.V. Altunin: Thermophysical Properties of Carbon Dioxide, Collets, London 1968.

[6] A.L. Horvath: Physical Properties of Inorganic Compounds (SI Units), Arnold, London 1975.

[7] S. Angus, B. Armstrong, K. Renck: Carbon Dioxide – International Tables of the Fluid State (IUPAC), vol. 3, Pergamon Press, Oxford-New York 1976.

[8] J.B. van Helmont: Ortus Medicinae, ca. 1650.

[9] A.L. Lavoisier, P.S. Laplace, Mem. Acad. Sci. Paris histoire et memoires (1780) 359, (1784) 387.

[10] Recherches chimiques sur la végétation (1804; Chemical Research on Vegetation).

[11] H. D. Roth, Angew. Chem. Int. Ed., 1989, 28, 1193–1207.

[12] M. Faraday, Philos. Trans. R. Soc. London 113 (1823) 193.

[13] M. Faraday, Philos. Trans. R. Soc. London 135 (1845) 155.

[14] J. Natterer, J. Prakt. Chem. 31 (1844) 375.

[15] W. Raydt, Polytech. Notizbl. 37 (1882) 196; DE33168, 1885.

[16] www.co2now.org

[17] Tyndall J. 1859a. On the transmission of heat of different qualities through gases of different kinds Proceedings of the Royal Institution 3: 155–158.

[18] Tyndall J. 1861. On the absorption and radiation of heat by gases and vapours. Philos. Mag. 22: 169–194 and 273–285.

[19] S. Arrhenius 1896. On the influence of carbonic acid in the air upon the temperature of the ground The London, Edinburgh and Dublin Philosophical Magazine and Journal of Science 41: 237–276.

[20] Yamasaki A. Journal of Chemical Engineering of Japan, 2003, 36(4): 361–375.

[21] IPCC Fourth Assessment Report, Working Group III. Mitigation. Cambridge University Press, Cambridge, UK, 2007.

[22] IEA GHG, 2002.

a) Building the Cost Curves for CO_2 Storage, Part 1: Sources of CO_2, PH4/9, July, pp 48.

b) Opportunities for Early Application of CO_2 Sequestration Technology, Ph4/10, September, 91 pp.

[23] R. Carapellucci, A. Milazzo. Proceedings of the Institution of Mechanical Engineers Part A: Journal of Power and Energy, 2003, 217: 505–517.

[24] C. Stewart, M. Hessami. *Energy Conversion and Management,* 2005, 46: 403–420.

[25] K. Riahi, E. S. Rubin, L. Schrattenholzer. *Energy*, 2004, 29: 1309–1318.

[26] T. B. Johansson, N. Nakicenovic, A. Patwardhan, L. Gomez-Echeverri. Global Energy Assessment (GEA, IIASA), Cambridge University Press, 2012.

[27] Herzog H J, Drake E M. *Annual Review of Energy and the Environment*, 1996, 21: 145–166.

[28] **GCCSI , 2011a** : *The Global Status of CCS, 2010.* www.globalccsinstitute.com/resources/publications/global-status-ccs-2010.

[29] P. H. M. Feron, C. A. Hendriks. *Oil and Gas Science and Technology-Rev*, IFP, 2005, 60(3): 451–459.

[30] IPCC, RCCCS. Special report on carbon dioxide capture and storage. Cambridge, University Press, Cambridge, United Kingdom/New York, NY, USA, p. 442, 2005

[31] L. C. Elwell, W. S. Grant. Technology options for capturingCO2-Special Reports. Power 2006, 150(8).

[32] D. J. Fauth, E. A. Frommell, J. S. Hoffman, R. P. Reasbeck, H.W. Pennline. *Fuel Processing Technology*, 2005, 86(14-15): 1503–1521.

References

---

[33] K. P. Resnik, J. T. Yeh, H. W. Pennline. *International Journal of Environmental Technology and Management*, 2004, 4(1-2): 89–104.

[34] J. T. Yeh, K. P. Resnik, W. Pennline. *Fuel Processing Technology,* 2005, 86(14-15): 1533–1546.

[35] G. P. Knowles, S. W. Delaney, A. L. Chaffee. *Industrial and Engineering Chemistry Research*, 2006, 45(8): 2626–2633.

[36] H. Yoshitake, T. Yokoi, T. Tatsumi. *Chemistry of Materials*, 2003, 15: 4536–4538.

[37] C. Song et al. *Catalysis Today*, 2006, 115: 2–32.

[38] X. Xu, C. Song, B. G. Miller, A. W. Scaroni. *Fuel Processing Technology*, 2005, 86(14-15); 1457–1472.

[39] H. Y. Huang, R. T. Yang, D. Chinn, C. L. Munson. *Industrial and Engineering Chemistry Research*, 2003, 42(12): 2427–2433.

[40] G. P. Knowles, J. V. Graham, S. W. Delaney, A. L. Chaffee. *Fuel Processing Technology.* 2005, 86: 1435–1448.

[41] X. Xu, C. S. Song, J. M. Andresen, B. G. Miller, A. W. Scaroni. *Energy and Fuels*, 2002, 16: 1463–1469.

[42] M. M. Maroto-Valer, D. J. Fauth, M. E. Kuchta, Y. Zhang, J. M. Andresen. *Fuel Processing Technology*, 2005, 86: 1627–1645.

[43] B.P. Spigarelli, S.K. Kawatra. J. CO2 Utilization 1 (2013) 69–87.

[44] S. Choi et al. Chem Sus Chem 2 (2009) 796–854.

[45] A. Sayari et al. Chem. Eng. J. 171 (2011) 760–774.

[46] D. Shekhawat, D. R. Luebke, H. W. Pennline. National Energy Technology Laboratory, United States Department of Energy, 2003.

[47] P. Bernardo, E. Drioli, G. Golemme. Ind. Eng. Chem. Res. 2009, 48, 4638–4663.

[48] R. Bredesen, K. Jordal, O. Bolland. Chem. Eng. Process.: Process Intensif. 2004, 43, 1129–1158.

[49] A. S. Damle, T. P. Dorchak. *Journal of Energy and Environment Research*. 2001, 1(1): 77–89.

[50] H. Yang et al. Journal of Environmental Sciences 20(2008) 14–27

[51] J. C. Abanades, B. Arias, S. Brandani. International Journal of Greenhouse Gas Control 40 (2015) 126–166

[52] D. Shekhawat, D. R. Luebke, and H. W. Pennline; National Energy Technology Laboratory and United States Department of Energy. Topical Report Dec 2003.

[53] M. Rydén, A Lyngfelt. *International Journal of Hydrogen Energy*, 2006, 31:1271–1283.

[54] A. Lyngfelt, T. Mattisson. Efficient Carbon Capture for Coal Power Plants. Weinheim:WILEY-VCH Verlag GmbH & Co. KGaA, 2011.

[55] P. Sun, J. R. Grace, C. J. Lim, E. J. Anthony. *Energy and Fuels*, 2007, 21: 163–170.

[56] V. Manovic, E. J. Anthony. *Environmental Science and Technology,* 2007, 41: 1420–1425.

[57] A. MacKenzie, D. L. Granatstein, E. J. Anthony, J. C. Abanades. *Energy and Fuel*, 2007, 21: 920–926.

[58] J.R. Hufton, , S. Mayorga, S. Sircar. *AIChE J*, 1999, 45, 248-254.

[59] D. J. Fauth, E. A. Frommell, J. S. Hoffman, H.W. Pennline.*Fuel Processing Technology*, 2005, 86(14-15): 1503–1521.

[60] K. Essaki, K. Nakagawa, M. Kato, H. Uemoto. *Journal of Chemical Engineering of Japan*, 2004, 37(6): 772–777.

[61] M. Kato, K. Nakagawa, K. Essaki. *International Journal of Applied Ceramic Technology*, 2005, 2(6): 467–475.

[62] R. Zevenhoven, S. Eloneva, S. Teir. *Catal. Today* 2006, *115*, 73.

[63] M. Aresta, A. Dibenedetto, I. Tommasi. *Energy Fuels* 2001, *15*,269.

[64] C. S. Song. *ACS Symp. Ser.* 2002, *809*, 2.

[65] P. Tundo, M. Selva. *Acc. Chem. Res.* 2002, *35*, 706-716.

[66] S. Kaneco, K. Iiba, K. Ohta, T. Mizuno. *Energy Sources* 2000, *22*, 127.

[67] Intergovernmental Panel on Climate Change (IPCC). *Carbon dioxide capture and storage*, Sect. 7.3.4, p. 334. New York, NY: Cambridge University Press, 2005.

[68] J. De Heer. J. Chem. Educ., 1957, 34 (8), p 375.

---

[69] International Fertilizer Industry Association, Production and trade statistics 2011, http://www.fertilizer.org/ifa/HomePage/STATISTICS/Production-and-trade

[70] S. A. French, A. A. Sokol, S. T. Bromley, C. R. A. Catlow and P. Sherwood, Top. Catal., 2003, 24, 161–172.

[71] F. Fischer and H. Tropsch, Brennst.-Chem., 1928, 9, 39.

[72] D. Pakhare and J. Spivey. Chem. Soc. Rev., 2014, 43, 7813

[73] K. M. Kerry Yu and S. C. Tsang, Catal. Lett., 2011, 141, 259–265.

[74] M. Saito and K. Murata, Catal. Surv. Asia, 2004, 8, 285–294.

[75] R. Raudaskoski, E. Turpeinen, R. Lenkkeri, E. Pongracz and R. L. Keiski, Catal. Today, 2009, 144, 318–323.

[76] (a) O.-S. Joo, K.-D. Jun and J. Yonsoo, Stud. Surf. Sci. Catal., 2004, 153, 67–72; (b) M.-J. Choi and D.-H. Cho, Clean: Soil, Air, Water, 2008, 36, 426–432.

[77] G. J. Kraaij and M. Weeda, Report E-08-063, ECN, The Netherlands, 2008.

[78] Carbon dioxide. Ulmann's Encyclopedia of Industrial Chemistry, 2014.

[79] Y. Maenaka, T. Suenobu and S. Fukuzumi, Energy Environ. Sci., 2012, 5, 7360–7367.

[80] J. F. Hull, Y. Himeda, W.-H. Wang, B. Hashiguchi, R. Periana, D. J. Szalda, J. T. Muckerman and E. Fujita, Nat. Chem., 2012, 4, 383–388.

[81] F. Cavani, G. Centi, S. Perathoner and F. Trifirò, Sustainable Industrial Chemistry, Wiley-VCH, Weinheim (Germany), 2009.

[82] Y. Feng, W. Yang and W. Chu. International Journal of Chemical Engineering Volume 2015, Article ID 795386, 7 pages http://dx.doi.org/10.1155/2015/795386

[83] S. Tada, T. Shimizu, H. Kameyama, T. Haneda and R. Kikuchi, Int. J. Hydrogen Energy, 2012, 37, 5527–5531.

[84] T. Abe, M. Tanizawa, K. Watanabe and A. Taguchi, Energy Environ. Sci., 2009, 2, 315–321.

[85] J. Ralston and E. Fareid, Catalytic CO2 Recycle (CCRTM) Technology, Proceedings 7th Power Plant Air Pollutant Control "Mega" Symposium 2008, Baltimore, US, August 2008, vol. 1, pp. 1–12.

[86] H. Kolbe. Ann. Chem. Pharm. 1860, 113, 125-127.

[87] R. Schmitt. J. Prakt. Chem. 1885, 31, 397-411.

[88] M. D. Archer et al. International Energy Agency Executive Conference on Solar Photoconversion Processes for Recycling CO_2 from the atmosphere: an Assesment of Energy. Research and Industrial Implications. Mar 13-16 1990, Colorado Springs, CO, 1990: p. 9.

[89] A. Ion, C. Van Doorslaer, V. Parvulescu, P. Jacobs, D. De Vos, Green Chem. 10 (2008) no. 1, 111.

[90] K. Tominaga. *Catal. Today* 2006, *115*, 70.

[91] K. Tominaga; Y. Sasaki; M. Saito; K. Hagihara; T. Watanabe. *J.Mol. Catal.* 1994, *89*, 51.

[92] K. Tominaga; Y. Sasaki; T. Watanabe; M. Saito. *Stud. Surf. Sci.Catal.* 1998, *114*, 495.

[93] Evonik Oxeno, WO2011157788, 2012 (R. Franke, D. Fridag, B. Hamers, H.-W. Zanthoff, M. Blug, J. Strautmann, S.Nordhoff).

[94] B.R. Eggins, J. McNeill. J. Electroanal. Chem. 1983.148.17.

[95] Y. Hori et al. Chem. Lett. 1986, 897.

[96] G. Silvestri. In *Carbon Dioxide as a Source of Carbon, Biochemicaland Chemical Uses*; Aresta, M., Forti, G., Eds.; D. Reidel: Dordrecht, Holland, 1987; Vol. 206.

[97] M. Tokuda; T. Kabuki; Y. Katoh; H.Suginome. *Tetrahedron Lett.* 1995, *36*, 3345.

[98] A. Sasaki; H. Kudoh; H. Senboku; M. Tokuda. In *Novel Trends in Electroorganic Synthesis*; Torii, S., Ed.; Springer-Verlag: Tokyo,1998.

[99] J.H. Clements. Industrial & Engineering Chemistry Research, 2003. 42(4): p. 663-674.

[100] B. Schaffner, S. Schaffner, S. P. Verevkin and A. Borner. *Chem. Rev.* 2010**, *110,* 4554–4581

[101] M. Lissel, A. Rohani-Derfuli, G. J. Vogt, *Chem. Res.* (S) 1989, 312.

[102] E. B. Hodge. US 4,751,239, Jun.14, 1988.

[103] M. Buzzolini. US 3,931,275, Jan. 6, 1976.

[104] M. Acemoglu; S. Bantle; T. Mindt; F. Nimmerfall. *Macromolecules* 1995**, *28* (9), 3030-3037.

References

[105] Zhu, K. J.; Hendren, R. W.; Jensen, K.; Pitt, C. G. *Macromolecules* 1991, 24 (8), 1736-1740.

[106] Wang, H.; Dong, J. H.; Qiu, K. Y.; Gu, Z. W. *Journal of Polymer Science Part A: Polymer Chemistry* 1998, 36 (8), 1301-1307.

[107] Ishida, N.; Hasegawa, H.; Saaki, U.; Ishikawa, T.; (Nippon Oil Co Ltd., Tokio, JP) US 5,391,311, Feb. 21, 1995.

[108] Ishida, N.; Sakamoto, T.; Hasegawa, H.; (Nippon Oil Co. Ltd, Tokio, JP) US 5,370,809, Dec. 6, 1994.

[109] Pacheco, M. A.; Marshall, C. L. *Energy Fuels* 1997, *11* (1), 2-29.

[110] Ueda, Y.; Takeyama, N.; Ueki, H.; Kusumoto, T., *Chem. Abstr.* 1994, *120*, 334979t.

[111] Azumato, A.; Ishida, T., *Chem. Abstr.* 1971, *74*, 65062u.

[112] Imaki, S.; Kawakami, I., *Chem. Abstr.* 1989, *111*, 174080b.

[113] H-J. Buysch. Carbonic Esters. Ullmann's Encyclopedia of Industrial Chemistry, 2012.

[114] Beilstein, 3 (III), 4, 6.

[115] Azeotropic Data, Advances in Chemistry Series 116, American Chem. Soc.

[116] J. Chem. Eng. Data, Int. Data Series, Sel. Data Mixtures, Ser. A, 1992/1993.

[117] Clayden, Greeves, Warren and Wother, Organic Chemistry, OUP Oxford pag. 237-238.

[118] Z. Du, Y. Xiao, T. Chen and G. Wang. Catalysis Communications 9 (2008) 239–243.

[119] D. Delledonne, F. Rivetti, U. Romano. J. Organomet. Chem. 1995, 448, C15-C19

[120] (a) Ger. Pat. 109,933 (Chemische Fabrik von Heyden) 1900 Friedl, 1901, 5. (b) Ger. Pat. 116,386 (Chemische Fabrik von Heyden) 1900 Friedl, 1904, 6, 1160.

[121] Schnell, H. (Farbenfabriken Bayer AG).Interscience Publishers: New York, 1964; Vol.9, p 91.

[122] J. Nemirowsky. Journal für Praktische Chemie, 1883. **28**(1): p. 439-440.

[123] a) National Distillers, US 3 114 762, 1960. (J. L. Mador, A. U. Blackham). b) Union Oil, US 3 227 740, 1963 (D. M. Fenton). c) SNAM Progetti, US 3 846 468, 1970 (E. Perotti, G. Cipriani). d) Rohm, US 3 952 045, 1973 (W. Ganzel, K. Kabs, G. Schroder). e) SNAM Progetti, US 3 980 690, 1973 (G. Ciprani, E.Perotti).

[124] Chem. Eng. (N.Y.) 90 (1983) no. 9, 15.

[125] Anic, US 4 218 391, 1980 (U. Romano, R. Tesei, G. Cipriani, L. Miucci).

[126] Enichem Synth., EP 685 453 A1, 1995 (F. Rivetti, D. Delledonne).

[127] Enichem Synth., EP 365 083 A1, 1988 (U. Romano, F. Rivetti).

[128] JGC Corp., JP 9 010 591 A2, 1995 (K. Takiguchi, K.Mori).

[129] Quantum Chem. Corp., US 5 171 874, 1989 (D. W.Smith, S. D. Landau).

[130] Enichem Synth., EP 558 128 A2, 1992 (F. Rivetti, D.Delledonne, D. Dreoni).

[131] F. Rivetti, U. Romano, D. Delledonne, Symp. Amer.Chem. Soc., Symp. Ser. 626 (1996) 78.

[132] J. E. Hallgren, G. M. Lucas, R. O. Matthews, J. Organomet. Chem. 204 (1981) no. 1, 135 – 138.

[133] Fukuoka, S.; Ogawa, H.; Watanabe, T. (Asahi Chem. Ind. Co. Ltd.) Jap. Pat. 01 16 551, 1989; *Chem. Abstr.* 1990, *112*, 76618j.

[134] Bayer, US 5 625 091, 1995 (H.-J. Buysch, C. Hesse, J. Rechner).

[135] A. Gelbein, R. Piccolini, Chemtech. (1996) May, 30.

[136] Paquin, A. M. *Z. Naturforsch.* 1946, *1*, 518.

[137] Exxon, WO 9 517 369, 1993 (R. Y. Salch, R. C. Michaelson, E. Suciu, B. Kuhlmann).

[138] Ball, P.; Fullmann, H.; Schwalm, R.; Heitz, W. C. *Mol. Chem*. 1984, *1*, 95.

[139] Mitsubishi, EP 866 051 A1, 1997 (M. Mizukami, Y. Arai, H. Harada, T. Oshida, H. Ohgi).

[140] Ball, P.; Fullmann, H.; Heitz, W. *Angew. Chem., Int. Ed. Engl.* 1980, *19* (9), 718.

[141] Q. Li, W. Zhang, N. Zhao, W. Wei and Y. Sun. Catalysis Today 115 (2006) 111–116.

[142] Idemitsu, JP 9 104 658 A, 1995 (M. Ito).

[143] *Beilstein Handbuch der Organischen Chemie*; Springer-Verlag: Berlin, 1921; Vol. III, pp 3, 5.

[144] (a) Weisz, I.; Havelka, F.; Pellek, S.; Kuncsik-Bojtos, K.; Marosvolgyi, S. (Eszakmagyarorszagi, vegyimuvek) *Hung. Teljes* 1977, *11*, 221.

(b) Heinberger, C. A. (thioApex Inc.) U.S. Pat. 2,648,678, 1953; *Chem. Abstr*. 1954, *48*, 8260a. (c) Kenichi, F.; Shigeo, Y.; Hideo, T.; Hisao, K. *Kogyo Kagaku Zasshi* 1960, *63*, 2146. (d) Ikeda, S.; Soga, K.; Hosoda, S.; Samejima, H.; Takeyama, T. (Mitsubishi Petrochem. Co. Ltd.) Jap. Pat. 135,905, 1978; *Chem. Abstr*. 1979, *90*, 103604m. (e) Shikata, K.; Shigemune, T. (Tokuyama, Soda Co. Ltd.) Jap. Pat. 14,920, 1977; *Chem. Abstr*. 1979, *90*, 203503x. (f) Shikata, K.; Shigemune, T. (Tokuyama, Soda Co. Ltd.) Jap. Pat. 16,426, 1979; *Chem. Abstr*. 1979, *91*, 38918x. (g) Sakai, S.; Fujinami, T.; Sato, S. (Adeka

Argus Chem. Co. Ltd.) Jap. Pat. 38,327, 1980; *Chem. abstr*. 1980, *93*, 149787a.

[145] Lissel, M.; Dehmlow, E. V. *Chem. Ber*. 1981, *114*, 1210.

[146] Rokicki, G.; Pawlicki, J.; Kuran, W. *Polymer J*. 1982, *14* (11), 839.

[147] F. Chu et al. Tetrahedron Letters 40 (1999) 1847-1850.

[148] Y. R. Jorapur and D. Y. Chi. *J. Org. Chem.* 2005, *70*, 10774-10777.

[149] A-A. G. Shaikh, S. Sivaram. Chem. Rev. 1996, 96, 951-976.

[150] H. Wang, L.-X. Wu, Y.-C. Lan, J.-Q. Zhao, J.-X. Lu: Int. J. Electrochem. Sci. 6 (2011) 4218.

[151] S. Zhang, Y. Chen, F. Li, X. Lu,W. Dai, R. Mori. Catal. Today 115 (2006) nos. 1–4, 61.

[152] Aresta, M.; Dibenedetto, A. *J. Mol. Catal. A: Chem.* 2002, *182*, 399.

[153] Aresta, M.; Dibenedetto, A.; Dileo, C.; Tommasi, I.; Amodio, E. *J. Supercrit. Fluids* 2003, *25*, 177.

[154] Darensbourg, D. J.; Holtcamp, M. W. *Coord. Chem. ReV*. 1996, *153*-155.

[155] Lu, X. B.; Zhang, Y. J.; Jin, K.; Luo, L. M.; Wang, H. *J. Catal.* 2004, *227*, 537.

[156] Lu, X. B.; He, R.; Bai, C. X. *J. Mol. Catal. A: Chem.* 2002, *186*, 1.

[157] Paddock, R. L.; Nguyen, S. T. *J. Am. Chem. Soc.* 2001, *123*, 11498.

[158] Darensbourg, D. J.; Fang, C. C.; Rodgers, J. L. *Organometallics* 2004, *23*, 924.

[159] Shen, Y. M.; Duan, W. L.; Shi, M. *J. Org. Chem.* 2003, *68*, 1559.

[160] Lu, X. B.; Liang, B.; Zhang, Y. J.; Tian, Y. Z.; Wang, Y. M.; Bai, C. X.; Wang, H.; Zhang, R. *J. Am. Chem. Soc.* 2004, *126*, 3732.

[161] Jing, H. W.; Edulji, S. K.; Gibbs, J. M.; Stern, C. L.; Zhou, H. Y.; Nguyen, S. T. *Inorg. Chem.* 2004, *43*, 4315.

[162] Kim, Y. J.; Cheong, M. *Bull. Korean Chem. Soc.* 2002, *23*, 1027.

[163] Sun, J. M.; Fujita, S.; Arai, M. *J. Organomet. Chem.* 2005, *690*,3490.

[164] Kawanami, H.; Sasaki, A.; Matsui, K.; Ikushima, Y. *Chem. Commun.* 2003, 896.

[165] Sun, Y. H. Stud. Surf. Sci. Catal. 2004, 153, 9.

[166] Wang, J. Q.; Kong, D. L.; Chen, J. Y.; Cai, F.; He, L. N. *J. Mol.Catal. A: Chem.* 2006, *249*, 143.

[167] Srivastava, R.; Srinivas, D.; Ratnasamy, P. *Appl. Catal., A* 2005, *289*, 128.

[168] Yano, T.; Matsui, H.; Koike, T.; Ishiguro, H.; Fujihara, H.; Yoshihara, M.; Maeshima, T. *Chem. Commun.* 1997, 1129.

[169] Yamaguchi, K.; Ebitani, K.; Yoshida, T.; Yoshida, H.; Kaneda, K. *J. Am. Chem. Soc.* 1999, *121*, 4526.

[170] Ramin, M.; van Vegten, N.; Grunwaldt, J. D.; Baiker, A. *J. Mol. Catal. A: Chem.* 2006, *258*, 165.

[171] Yasuda, H.; He, L. N.; Sakakura, T. *Stud. Surf. Sci. Catal.* 2003, *145*, 259.

[172] Doskocil, E. J. Microporous Mesoporous Mater. 2004, 76, 177.

[173] Yasuda, H.; He, L. N.; Takahashi, T.; Sakakura, T. *Appl. Catal., A* 2006, *298*, 177.

[174] Fujita, S.; Bhanage, B. M.; Ikushima, Y.; Shirai, M.; Torii, K.; Arai, M. *Catal. Lett.* 2002, *79*, 95.

[175] Mori, K.; Mitani, Y.; Hara, T.; Mizugaki, T.; Ebitani, K.; Kaneda, K. *Chem. Commun.* 2005, 3331.

[176] Sankar, M.; Tarte, N. H.; Manikandan, P. *Appl. Catal., A* 2004, *276*, 217.

[177] X. H. Zhang, N. Zhao, W. Wei, Y.H. Sun. Catal. Today 115 (2006) 102.

[178] R.A. Watile, K. M. Deshmukh, K.P. Dhake and B. M. Bhanage. Catal. Sci. Technol., 2012, 2, 1051-1055.

[179] Kihara, N.; Hara, N.; Endo, T. *J. Org. Chem.* 1993, *58*, 6198.

[180] V. Calo, A. Nacci, A. Monopoli, A. Fanizzi, Org. Lett. 4 (2002) 2561.

[181] Sun, J. M.; Fujita, S. I.; Zhao, F. Y.; Arai, M. *Appl. Catal., A* 2005,*287*, 221.

[182] T. Sakakura, J-C. Choi and H. Yasuda. Chem. Rev. 2007, 107, 2365□2387

[183] Lu, X. B.; Liang, B.; Zhang, Y. J.; Tian, Y. Z.; Wang, Y. M.; Bai, C. X.; Wang, H.; Zhang, R. *J. Am. Chem. Soc.* 2004, *126*, 3732.

[184] Inoue, S. *Gendai Kagaku* 2005, *408*, 42.

[185] Coates, G. W.; Moore, D. R. *Angew. Chem., Int. Ed.* 2004, *43*, 6618.

[186] D. J. Darensbourg. Chem. Rev., 2007, 107, 2388.

[187] P. P. Pescarmona and M. Taherimehr. Catal. Sci. Technol., 2012, **2**, 2169-2187

[188] He, L. N.; Yasuda, H.; Sakakura, T. *Green Chem.* 2003, *5*, 92.

[189] Sako, T.; Sahashi, R.; Fujita, Y. *Kobunshi Ronbunshu* 2005, *62*, 275.

[190] Q. Cai, B. Lu, L. Guo and Y. Shan. Catalysis Communications 10 (2009) 605–609

[191] Oshima, Y.; Kohno, K.; Choi, J.-C.; Sakakura, T. *87th Annual Meeting of Japan Chemical Society*, Chiba, Japan, March 27-30, 2006; Japan Chemical Society: Abstract 2PA059.

[192] Sakakura, T.; Choi, J.-C.; Saito, Y.; Sako, T. *Polyhedron* 2000, *19*, 573.

[193] Choi, J.-C.; Sakakura, T.; Sako, T. *J. Am. Chem. Soc.* 1999, *121*, 3793.

[194] Zhao, T. S.; Han, Y. Z.; Sun, Y. H. *Fuel Process. Technol.* 2000, *62*, 187.

[195] Dibenedetto, A.; Pastore, C.; Aresta, M. *Catal. Today* 2006, *115*, 88.

[196] S. Huang, J. Ma, J. Li, N. Zhao, W. Wei, Y. Sun, Catalysis Communications 9 (2008) 276–280.

[197] Abulimiti, I.; Oshima, Y.; Choi, J.-C.; Sakakura, T. *54th Symposium on Coordination Chemistry of Japan*, Kumamoto, Japan, September 23-25, 2004; Japan Society of Coordination Chemistry: Abstract 1PA040.

[198] Ballivet-Tkatchenko, D.; Burgat, R.; Chambrey, S.; Plasseraud, L.; Richard, P. *J. Organomet. Chem.* 2006, *691*, 1498.

[199] Bloodworth, A. J.; Davies, A. G.; Vasishtha, S. C. *J. Chem. Soc. C* 1967, 1309.

[200] Yamazaki, N.; Nakahama, S.; Higashi, F. *Rep. Asahi Glass Found. Ind. Technol.* 1978, *33*, 31.

[201] T. Sakakura, J. Choi, Y. Saito, T. Sako, Polyhedron 19 (2000) 573.

[202] Tomishige, K.; Ikeda, Y.; Sakaihori, T.; Fujimoto, K. *J. Catal.* 2000, *192*, 355.

[203] Jung, K. T.; Bell, A. T. *Top. Catal.* 2002, *20*, 97.

[204] Tomishige, K.; Furusawa, Y.; Ikeda, Y.; Asadullah, M.; Fujimoto, K. *Catal. Lett.* 2001, *76*, 71.

[205] M. Honda, A. Suzuki, B. Noorjaham and K. Tomishige. Chem. Commun., 2009, 4596–4598.

[206] M. Tamura, M. Honda, Y. Nakagawa, and K. Tomishige. *J Chem Technol Biotechnol* 2014; 89: 19–33.

[207] Jiang, C. J.; Guo, Y. H.; Wang, C. G.; Hu, C. W.; Wu, Y.; Wang, E. B. *Appl. Catal., A* 2003, *256*, 203.

[208] Wu, X. L.; Xiao, M.; Meng, Y. Z.; Lu, Y. X. *J. Mol. Catal. A: Chem.* 2005, *238*, 158.

[209] Wu, X. L.; Meng, Y. Z.; Xiao, M.; Lu, Y. X. *J. Mol. Catal. A: Chem.* 2006, *249*, 93.

[210] Kizlink, J.; Pastucha, I. *Collect. Czech. Chem. Commun.* 1995, *60*, 687.

[211] Tian, Y.; Qin, Y.; Chen, L.; Fang, J.; Wang, L. *Prepr. Symp.Am.Chem. Soc., Div. Fuel Chem.* 2002, *47*, 267.

[212] Sakakura, T.; Choi, J.-C.; Saito, Y.; Sako, T. *Polyhedron* 2000, *19*, 573.

[213] Tanaka, Y.; Sawamura, N.; Iwamoto, M. *Tetrahedron Lett.* 1998, *39*, 9457.

[214] Ballivet-Tkatchenko, D.; Douteau, O.; Stutzmann, S. *Organometallics* 2000, *19*, 4563.

[215] Ghosh, R.; Nethaji, M.; Samuelson, A. G. *Chem. Commun.* 2003, 2556.

[216] Moore, D. R.; Cheng, M.; Lobkovsky, E. B.; Coates, G. W. *J. Am.Chem. Soc.* 2003, *125*, 11911.

[217] K. Tomishige, H. Yasuda, Y. yoshida, M. Nurunnabi, B. Li, K. Kunimori, Catalysis Letters 95 (2004) 45–49.

[218] K. Tomishige, H. Yasuda, Y. Yoshida, M. Nurunnabi, B. Li, K. Kunimori, Green Chemistry 6 (2004) 206–214.

[219] I.-H. Lin, C.-S. Tan, Journal of Chemical and Engineering Data 53 (2008) 1886–1891.

[220] E. De Silva, W. Dayoub, G. Mignani, Y. Raoul and M. Lemaire. Catalysis Communications 29 (2012) 58–62.

[221] M. Honda, M. Tamura, Y. Nakagawa and K. Tomishige. ChemSusChem 2013, 6, 1341 – 1344.

[222] M. Tamura, H. Wakasugi, K. Shimizu, A. Satsuma, Chem. Eur. J. 2011, 17, 11428– 11431.

[223] Sridharan, R.; Mathai, I. M. *J. Sci. Ind. Res.* 1974, *33*, 178.

[224] J. F. Knifton, R. G. Duranleau, J. Mol. Catal. 67 (1991) 389.

[225] Mitsubishi, JP 6 048 993 A2, 1992 (M. Dotani, T. Ookawa).

[226] Mobil Oil, US 5 498 743 A, 1994 (S. S. Shi, M. Wu, T. Yan).

[227] Mitsui Toatsu, JP 6 345 696 A2, 1993 (K. Inoue, H. Ookubo).

[228] Nippon Catal. Chem., JP 6 107 601 A2, 1992, JP 6 238 165 A2, 1993 (M. Kirishiki, Y. Onda, H. Tsuncki).

[229] Texaco, US 5 214 182 A, 1991 (J. F. Knifton).

[230] Bayer, DE 4 208 875 A1, 1992 (F.-J. Mais, H.-J. Buysch).

[231] Daicel, JP 3 044 353 A, 1989 (K. Honda et al.).

[232] Mitsui Toatsu, JP 6 336 461 A2, 1993 (K. Inoue, H.Ookubo).

[233] Asahi, JP 63 238 043 A2, 1993 (M. Tojo, S. Fukuoka).

[234] UCC, EP 478 073 A2, 1990 (K. S. Wayne, R. B. Claude).

[235] Daicel, JP 63 140 066 A2, 1988 (S. Oda).

[236] Texaco, EP 255 252 B1, 1986 J. F. Knifton).

[237] Bayer, EP 499 924 A1, 1991 (H.-J. Buysch, A. Klausener).

[238] (a) Duranleau, R.; Nieh, E.; Knifton, J. Process for Production of Ethylene Glycol and Dimethyl Carbonate. U.S. Patent 4,691,041, 1987.

(b) Knifton, J. Prcoess for Cogeneration of Ethylene Glycol and Dimethyl Carbonate. U.S. Patent 5,214,182, 1993.

[239] Chem. Eng. News, 1992, May 4, 25.

[240] Bayer,DE 4 129 316 A1, 1991 (H.-J. Buysch, A. Klausener, R. Langer, F.-J. Mais).

[241] Bayer, EP 569 812 A1, 1992 (P. Wagner, F.-J. Mais, H.- J. Buysch, R. Langer, A. Klausener).

[242] R. S. Hiwale, N. V. Bhate, Y. S. Mahajan and S. M. Mahajani. Intern.Journal of Chemical Reactor Engineering Vol 2, 2004, Review R1.

[243] M. M. Sharma and S. M. Mahajani. Reactive distillation: status and future direction. Book published online 2003.

[244] N. Ishida, T. Ishikawa, US Pat., 5 391 311, 1995; A. Ansmann and D. Hoffmann, WO Pat., 2003005981, 2003.
 S. L. Giolito, J. C. Goswami and E. D. Weil, US Pat., 4 403 056, 1983.

[245] M. Selva, M. Noè, A. Perosa and M. Gottardo. Org. Biomol. Chem., 2012, 10, 6569.

[246] H. Mutlu, J. Ruiz, S. C. Solleder and M. A. R. Meier. Green Chem., 2012, 14, 1728

[247] S. Carloni, D. E. De Vos, P. A. Jacobs, R. Maggi, G. Sartori and R. Sartorio, J. Catal., 2002, 205, 199.

[248] B. Veldurthy and F. Figueras, Chem. Commun., 2004, 734.

[249] B. Veldurthy, J. M. Clacens and F. Figueras, Eur. J. Org. Chem., 2005, 1972.

[250] M. L. Kantam, U. Pal, B. Sreedhar and B. M. Choudary, Adv. Synth. Catal., 2007, 349, 1671.

[251] Y.-X. Zhou, S.-G. Liang, J.-L. Song, T.-B. Wu, S.-Q. Hu, H.-Z. Liu and B.-X. Han, Acta Phys. -Chim. Sin., 2010, 26, 1.

[252] Tundo, P.; Trotta, F.; Moraglio, G.; Ligorati, F. *Ind. Eng. Chem. Res.* 1988, *27*, 1565.

[253] D. J. Brunelle, "Polycarbonates", Kirk-Othmer Encyclopedia of Chemical Technology.

[254] S. Fukuoka, M. Kawamura, K. Komiya and S. Konno et al. *Green Chemistry*, 2003, 5, 497-507.

[255] P. Tundo, F. Trotta, G. Moraglio and F. Ligorati, *Ind. Eng. Chem. Res.*, 1988, 27, 1565-1571.

[256] (*a*) S. Fukuoka, M. Tojo and M. Kawamura, *World Pat.* WO 91/09832 A1, July 11, 1991 (Priority: Dec. 28, 1989);

(*b*) S. Fukuoka, M. Tojo and M. Kawamura, *Jap. Pat.*, 4-224547 A1, Aug. 13,]u; 7-91234 B2, Oct. 4,]u, to Asahi Kasei Corp.

[257] (a) Malkemus, J. U.S. Patent 2,627,524, 1953. (b) Coury, A.; Hobot, C. U.S. Patent 4,883,854, 1989.

[258] Angeles, E.; Santilla´n, A.; Martinez, I.; Ramirez, A.; Moreno, E. *Synth. Commun.* 1994, *24*, 2441.

[259] Doya, M.; Kimizuka, K.; Kanbara, Y. European Patent 638,541, 1995.

[260] Henkelmann, J.; Ru¨ hl, T. U.S. Patent 5,783,706, 1998.

[261] Anderson, A. (Du Pont). U.S. Patent 5,977,262, 1999.

[262] *Alkylene Carbonates in the Preparation of Hydroxyalkylcarbamates* (technical bulletin); Huntsman Petrochemical Corporation: Austin, TX, 2000.

[263] J. H. Park, J. Y. Jeon, J. J. Lee and B. Y. Lee Macromolecules 2013, 46, 3301−3308

[264] Darensbourg, D. J.; Wilson, S. J. Green Chem. 2012, 14, 2665.

[265] Lu, X. B.; Ren, W. M.; Wu, G. P. Acc. Chem. Res. 2012, 45, 1721.

[266] Kember, M. R.; Williams, C. K. J. Am. Chem. Soc. 2012, 134,15676.

[267] S, S.; Min, J. K.; Seong, J. E.; Na, S. J.; Lee, B. Y. Angew. Chem.,Int. Ed. 2008, 47, 7306.

[268] Cyriac, A.; Lee, S. H.; Varghese, J. K.; Park, E. S.; Park, J. H.; Lee,B. Y. Macromolecules 2010, 43, 7398.

[269] H. M. Bolt; Gansewendt, B. *Crit. Rev. Toxicol.* 1993, *23*, 237–253.

[270] L. A. Pokier et al. Cancer res. 1975, 35, 1411.

[271] J. Mc Cann et al. Proc. Nati. Acad. Sci. USA 1975, 72, 5135.

[272] P. Ziosi, T. Tabanelli, G. Fornasari, S. Cocchi, F. Cavani and P. Righi. Catal. Sci. Technol., 2014,4, 4386

[273] Z. Wang, China Chem. Rep., 2005, 12.

[274] Hugo Reinsch (1839) *Repertorium für die Pharmacie*, **68** : 49-58.

[275] J.Varagnat, *Ind.Eng.Chem.Prod.Res.Dev.*, 15 (1976) 212.

[276] P.Maggioni, F.Minisci, *Chim.Ind.*, (Milano) 59, (1977), 239.

[277] S.Umemura, N.Takamitu, T.Hamamoto, N.Kuroda. Ube Industries, US 4 078 006, 1976, JP-Kokai 50 130 727, 1974,

[278] J.A.Horsely, S.R.Vatcha, F.Trifirò, F.Cavani, *Catalytic Division*, 4193, SO, 1994.

[279] Mitsubishi Kasei, Co., Ltd., JP-Kokai, 5855 439, 1981 (T.Maki, K.Murayama).

[280] W-J. Liu, H. Jiang and H-Q. Yu. Green Chem., 2015, 17, 4888-4907.

[281] J. Zakzeski, P. C. A. Bruijnincx, A. L. Jongerius and B. M. Weckhuysen, Chem. Rev., 2010, 110, 3552–3599

[282] R. Beauchet, F. Monteil-Rivera, and J.M. Lavoie. Bioresource technology, 2012. 121: p. 328-334.

[283] J.M. Lavoie, , W. Baré, and M. Bilodeau. Bioresource technology, 2011. 102(7): p. 4917-4920.

[284] *Chem.Mark.Rep.*, 7, 33, Maggio 1990

[285] Miner, C. S. and Dalton, N. N., Editors. Glycerol, American Chemical Society Monograph Series. Reinhold Publishing Company, New York. 1953. p. 1.

[286] A. Behr, J. Eilting, K. Irawadi, J. Lechinski and F. Lindner, Green Chem., 2008, 10, 13–30.

[287] M. Ayoub and A. Z. Abdullah, Renewable Sustainable Energy Rev., 2012, 16, 2671–2686.

[288] J. J. Bozell and G. R. Petersen. *Green Chem.*, 2010, **12**, 539–554

[289] D. Cespi, F. Passarini and F. Cavani. Green Chem., 2015, 17, 343–355

[290] Kirk-Othmer Encyclopedia of Chemical Technology "Ethanol"

[291] Ullmann's encyclopedia of industrial chemistry "Ethanol"

[292] C. E. Wyman, *Trends Biotechnol.*, 2007, 25, 153–157.

[293] J. Rass-Hansen, H. Falsig, B. Jorgensen and C. H. Christensen, *J. Chem. Technol. Biotechnol.*, 2007, 82, 329–333.

[294] A. Morschbacker, *Polym. Rev.*, 2009, 49, 79–84.

[295] C. H. Christensen, B. Jorgensen, and A. Riisager, *Angew. Chem., Int. Ed.*, 2006, 45, 4648–4651.

[296] H.-D. Hahn, G. Dämbkes, N. Rupprich, H. Bahl, Ullmann's Encyclopedia of Industrial Chemistry, Vol. 6, Wiley-VCH Verlag GmbH & Co. KGaA, Weinheim (2012) pp. 417-430.

[297] T. Tsuchida, J. Kuboa, T. Yoshioka, S. Sakuma, T. Takeguchi, W. Ueda, J. Catal., 259 (2008) 183-189

[298] M. León, E. Díaz, A. Vega, S. Ordóñez, A. Auroux, Appl. Catal. B, 102 (2011) 590–599

[299] B. G. Harvey, H. A. Meylemans, J. Chem. Technol. Biotechnol., 86 (2011) 2

[300] N. Qureshi, T. C. Ezeji, Biofuels, Bioprod. Bioref., 2 (2008) 319

[301] M .R. Harper, K. M. V. Geem, S. P. Pyl, S. S. Merchant, G. B. Marin, W. H. Green, Combust. Flame, 158 (2011) 2075

[302] R. Horyń, R. Klimkiewicz, Appl. Catal. A, 370 (2009) 72-77

[303] G. Pavarelli, J. Velasques-Ochoa, A. Caldarelli, F. Puzzo, F. Cavani and J-L. Dubois. ChemSusChem 2015, 8, 2250 – 2259.

[304] D. Zhao, Q. Huo, J. Feng, B .F. Chmelka, G. D. Stucky, J. Am. Chem. Soc. (1998), 120, 6024.

[305] B. Zornoza, S. Irusta, C. Tellez, J. Coronas, Langmuir (2009), 25, 5903.

[306] L. Cao, T. Man, M. Kruk, Chem. Mater. (2009), 21, 1144.

[307] R. Ryoo, C. H. and Ko, J. Phys. Chem. B (2000), 104, 11465.

[308] G. Soler-Illia, C. Sanchez, B. Lebeau, J. Patarin, Chem. Rev. (2002), 102, 4093.

[309] N. Hiyoshi, K. Yogo, T. Yashima, Microporous and Mesoporous Materials (2005), 84, 357-365.

[310] S. Hao, H. Chang, Q. Xiao, Y. Zhong, W. Zhu, J. Phys. Chem. (2011), 115, 12873–12882.

[311] Q. Wei, Z. R. Nie, Y. L. Hao, L. Liu, Z. X. Chen, J. X. Zou, J. Sol-Gel Sci. Technol. (2006), 39, 103-109.

[312] W.G. Klemperer, V. V. Mainz, S. D. Ramamurthi "Better ceramics through chemistry III". Materials Research Society: Pittsburgh, PA, 1998.

[313] Zhang et al. Catalysis Today 115 (2006) 102–106.

[314] A. g. patil, U.R. Kapadi, D. G. Hundiwale, *J. of Scientific and Industrial Research*, 2005, 64, 364-366.

[315] H. Cui, T. Wang, F. Wang, , C. Gu, P. Wang, Y. Dai, *J. of Supercritical Fluids*, 2004, 30, 63-69.

316 J. Gmehling, J. Menke, J. Krafczyk, K. Fischer, J.-C. Fontaine, and H. V. Kehiaian, *Azeotropic data for binary mixture.*

317 L. Wang, X. Han, J. Li, X. Zhan and J. Chen. Separation Science and Technology Volume 46, Issue 9, 2011 pages 1396-1405

[318] G. Iluminati and U. Romano, German Patent 2,528,368 (1976); Chem. Abstr., 84, 164777 (1974).

[319](a) R. S. Hanslick, W. F. Bruce, A. Mascitti Org. Synth., Coll. Vol. 4, 1963, 788; (b) *The Chemistry of Non-Aqueous Solvents*, J. J. Lagowski, Ed.; Academic Press, Inc. (London) Ltd, 1976; (c) H. Mayr; U. von der Brueggen*Chem. Ber.* 1988, *121*, 339-346.

[320]K. R. Fountain, M. Pierschbacher J. Org. Chem., 1976, 41(11), 2039-2042.

[321] (a) L. Troisi, C. Granito, S. Perrone, F. Rosato*Tetrahedron Lett.*2011, 52, 4330–4332; (b) Y.-F. Jing, R.-T. Liu, Y.-H. Lin, X.-G. Zhou, *Sci. China Chem.*2014, 57(8), 1117–1125.

[322](a) H. A. Belfadhel, H.-P. Brack, R. Godoy-Lopez, D. J. Patrick, M. Willemsem, Sabic Innovative Plastics IP B.V., US Pat. 7,977,447, B2 (July 12, 2011); (b) Y. Fu, T. Baba, Y. Ono *Appl. Catal. A: General*1999, *178*, 219-223.

[323] (a) P. J. McCloskey, T. B. Burnell, D. J. Brunelle, E. W. Shanklin, P. M. Smilgelski, Jr, G. Kailasam, General Electric Company, US Pat. 6,420,588 B1 (July 16, 2002); (b) Y. Dai, Y. Wang, J. Yao, Q. Wang, L. Liu, Wei Chu, G. Wang *Catal. Lett.*2008, *123*, 307–316

[324] J. J. Zuckermann. J. *Chem. SOC.* 1963, 1322-1324.

[325] S.M. Gross, W.C. Bunyard, K. Erford, G.W. Roberts, D.J. Kiserow, J.M. Desimone,J. Polym. Sci. A 40 (2002) 171–178.

[326] S. Fukuoka, M. Kawamura, K. Komiya, M. Tojo, H. Hachiya, K. Hasegawa, M.Aminaka, H. Okamoto, I. Fukawa, S. Konno, Green Chem. 5 (2003) 497–507.

[327] B. Veldurthy, J.M. Clacens, F. Figueras, Eur. J. Org. Chem. (2005) 1972–1976.

[328] S. Gryglewicz, F.A. Oko, G. Gryglewicz, Ind. Eng. Chem. Res. 42 (2003)5007–5010.

[329] K. Ishida, T. Aida and T. Yamamoto. US 2011/0117147 A1.

[330]M. Selva, A. Perosa, M.Fabris *Green Chem.*2008, *10*, 1068–1077

[331] S. Pan, L. Zheng et al Chin. J. Catal., 2012, 33: 1772–1777.

[332] Aresta, M., Dibenedetto, A., Nocito, F., et al., 2006. J. Mol. Catal. A Chem. 257, 149-153.

[333] Dibenedetto, A., Angelini, A., Aresta, M., 2011 Tetrahedron 67, 1308-1313.

[334] S. Fujita et al. Journal of Catalysis 297 (2013) 137–141

[335] M. O. Sonnati et al. Green Chem., 2013, 15, 283.

[336] J. R. Ochoa-Gòmez et al. Applied Catalysis A: General 366 (2009) 315–324

[337] A. Dibenedetto et al. Tetrahedron 67 (2011) 1308e1313

[338] J.S.Clarskson, A.J. Walker and M.A. Wood. (2001) Org. Process Res. Dev. 5:630-635

[339] Y. Zhen et al. Macromol Chem Phys (2005) 206:607-612

[340] J.A. Kenar, G. Knothe. J. Am. Oil Chem Soc. (2008) 85, 365-372.

[341] F. Comelli, et al. J. Chem. Eng. Data 41 (1996) 534.

[342] T. Keller, J. Holtbruegge, A. Gòrak. Chemical Engineering Journal 180 (2012) 309– 322

[343] T. Keller et al. Ind. Eng. Chem. Res. 2011, 50, 11073–11086

[344] Z. L. Shen et al. Catalysis Letters Vol. 91, Nos. 1–2, November 2003

[345] H-J. Buysch. "Carbonic esters" Ullmann's Encyclopedia of Iindustrial Chemistry 2012.

[346] J. Tsuji et al. *J. Org. Chem.* 1985,50, 1523-1529

[347] F. Manjholinho et al. *Eur. J. Org. Chem.* 2012, 4680–4683

[348] O. Kreye et Al. Tetrahedron 71 (2015) 293e300

[349] C. Bolchi et Al. *Asymmetry* 14 (2003) 3779–3785

[350] A. Rhouf et Al. Tetrahedron Letters. 54 (2013) 6420-6422.

[351] I. Sànchez et Al. Eur. J. Med. Chem. 35 (2000) 663−676

[352] C. Bolchi et Al. J. Org. Chem. 2014, 79, 6732−6737

[353] S. Wang et Al. Arch. Pharm. Chem. Life Sci. 2014, 347, 32–41

[354] M. Ilìc et Al. European Journal of Medicinal Chemistry 62 (2013) 329e340

[355] C. L. Bolivar-Diaz et Al. Applied Catalysis B: Environmental 129 (2013) 575– 579

[356] R. Bai et Al. Green Chem., 2013, 15, 2929

[357] T. P.Vishnyakova; I. A. Golubeva; E. V. Glebova. Russ. Chem. Rev. (Engl. Transl.) 1985, 54, 249-261.

[358] P.Y.S. Lam et al; Science 1994, 263, 380-384.

[359] G. Semple et al. J. Med. Chem. 1997, 40, 331-341.

[360] T. W. vonGeldern; J. Med. Chem. 1996, 39, 968-981.

[361] B. S. Furniss, A. J. Hannaford, P. W. G. Smith, A. R. Tatchell. Vogel's Textbook of Practical Organic Chemistry, 5th Edn.; Wiley: New York, 1989.

[362] L. A. Paquette. *Encyclopedia of Reagents for Organic Synthesis*; Wiley: New York, 1995, Vol. 3, 5105.

[363] G. Lamoureux and C. Aguero. Special Issue Reviews and Accounts, Arkivoc 2009 (i) p. 251-264 (ISSN 1551-7012).

[364] N. Ballarini, F. Cavani, L. Maselli, S. Passeri, S. Rovinetti. Journal of Catalysis 256 (2008) 215–225.

[365] F. Cavani et al. Journal of Catalysis 269 (2010) 340–350.

[366] (a) Shieh, W.-C.; Dell, S.; Repic, O. *Org. Lett.* 2001, *3*, 4279. (b) Ouk, S.; Thiébaud, S.;Borredon, E.; Le Gars, P. *Green Chem*. 2002, *4*, 431. (c) Shen, Z. L.; Jiang, X. Z.; Mo, W. M.; Hu, B. X.; Sun, N. *Green Chem.* 2005, *7*, 97. (d) Rajabi, F.; Saidi, M. R. *Synth.Commun*. 2004, *34*, 4179.

[367] Shieh, W.-C.; Dell, S.; Repic, O. *J. Org. Chem.* 2002, *67*, 2188.

[368] M. Selva, P. Tundo. J. Org. Chem. 2006, 71, 1464.

[369] P. Tundo, M. Selva and A. Bomben. Org. Synth. 1998,76, 169-177.

[370] M. Selva, P. Tundo and A. Perosa. J. Org. Chem. 2003, 68, 7374-7378

[371] P. Tundo, F. Trotta, G. Moraglio and F. Ligorati. *Industrial & Engineering Chemistry Research,* vol. 27, pp. 1565-1571, 1988.

[372] R. Luque, J. M. Campelo and A. A. Romero. New J. Chem., 2006, 30, 1228-1234.

[373] Y. Li, B. Xue, X. He. Catalysis Communications 10 (2009) 702–707.

[374] B. Xue et al. *Journal of molecular catalysis A: chemical*, vol. 357, pag. 50-58, 2012.

[375] S. Udayakumara, A. Pandurangan, P.K. Sinha. Applied catalysis A: general, Vol. 272, pp. 267–279, 2004.

[376] A. Perosa, M. Selva, P. Tundo, F. Zordan. Synlett 2000, No. 1, 272–274

[377] Horsley LH (1952, 1962) Azeotropic Data I and II. American Chemical Society, Washington D.C.

[378] Naumann HJ, Schaefer H, Oberender H, Timm D, Meye H, Pohl G (1977) Chem. Techn, Heft 1, p 38.

[379] .S. 4,092,360 Pat (March 30, 1978).

[380] H.Fiege, Heinz-Werner Voges, T.Hamamoto, et al., Phenol Derivatives, Ullmann's Encyclopedia of Industrial Chemistry, Wiley-VCH, 2012.

[381] H. Fiege, Cresols and Xylenols, Ullmann's Encyclopedia of Industrial Chemistry, 7th Ed., Wiley-VCH

[382] G. Moon, W. Bohringer, C.T. O'Connor, Catal. Today, 97 (2004) 291

[383] A. Vinu et al. J. Mol. Catal. A: Chem. 230 (2005), 151-157.

[384] K. Tanabe, T. Nishizaki, Proceed. 6th ICC, G.C. Bond et al. (Eds), The Chemical Society, London (1977), p. 863.

[385] K. Tanabe, Studies in Surface Science and Catalysis , 20 (1985) 1.

[386] Z. Strassberger, S. Tanase and G. Rothenberg. *Eur. J. Org. Chem.* **2011***, 5246-5249.*

APPENDIX:

DIMETHYL CARBONATE AS A GREEN SOLVENT FOR PHOTOOXIDATION PROCESSES

Summary

1 INTRODUCTION

1.1 Photochemistry: general introduction

"Photochemistry has only been developed to a very slight extent; perhaps because chemists have been attracted by problems which seemed more urgent, photochemistry is still in its infancy.[...] On the arid lands there will spring up industrial colonies without smoke and without smokestacks; forests of glass tubes will extend over the plains and glass buildings will rise everywhere; inside of these will take place the photochemical processes that hitherto have been the guarded secret of the plants, but that will have been mastered by human industry which will know how to make them bear even more abundant fruit than nature, for nature is not in a hurry and mankind is. [...] If our black and nervous civilization, based on coal, shall be followed by a quieter civilization based on the utilization of solar energy that will not be harmful to progress and to human happiness. The photochemistry of the future should not however be postponed to such distant times; I believe that industry will do well in using from this very day all the energies that nature puts at its disposal. So far, human civilization has made use almost exclusively of fossil solar energy. Would it not be advantageous to make better use of radiant energy?"

Giacomo Ciamician, "The photochemistry of the future" 1912.[1]

Giacomo Ciamician, in his inspiring paper, 1912, outlined his vision for the future role of photochemistry in the progress of industry and human civilization. During the last century, , photochemistry has made significant improvement that will be underlined in the following pages, even if the applications of photochemical transformations on an industrial scale remain relatively scarce.[2,3,4] The term "photochemistry" includes all the chemical transformations which occur due to the absorption of light. The photosynthesis process utilized by plants is an excellent example of a photochemical transformation, where carbon dioxide and water are transformed to sugars and oxygen with the following general reaction:

$$6\ CO_2\ +\ 6\ H_2O\ \xrightarrow{\text{Light}}\ C_6H_{12}O_6\ +\ 6\ O_2$$
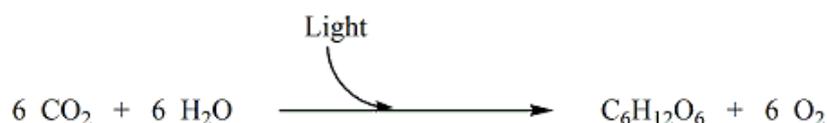
Scheme 1.1: General reaction involves in photosynthesis.

This process was firstly discovered by Priestly in the eighteenth century.[5] Since then, a variety of organic photochemical reactions have been developed, such as rearrangements, [6,7] cycloadditions[8,9] , cyclizations,[10,11] reductions, [12,13] and oxidations.[14,15]

In particular, this chapter will focus on photooxidation, which is one of the main focuses of the group of Professor Sir Martyn Poliakoff, University of Nottingham. A three month project was undertaken in this group at Nottingham to investigate the viability of DMC as a photooxidation solvent. The work was carried out from September to December 2015 and the results of the project form the bulk of this chapter.

1.2 The photooxidation process

Adding oxygen to a molecule is a frequent task in organic synthesis, nevertheless some of the traditional reagents commonly used in laboratories often come with big problems with regards to their safety, with many being toxic, flammable and explosive (e.g osmium tetroxide, chromate/dichromate compounds, oxone and peracids to name a few).[16] Cost is also often a large factor in the decision to use these compounds. Considering all these aspects, molecular oxygen is the ideal, ubiquitous reagents for these types of reactions. However, the ground state of molecular oxygen, a triplet state $^3O_2$ or $^3\Sigma_g$, is often poorly reactive towards organic substrates.

In order to overcome this problem, the photo-oxidation process requires a suitable light source and a particular photo-catalyst (or photosensitizer) able to excite the molecular oxygen from the (inert) triplet ground state to the excited and reactive singlet oxygen state: $^1O_2$ or $^1\Delta_g$.

Singlet oxygen ($^1O_2$) show a characteristic electrophilic reactivity, often in mild reaction conditions, and is the reason why photo-oxidations are considered a complementary alternative to standard oxidation methods. Nowadays, few of these reactions are industrially applied, for example for the productions of perfumes and fragrances by the oxidation of terpenes. [17,18,19] An example is the synthesis of Rose Oxide from citronellol developed by Symrise in Germany (>100 t/year). Great interest of the industry was focused in the photosynthesis of valuable compounds and efficiently scaled up.[20] We will discuss in detail about singlet oxygen, photosensitizers and photo-oxidation reactions in the following chapters.

1.2.1 Singlet oxygen: properties

As written before, the ground state of molecular oxygen is the triplet state $^3O_2$ but two possible excited states of this molecule are also available as depicted in the following molecular orbital diagram (Fig. 1.1).
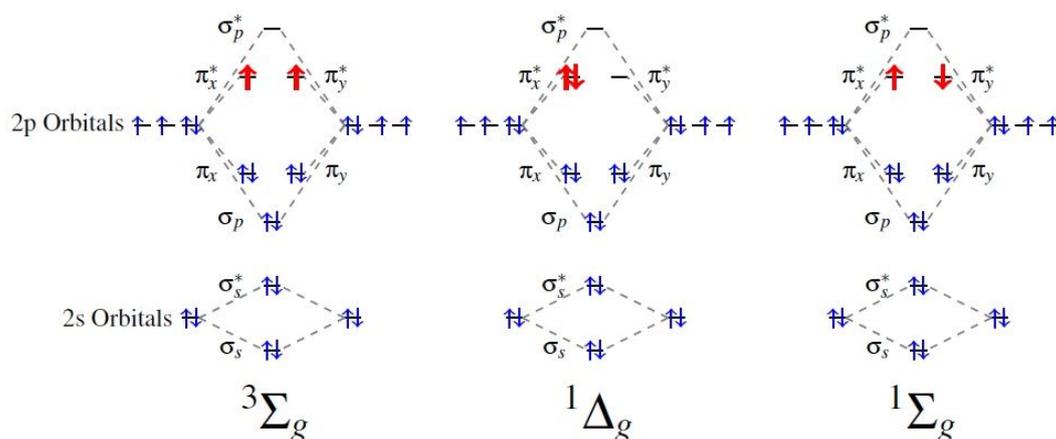

Fig. 1.1 Molecular orbital of the dioxygen molecule (O_2) at ground and at the two lowest exited states[71]

It is worth noting that oxygen has an open-shell triplet ground state $^3\Sigma g$, where two electrons occupy two antibonding π* orbitals with parallel spins. Of the two different excited levels the $^1\Sigma g$ state is very short-lived and rapidly relaxes to the lowest excited state of singlet oxygen, or $^1\Delta g$, through a spin-allowed transition.[21] Singlet oxygen, with an energy level of 22.4 Kcal/mol above the ground state is the active species involved in most of the photochemical oxidations .[22,23]

One of the most important parameters for these kinds of reactions is the singlet oxygen lifetime. As a matter of fact, transitions between $^3O_2$ ground state and $^1O_2$ are strictly spin, symmetry and parity forbidden, this lead to the relatively long lifetime of the excited state (t = 59 ms in CCl_4 at room temperature).[24] This aspect will be discussed in detail in the following section. On the other hand, for the same reason, the direct excitation of $^3O_2$ to $^1O_2$ via absorption of light is an ineffective process.[25] This entails the needs to use a photosensitizer that is able to facilitate the energy transfer from the light source and promote the excitation of the oxygen.

1.2.2 Photosensitisers

Singlet oxygen can be generated at least in three different pathways:

i. Photosensitisation via a photochemical reaction involving the excitation with a light source;

ii. Chemical reactions, often decomposition of peroxides (e.g. the reaction of sodium hypochlorite, NaOCl, and hydrogen peroxide H_2O_2);[26]

iii. Microwave discharging of gaseous O_2.[27]

However, the photosensitisation mechanism remains the most investigated. Since the direct absorption of light and the corresponding excitation of oxygen is an inefficient process, it is necessary to use photosensitizers able to absorb light and enhance the energy transfer to the oxygen molecules. This process can occur with two different mechanisms.

In the first one (namely the "Type I" photosensitized oxidation), the photosensitizer is able to absorb light and excited itself from the ground state S_0 to the first singlet excited state S_1; then through an intersystem-crossing (ISC), S_1 relaxes to the triplet state T_1. After that, this particular state can undergo different reactions with organic substrate or directly to the oxygen molecules. In both cases, these reactions form radicals (e.g O_2^{-}) that undergo further reactions.

In the case of the "Type II" the photosensitizer, excited in the same manner as the previous mechanism to the triplet state T_1, while relaxing again to the ground state S_0, is able to transfer enough energy to one triplet oxygen ($^3O_2$) molecule to promote the excitation to the singlet form ($^1O_2$).[28,29] This particular pathway, represented in Fig. 1.2, is particularly interesting as the photosensitizer is not consumed and can be used in catalytic amount. The improvement of the photosensitizer and their immobilization over heterogeneous systems will provide a green and sustainable route to $^1O_2$.[30]
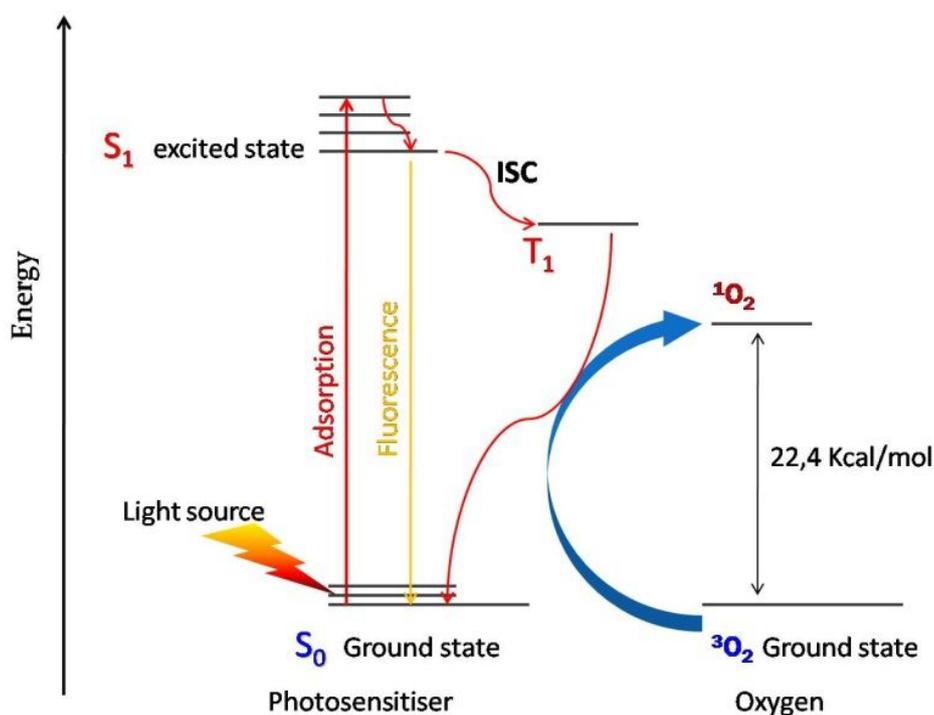
Fig. 1.2: Jablonski diagram for the Type II photo-oxidation pathway

It is important to underline that, for the desired Type II photo-oxidation mechanism, the T_1 exited state of the photosensitizer should be higher in energy or at least at the same energy level of the excited singlet oxygen, or it will be unable to transfer enough energy.
In this way the efficiency of a photochemical process is strictly dependent on the efficiency of the photosensitizer and can be described by its quantum yield:[31]

$$\Phi = \frac{amount\ of\ product\ formed}{number\ of\ photons\ adsorbed}$$

In an ideal situation, all absorbed photons result in a chemical transformation and thus $\Phi = 1$. However, a quantum yield of more than 0.3 is considered to be a fairly efficient process.[32]

There are a number of photosensitizers already commercially available and in this thesis we will consider some of the most common. In particular, two porphyrin-based photosensitizers, meso-tetraphenylporphyrin (TPP) (1) and 5,10,15,20-tetrakis(pentafluorohenyl) porphyrin (TPFPP) (2); and the more inexpensive Rose Bengal (3,4), Eosin Y (6) and Methylene Blue (5). The molecular structure of the photosensitizers considered is shown below (Fig. 1.3).
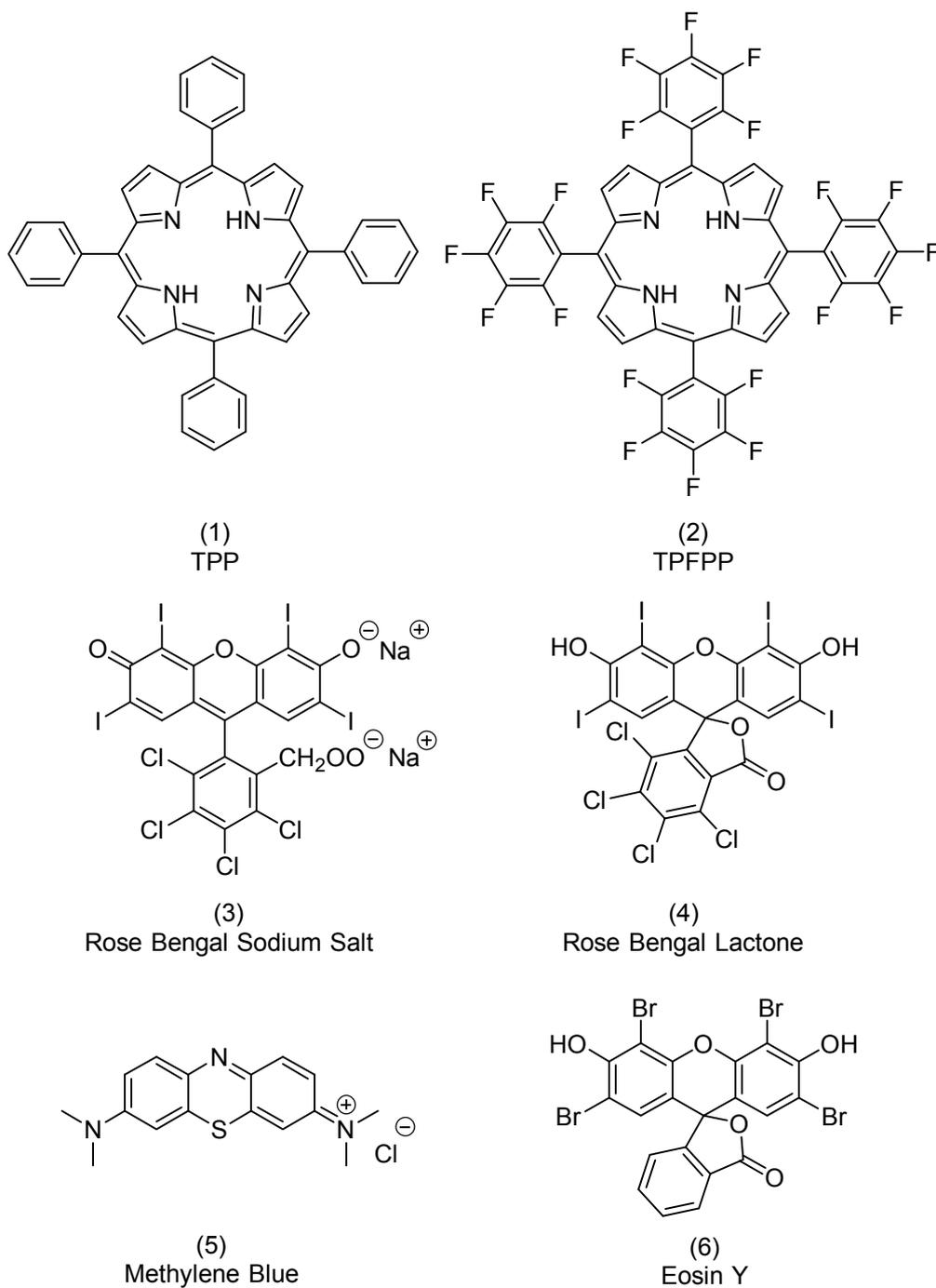
(1)
TPP

(2)
TPFPP

(3)
Rose Bengal Sodium Salt

(4)
Rose Bengal Lactone

(5)
Methylene Blue

(6)
Eosin Y

Fig. 1.3 Chemical structures of a range of common photosensitizers

## 1.2.3 Singlet oxygen lifetime: effect of solvent

It is important to notice that photochemical processes produce very active species. Their lifetime should be considered. Once singlet oxygen is generated, after energy transfer from the excited photosensitizer (Type II, see section 1.2.2), it decays back to the ground state following two different processes i.e. non-radiative and radiative processes. The non-radiative mode is almost 10^4 times faster than the radiative process and represents the primary mode of $^1O_2$ relaxation in solution. The radiative decay results in a characteristic phosphorescence emission at 1270 nm detected solution by time-resolved laser spectroscopy. The rate of the decay of this phosphorescence gives the lifetime in the medium studied. Interaction with molecules (solvent, substrate) can greatly shorten the $^1O_2$ lifetime. The ability of a molecule to quench $^1O_2$ in solution has been well studied by Hurst and Schuster suggesting an exchange energy transfer. In this way, the lifetime of singlet oxygen is closely dependent of the nature of solvent and the interactions with O-H and aromatic C-H bonds. Solvents with larger vibrational frequencies are easier to excite, and are more efficient quenchers of $^1O_2$.[33] Thus, large variations were observed in various solvent and polarity (Table 1.1). Halogenated solvents stabilize the singlet oxygen because of the low overlapping of the vibration modes and deuterated solvents increase lifetime of singlet oxygen due to a poor energy acceptor character of C-D and O-D bonds compared with C-Hand O-H.[34]

Solvent	$^1O_2$ Lifetime (µs)
Carbon tetrachloride	59000
Hexafluorobenzene	21000
Chloroform	229
Dichloromethane	99
Acetonitrile	77
Acetone	51
Ethyl acetate	45
Butanone	43
n-hexane	33
Benzene	30
Toluene	29
2-propanol	22
Pyridine	20
Ethanol	14.5
Methanol	10
Water	3

Table 1.1: Singlet oxygen lifetime in various solvents[35]

1.2.4 Singlet oxygen photochemistry

As described previously, singlet oxygen is a highly active form of oxygen due to its vacant molecular orbital (see Fig.1). Indeed, three main modes of reactivity of $^1O_2$ are known as shown in the following Scheme 1.2.[36]
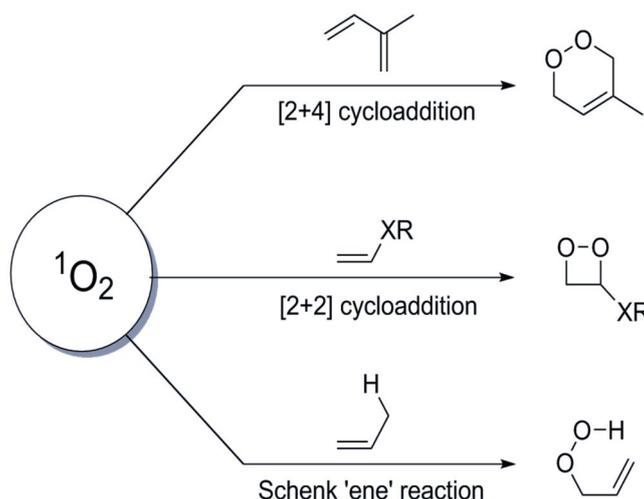

Scheme 1.2: Singlet oxygen modes of reaction with olefins.[36]

Most the oxygen singlet reactions with olefins could be divided into 3 groups depending on the reactivity/activation properties of the olefin.

A beautiful review of the peculiar reactivity of various olefins with $^1O_2$ was carried out by Prein and Adam.[36]

Conjugated olefins usually undergo a [2+4] cycloaddition forming an endoperoxide following a stepwise pathway.[37,38,39]
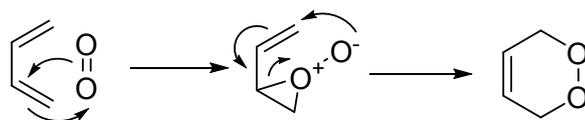

Scheme 1.3 [2+4] cycloaddition mechanism of singlet oxygen with conjugated olefins.

In particular, the [2+4] cycloaddition reaction is similar to Diels-Alder reaction, in which conjugated dienes react with a dienophile, represented by the $^1O_2$ moiety.[40] Furthermore, the [2+4] cycloaddition reactions of $^1O_2$ have also been observed in heterocyclic systems, such as furans and pyrroles. [41,42]

On the other hand, electron rich olefins react with $^1O_2$ giving preferably 1,2-dioxetanes via a [2+2] cycloaddition reactions.

The last group is the well-known Schenk Ene reaction with inactivated olefins bearing allylic hydrogen form allylic hydroperoxide. It has been described as an "indirect substitutive addition in the allylic position". It is a valuable, often regioselective, synthetic pathway to allylic hydroperoxides which have proven to be useful chemical intermediates in the production of allylic alcohols (via reduction), epoxy alcohols and functionalized enones.[43,44,45]

Within the [2+4] cycloaddition category, we can find the first photo-oxidation reaction, which was discovered in 1928 by Windaus and Brunken, in which ergosterol is oxidized with $^1O_2$ in the presence of a dye.[46] A similar example is the photo-cycloaddition of α-terpinene with $^1O_2$ to producing ascaridole which is a valuable compound that naturally occurs in some South American plants (e.g. peumus boldus). It is mainly used as an anthelmintic drug to expel paretic worms from body and plants (Scheme 1.4).[47]
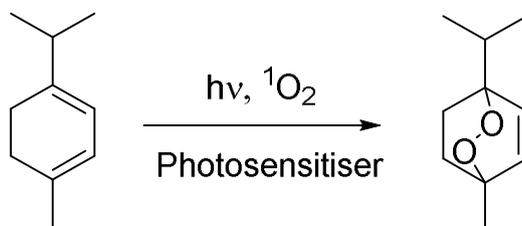
Scheme 1.4 α-terpinene oxidation to ascaridole.

It was successfully synthesized in 1944 by Schenck and Ziegler using chlorophyll as photosensitiser in the presence of oxygen and light.[48]
Schenck also reported, in 1943 another important photo-oxidation reaction, namely the hydroperoxidation of alkenes with singlet oxygen.[49]

In compounds without conjugated diene groups, the Schenck reaction is always in competition with the [2+2] cycloaddiction reaction, although the [2+2] often occurs in the absence of an allylic proton.
This reaction leads to the formation of dioxoetanes and is normally favored increasing the solvent polarity or lower the reaction temperature.[50]
The mechanism of the Schenk-ene reaction is not completely clear yet, given the difficulties of studying electronically excited molecules by theoretical methods; the most supported ones are the stepwise mechanism.
The latter proceeds via a three-step pathway, as shown in the following scheme (Scheme 1.5), as described by Gorman.[51]
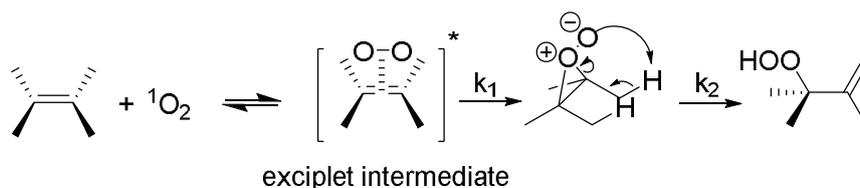
Scheme 1.5 Stepwise mechanism of the Schenck-ene reaction of singlet oxygen and olefins.

Wide investigations have been accomplished in order to understand the conformational, steric hindrance and electronic effects of the substituent of the starting material, joined to the reaction solvent effects on the products distribution and reaction rates.[52,53,54]

As mentioned earlier (Chapter 1.2), one of the famous industrial application of photochemistry was the synthesis of Rose Oxide, a fragrance found in roses and rose oil. The synthetic pathway includes the Schenck-ene reaction with the formation of the allylic hydroperoxides, which are then quenched with sodium sulfite and finally a dehydration reaction yields the desired product as shown in Scheme 1.6.
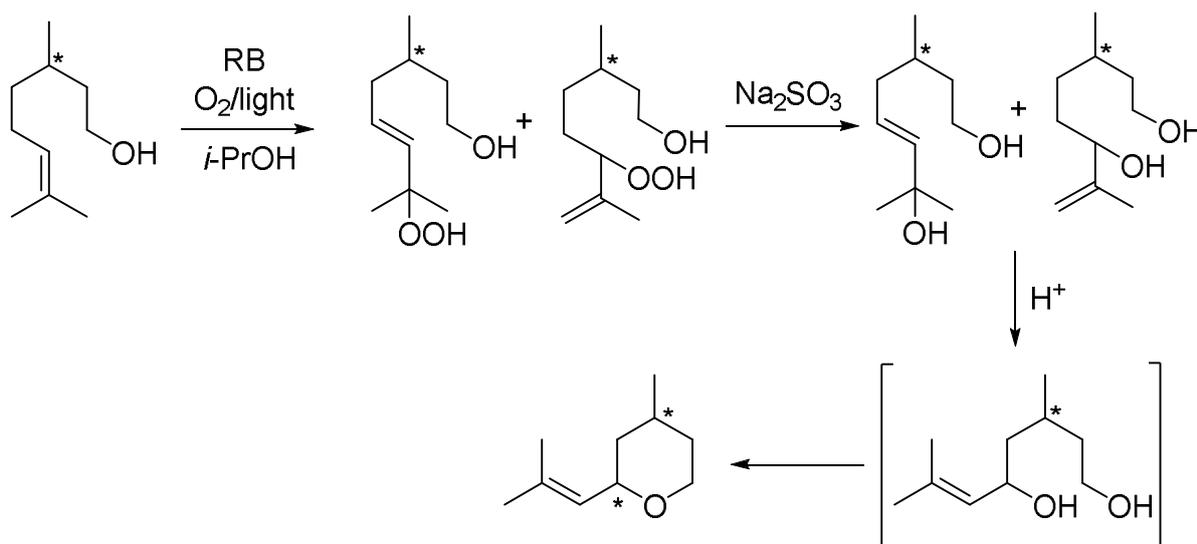
Scheme 1.6 Industrial scale production of Rose Oxide.

1.2.5 *Scale-up: batch and continuous flow reactors comparison*

Although there are successful examples of applied photochemistry on industrial scales shown in the previous chapter, the scale-up of these kind of reactions is often challenging. This is partly related to the use of traditional batch reactors, unsuitable for the scale-up of these photochemical reactions. In fact, the larger is the volume of the batch reactor, the less light would be able to penetrate uniformly through the reaction mixture, a problem that is usually restricted by decreasing the concentration of the reaction mixture.[55]

This behavior is described also in the Bouguer-Lambert-Beer law, which correlates the absorbance of the solution with the pathlength of the radiation (l) and the concentration of the analyte (c) with the extinction coefficient (ε) of the absorbing species in the following equation:

$$A = \varepsilon\, c\, l$$

On the other hand, working in flow and designing new thin tubular reactors in order to maximize the light penetration, would lead to many benefits to overcome these limitations:

1) Decreasing of the reactor volume, without losing productivity;
2) Conditions considered unsafe for batch reactors, may be explored in flow as a results of the relatively small reactor volume used;[56]
3) Versatile and more accurate control on the reaction conditions, for example the residence time in order to avoid stockpiling of intermediates and products inside the reactor, limiting the degradation and maximize the productivity;[55,56]
4) Enhance heat and mass transfer;[55,57]
5) Avoid of the cyclical repetition of load/unload and heating/cooling operation characterizing of the batch processes, operate at optimal condition for long period of time;
6) Multi-step reaction can be safely conducted in flow, since the reagents can be added downstream;[58]
7) Easier online analysis that lead to an easier automation of these processes.[58]

Finally, photochemical processes typically require mild condition thanks to the characteristic reactivity of active species generated by the adsorption of photons (e.g. singlet oxygen) or the nature of the products and intermediates formed (e.g. hydroperoxide) and generally results in a higher atom economy.[59]

All these features make continous flow an attractive option for the application of photochemistry processes on larger scale.

1.3 Alternative solvents

The solvents commonly used in traditional chemical processes are volatile organic compounds (VOCs) which are often highly flammable and can cause adverse health effects (e.g. eye irritation, headaches and allergic skin reactions). Moreover, some VOCs are also known or suspected carcinogens.

Furthermore, VOCs are able to form low-level ozone and smog through free radical air oxidation processes.

For all these reasons it is not surprising that over the past 10 years, the research has been focussed in the development of greener and safer alternative solvents.[60]

In this way, many alternative solvent has been proposed in particular:

- supercritical fluids (e.g. sc-CO_2 and sc-H_2O);
- water;
- ionic liquids;
- fluorous solvents,
- bio-alcohols;
- organic carbonates.

Each of them are characterized by very different physical chemical properties, such as volatility and polarity characteristic, for these reason they shows advantages and disadvantages and the choice among them is strictly depended on the applications.[61]

In 2007, Clark et al. created a scoring system to grade the most high-profile types of alternative solvents, considering five main criteria:

1. key solvent properties;
2. ease of separation and reuse;
3. health and safety;
4. cost of use;
5. cradle-to-grave environmental impact.

From this grading system, both supercritical carbon dioxide (scCO_2) and water (H_2O) are high scored alternative solvents.

However, especially for sc-CO_2 the relatively poor solvent power for many chemicals is counterbalanced by the utilisation of eco-friendly co-solvents and its more desirable handing, ease of separation and low environmental impact.

1.4 Dimethyl carbonate: a greener solvent for chemical reactions

DMC (Fig. 1.4) is considered as an eco-friendly reactive chemical intermediate and, thanks to its high boiling point and high solvency it's considered a good aprotic polar solvent. In fact, with a boiling point of 90 °C at atmospheric pressure, it's able to limit the emission of volatile organic compound (VOCs) in the atmosphere, compared to other oxygenated solvent such as esters or ketones.
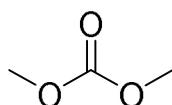

Fig. 1.4 Dimethyl carbonate (DMC)

It was introduced in the early eighties in the market of the chemical intermediates by Enichem (Italy) that has started to produce DMC on industrial scale using a clean and innovative process (phosgene-free). This synthesis, described also in the chapter 1.3.3.2 of the main part of the thesis, consisted on the oxidative carbonylation of methanol in the presence of a copper compound catalyst (Scheme 1.7). [62,63]

1° Step:

2° Step:
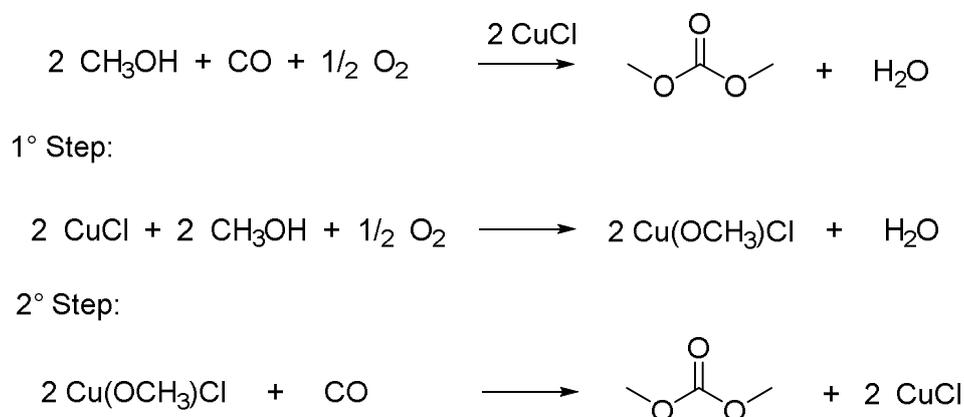
Scheme 1.7 Enichem synthesis of DMC by oxidative carbonylation of methanol**.**

DMC is a not toxic, mutagenic nor irritating compound that shows a good biodegradability in the environment.[64] For these reasons, in the pharmaceutical industry, it is increasingly used as an extraction solvent replacing toluene. Moreover, DMC is a relatively highly oxidized compound so it is a solvent of choice for oxidation processes. Despite this, there are only few examples of oxidation in DMC in the literature, for examples for the palladium-catalyzed cyclocarbonylation reactions or the ruthenium tetraoxide oxidations.[65,66] R. Bernini et al. in 2007 reported the utilization of DMC as an environmentally friendly reaction medium for methyltrioxorhenium-catalyzed oxidations

of a wide range of substrates (mainly phenols and aromatics). Furthermore, they reported that the use of DMC shortens the reaction times and lowers the required amount of catalyst on the respect of other traditional solvent, behavior closer to ionic liquids.[67]Finally, DMC was previously used in a photochemical oxidation as a co-solvent with scCO$_2$ by Poliakoff et al. to solubilize the photosensitizer (TPFPP) which was insoluble into the starting material (citronellol). This work demonstrate the non-reactivity of DMC with singlet oxygen.[87]

The same group studied the effect of DMC as methylating agent of some alcohols in scCO$_2$ leading to higher selectivity toward methyl ethers.[68]

2 AIM OF THE WORK

The aims of this piece of the work are regarded to the study dimethyl carbonate (DMC) as an alternative solvent (or co-solvent) for synthetic photochemistry using singlet oxygen ($^1O_2$).

In particular the following aspects have been investigated:

➢ Singlet oxygen lifetime determination in DMC by mean of laser excitation and analysis of the characteristic phosphorescence emission of 1O2 at 1270 nm;

➢ We have studied two different reactions:

   1. the first is the model photo-oxidation reaction of α-terpinene to ascaridole, the cyclic endoperoxide (Scheme 3);
   2. the second one is the citral photo-oxidation to allylic hydroperoxides.

➢ In particular, the reactivity in DMC was compared with other common solvents, primarily with ethanol, another "green" solvent for these reactions;
➢ Especially for the citral oxidation in batch a complete comparison with the reactivity obtained with different photosensitizer and the possible explanation of these trends have been reported;
➢ Finally, comparisons between the reactions performed in batch and the same performed in an implemented and optimized flow reactor, at high pressure using liquid/supercritical CO_2 and DMC as co-solvent in order to solubilized the reagent mixture and the photosensitizer is reported.

3 EXPERIMENTAL

3.1 Light sources

Photochemical batch experiments were irradiated using a vertically positioned 5 x Citizen Electronics Co. Ltd 1000 lumen white light LED arrays (CL-L233-C13N1-C). This LED array is mounted on a commercially available aluminium heat sink which has two fan attached for cooling, as shown in Fig. 3.1.

Fig. 3.1 Photographs of the LEDs array for batch reactions.

These kind of wide wavelength white light emitting LEDs were chosen in order to allow us to study different photosensitizer for ours particular reactions.

In the same way, for the high pressure continuous flow reactor, three similar array of 5 x Citizen Electronics Co. Ltd 1000 lumen white light LEDs, vertically positioned but mounted onto the end of a stainless steel block that contains an internal channel to allow for circulation of a coolant (typically water:ethylene glycol=1:1 in volume), were used (Fig. 3.2).

Fig. 3.2 Photographs of the LEDs array for continuous flow reactions, optimized with an efficient temperature control via internal circulation of a coolant.

The LEDs light emitted intensity is controlled simultaneously by a single control box to ensure that the light provided to the reactor is uniform (Fig. 3.3).

Fig. 3.3 Photograph of the LEDs controller.

3.2 Reactor systems

3.2.1 Batch apparatus

The reactions in batch were carried out using a two-necked 25 mL round bottom flask equipped with a magnetic stirrer and a reflux condenser on the top neck. Needle plastic caps were putted over the other neck in order to allow the insertion and bubbling of the oxygen stream into the mixture, the second cap were placed at the top of the condenser for the releasing of the gas (Fig. 8).
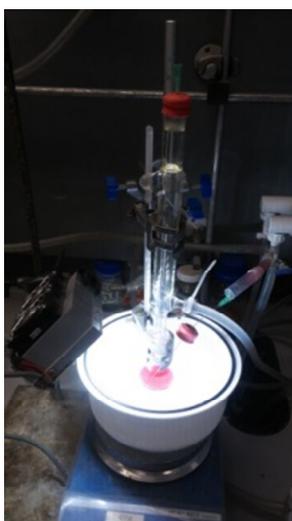

**Fig. 3.4** Photograph of the batch reaction system.

The reactions were performed at atmospheric pressure and the temperature was fixed at 5 °C inserting the flask in an ice bath and irradiating with the LEDs.

3.2.2 High pressure flow reactor system (rig)

All the photo-oxidation reactions in flow were conducted in the high pressure rig shown in the following Scheme 3.1.
Each piece of the equipment of the rig is connected by 316 stainless steel tubing with an outer diameter of 1/16″ using Swagelok® fittings where it is necessary. Manual valves are preferably provided by the High Pressure Equipment Company (HiP 15-11AF1) or Scientific Systems, Inc (SSI, flat valves).
Every part of the rig united with the standard operating procedure will be discussed in the following pages.
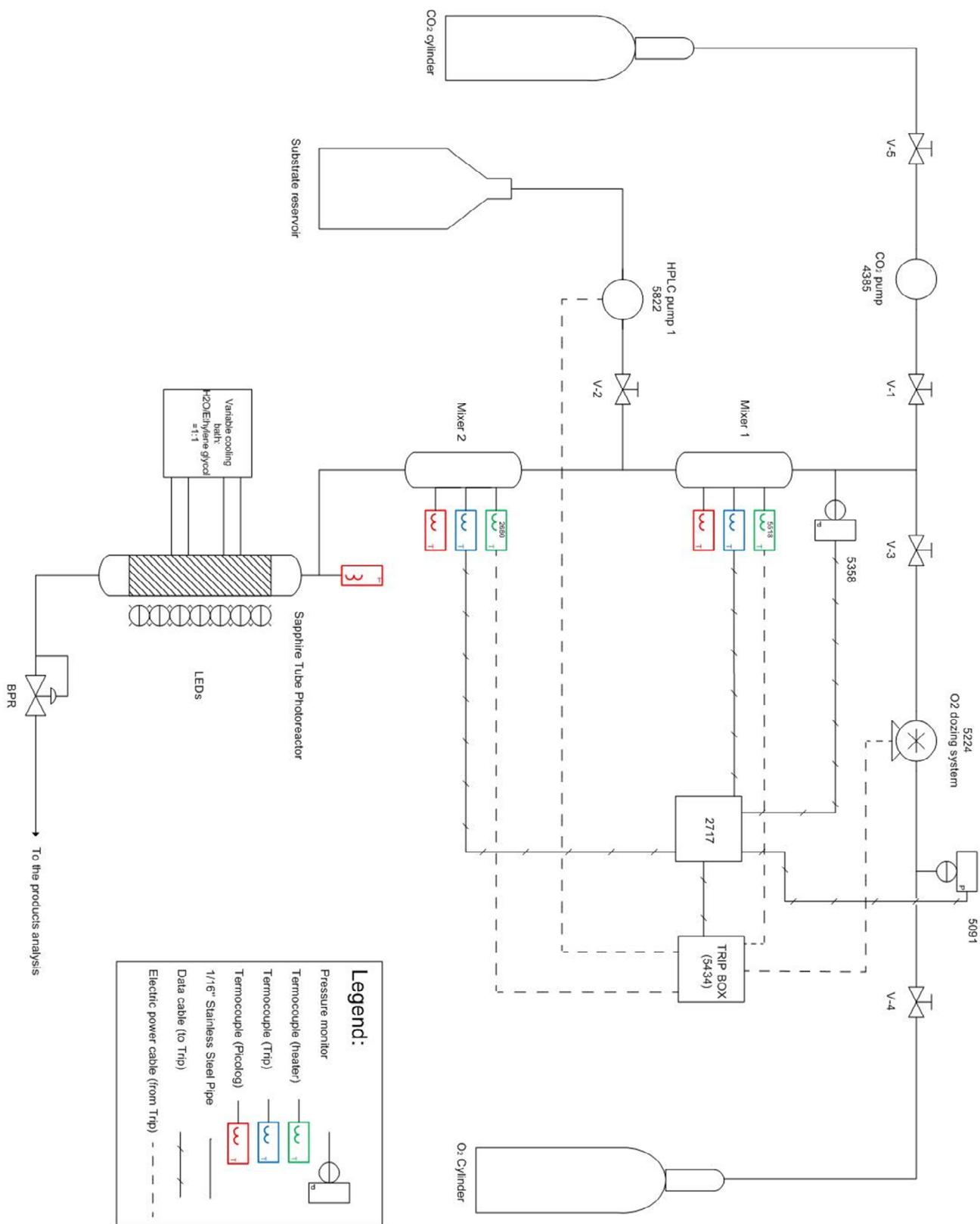
Scheme 3.1 Schematic of the rig used for the photo-oxidation at high pressure in flow.

The pressurization of the system: the CO$_2$ pump and the Back Pressure Regulator (BPR)

The CO$_2$ pump used in this work was a Jasco™ PU-1580-CO2 pump which deliver liquid CO$_2$ (at -10 °C).

The efficiency of the CO$_2$ pumps was tested connecting the pump to a mass-flow meter.

This is particularly important for our oxidation reaction in order to achieve the desired ratio of dilution between the organic flow and the oxygen stream.

As a matter of fact the flammability limits change regarding the solvent and the starting material used in each reaction; however the "golden rule" is that oxygen should never exceed the 8mol.%.[69]

The CO$_2$ pump is never turned off, and when not in use, it remains isolated from the other part of the rig and under a pressure of CO$_2$. This is because the pump check valves are sensitive to changes in their environment and would fail under repeated warming and cooling cycles.

The system is pressurized with CO$_2$ and the pressure was controlled using a Jasco™ BP-1580-81 back pressure regulator (BPR).

The temperature of the BPR can be controlled and was set to 50°C (BPR) to assist in blockage prevention. The BPR is always flushed with iso-propanol after each rection, to prevent blockage or restricted motion of the needle.

The oxygen dosing apparatus: the Rheodyne

To supply and dose the desired amount of oxygen in the reactor system, a six port Rheodyne® 70 series 2-position switching valve is used, as illustrated in Fig. 3.5.
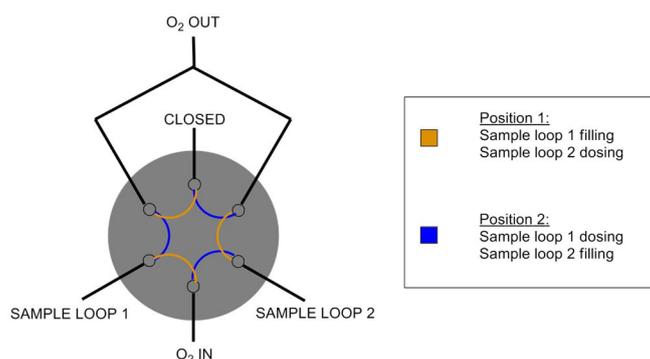

Fig. 3.5 Schematic of the Rheodyne dosing system.

The Rheodyne is characterized by two sample loops and two different positions.

A 3-slot rotor seal joins pairs of the six ports together such that, at any one time, one of the loops acts as reservoir and is filled with O$_2$ while the second one is supplying O$_2$ to the system due to the pressure difference between the oxygen cylinder and the rig.

The rotor position is then switched such that the 3-port rotor joins two different ports together, so that the first loop now is supplying oxygen to the system and the second one is filling with oxygen.

The concentration of O_2 in the CO_2 stream can be varied by changing:

- the volume of the sample loops, in our case 10 µl;
- the frequency of switching the position of the 3-port rotor;
- the pressure gap between the cylinder and the desired pressure of the reaction (at least 20 bar);
- the desired organic reagents and CO_2 flow rates.

Considering the desired O_2:substrate ratio, careful calculation must be undertaken to determine the appropriate switching rate for the O_2 dosage unit taking into account all the parameter cited above, whilst ensuring that the concentration of O_2 in the CO_2 stream does not exceed 8%. The optimum switching rate is between ca. 4 and 14 seconds. Indeed, if the loops volume is too big (i.e. > 300 µL), or the switching rate too slow, then large bubbles of O_2 will mean uneven mixing and spikes in the O_2 concentration.[70]

Conversely, if the switching rate is too fast, this can result in damage to the rotor seal and can cause leaking of O_2 directly from the cylinder into the reactor system.

Finally, it is critical to maintain the O_2 cylinder pressure at least at 20 bar higher than the desired system pressure in order to continuing the feeding of oxygen and to prevent any possibility of back-flow of the organic material of the rigs into the oxygen line that represents a major potential hazard.

The organic alimentation system

The organic mixture of the starting material, the solvent and the photosensitizer is delivered using a Jasco™ PU-980 high performance liquid chromatography (HPLC) pumps (Fig. 3.6).

The efficiency of the HPLC was tested by recording the amount of time required to fill a known volume flask at a fixed flow rate at the pressure of the experiments (100 bar).

Fig. 3.6 Photograph of the Jasco™ PU-980 HPLC pump.

The safety trips and the computer recording and control system (Picolog)

In case of exceeding of alarm values of pressure or temperature, a safety trip system is set in order to shuts down the heating blocks of the mixers, the feeding of oxygen (Rheodyne) and the feeding of the organics, to prevent failures.

In particular the alarm values are set as follow:

- the over-temperature of the heating blocks controlling the temperature of the two mixers are set 10 °C over the desired temperature;
- the system over-pressure is set 10 bar over the operating pressure of the system;
- the oxygen over-pressure of the oxygen from the cylinder (typically set to 220 bar);
- the oxygen under-pressure in order to prevent back flow of organics from the rig to the cylinder: this value must be set higher than the system over-pressure limit.

When one of the parameters exceed or drops below the alarm limit the heaters and the alimentation of oxygen and reagents are switched off, but the CO_2 pump continues to work in an attempt to clear a possible reactor blockage safely and to further dilute the oxygen in the system. The CO_2 pump has an inbuilt pressure trip which will turn the CO_2 pump off in the event that flowing CO_2 does not clear the blockage. Moreover, the BPR is not connected to the trip system so it can fully open and vent the entire contents of the rig. Reactor and mixers temperatures, besides of oxygen and system pressures are simultaneously monitored and recorded via connection of the relevant device to a Pico® Technology TC-08 PicoLogger and by using the PicoLog logging software. This is especially important during continuous flow experiments as it can indicate the time of a system trip and enable identification of the cause.

The heating mixers and the sapphire tube photo reactor

The rig is characterized by the presence of two different mixing chambers (mixers) located before the sapphire tube photo reactor. The mixers consists of a stainless steel tube of 1/4" of outer diameter and around 8 cm in length, packed with sand retained at its end by suitable filters (Fig. 3.7).

Fig. 3.7 Photograph of one of the mixers and aluminum heating block used.

The first mixer is designed to mix CO_2 with O_2 at 40 °C; the second one is useful to mix the organic material with the CO_2-O_2 stream at 25 °C.

The temperature of the mixers is controlled via heated aluminum blocks which are held around the stainless steel tube.

The desired temperature of the heating blocks is controlled by programmable proportional integral derivative (PID) controllers (Eurotherm 2216) which monitor the temperature via K-type thermocouples.

A new generation of sapphire tube reactor was used for the high pressure photo oxidation experiments reported in this Thesis.

The main component is a sapphire tube (Saint-Gobain Crystals, 0.4" outer diameter, 0.04" wall thickness, 4.7" in length) filled with glass balls to maximize the mixing of the mixture. This tube is held in place by a pair of EPDM O-rings and connected to the flow system using 1/8" Autoclave Engineer fittings.

In particular, this sapphire tube reactor was designed and constructed at the University of Nottingham and widely described in the work of Jessica Bellamy in 2014.[71]

This optimized reactor demonstrated increased efficiency and better temperature control.

The reactor, in fact, has a minimal space (ca. 2 mm) between the sapphire tube and the LEDs, which is sealed using a wide Lexan™ polycarbonate tube surrounding the sapphire tube in which the coolant mixture of ethylene glycol/water can flow into this space and, via circulation with a suitable unit (Julabo F250), this allows to control and keep constant the internal reactor temperature.

Other 2 mm divide the Lexan tube to the three LEDs arrays, which are placed and fixed at 120° around the reactor in order to provide maximum irradiation to the reaction mixture (Fig.3.8).

The maximum operating pressure of this reactor is 200 bar at standard operating conditions.
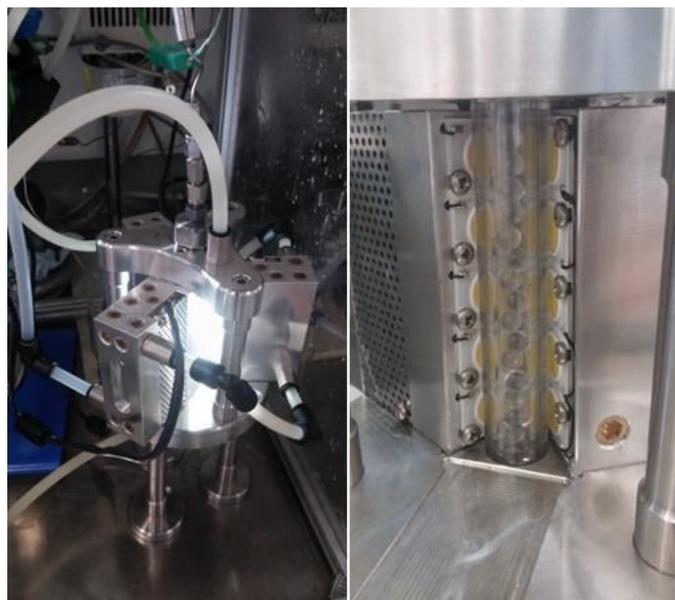
Fig. 3.8 Photograph of the photo-oxidation reactor and the particular of the sapphire tube containing the glass balls in order to maximize the mixing of the solution.

The Standard Operating Procedure

Start-up procedure:
-   check the O_2 cylinder pressure (should be high enough for the desired reaction condition);
-   accurate calculation of the required pump flow rates, Rheodyne switching time and sample loop sizes for the reaction to be performed, be sure that the oxygen does not exceed 8 mol.%;
-   attach the correct sample loops to the Rheodyne dosing unit (5224).
-   ensure that all thermocouples are correctly attached, that all pressure transducers are calibrated and working, and that the pressure and temperature trips are working and set correctly;
-   start the Picologger recording on the PC;
-   set the BPR (4272) to hold 60 bar;
-   set the CO_2 pump (4385) to 5 ml/min and start the pump;
-   open valve V1 to allow CO_2 to enter the system. The reading on the system pressure monitor (5358) should increase;
-   increase the BPR (4272) setting to hold the desired reaction pressure: 100 bar;
-   allow the system time to reach pressure;
-   set the CO_2 pump (4385) to the desired flow rate for the reaction;
-   set the mixer heaters A (2680) and B (5518), and cooling baths (Julabo F250) to the desired temperatures (-10°C).
-   allow the system time to reach temperature and to settle.
-   set the correct switching time on the Rheodyne dosing unit (5224);
-   start the Rheodyne dosing unit (5224), and open valve V3 to allow oxygen to enter the system;
-   allow the system time to equilibrate;
-   make a solution of any reagents and co-solvents and use it to prime HPLC pump 1 (5822).
-   start your chosen light source;
-   set HPLC pump 1 (5822) to the required flow rate, start it and open V2 to allow organic material to enter the rig.

Shutdown procedure:
-   switch off the light source;
-   close valve V2 then stop HPLC pump 1 (5822).
-   close valve V3 then turn off the Rheodyne dosing unit (5224).
-   after 10 minutes, turn off mixer heaters A (2680) and B (5518), and cooling bath ((Julabo F250).
-   allow the system to purge with CO_2 and the temperature to equilibrate.

- release the pressure slowly by reducing the set pressure at the BPR (4272) to 60 bar in roughly 20 bar increments, allowing approximately 10 seconds in between.
- close valve V1 and stop the CO_2 pump (4385).
- release the pressure slowly by reducing the set pressure at the BPR (4272) to atmospheric pressure in 20 bar increments, allowing approximately 10 seconds in between.

3.3 Products analysis

The analysis of the reaction products were performed by ^{1}H and ^{13}C NMR using a Bruker DPX300 spectrometer.

The sample collected from the batch and flow reactors were first concentrated by removing the reaction solvent using a mild condition (low temperature) rotary evaporator; due to the high volatility of α-terpinene the analysis of the samples for the ascaridole synthesis were analyzed as crude.

In particular, the conversion of the starting materials and the yield of products were calculated by ^{1}H-NMR signals integration using biphenyl as internal standard (1/10 mol respect to the starting material) in $CDCl_3$.

The ^{1}H-NMR of α-terpinene and citral are reported in Fig. 3.9 and Fig. 3.10 respectively.
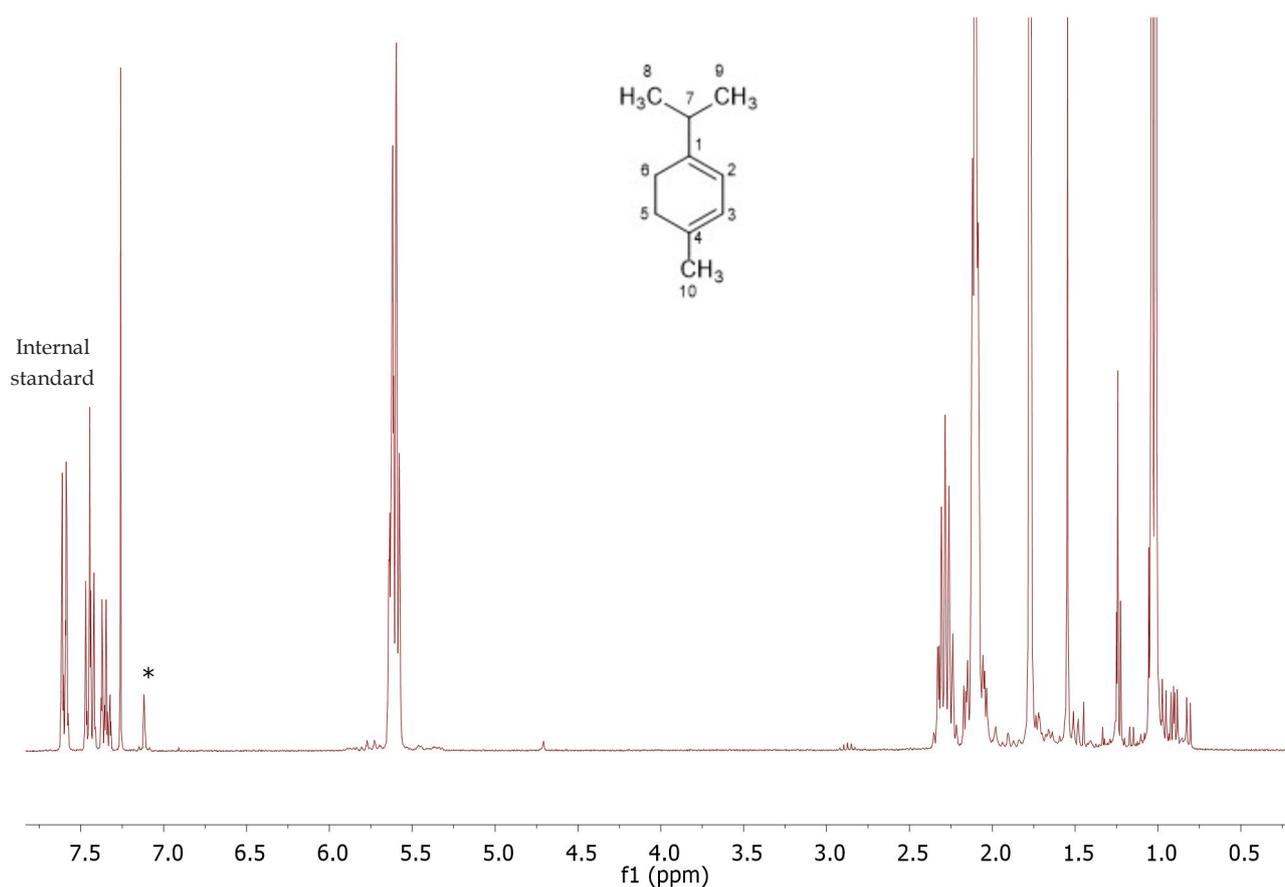

Fig. 3.9 ^{1}H-NMR of α-terpinene (300MHz, $CDCl_3$, 25°C) δ: 1,02-1,06 (d, 6H, C 8-9), 1,78 (s, 3H, C 10), 2,10 (t, 4H, C 5-6), 2,29 (m, 1H, C7), 5,63 (m, 2H, C2-3).

From the internal standard (biphenyl) signal integrations it is possible to obtain both the conversion value of the catalytic tests and the starting material purity.

In particular, the graph above shows the H-NMR of the α-terpinene in the presence of the internal standard, allowing us to calculate that terpinene contains around 5% of impurities, namely p-cymene (* in the figure above).

In particular, for the terpinene conversion calculations was considered the integration of the 2H signal around 5,63 ppm and the corresponding shift and formation of a d-d signal around 6,4 ppm (2H) was considered for the ascaridole yield
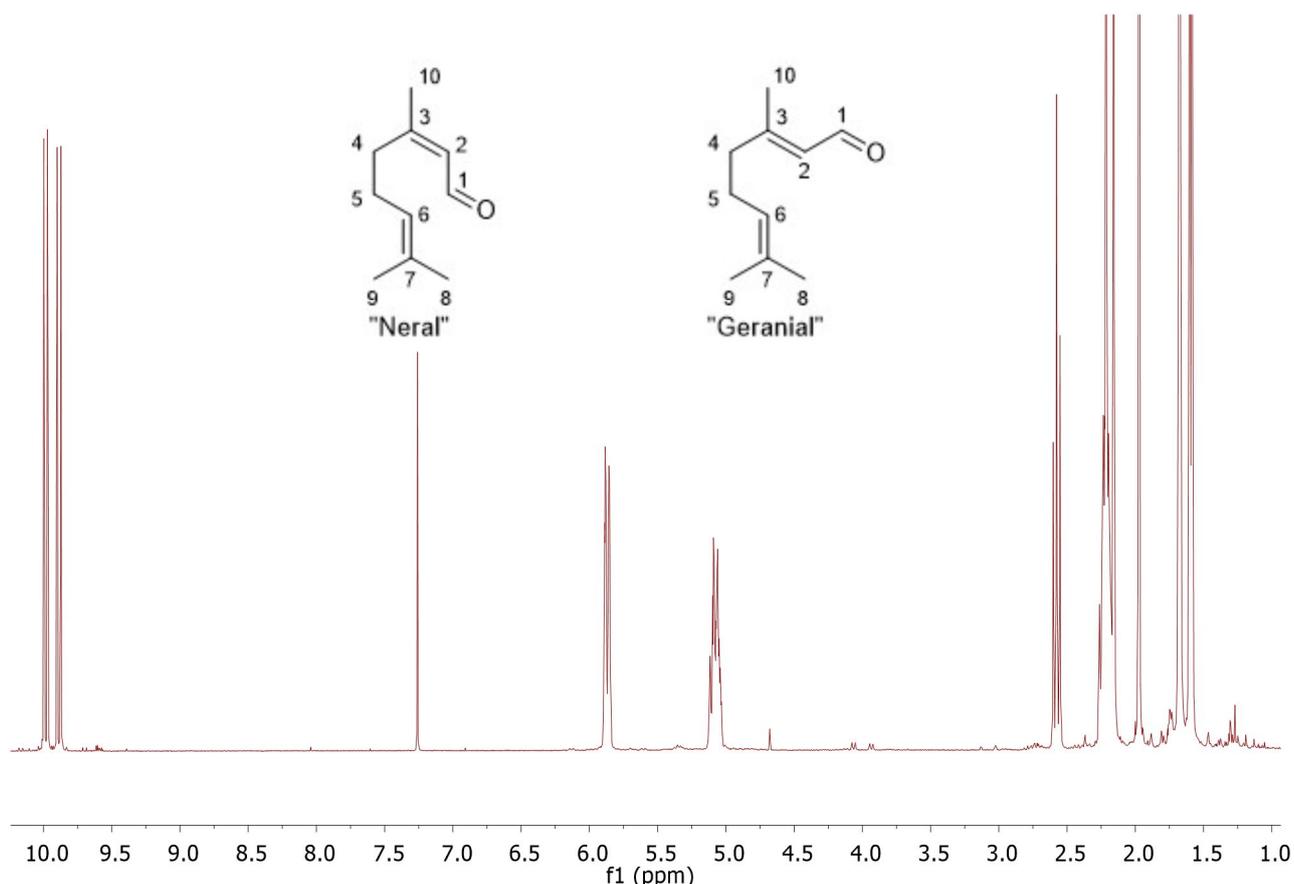
.

Fig. 3.10 ^{1}H-NMR of citral, mixture of 1:1 of neral and geranial (300MHz, CDCl$_3$, 25°C) δ: 1,58 (s, 3H, C 8 Neral), 1,60 (s, 3H, C8 Geranial), 1,68 (s, 3H, C 9, Citral), 1,98 (s, 3H, C 10, Neral), 2,16 (s, 3H, C10, Geranial), 2,17-2,26 (m, 2H, C5 Citral, t, 2H, C4, Neral), 2,58 (t, 2H, C4, Geranial), 5,03-5,13 (m, 1H, C6, Citral), 5,85-5,89 (m, 1H, C2, Citral), 9,87-9,90 (d, 1H, C1, Neral) and 9,97-10 (d, 1H, C1, Geranial).

In particular, for the calculations of the citral conversion were considered both the signals at 5,03-5,13 (1H) and the signals of the CH$_3$ at 1,58 and 1,60 ppm. An average of the two values gives the correct citral conversion.

For the products yields, we always observe the formation of four different signals from 8 to 9 pmm. These signals correspond to the expected –OOH of the products, however due to their broadness they cannot be considered for a reliable yield calculation.[91]

The formation of three different signals around 4,3; 3,3 and 2,9 pmm were considered for the hydroperoxides yield calculatons.

In the following figure is reported a typical ^{1}H-NMR of a reaction sample analysis (Fig. 3.11).
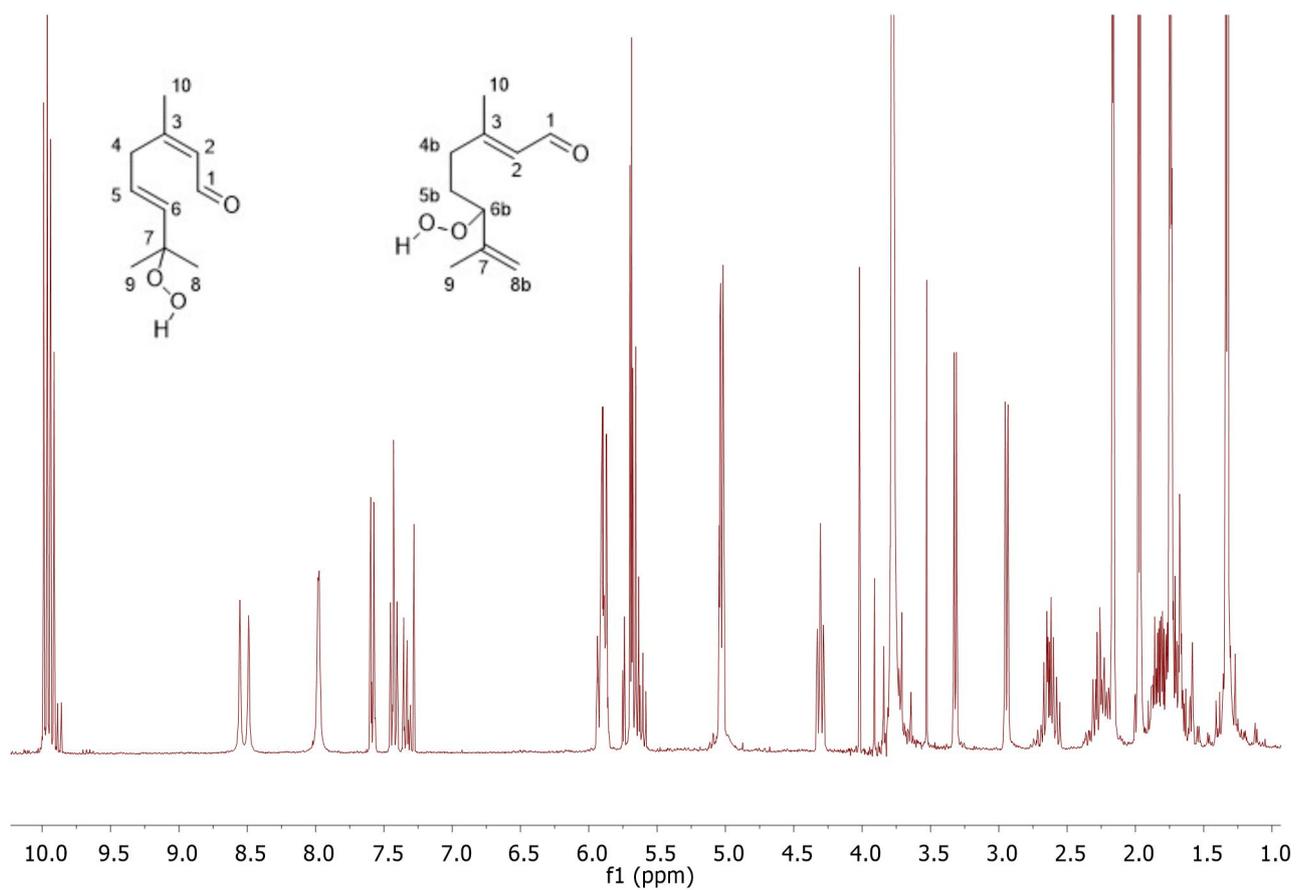
Fig. 3.11 ^{1}H-NMR of citral hydroxides, mixture of the four expected products (300MHz, CDCl$_3$, 25°C) δ: 1,30, 1,31 (s, 3H, C9), 1,72 (3H, C 8), 1,94 (3H, C 10), 2,13 (3H, C10), 2,15-2,28; 2,53-2,64 (m, 2H, C4b, m, 2H, C5b), 2,9-3,3 (d-d, 1H, C4), 4,3 (t, 1H, C6b), 4,98-5,01 (2H, C9b), 5,55-5,67 (m, 2H, C5-C6) and 5,80-5,90 (m, 1H, C2), 8,25;8,27;8,77;8,83 (s –OOH) and 9,82-9,96 (d, 1H, C1).
Biphenyl (I.S.) signals from 7,27 to 7,57 ppm; DMC (reaction solvent) 3,75 ppm (s, 6H).
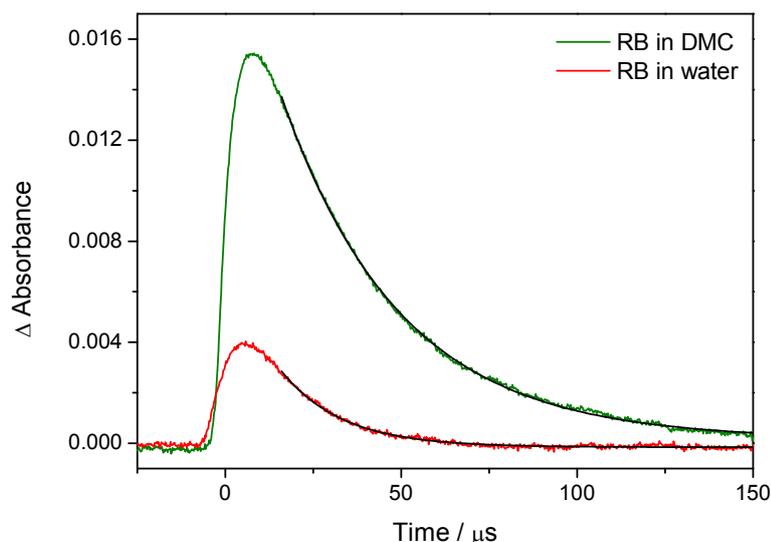
4 RESULTS AND DISCUSSION

4.1 Singlet oxygen lifetime in dimethyl carbonate (DMC)

Singlet oxygen lifetime in DMC were determined by means of laser excitation at 532 nm of an oxygen-saturated diluted solution of Rose Bengal sodium salt in DMC.

The $^1O_2$ characteristic phosphorescence decay emission at 1270 nm was monitored for the lifetime determination following the scheme reported below.

Scheme 4.1 Excitation mechanism of singlet oxygen using Rose Bengal as photosensitizer

Wavelength-discrimination was achieved using a 1270 nm bandpass filter. Interestingly, no signal was detected when a 1250 nm bandpass filter was used instead, indicating that the source of emission is narrow-band, consistent with emission from $^1O_2$.

The results obtained both in DMC and in water (for reference) are reported in the following figure.

Fig. 4.1 $^1O_2$ lifetime determination through the characteristic decay emission at 1270 nm. The laser used is a GCR-12 (Spectra-Physics) Nd:YAG 532 nm with a 6 ns pulse-width at a power of ca. 10 mJ/pulse and a 10 Hz repetition rate. The measurements shown are 16-pulse averages.

Single exponential decays were fitted to the data, giving lifetimes of 34 μs and 17 μs for the samples in DMC and water respectively. The latter value is clearly too large for the decay of $^1O_2$ in water (it has been measured as 5 μs before), which is likely due to the limited time-resolution of the detector. Using this value as our shortest measureable, 34 μs is likely the lifetime of $^1O_2$ **under these conditions**. It should be noted that the proper $^1O_2$ lifetime in DMC is likely to be somewhat longer since many factors such as self-quenching, quenching by the photosensitizer, and impurities have not been accounted for (and are very difficult to take into account).

The different intensities are likely due to quenching of the $^1O_2$ population in water as well as lower solubility of O_2 in water, both resulting in a lower emission intensity.

4.2 Ascaridole synthesis

The well-known [2+4] cycloaddiction of singlet oxygen to α-terpinene to yield the corresponding endoperoxide (ascaridole) was chosen and firstly investigated as model reaction to start to investigate the possibility to use dimethyl carbonate (DMC) as greener solvent for the photochemistry (Scheme 4.2).
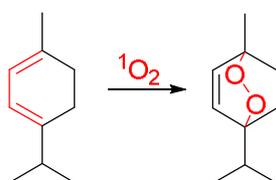
Scheme 4.2 The photo-oxidation of α-terpinene with singlet oxygen to yield ascaridole.

In particular we have studied the influence of the reaction solvent in the batch reaction condition (as explained in the Experimental chapter 3.2.1), using as photo sensitizer the TPFPP.

This porphyrin show a good solubility in DMC and is known to be soluble in sc-CO_2, features that facilitates the applicability of this process to the high pressure continuous flow system, since the reaction proceed in a homogeneous single phase system.[72]

Moreover, these photosensitizers (such as TPFPP and TPP) are meso-substituted porphyrins characterized by higher chemical stability due to the presence of bulky substituents that avoid the formation of inactive dimers and limits destructive self-oxidation reactions, decreasing the electron density in the porphyrin rings.[73,74]

Furthermore, these porphyrins are highly efficient photosensitizers because the "Type II" mechanism of photosensitized oxidation to generate singlet oxygen is thought to be dominant (see Introduction 1.2.2).[75]

4.2.1 Batch reaction

The photo-oxidation of α-terpinene were firstly investigated in a batch using classical glassware at 5°C, using a TPFPP:α-terpinene ratio of 1:1500 (ca 0,067mol.%), and a concentration α-terpinene of 0,5 mol/L studying the influence of three different solvents mixture Ethanol:THF=1:1 in volume (blue line); Pure DMC (red line); Ethanol:DMC=1:1 in volume (green line). The results are shown in the following Fig. 4.2.
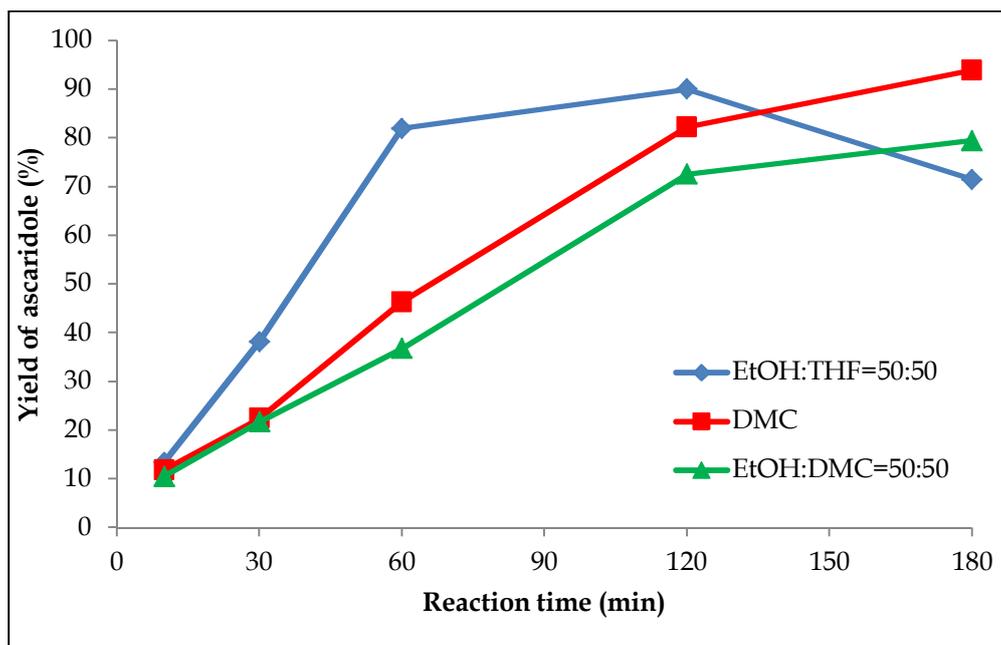

Fig. 4.2 Solvent influence in the photo-oxidation of α-terpinene with singlet oxygen to yield ascaridole; T=5°C, TPFPP 0,067mol.%, α-terpinene 0,5 mol/l.

From the graph above it appears that in the mixture of ethanol and THF the reactivity is faster. In this case, we have used a mixture of ethanol and THF instead of pure ethanol due to the low solubility of TPFPP in the alcoholic solvent and because we wanted to avoid the utilization of chlorinated co-solvent. However, using THF leads to two main problems:

- ascaridole seems to be not stable and start to decompose after 120 minutes of reaction;
- THF itself is not stable in the presence of singlet oxygen, and forms a charge transfer complex with oxygen;[76] moreover it can react leading to the formation of other endoperoxide byproducts by the following reaction scheme (Scheme 4.3).[77,78]
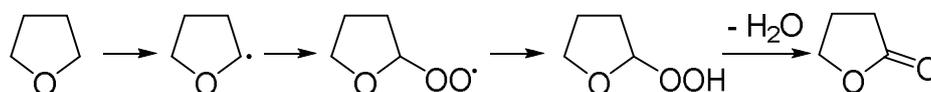
Scheme 4.3 THF possible reaction with singlet oxygen.

Conversely, DMC shows a very good reactivity that allows us to obtain the higher ascaridole yield (ca. 94%) after three hours of reaction. Moreover, the addition of ethanol to the DMC results in a slower reaction; that is probably due to the lower singlet oxygen lifetime in ethanol compare to DMC and is detrimental for the reaction.

However, DMC allow to obtain an interesting reactivity using the TPFPP as photosensitizer and it was chosen for further investigations and optimizations in the high pressure flow rig.

4.2.2 High pressure flow reaction

Supercritical fluids (SCFs) have many interesting and unusual properties that make them useful media for separations and spectroscopic studies as well as for reactions and synthesis.[79] In many cases, CO_2 is seen as the most viable supercritical solvent because of its relatively mild critic point conditions (T_c=31°C and P_c=74bar) moreover, it is non-toxic, non-flammable and relatively inert.

For example, CO_2 is inert to free radical chemistry so it is an interesting alternative solvents for polymerisation processes initiated by free radicals.[80,81]

Moreover, scCO_2 cannot be oxidised and, therefore oxidation reactions using air or oxygen (completely miscible in this solvent) have been extensively investigated.[82]

Although scCO_2 is a weak solvent compared to most of the conventional VOCs, it solvency can be increased by addition of a co-solvent or surfactant.[83,84]

Finally, scCO_2 often allow to obtain higher reaction rate because of the increasing of the molecular diffusivities due to the fact that it has a lower density and viscosity than conventional liquid solvents.[85]

For all these reasons, scCO2 have been widely investigated by the Poliakoff's group for a wide range of photo-oxidations in high-pressure flow reactors.[86,87,88]

The same solution of α-terpinene in DMC, TPFPP (0,067mol%) and biphenyl as internal standard was prepared for the high pressure continuous flow tests.

At the beginning we performed one test at atmospheric pressure, without co-feeding CO_2, at 5°C) in order to study the implementation due to the new, optimized design of the flow photo-reactor; feeding an equimolar amount of oxygen respect to the α-terpinene. The results are represented in Fig. 4.3.
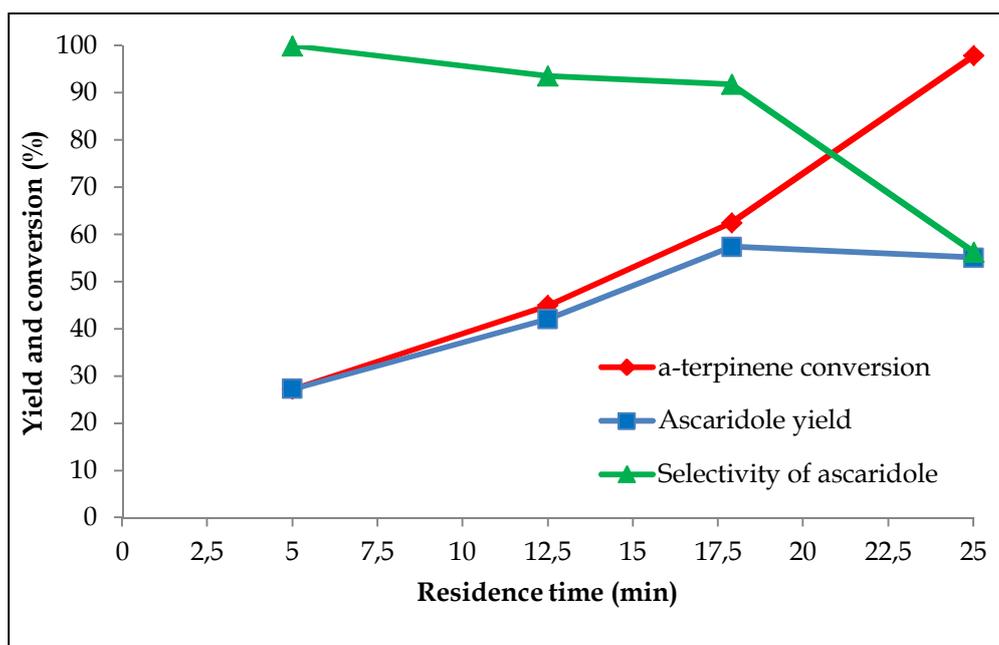
Fig. 4.3 Photo-oxidation of α-terpinene with singlet oxygen to yield ascaridole in a continuous flow reactor; atmospheric pressure, T=5°C, variable organic flow rate. α-terpinene:oxygen:TPFPP=1:1:0,00067, α-terpinene 0,5 mol/L in DMC.

The continuous flow photo-reactor allow us to greatly increase the reaction rate, allow us to obtain around 60% of ascaridole yield with 18 minutes of residence time inside the reactor, while in batch after 30 minutes we obtain only 20% of product yield.

However, for longer residence time of the organic flow inside the sapphire tube, the selectivity in ascaridole rapidly drops below 60%.

This is probably due to the decomposition of the formed ascaridole that lead to the formation of byproducts such as alcohols and aromatics (namely p-cymene derivatives).

Moreover, feeding stoichiometric amount of oxygen at atmospheric pressure means that part of the oxygen is not completely solubilized in the organic solution, this lead to an incomplete conversion of alpha-terpinene at low residence time and to the formation of heavy dimers with hydroperoxides groups bridging between two molecules of the starting materials. Some of the hypothesized by-products (from the mass-spec analysis) are reported below (Fig. 4.4).
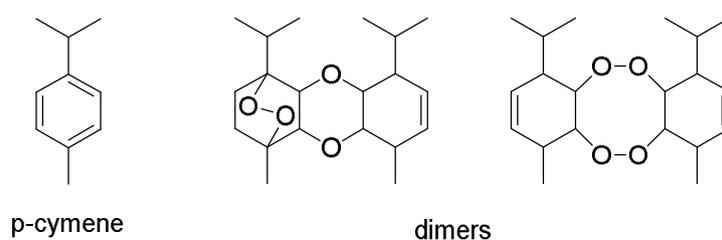

Fig. 4.4 Ascaridole byproducts.

After having realized these aspects of the reaction, we have decided to feed the same organic mixture, co-feeding a constant flow of 1 ml/min liquid CO_2 at 100 bar at the same, relatively low, temperature (5 °C). These reaction conditions, milder than those usually used for similar the photo-oxidation in $scCO_2$ (e.g. 40 °C and 180 bar),[89,90] allow us to test the reactivity of α-terpinene in a DMC and liquid CO_2 mixture. Also in this case the influence of different organic flow rates, and consequently different concentration of the starting material in the overall flow, and different residence times were investigated (Fig. 4.5).
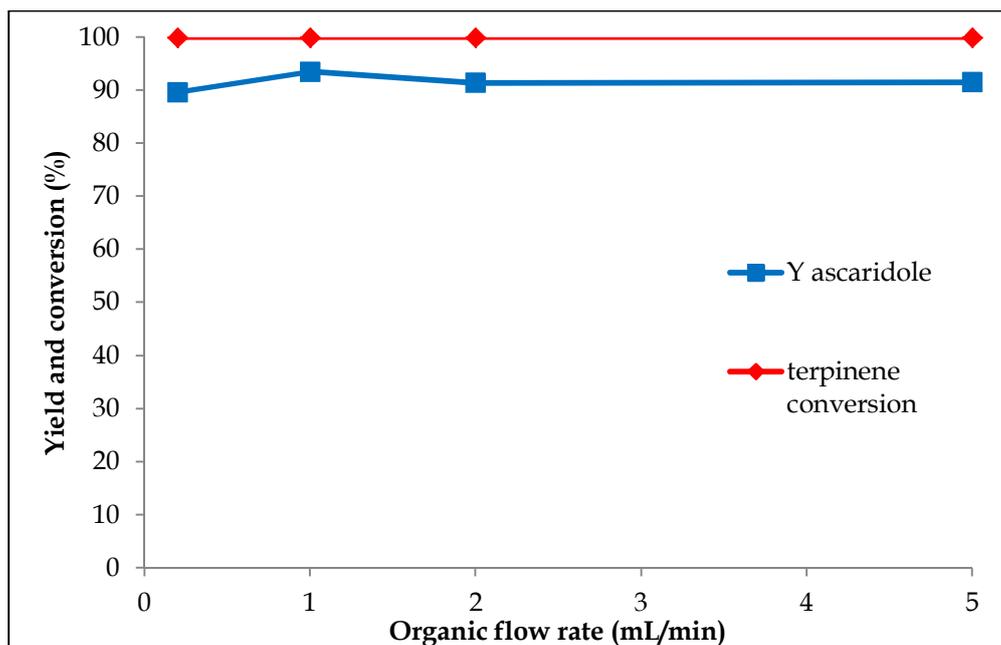

Fig. 4.5 Photo-oxidation of α-terpinene with singlet oxygen to yield ascaridole in a continuous flow reactor; 100 bar, T=5 °C, 1 ml/min of CO_2, variable organic flow rate.
α-terpinene:oxygen:TPFPP=1:2:0,00067, α-terpinene 0,5 mol/l in DMC.

The photo-oxidation reaction of α-terpinene performed in the conditions described above show a surprisingly stability in the wide range of organic flow rates tested; with complete conversion of the starting material also for very low residence time.
Moreover the selectivities of ascaridole remain virtually unchanged (>90%).
These are interesting results show that the use of liquid CO_2 as solvent and DMC as co-solvent in relatively mild conditions are viable.
For a better understanding of the dilution rate of α-terpinene and of the residence time look at the table below (Table 4.1).

Organic flow rate (ml/min)	Liquid CO_2 flow rate (ml/min)	Overall flow rate (ml/min)	Photo-reactor Volume (ml)	Residence time (sec)	α-terpinene final concentration (mol/l)
0,2	1	1,2	2,5	125	0,083
1	1	2	2,5	75	0,25
2	1	3	2,5	50	0,33
5	1	6	2,5	25	0,42

Table 4.1 Residence time and dilution calculation for the high pressure continuous flow photo-oxidation test of α-terpinene.

In conclusion, we have proved the importance of DMC as co-solvent for the model photochemical oxidation of terpinene to ascaridole, helping to solubilized the photosensitizer and allowing to obtain a stable system in wich ascaridole doen not undergoes to a fast decomposition.

Taking into account this encouraging results we decided to move our attention to another photo-oxidation studied at the Poliakoff's group: the citral photo-oxidation with singlet oxygen.

The photo-oxidation of citral will be discussed thereafter. Citral is an acyclic monoterpenoid a major constituent of lemongrass among well know others such as myrcene, citronnellol and geraniol. Terpenoids are volatile compounds that are defined as a group of molecules with a general formula of $(C_5H_8)_n$. The n value allow the classification of these compounds from the most simple (isoprene, C5) to more complex structures. These compounds are widely available from renewable sources and constitute a class of materials that can be transformed into valuable fine chemicals. Indeed, various very important processes were developed for the synthesis of perfume, flavor and pharmaceuticals. One of this process was described earlier in this thesis.

4.3 Citral hydroperoxides synthesis

After the results obtained in the synthesis of ascaridole we studied another less-investigated reaction: the Schenk-ene oxidation of citral with singlet oxygen.

Citral is a mixture of two different isomers: the (Z)-3,7-dimethylocta-2,6-dienal (also named Neral) and the (E)- 3,7-dimethylocta-2,6-dienal (Geranial) so the Schenck-ene reaction can lead to the formation of four different allylic hydroperoxides (Scheme 4.4).
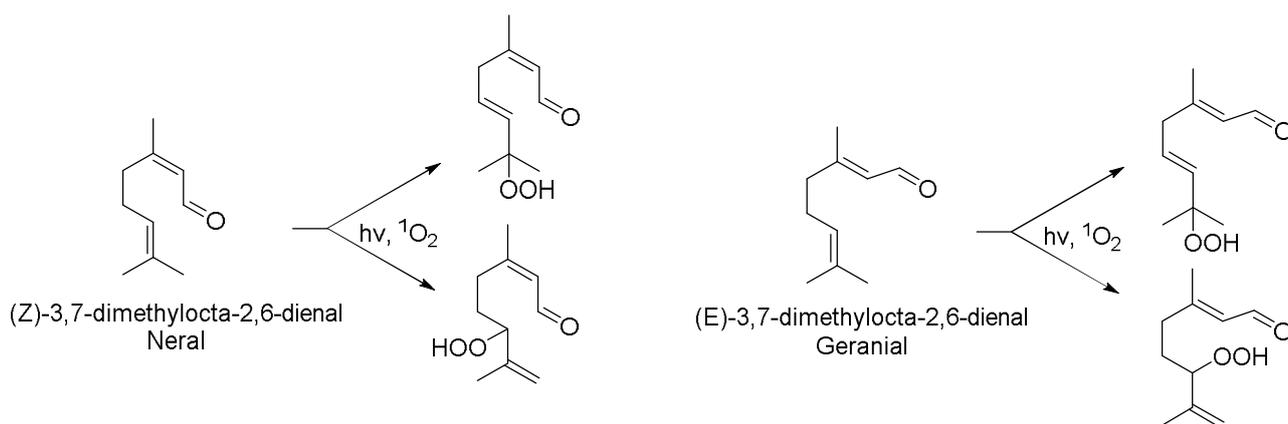
Scheme 4.4 Citral oxidation to hydroperoxides.

As reported in the literature, the reaction with $^1O_2$ is selective toward the oxidation of the unconjugated double bond, while the utilization of other oxidant, namely H_2O_2 lead to the formation of a mixture of oxidized compound of both of the double bonds (especially epoxides).[91]
Indeed the electrons of the conjugated double bond are being withdrawn by the aldehyde group, therefore it is less nucleophilic towards singlet oxygen and incredibly slow to react. In this way, the reactivity of singlet oxygen is very similar to that of carbenes, i.e. requires an electron rich nucleophilic alkene.

4.3.1 Batch reaction: photosensitizers screening

The citral photo-oxidation reaction with $^1O_2$ was firstly investigated in a simple batch reactor system in order to identify which photosensitizer would be best and in which solvent system it would work best.
The main problem with some of the photosensitizers used is related to the low solubility in DMC, but whenever it was possible, a complete analysis of the solvent influence from pure DMC to pure ethanol was performed. The photosensitizers studied and the solubility in ethanol and DMC are shown in the following page (Table 4.2) in which the photosensitizers structures and the solubility both in ethanol and DMC are shown.
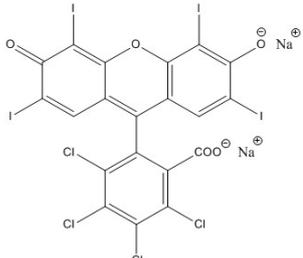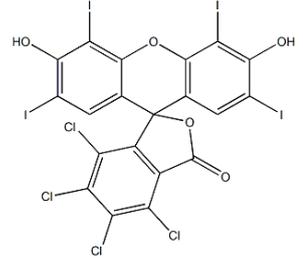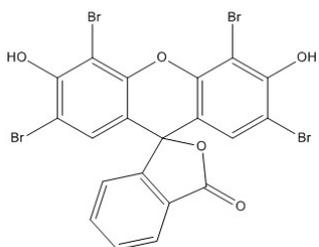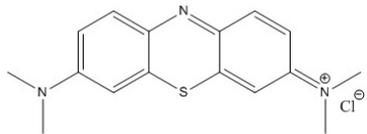
Photosensitizer	Solubility in ethanol	Solubility in DMC
Rose Bengal Na salt	Soluble	Partially soluble
Rose Bengal Lactone	Soluble	Soluble
Eosin Y	Soluble	Partially soluble
Methylene Blue	Soluble	Partially soluble
Meso-tetraphenylporphyrin (TPP)	Partially soluble	Soluble
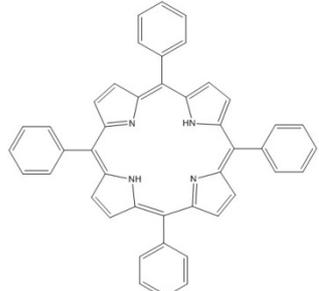
Table 4.2 Photosensitizers studied and the solubility in DMC and ethanol.

The reaction condition adopted for all of these batch reactions were as follow:

Citral concentration in the solvent (o solvent mixture): 0,5 mol/l;
The solvent mixture ratio refers to a volume ratio;
Photosensitizer amount: 0,1 mol.% (1/1000 on respect to citral);
T = 5 °C;
Oxygen bubbling in the mixture.

Depending on the photosensitizer used, the results obtained follows two opposing trends that will be explained in the following pages.

The lactone group effect on the photosensitizer: Rose Bengal Lactone and EosinY

Two of the major and cheaper photosensitizers commercially available are Rose Bengal the lactone form and Eosin Y. In particular Eosin Y is of particular interest because of its low cost and toxicity.[92] Moreover, the two molecules are strikingly similar and are characterized by the presence of a lactone group (see Table 4.2). So is not surprisingly that they show similar behavior when used for the citral photo-oxidation reaction.
The results obtained with Rose Bengal Lactone of citral conversion and yield on the hydroperoxides products are show below (Fig. 4.6).
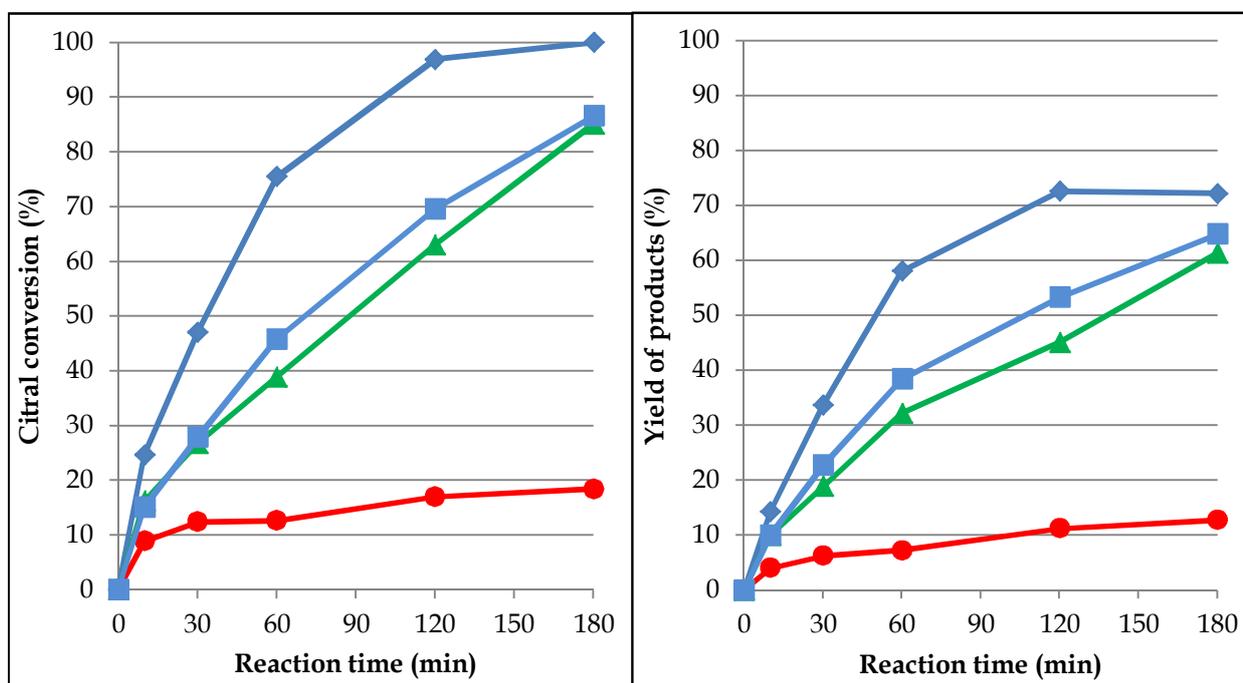

Fig. 4.6 Batch photo-oxidation of citral with singlet oxygen using Rose Bengal Lactone.
Solvent influence analysis, citral conversion trends (left) and hydroperoxides products yields (right).
♦ Ethanol(dark blue); ■ Ethanol:DMC=9:1(light blue); ▲Ethanol:DMC=1:1(green); ● DMC (red).

A clear trend was obtained with a faster reaction rate are observed when using ethanol as reaction solvent, it was noted that progressively increasing of the amount of DMC was detrimental for the conversion of citral. Similar behaviors are obtained using EosinY as photosensitizer (Fig. 4.7).
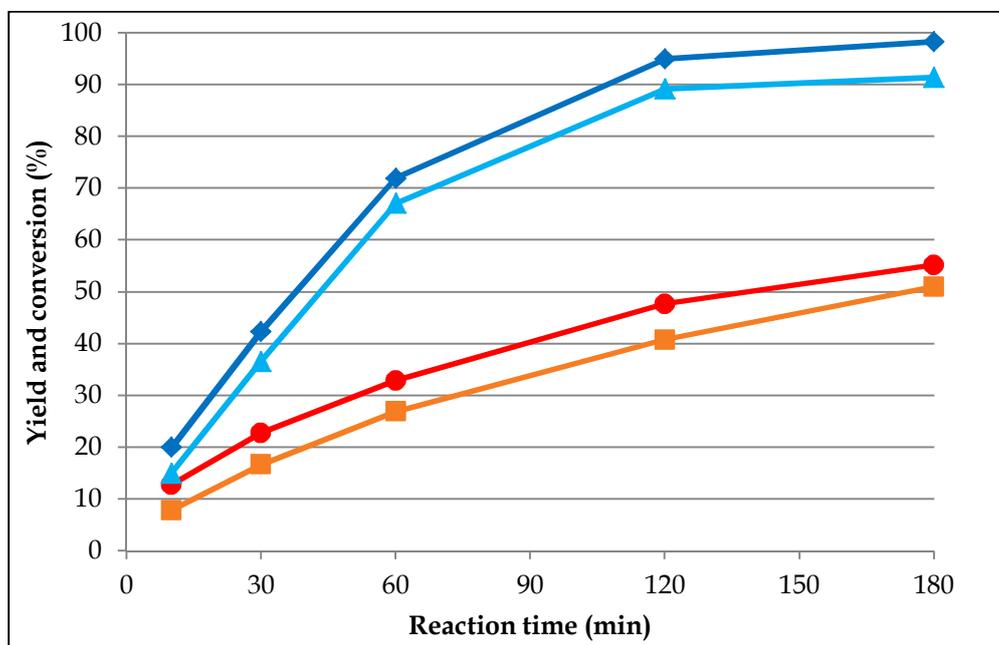

Fig. 4.7 Batch photo-oxidation of citral with singlet oxygen using EosinY.
Solvent influence analysis between pure ethanol (♦ citral conversion blue and ▲ product yields light blue) and a mixture rich of DMC (DMC:Ethanol=8:1, ● citral conversion in red and ■ product yields orange).

Also in the case of Eosin Y using DMC lead to a slower reaction rate. Considering only the singlet oxygen lifetime measurement (greater in DMC than in ethanol) we would expect completely opposite trends.

Moreover, especially when Rose Bengal is used as photosensitizer, we obtain very low selectivity in the desired hydroperoxide products with the formation of new byproducts never detected with other photocatalysts.

It is clear that some incompatibility between lactone bearing photosensitizers and the DMC occurs which will have to be investigated in the future.

Probably DMC faster the decomposition (or bleaching) of this photosensitizers in the reaction conditions.

The UV-Vis absorbance profile of Rose Bengal Lactone in different solutions are reported (Fig. 4.8).
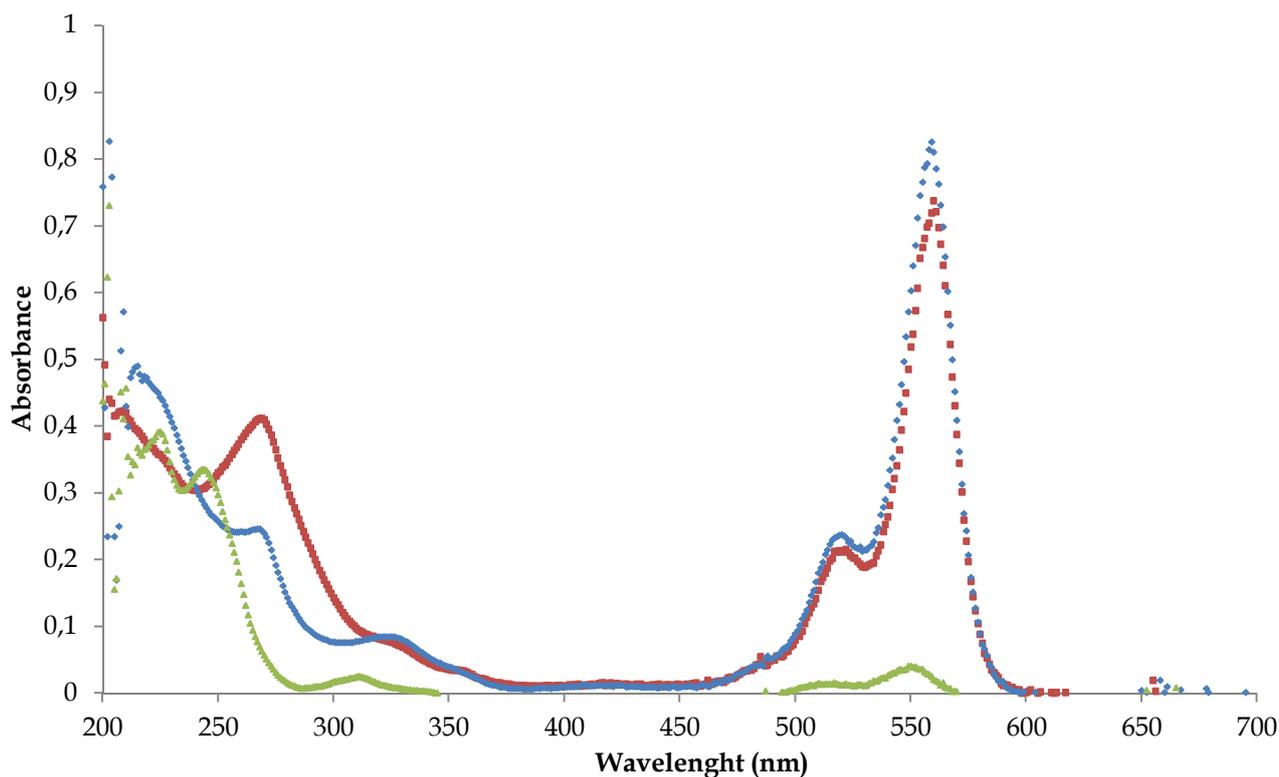
Fig. 4.8 UV-Vis absorbance test of three different Rose Bengal Lactone form solution (0,5*10⁻⁵ mol/l) in: Ethanol (red spots); Ethanol:DMC=1:1 (blue spots); DMC (green spots).

A clear modification of the absorbance profile of Rose Bengal Lactone show a detrimental effect of DMC in the absorption of the photocatalyst. Indeed, while the bands in the UV region are shifted to lower wavenumbers the bands around 550 nm almost disappears.

This can be explained both by a different and detrimental coordination of the solvent to the photosensitizer and its decomposition to a colorless compound that doesn't adsorb and it completely inactive for our purpose.

The DMC improvement

In this chapter we will discuss the improvement achieved by the use of DMC as reaction solvent with three different photosensitizers: Methylene blue, Rose Bengal sodium salt and finally a porphyrin, TPP.

Methylene blue is another common dye used for photo-oxidation reaction, however in previous work was found that the hydroperoxide products are less stable in the presence of this photosensitizer compared to the others tested.

This is due to further interactions that lead to consecutive reactions toward other byproducts.

In our tests we have confirmed this behavior but surprisingly using DMC as reaction solvent decreased the rate of decomposition of peroxide products and gave a better overall conversion than Rose Bengal and EosinY (Fig. 4.9).
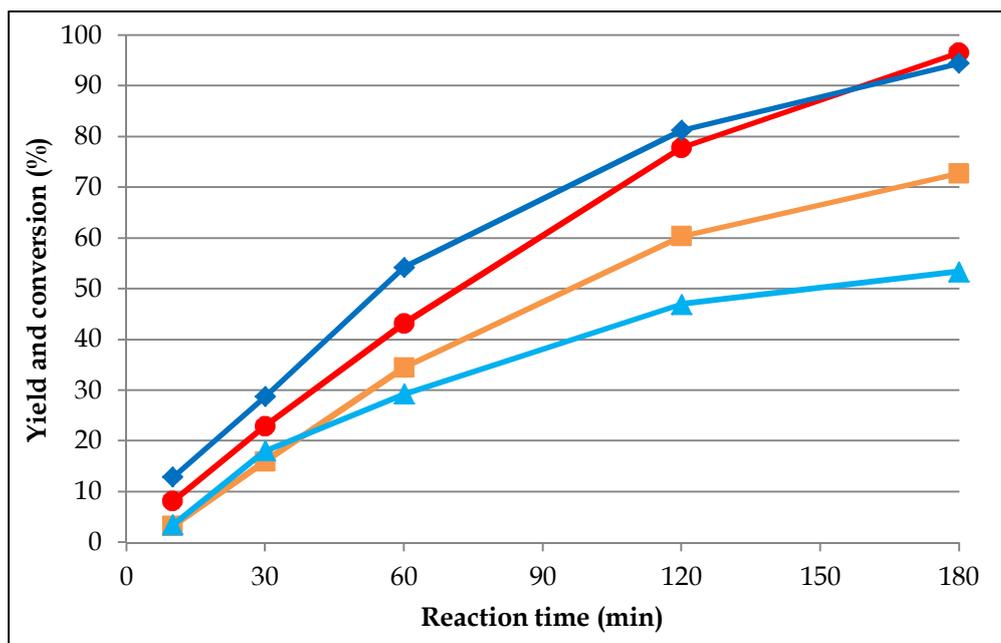
Fig. 4.9 Batch photo-oxidation of citral with singlet oxygen using Methylene Blue.
Solvent influence analysis between pure ethanol (♦ citral conversion blue and ▲ product yields light blue)
and a mixture of DMC:Ethanol=1:1, (● citral conversion in red and ■ product yields orange).

Interestingly, after the unpromising results obtained with Rose Bengal Lactone we decided to try also the other commercially available and cheaper form of this photosensitizer: Rose Bengal sodium salt.
The results obtained are shown in the two graphs below (Fig. 4.10).
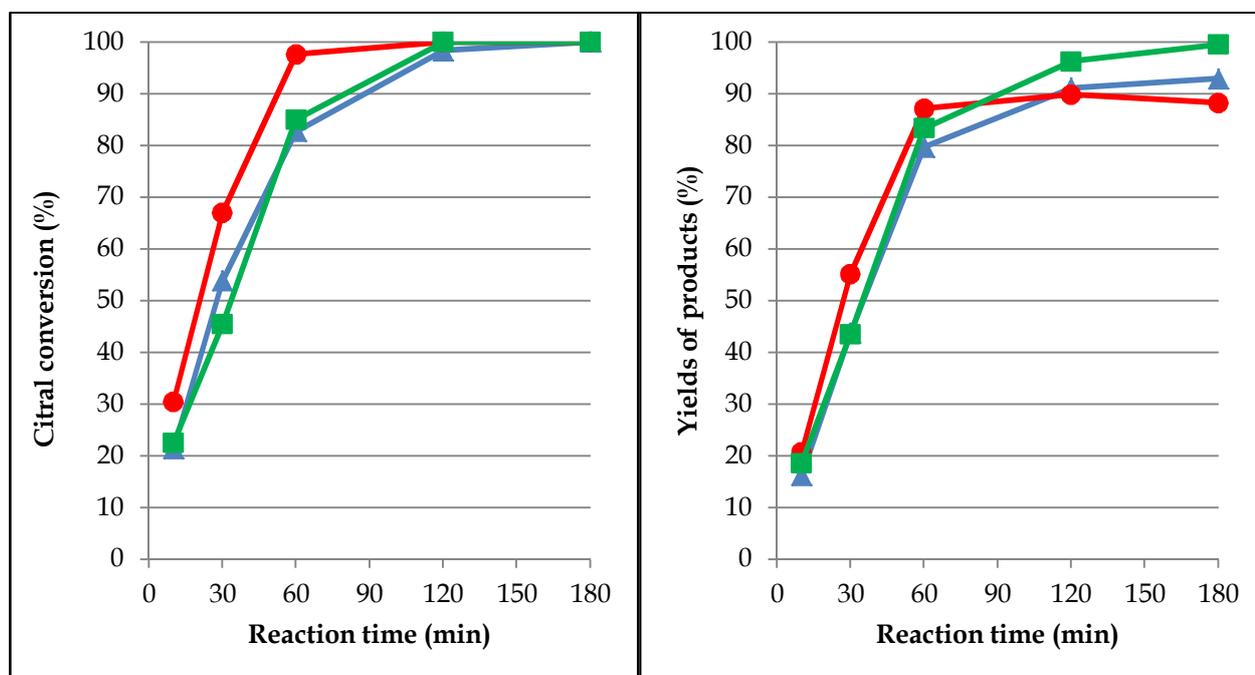

Fig. 4.10 Batch photo-oxidation of citral with singlet oxygen using Rose Bengal Na salt.
Solvent influence analysis, citral conversion trends (left) and hydroperoxides products (right).
▲ Ethanol; ■ Ethanol:DMC=1:1,45; ● Ethanol:DMC=1:1.

Adding a small quantity of DMC results in an improvement for the reaction kinetics (eg ethanol:DMC=1:1 in red), however continuing to increase the ratio of DMC to ethanol in the mixture finally lead to results similar to the using pure ethanol as the reaction solvent. Probably with some of the photosensitizer we have two different and conflicting effects:

- The increasing of the oxygen lifetime that faster the reactions;
- The stronger coordinating effect of DMC to the photosensitizer and the consequence decreasing of some of the absorption bands;

Finally another porphyrin (TPP) was tested as photosensitizer. This photo catalyst, cheaper compared the more substituted TPFPP, show good solubility in DMC. The results obtained by the photo-oxidation of citral are shown in the following Graph (Fig. 4.11).
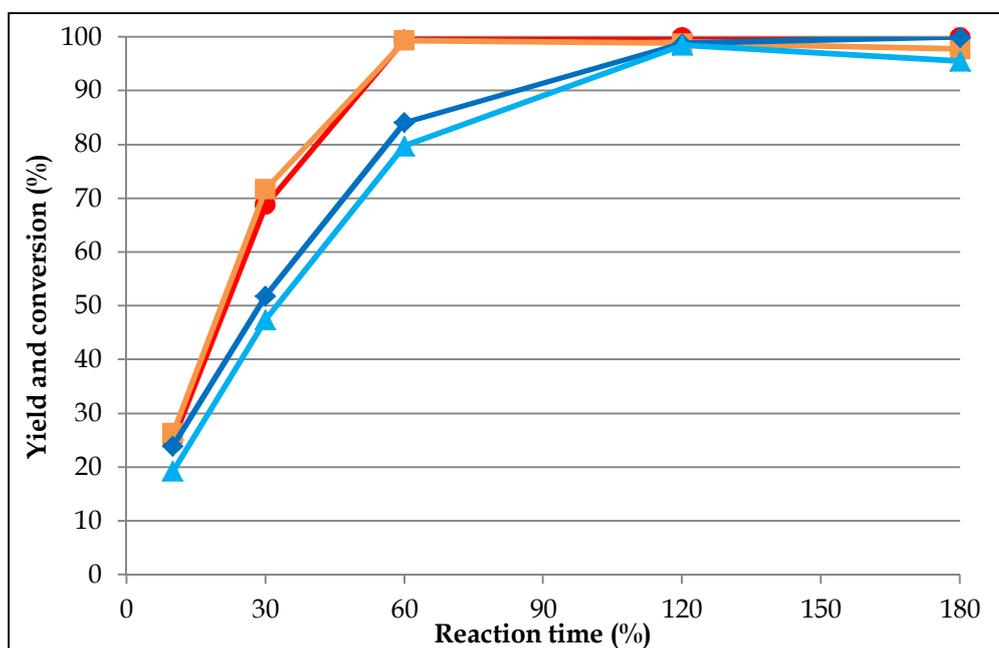
Fig. 4.11 Batch photo-oxidation of citral with singlet oxygen using TPP.
Solvent influence analysis between a mixture of ethanol and DMC (ethanol:DMC=1:1; ♦ citral conversion blue and ▲ product yields light blue) and pure DMC (● citral conversion in red and ■ product yields orange).

TPP show the best reactivity in DMC as solvent allowing us to obtain complete conversion and yield of the desired products in 1 hour of reaction. Moreover, the hydroperoxides start to decompose with a slow rate after 2 hours of reaction.

This stable reactivity and the good solubility in DMC convinced us to choose TPP as photosensitizer for further investigation in the high-pressure continuous flow reactor.

All the results obtained from the citral oxidation in batch are summarized in the following table for convenience (Table 4.3).

Photosensitiser	Conc.	Solvent	Time (min)	10	30	60	120	180
Rose Bengal Na salt	0,1 mol.%	EtOH	Citral conversion (%)	21.4	53.8	82.7	98.3	100
			Hydroperoxides yields (%)	16.2	43.7	79.7	91.1	92.9
Rose Bengal Na salt	0,1 mol.%	EtOH:DMC=1:1	Citral conversion (%)	30.4	67	97.6	100	100
			Hydroperoxides yields (%)	20.6	55.1	87.1	89.8	88.2
Rose Bengal Na salt	0,006 mol.%	DMC	Citral conversion (%)	12	13.6	16.3	20.4	19.4
			Hydroperoxides yields (%)	2.5	4.8	7.5	11.3	12.8
Rose Bengal Lactone	0,1 mol.%	EtOH	Citral conversion (%)	24.7	47.1	75.5	96.9	100
			Hydroperoxides yields (%)	14.3	33.7	58.1	72.6	72.2
Rose Bengal Lactone	0,1 mol.%	EtOH:DMC=9:1	Citral conversion (%)	15.1	27.9	45.8	69.6	86.6
			Hydroperoxides yields (%)	10	22.7	38.4	53.3	64.8
Rose Bengal Lactone	0,1 mol.%	EtOH:DMC=1:1	Citral conversion (%)	16.2	26.8	38.9	63.1	85.1
			Hydroperoxides yields (%)	10	18.9	32.2	45.1	61.4
Rose Bengal Lactone	0,1 mol.%	DMC	Citral conversion (%)	8.9	12.4	12.6	17	18.4
			Hydroperoxides yields (%)	4	6.2	7.2	11.2	12.7
Eosin Y	0,1 mol.%	EtOH	Citral conversion (%)	20	42.4	72	95	98.3
			Hydroperoxides yields (%)	15	36.6	67.1	89.2	91.4
Eosin Y	0,1 mol.%	EtOH:DMC=1:8	Citral conversion (%)	12.8	22.8	32.9	47.7	55.2
			Hydroperoxides yields (%)	7.9	16.7	26.9	40.8	51
Methylene Blue	0,1 mol.%	EtOH	Citral conversion (%)	12.9	28.8	54.3	81.3	94.5
			Hydroperoxides yields (%)	3.5	18.1	29.3	47	53.4
Methylene Blue	0,1 mol.%	EtOH:DMC=1:1	Citral conversion (%)	8.1	22.9	43.2	77.8	96.6
			Hydroperoxides yields (%)	3.3	16	34.5	60.4	72.8
TPP	0,1 mol.%	EtOH:DMC=1:1	Citral conversion (%)	24	51.9	84.1	98.8	100
			Hydroperoxides yields (%)	19.3	47.5	79.8	98.5	95.5
TPP	0,1 mol.%	DMC	Citral conversion (%)	25.1	68.8	99.5	100	100
			Hydroperoxides yields (%)	25	68	99.3	98.8	97.7

Table 4.3 Batch reactor results for the photo-oxidation of citral with $^1O_2$ with different photosensitizers and different reaction solvents: DMC, ethanol and mixture of the two.

4.3.2 High-pressure continuous flow reaction

As a result of the in-depth study conducted in the batch reactor, we have decided to focus our attention in the in-flow implementation of the reactivity of citral in the presence of TPP as photosensitizer using DMC as solvent.

In particular using the same reagent solution used for the batch reaction, we firstly investigated the following reaction conditions (already tested also for the α-terpinene oxidation):

Citral concentration in DMC: 0,5 mol/l;

Photosensitizer amount: 0,1mol.% (1/1000 on respect to citral);

T = variable from 1 to 6°C (depending on the organic flow rate, exotermic reaction);

P = 100 bar; co-feeding a liquid CO_2 flow of 1 ml/min;

Oxygen:citral ratio = 2:1.

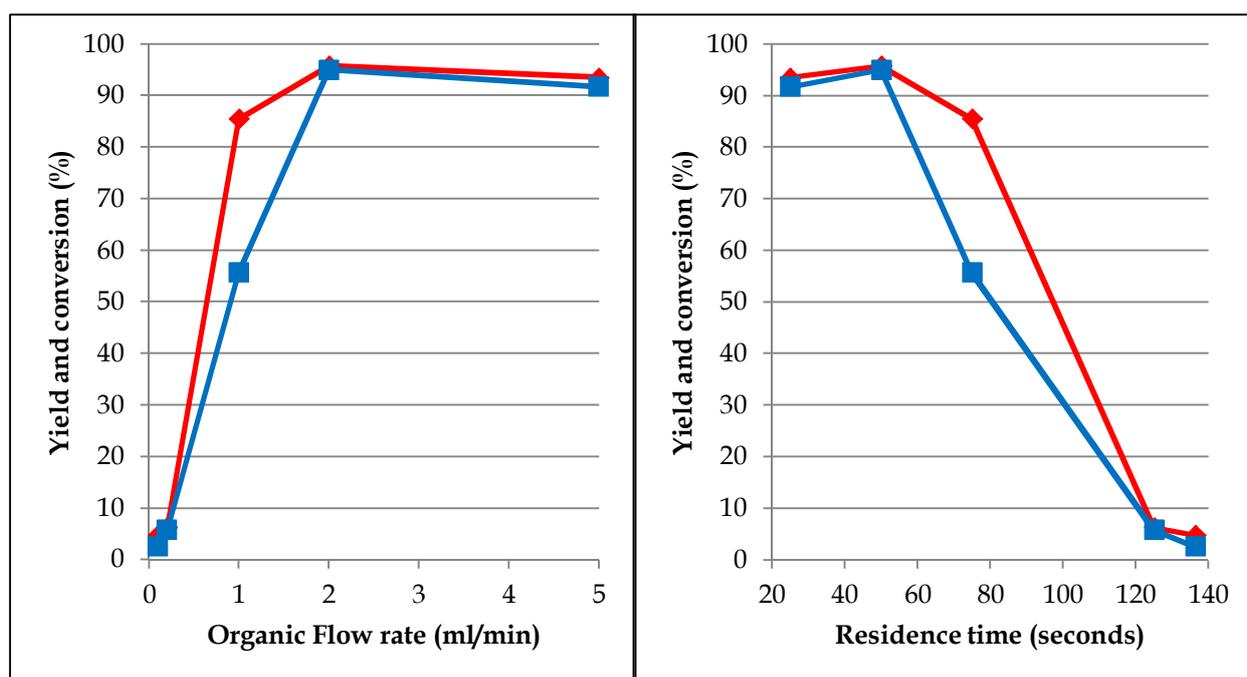The results obtained are shown in the following graphs (Fig.4.12).

Fig. 4.12 Photo-oxidation of citral with singlet oxygen in the high-pressure continuous flow system. TPP 0,1 mol.%, P= 100bar T= 1-6°C, 1 ml/min of liquid CO_2.
Citral conversion ♦ (red) and hydroperoxides yield ■ (blue) refer to the organic flow rate (left) and the residence time (τ) in the reactor (right) considering τ = V reactor/overall flow rate.

It is immediately evident the ostensible contradiction of these results. Indeed, at higher residence times, where we would expect the maximum conversion of the starting material, we observe almost no reactivity at all.

Moreover, we reach a maximum yield and conversion with 2 ml/min of organic flow rate (corresponding to ca. 50 seconds of residence time inside the sapphire tube), that starts to decrease with further increasing of the overall flow rate.

While this effect is easily explained with the decreasing of the residence time below the limit required to achieve complete conversion; the first observation can only be explained if we consider another important parameter: the dilution of the reagents solution in the overall flow.

As a matter of fact, co-feeding a certain amount of liquid CO_2 lead to a dilution of the reaction mixture in the overall flow (Table 4.4).

Organic flow rate (ml/min)	Liquid CO_2 flow rate (ml/min)	Overall flow rate (ml/min)	Photo-reactor Volume (ml)	Residence time (sec)	Citral final concentration (mol/l)
0,1	1	1,1	2,5	136	0,045
0,2	1	1,2	2,5	125	0,083
1	1	2	2,5	75	0,25
2	1	3	2,5	50	0,33
5	1	6	2,5	25	0,42

Table 4.4 Residence time and dilution calculation for the high pressure continuous flow photo-oxidation test of citral with TPP, P=100bar, T variable for the exotermicity of the reaction from 1 to 6 °C.
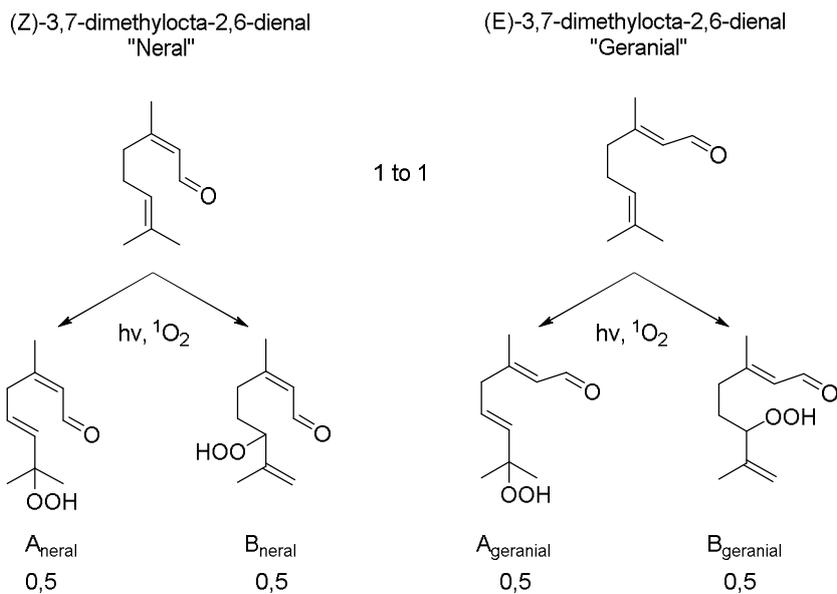
To prove the detrimental effect of an excessive dilution of the reagents, we have performed another test choosing the dilution of the best condition observed (at 2 ml/min of organic flow: final concentration 0,33mol/l) and changing the CO_2 and organic flow in order to have the same residence time at 0,2ml/min of organic flow with a residence time of 125 seconds.

In this way, feeding the organic mixture at 0,8 ml/min and co-feeding liquid CO_2 at 0,4 ml/min an outstanding results of 99% of citral conversion with complete selectivity towards the hydroperoxides products is obtained

A complete analysis of the allylic hydroperoxides obtained in flow tests at high conversion value has been performed.

Interestingly, from the ^{1}H-NMR all the signals integrations (especially the hydroperoxide hydrogen and the aldehyde signals) clearly shows the formation of the four expected hydroperoxides products with very similar yields (Fig. 4.13 and Fig. 4.14).

Indeed, starting from an 1:1 mixture of Neral and Geranial the products distribution are as follow (Scheme 4.5).

(Z)-3,7-dimethylocta-2,6-dienal
"Neral"

(E)-3,7-dimethylocta-2,6-dienal
"Geranial"

1 to 1

hv, $^1O_2$

hv, $^1O_2$

A_{neral}
0,5

B_{neral}
0,5

$A_{geranial}$
0,5

$B_{geranial}$
0,5

Scheme 4.5 Citral photo-oxidation with singlet oxygen, products distributions.

Fig. 4.13 ^{1}H-NMR (300MHz, CDCl$_3$, 25°C) of the reaction mixture obtained in the high-pressure flow reaction system at almost complete conversion of the starting material. Four hydroperoxides (-OOH) signals are detected at 9,55; 9,57; 9,07 and 9,11 ppm.
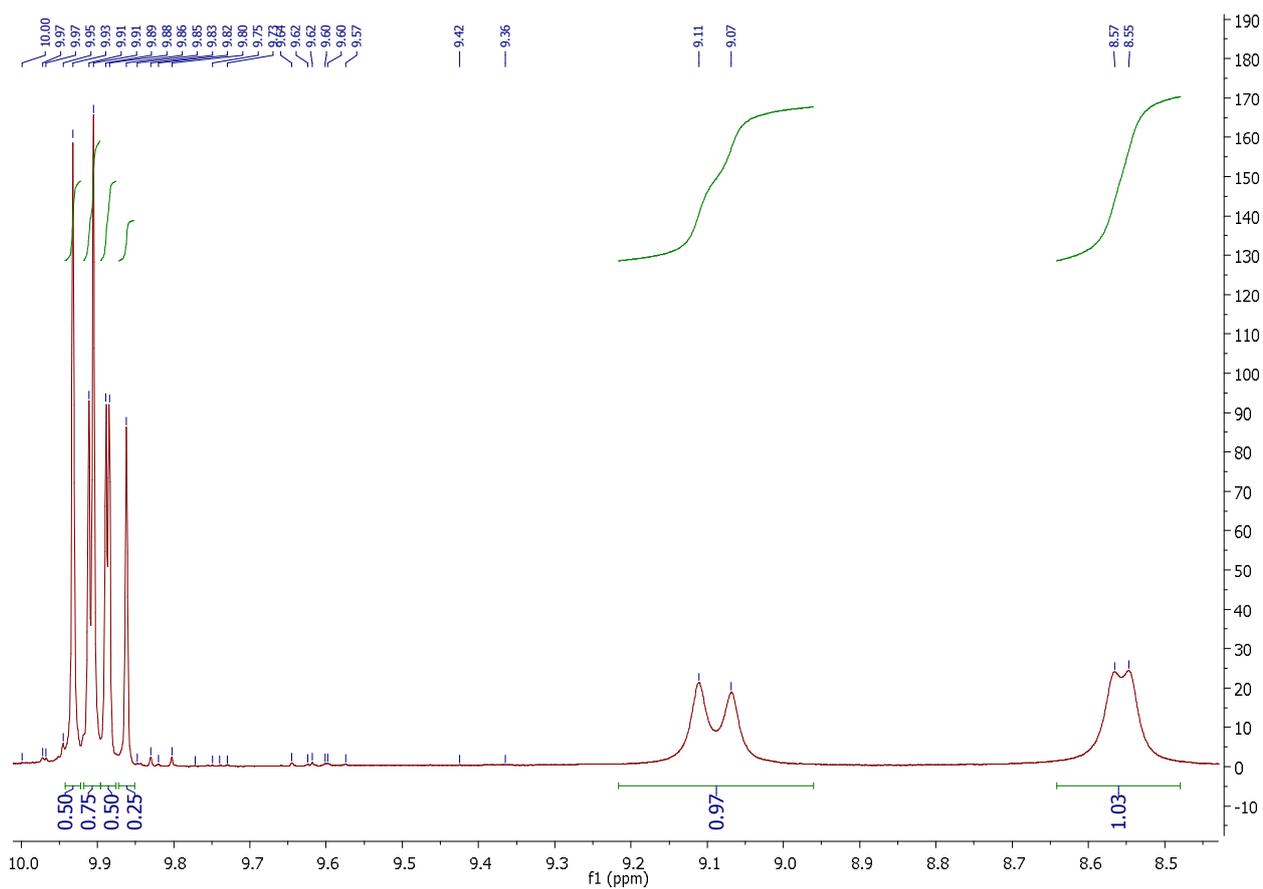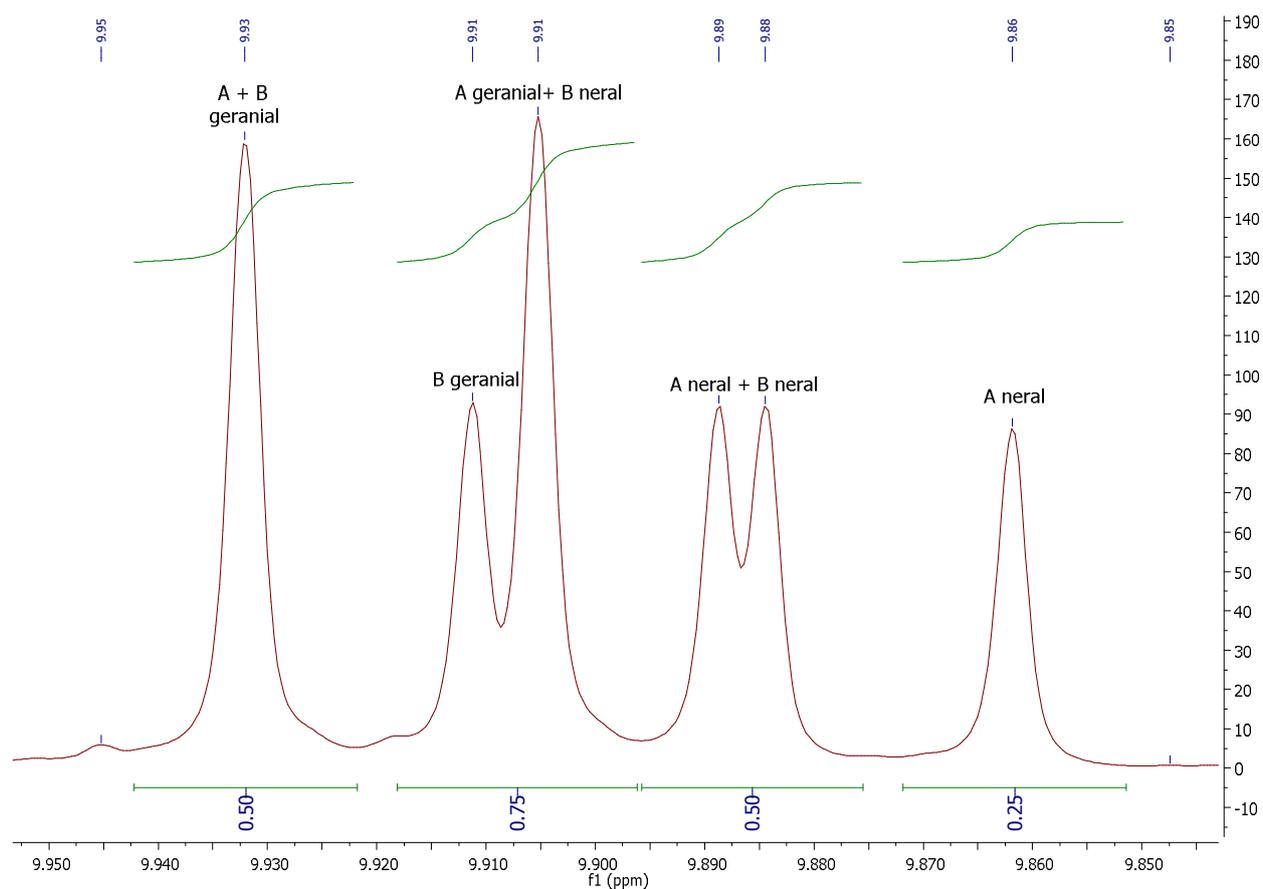
Fig. 4.14 ^{1}H-NMR (300MHz, CDCl$_3$, 25°C) of the reaction mixture obtained in the high-pressure flow reaction system at almost complete conversion of the starting material. Zoom in the aldehyde (CHO) region with the integration value and the hypothesized attribution of each pair of signals to one of the products proposed in Scheme **4.5**

Finally, in order to increase the miscibility of the system and enhance the kinetics we decided to make the same test, with the same organic mixture of reagents and photosensitizer but increasing the system pressure and temperature in order to work in the supercritical conditions of the CO$_2$ (P system = 140 bar and T= 40 °C).

Surprisingly we have obtained exactly the same behavior obtained in liquid CO$_2$.

This means that the conditions are optimal in liquid CO$_2$, probably because the conversion of triplet to singlet oxygen is already high enough that an extra miscibility enhancement due to the scCO$_2$ is not required. So this reactions does not necessarily required harsher conditions and moreover the reproducibility of these flow reactions have been proved.

5 CONCLUSIONS

In conclusion, the work performed during my time at the School of Chemistry, University of Nottingham under the supervision of Prof. Sir Martyn Poliakoff, from September to December 2015, allowed us to obtain the following results:

- ✓ DMC shows a greater singlet oxygen lifetime compared to ethanol and other considered "green" solvents (namely water, methanol etc.);
- ✓ DMC show a good stability in the oxidizing condition used for the reactions analyzed and could be considered as a green alternative for chlorinated solvents for these kind of reaction (low solubility in water).

- ✓ For the α-terpinene photo-oxidation with singlet oxygen in the presence of a porphyrin as photosensitizer (TPFPP), the utilization of DMC allow us to obtain promising results both in batch and in flow reactions;
- ✓ Furthermore, in the high-pressure flow test, co-feeding liquid CO_2 in milder condition compared to the usually utilized for the sc-CO_2 test we are able to obtain a stable system with complete conversion and high selectivity for ascaridole (>90%) for a wide series of residence time and organic flow rates. With the higher flow rate tested (but is probably a not limiting value) we are able to obtain an ascaridole productivity of 0.135 mol/h.

- ✓ A wide series of photosensitizer were investigated in a batch reactor system for the citral oxidation to the corresponding hydroperoxides.

We have found mainly two different behaviours:

- ✓ With porphyrins (TPP), Rose Bengal Sodium salt and methylene blue the utilization of DMC shows an increase in the rate of photooxidation, compared to the other solvents tested, toward the desired products;
- ✓ With photosensitizers characterized by the presence of a lactone group (Rose Bengal Lactone and Eosin Y) we have obtained opposite results, this is probably due to the different coordination in DMC compared to other solvents and to the decomposition of the photosensitizer that lead to lower absorbance and activities, but further experiments need to be carried out to further understand this observations.

In particular, TPP shows the best reactivity in batch reactions so it was chosen for further investigation in flow.

✓ In the same "milder" reaction conditions of the terpinene oxydation (co-feeding liquid CO_2 at 100 bar and 5 °C) we have obtained an interesting behaviour: the reaction seems to be stable toward changes of residence time but is dramatically affected by the dilution of the starting material in the overall flow.

✓ In the optimized conditions, feeding 0,8 ml/min of the citral solution in DMC, using TPP (0,1 mol.%) as photosensitizer and co-feeding liquid CO_2 0,4 ml/min at 100 bar and 5 °C we were able to obtain 99% of yield into the desired hydroperoxides products in the same ratio ca. 25% each.

✓ Finally, conducting the test in supercritical CO_2 (P system = 140 bar and T = 40 °C), we have obtained the same results as in milder condition; this means that supercritical conditions are not related to the rate limiting factors of the reaction. (i.e. good mixing of gases in the sc phase)

6 REFERENCES

[1] G. Ciamician, Science, 1912, 36, 385–394.

[2] E. Coyle, Ph.D. thesis, School of Chemical Sciences, Dublin City University, 2010.

[3] A. M. Braun, M. T. Maurette and E. Oliveros, Photochemical Technology, Wiley-VCH: New York, 1991.

[4] K. H. Pfoertner, J. Photochem. Photobiol. A, 1990, 51, 81–86.

[5] H. D. Roth, Angew. Chem. Int. Ed., 1989, 28, 1193–1207.

[6] H. E. Zimmerman and O. D. Mitkin, J. Org. Chem., 2007, 72, 6091-6096.

[7] R. L. Varma, V. B. Ganga and E. Suresh, J. Org. Chem., 2007, 72, 1017-1019.

[8] J. J. Sahn and D. L. Comins, J. Org. Chem., 2010, 75, 6728-6731.

[9] M. Nagarathinam, A. M. P. Peedikakkal and J. J. Vittal, Chem. Commun., 2008, 42, 5277-5288.

[10] G. Bucher, A. A. Mahajan and M. Schmittel, J. Org. Chem., 2008, 73, 8815-8828.

[11] V. Rey, S. M. Soria-Castro, J. E. Arguello and A. B. Penenory, Tetrahedron Lett., 2009, 50, 4720-4723.

[12] A. M. Khenkin, I. Efremenko, L. Weiner, J. M. L. Martin and R. Neumann, Chem.-Eur. J., 2010, 16, 1356-1364.

[13] M. P. Juliarena, R. O. Lezna, M. R. Feliz, G. T. Ruiz, S. Thomas, G. Ferraudi and I. Carmichael, J. Org. Chem., 2006, 71, 2870-2873.

[14] Y. H. Gao, J. F. Chen, X. J. Zhuang, J. T. Wang, Y. Pan, L. M. Zhang and S. Q. Yu, Chem. Phys., 2007, 334, 224-231.

[15] A. Astarita, F. Cermola, M. DellaGreca, M. R. Iesce, L. Previtera and M. Rubino, Green Chem., 2009, 11, 2030-2033.

[16] B. R. Travis, R. S. Narayan and B. Borhan; Chem. Soc., 2002, 124 (15), pp 3824–3825

[17] P. Esser, B. Pohlmann and H. D. Scharf, Angew. Chem. Int. Ed., 1994, 33, 2009-2023.

[18] J. Mattay, Chem. unserer Zeit, 2002, 36, 98-106.

[19] M. Oelgemoller, C. Jung, J. Ortner, J. Mattay and E. Zimmermann, Green Chem., 2005, 7, 35-38.

[20] N. Monnerie and J. Ortner, J. Sol. Energy Eng. Trans.-ASME, 2001, 123, 171-174.

[21] B. Ranby and J. F. Rabek, Singlet Oxygen-Reactions with Organic Compounds and Polymers, JOHN WILEY & SONS, London, 1978.

[22] S. Lacombe and T. Pigot, in Photochemistry, ed. A. Albini, Royal Society of Chemistry, 2010, pp. 307–329.

[23] E. L. Clennan and A. Pace, Tetrahedron, 2005, 61, 6665–6691.

[24] F. Wilkinson, W. P. Helman and A. B. Ross, J. Phys. Chem. Ref. Data, 1995, 24, 663–1012.

[25] A. Sivery, A. Barras, R. Boukherroub, C. Pierlot, J. M. Aubry, F. Anquez and E. Courtade, J. Phys. Chem. C, 2014, 118, 2885–2893.

[26] P. L. Alsters, W. Jary, V. Nardello-Rataj and J. M. Aubry, Org. Process Res. Dev., 2010, 14, 259-262.

[27] T. Foldes, P. Cermak, M. Macko, P. Veis and P. Macko, Chem. Phys. Lett., 2009, 467, 233-236.

[28] A. Greer, Acc. Chem. Res., 2006, 39, 797–804.

[29] P. R. Ogilby, Chem. Soc. Rev., 2010, 39, 3181–3209.

[30] X. Han, R. A. Bourne, M. Poliakoff and M. W. George. Chem. Sci., 2011, 2, 1059

[31] S. E. Braslavsky, Pure Appl. Chem., 2007, 79, 293–465.

[32] E. Coyle, Ph.D. thesis, School of Chemical Sciences, Dublin City University, 2010.

[33] Clennan, E.L.; Pace, A. *Tetrahedron* 2001, 61, 6665

[34] Alexander P. Darmanyan and William S. Jenks *J. Phys. Chem.* A 1998, *102*, 7420-7426

[35] a) Schmidt, R., *J. Am. Chem. Soc.* 1989, *111*, 6983. b) Gorman, A. A.; Rodgers, M. A. J. Singlet Oxygen; Scaiano, J. C., Ed.; CRC Press: Boca Raton, Florida, 1989; Vol. II, pp 229. C) Wilkinson, F.; Helman, W. P.; Ross, A. B *J. Phys. Chem.* 1995, 24, 663.

[36] M. Prein and W. Adam, Angew. Chem. Int. Ed., 1996, 35, 477–494.

[37] M. J. S. Dewar; W. Thiel, J. Am. Chem. Soc. 1977, 99, 2338-2339

[38] Grdina, M. B.; Orfanopoulos, M.; Stephenson, L. M. J. Am. Chem. Soc. 1979, 101, 3111- 3112

[39] A. Maranzana; G. Ghigo; G. Tonachini, J. Am. Chem. Soc. 2000, 122, 1414-1423

[40] M. R. Iesce, in Synthetic Organic Photochemistry, ed. A. G. Griesbeck and J. Mattay, Marcel Dekker, 2005, pp. 299–363.

[41] T. Montagnon, M. Tofi and G. Vassilikogiannakis, *Acc. Chem. Res.*, 2008, **41**, 1001-1011.

[42] M. N. Alberti, G. C. Vougioukalakis and M. Orfanopoulos, *J. Org. Chem.*, 2009, **74**, 7274-7282.

[43] G. Ohloff, Pure Appl. Chem., 1975, 43, 481–502.

[44] W. Adam, M. Braun, A. Griesbeck, V. Lucchini, E. Staab and B. Will, J. Am. Chem. Soc., 1989, 111, 203–212.

[45] E. D. Mihelich and D. J. Eickhoff, J. Org. Chem., 1983, 48, 4135–4137.

[46] A. Windaus and J. Brunken, Justus Liebigs Ann. Chem., 1928, 460, 225–235.

[47] *A. L. A. Lan,. (2003). Ecologia quimica. Plaza y Valdes. pp 323*

[48] G. O. Schenck and K. Ziegler, Naturwissenschaften, 1944, 32, 157–157.

[49] E. L. Clennan, in Synthetic Organic Photochemistry, ed. A. G. Griesbeck and J. Mattay, Marcel Dekker, 2005, pp. 365–390.

[50] E. W. H. Asveld and R. M. Kellogg, J. Am. Chem. Soc., 1980, 102, 3644–3646.

[51] A. Gorman, I. Hamblett, C. Lambert, B. Spencer and M. Standen, J. Am. Chem. Soc., 1988, 110, 8053–8059.

[52] M. N. Alberti and M. Orfanopoulos, *Synlett*, 2010, 7, 999-1026.

[53] S. D. Yardimci, N. Kaya and M. Balci, *Tetrahedron*, 2006, 62, 10633-10638.

[54] J. J. Helesbeux, O. Duval, D. Guilet, D. Seraphin, D. Rondeau and P. Richomme,*Tetrahedron*, 2003, 59, 5091-5104.

[55] S. G. Newman and K. F. Jensen, Green Chem., 2013, 15, 1456–1472.

[56] B. Gutmann, J.-P. Roduit, D. Roberge and C. O. Kappe, Angew. Chem. Int. Ed., 2010, 49, 7101–7105.

[57] A. E. Rubin, S. Tummala, D. A. Both, C.Wang and E. J. Delaney, Chem. Rev., 2006, 106, 2794–2810.

[58] H. Lange, C. F. Carter, M. D. Hopkin, A. Burke, J. G. Goode, I. R. Baxendale and S. V. Ley, Chem. Sci., 2011, 2, 765–769.

[59] S. Protti, D. Dondi, M. Fagnoni and A. Albini, Pure Appl. Chem., 2007, 79, 1929–1938.

[60] R. A. Sheldon, *Green Chem.*, 2005, **7**, 267-278.

[61] J. H. Clark and S. J. Tavener, *Org. Process Res. Dev.*, 2007, 11, 149-155.

[62] U. Romano; F. Rivetti, U.S. Patent 4,318,862, 1979.

[63] U. Romano, R. Tesei, M. Massi Mauri, P. Rebora, Ind. Eng. Chem. Prod. Res. Dev., 1980, 19, 396.

[64] P. Tundo; M. Selva. Acc. Chem. Res. 2002, 35, 706–716.

[65] G. Vasapollo; G. Mele; A. Maffei; R. Del Sole, Appl. Organomet. Chem. 2003, 17, 835–839.

[66] J. Cornely; L. M. Su Ham; V. Meade; V. Dragojilovic, Green Chem. 2003, 5, 34–37.

[67] R. Bernini et al. Tetrahedron 63 (2007) 6895–6900.

[68] P.N. Gooden, Ph.D. Thesys, The University of Nottingham, 2006.

[69] B. Lewis and G. von Elbe, *Combustion, Flames and Explosions of Gases*, Academic Press Inc. (London), 1987.

[70] A. O. Chapman, Ph.D. thesis, University of Nottingham, 2007.

[71] J. F. B. Bellamy, Ph.D. thesis, University of Nottingham, 2014.

[72] X. Han, Ph.D. thesis, The University of Nottingham, 2010.

[73] M. W. Grinstaff, M. G. Hill, J. A. Labinger and H. B. Gray, *Science*, 1994, **264**,1311-1313.

[74] T. G. Traylor, Y. S. Byun, P. S. Traylor, P. Battioni and D. Mansuy, *J. Am. Chem.Soc.*, 1991, **113**, 7821-7823.

[75] C. Tanielian and C. Wolff, *J. Phys. Chem.*, 1995, **99**, 9825-9830.

[76] Jan F. Rabek, Young J. Shur, B. Rårnby Polym. Chem. 1975, 13(6), 1285–1295

[77] Org. Biomol. Chem., 2015, 13, 4686-4692

[78] C.S. Foote; S. Wexler, J. Am. Chem. Soc., 86, 3879 (1964).

[79] G. Brunner, Supercritical Fluids as Solvents and Reaction Media, Elsevier, London,2004.

[80] T. Casimiro, A. M. Banet-Osuna, A. M. Ramos, M. N. da Ponte and A. Aguiar-Ricardo, *Eur. Polym. J.*, 2005, 41, 1947-1953.

[81] H. Y. Tai, J. Liu and S. M. Howdle, *Eur. Polym. J.*, 2005, **41**, 2544-2551.

[82] T. Y. Zhang, H. B. Fan and L. Zhong, *Prog. Chem.*, 2008, **20**, 1270-1275.

[83] H. K. Bae, J. H. Jeon and H. Lee, *Fluid Phase Equilib.*, 2004, **222**, 119-125.

[84] M. Sagisaka, J. Oasa, S. Hasegawa, R. Toyokawa and A. Yoshizawa, *J. Supercrit.Fluids*, 2010, **53**, 131-136.

[85] C. E. Bunker, H. W. Rollins, J. R. Gord and Y. P. Sun, *J. Org. Chem.*, 1997, **62**, 7324-7329.

[86] A. O. Chapman, G. R. Akien, N. J. Arrowsmith, P. Licence and M. Poliakoff, *Green Chem.*, 2010, **12**, 310-315.

[87] R. A. Bourne, X. Han, M. Poliakoff and M.W. George Angew. Chem. Int. Ed. 2009, 48, 5322 –5325

[88] Xue Han, Richard A. Bourne, Martyn Poliakoff and Michael W. George *Green Chem.*, 2009, **11**, 1787–1792

[89] J. F. B. Hall, X. Han, M. Poliakoff, R. A. Bourne and M.l W. George, Chem. Commun., 2012, 48, 3073–3075.

[90] R. A. Bourne, X. Han, A. O. Chapman, N. J. Arrowsmith, H. Kawanami, M. Poliakoff and M.W. George, Chem. Commun., 2008, 4457–4459.

[91] E. M. Elgendy and S. A. Khayyat, Russian Journal of Organic Chemistry, 2008, Vol. 44, No. 6, pp. 814–822.

[92] Chem. Commun., 2014, 50, 6688